

https://dspace.org/

Weathering of coals from the Waterberg and Limpopo Coalfields, South Africa

Sebola, Mandy-Jane Tlou

2018

https://hdl.handle.net/10539/26054

Sebola, Mandy-Jane Tlou (2018) Weathering of coals from the Waterberg and Limpopo Coalfields, South Africa, University of the Witwatersrand, Johannesburg, <http://hdl.handle.net/10539/26054>

Downloaded from a DSpace repository. https://dspace.org/

Weathering of coals from the Waterberg and Limpopo Coalfields, South Africa

---

Submitted by

Mandy-Jane Tlou Sebola

A dissertation submitted in fulfilment of the degree of Master of Science in Geology in The Faculty of Science at the University of the Witwatersrand, Johannesburg.

Supervisor: Professor Gillian R. Drennan

Co-supervisor: Professor Nicola J. Wagner



31 May 2018

Declaration

I, Mandy-Jane Tlou Sebola declare that this dissertation is my own, original unaided work. It is being submitted for the Degree of Master of Science in the Faculty of Science at the University of the Witwatersrand, Johannesburg. It has not been submitted before for any degree or examination in any other University.

_____

Mandy-Jane Tlou Sebola

Signed at Johannesburg on the____day of May 2018

Abstract

This study investigated the effects of weathering on coal from the Waterberg and Limpopo Coalfields with the aim to understand how the quality of these coals changed during the early stages of oxidative weathering under dry and wet conditions.

Coal was sampled from freshly exposed seams in both coalfields to provide, as best as possible, an un-weathered parent sample from which the extent of weathering could be determined. The Middle Seam was sampled from the Limpopo Coalfield whereas Benches 3, 5, 9B and 11 were sampled from the Waterberg Coalfield. This suite of samples enabled investigation into the impact of weathering on coals with similar properties but originating from different localities (Waterberg Coalfield vs Limpopo Coalfield), as well as coal with different properties originating from the same locality (Benches 3, 5, 9B and 11). Furthermore, the impact of weathering was studied on the coking properties (Middle Seam vs Bench 3) and heating properties using thermal coal (Bench 5).

The experiment was conducted over a duration of six months during which a subset of the samples from each coalfield was kept dry in perforated containers, whilst the remaining samples were frequently watered to simulate the effect of rainfall under controlled settings. The particle size of the samples was reduced to -1mm to enhance the surface area for a more rapid reaction. Thereafter the samples were left to weather outdoors, on the roof of a building at the University of the Witwatersrand, Johannesburg. The average temperature conditions affecting the samples during the research period ranged between 9.40-27.23 °C.

Several conventional coal analyses (proximate analysis, ultimate analysis, coal petrography, XRF & XRD) were used in conjunction with advanced techniques (EMPA, FE-SEM & Raman spectroscopy) to detect early signs of weathering on the organic and inorganic coal constituents. The impact of weathering on technological properties of the coal samples were investigated using calorific value, thermogravimetry and free swelling index.

After six months of weathering, very small changes were observed in the coal quality due to weathering. The chemical and petrographic composition of the coals remained relatively unaffected by weathering, whereas the mineral matter and swelling properties of the coals were more susceptible to weathering under wet conditions. The alteration of minerals was more evident in the samples that were watered throughout the experiment, irrespective of their original locality. These samples were characterized by the precipitation of gypsum on the surface of the wet coals, as well as the appearance of red calcite grains. Analysis of the red calcite grains revealed rare growth rims associated with the precipitation of siderite.

Although the findings of the thermogravimetric analysis suggested that the reactivity of the thermal coal had been slightly reduced by weathering (especially by weathering under wet conditions), the CV trend for this coal did not appear to be impaired. Hence, the effect of weathering on the heating properties of this sample are inconclusive.

Ultimately, after 6 months of exposure to weathering the quality of the coals remained very similar to their fresh parent samples. However, the swelling properties of the coking coals from each coalfield were diminished. Therefore, caution is advised for the stockpiling of the coking coals outdoors, which should not exceed longer than 4-6 months, especially in the case of the Waterberg coking coal.

Dedication

To my sister

Esther Mapula Onkarabile Sebola

9 August 2017

Acknowledgements

I am most grateful to my supervisors, Professors Gillian Drennan and Nicola Wagner who have spurred my interest in coal and have promoted my development in this field. Thank you for believing in me and supporting me through this research, especially through the many setbacks that we encountered and overcame. I truly appreciate all your guidance and support, which has helped me immensely and encouraged me. I am also grateful to Professor Wagner for training me on the petrographic microscope and providing guidance during the petrographic analysis.

I am grateful to the Council for Geosciences for funding my Master's degree and for covering the cost of many of the analyses that were pertinent to this study. Thank you to all the professionals from CGS who took the time to teach me how to conduct some of the analyses and those who also conducted the analyses on my behalf. Particularly, I would like to thank Dr Nandi Mulumbazo and Mr Supi Tlowana, for granting me access to the coal laboratory. Miss Nontle Mniki and Mr Ronald Ragoasha are thanked for assisting me with the various coal analyses. Thank you for your patience and willingness to train me on the various analysis techniques. Miss Nondumiso Dlamini, Mrs Corlien Cloete and Mr Teboho Motseri for conducting x-ray diffraction, x-ray fluorescence and sample preparation, respectively.

Coal of Africa is thanked for providing coal samples for the project. In particular, I would like to thank Mr John Sparrow, Miss Nthabiseng Masunyane and the staff at Vele Colliery for their contributions to my research.

Exxaro Coal is also acknowledged for kindly providing additional coal for the study. I would like to thank Mrs Karina Boekhoud, Mr Henk Lingenfelder and Mr Callie Van Heerden for kindly arranging my visit to the Grootegeluk Mine. I am grateful to Mr Coert Van Ryneveld for helping us to collect the samples.

Thank you to Mr Abraham for assisting me with sample preparation at the University of Johannesburg, Doornfontein Campus, and to Dr Raeesa Moola from the University of the Witwatersrand, who kindly allowed me to operate the Davis weather station during the course of the study. Dr Rudolph Erasmus is thanked for conducting Raman spectroscopy at the Microscopy and Microanalysis Unit at the University of the Witwatersrand. Dr Peter Horvath is thanked for conducting the electron microprobe analysis, at the Microscopy and Microanalysis Unit at the University of the Witwatersrand. Mr Brayner Nelwalani is thanked for conducting field emission scanning electron microscopy at the School of Chemical and Metallurgical Engineering, University of the Witwatersrand. Mrs Janet Smith is thanked for assisting me with the thermogravimetric analyses at the Clean Coal Technology Research (CCTR) laboratory at the University of the Witwatersrand.

To my parents, I thank you for being my biggest cheerleaders and for being my role models! I am ever grateful for your unwavering love and support, and for giving me the space I need to pursue my studies.

Finally, all glory to my Jesus who makes all things possible.

Contents

Declaration i

Abstract ii

Dedication iv

Acknowledgements v

List of Figures x

List of Tables xiii

List of Equations xiv

List of Abbreviations and Acronyms xv

Chapter 1: Introduction 1

1.1 Background to the study 1

1.2 Progress of coal weathering research in South Africa 4

1.3 Problem statement, Aim and Objectives 6

Chapter 2: Coal geology 9

2.1 Coal as a sedimentary rock 9

2.2 Coal forming processes and classification 10

2.3 The composition of coal 12

2.3.1 Organic coal constituents: Macerals 12

2.3.2 Inorganic coal constituents: Mineral matter 16

2.4 Overview of the Karoo Supergroup in South Africa 17

2.5 Overview of coalfields in South Africa 18

2.6 The Waterberg Coalfield 20

2.7 The Limpopo (Tuli) Coalfield 21

Chapter 3: Coal oxidation and weathering 24

3.1 Oxidative weathering of coal 24

3.2 Weathering during stockpiling 26

3.3 The effect of weathering on coal constituents 28

3.4 The effect of weathering on the technological properties of coal 30

3.5 Techniques for the detection of weathered coal 31

Chapter 4: Materials and methods 34
4.1 Sampling and sample preparation 34
4.2 Weather Station Assemblage 37
4.3 Chemical analyses 38
4.3.1 Proximate analysis 38
4.4.2 Ultimate analysis 42
4.5 Technological analyses 43
4.5.1 Calorific value (CV) 43
4.5.2 Thermogravimetric analysis (TGA) 44
4.5.3 Free swelling index (FSI) 45
4.6 Petrography 46
4.6.1 Maceral point count 46
4.6.2 Vitrinite reflectance 47
4.6.3 Abnormal Condition Analysis (ACA) 48
4.7 Mineralogy 48
4.7.1 X-ray diffraction (XRD) 49
4.7.2 X-ray Fluorescence (XRF) 49
4.7.3 Electron microprobe analysis (EMPA) 49
4.7.4 Field scanning electron microscopy (FE-SEM) 50
4.7.5 Raman Spectroscopy 50
4.8 Statistical analyses 51
Chapter 5: Results and discussion 53
5.1 Temperature measurements 53
5.2 Chemical analyses 54
5.2.1 Proximate results 54
5.2.2 Ultimate analysis 62
5.3 Calorific Value (CV) 76
5.4 Thermogravimetric analysis (TGA) 79
5.5 Free Swelling Index (FSI) 82

5.6 Mineralogy 84
5.6.1 Inorganic (mineral) composition of the coal 84
5.6.2 Mineral transformations due to weathering 87
5.6.3 Major oxide composition of coal ash 96
5.7 Petrography 101
5.7.1 Maceral point count 101
5.7.2 Vitrinite reflectance 105
5.7.3 Abnormal condition analysis (ACA) 106
Chapter 6: Conclusions and recommendations 112
6.1 Summary 112
6.2 Conclusions 112
6.3 Recommendations 116
References 117
Appendices 132
Appendix A. Ambient temperature measurements over the duration of the experiment. 132
Appendix B. Replicate (R) runs for the proximate analysis 139
Appendix C. Replicate (R) runs for the ultimate analysis 140
Appendix D. Replicate (R) runs for the calorific value (MJ/kg) 142
Appendix E. Critical values of the correlation coefficients for one-sided tests of the null hypothesis H0: $\rho = 0$. where degrees of freedom =sample size - 2 (Underhill and Bradfield, 2013). 143
Appendix F. Thermogravimetric analysis (TGA) for Bench 5 144
Appendix G. Carbonate analysis on various calcite grains (wt%) by EMPA 155
Appendix H. Raman spectroscopy 156
Appendix I. Major oxide composition (wt %) as determined by XRF 157
Appendix J. Presentations arising from this research project 160

List of Figures

Figure 1. Generalized mining operation showing points (circled in red) at which coal is likely to undergo weathering (Modified after Mangkusubroto, 2010). 1
Figure 2. The locations (circled in red) of the Waterberg and Limpopo Coalfields in South Africa (Hancox and Götz, 2014). 3
Figure 3. Deposition of coal into the peat swamp followed by an increase in rank with increasing temperature and burial pressure over time, including the subsequent effects of dykes and sills (Falcon and Snyman, 1986). 11
Figure 4. The extent of the Karoo Basin in South Africa (modified after Snyman and Barclay, 198918
Figure 5. Tentative correlation of stratigraphic units in the Main Karoo Basin, Ellisras Basin and Tuli Basin (modified after Johnson et al., 2006). 19
Figure 6. Geology of the Waterberg Coalfield (modified after Fourie et al., 2014). 20
Figure 7. The location of Vele Colliery (top right) on the Geological map of the Limpopo Coalfield (modified after Malaza, 2013). 22
Figure 8. Meteorological parameters driving weathering of a coal stockpile (modified after Zhang et al., 2016). 27
Figure 9. Flow diagram of the sampling, sample preparation and storage procedure. 35
Figure 10. Clear plastic containers on the roof of the Bernard Price Building, University of the Witwatersrand 36
Figure 11. Functions of the Davis Vantage Pro2 weather station (Davis, 2016). 38
Figure 12. Parameters on a burning profile determined by thermogravimetry (Norton, 1993). 45
Figure 13. Button profiles according to ISO 501:2012 46
Figure 14. Proximate results of the dry samples and their wet counterparts.* Inherent moisture content, ■ volatile matter (daf), ▲ ash content (db) and ●fixed carbon content (daf). 55
Figure 15. Ultimate results for the dry samples and their wet counterparts. ●hydrogen, ■ total sulphur and ▲nitrogen. 63
Figure 16. Total carbon (bar graph) and calculated oxygen (line graph) for the dry samples and their wet counterparts 71
Figure 17. The H/C ratio (♦) and the O/C ratio (●) for the dry samples and their wet counterparts. ... 74
Figure 18. The behaviour of the calorific value for the dry samples (●) and their wet counterparts (■). 76
Figure 18 continued19. The behaviour of the calorific value for the dry samples (●) and their wet counterparts (■). 77
Figure 20. DTG curves for B5 and its wet counterpart B5W showing temperature (x-axis) vs rate of mass loss 1 % min^{-1} (y-axis). 80

Figure 21. Trends in the free swelling index for coking coals the from the Middle Seam (MS) and Bench 3 (B3)..... 82
Figure 22. Example of the small extent of gypsum precipitated on the surface of B5W [A] compared to B5 after contamination by rainwater [B]..... 87
Figure 23. [A] Platy red calcite grains in sample B5W. [B]. The average chemical composition of fresh clear calcite in sample B5B compared to weathered clear calcite in B5W 6M and weathered red calcite grains in a rainwater contaminated sample B56M..... 88
Figure 24. Calcite (cal), pyrite (py) and siderite (sid) occurring with vitrinite (v) in sample B5W after six months of weathering, under oil immersion at x10 magnification [A] and electron microprobe back-scattered image at 200 μm [B]. 89
Figure 25. SEM back-scattered electron images and selected EDS data in coal sampled after 16 months of weathering. 91
Figure 26. SEM-EDS elemental maps of altered calcite grain after 16 months of weathering 92
Figure 27. SEM back-scattered electron images and selected EDS data in coal sampled after 16 months of weathering. 93
Figure 28. SEM back-scattered electron images and selected EDS data in coal sampled after 16 months of weathering. 94
Figure 29. SEM-EDS elemental maps of altered calcite grain after 16 months of weathering 95
Figure 30. $Fe_2O_{3\,(t)}$ (●) and CaO (■) trends for the dry samples and their wet counterparts..... 96
Figure 31. Photomicrograph of fresh macerals. Alternating bands of collotelinite in MSW M4 [A], Secretinite and fusinite in B11W M6 [B], Micrinite in B9 M4 [C], Fusinite in MS M4 [D], Cutinite and colloteliite in B5W M2 [E], Cutinite and collotelinite under fluorescent light in B5W M2 [F], Cutinite and collotelinite in B3W M6 [G], Cutinite and collotelinite under fluorescent light in B3W M6 [H]. ct= collotelinite, cut= cutinite, fu= fusinite, mic= micrinite, sc= secretinite. (Oil immersion at x500μm magnification). 103
Figure 32. Photomicrographs of fresh minerals as per the maceral point count. Quartz grains with clay minerals in B3 M6 [A], Clay minerals in B5 M4 [B], Calcite lath in B9W M6 [C], Calcite veins impregnating vitrinite in B3B [D], Pyrite veins crosscutting vitrinite in B3 M6 [E], Massive pyrite in B5 M2 [F], Pyrite nodules in B3W M2 [G] and MS M4 [H]. qrtz= quartz, clay= clay minerals, cal= calcite, py= pyrite. (Oil immersion at x500μm magnification).. 104
Figure 33. Photomicrographs of inherent oxidation rims occurring on fresh macerals in samples B5 M2 [A], B5W M4 [B], B5 M2 [C], and MS 4M [D], B3W M4 [E], B11W M6 [F], and after 16 months of weathering [G] and [H]. corp= corpogellinite, fu= fusinite, sc= secretinite. Oil immersion at x500μm magnification..... 108
Figure 34.Photomicrographs of cracks and fissures in samples B3W M4 [A], MSW M2 [B], MS M2 [C] and B3W M2 [D]; Examples of pseudovitrinite (primary origin) in samples B3W M4

[E], B3W M4 [F], B11 M6 [G], and B5W M4 [H]. Oil immersion at x500μm magnification. 109
Figure 35. Photomicrographs of various forms of altered calcite (bright red). Altered calcite veins in B3W M6 [A], Altered calcite lath in B11W M6 [B] and in B5W M4 [C], Altered calcite adjacent to pyrite in B11W M6 [D], Extensive alteration (white zone) associated with red altered calcite B3W M4 [E], Growth rims on the edge of calcite grain in sample collected after 16 months of weathering [F], Growth zones along the edge of altered calcite lath in B3W and sample collected after 16 months of weathering [H]. alt= alteration of calcite, py= pyrite, oxy rim= oxidation rim. Oil immersion at x500μm magnification. 110
Figure 36. Raman spectra of red calcite grains 156

List of Tables

Table 1. Observed signs of weathering due to oxidation in a previous study (Sebola, 2015). 4
Table 2. Contrast between coals from Gondwana and Laurasia (Falcon and Ham, 1988; Teichmüller, 1989; Kershaw and Taylor, 1992; Taylor et al., 1998; Malvadkar et al., 2004)..... 9
Table 3. Maceral classification according to the International Committee for Coal and Organic Petrology (ICCP, 1998; 2001; Pickel et al., 2017). 13
Table 4. Sample nomenclature and sampling intervals. 37
Table 5. Precision of the CHN method used by CGS. 43
Table 6. Macerals and mineral matter analysed in the study. 47
Table 7. Coal rank classification using SANS 10320: 2004. 48
Table 8. Summary of monthly average temperatures from 2 August 2016 to 6 February 2017. 53
Table 9. Statistical analysis of the proximate results 57
Table 10. Statistical analysis of the ultimate results 65
Table 11. Statistical analysis of the calorific value 78
Table 12. Summary of thermogravimetric analysis results 81
Table 13. Statistical analyses of coking coals MS and B3. 83
Table 14. Mineralogy of coal samples as determined by XRD (wt%). 85
Table 15. Statistical analyses of the total iron content ($Fe_2O_{3\,(t)}$) and calcium oxide (CaO)..... 99
Table 16.Maceral constituents including mineral matter (inc. mm) and mineral matter free (mmf) basis 102
Table 17. Random reflectance (Rr%) measurements for medium-rank C bituminous coal. 105
Table 18. Proportion of weathered vs fresh coal constituents as determined by the ACA (vol %) 111
Table 19. Statistically significant changes in the coal properties of the samples studied 114

List of Equations

Equation 1. Oxidation of coal……24

Equation 2. Oxidation of pyrite into sulphuric acid……...30

Equation 3. Precipitation of gypsum……...30

Equation 4. Calculation of fixed carbon by difference...…….38

Equation 5. Conversion of fixed carbon from air-dried basis (ad) to dry basis (db)……39

Equation 6. Conversion of fixed carbon from dry basis (db) to dry ash free basis (daf)……...39

Equation 7. Calculation of inherent moisture on an air-dried basis (ad).……...40

Equation 8. Calculation of volatile matter on an air-dried basis (ad)…….……..…40

Equation 9. Conversion of volatile matter from air-dried basis (ad) to dry basis (db)……40

Equation 10. Conversion of volatile matter from dry basis (db) to dry ash free basis (daf)……41

Equation 11. Calculation of ash content on an air-dried basis (ad)…….41

Equation 12. Conversion of ash content from an air-dried basis (ad) to dry basis (db)……41

Equation 13. Calculation of % oxygen content by difference…….42

Equation 14. Conversion of % elemental composition on an air-dried basis (ad) to dry basis (db)……42

Equation 15. Conversion of % elemental composition on dry basis (db) to dry ash free basis (daf)……42

Equation 16. Straight line equation…..……51

Equation 17. Calculation of the correlation of determination (R^2).……....51

Equation 18. Calculation of Pearson's correlation coefficient (p).……51

Equation 19. Calculation of the degree of freedom (d.f) ……...……52

List of Abbreviations and Acronyms

A : Ash

ACA : Abnormal Condition Analysis

ad : Air dried, includes Inherent Moisture (IM) only

alt : Alteration

ar : As Received, includes Total Moisture (TM)

ASTM : American Society for Testing and Materials

BSE : Back-scattered electron

BT : Burnout temperature

cal : Calcite

CBM : Coal bed methane

CCTR : Clean Coal Technology Research

CGS : Council for Geosciences

clay : Clay minerals

CoAL : Coal of Africa Limited

corp : Corpogelinite

ct : Collotelinite

cut : Cutinite

CV : Calorific value (MJ/kg)

daf : Dry Ash Free, excludes all Moisture and Ash

db : Dry Basis, excludes all Moisture

d.f. : Degree of freedom

EDS : Energy dispersive x-ray spectroscopy

EHT : Extra high tension

EMPA : Electron microprobe analysis

f_a : Aromaticity

FC : Fixed carbon

FSI : Free swelling index

FTIRS : Fourier transform infrared spectroscopy

inc. mm : Including mineral matter

ISO : International Organization for Standardization

ISS : Integrated Sensor Suite

IT : Initial/ignition temperature

IT_{FC} : Fixed carbon ignition temperature

LMB : Limpopo Mobile Belt

mic : Micrinite

MKB : Main Karoo Basin

mmf : Mineral matter free

MMU : Microscopy and microanalysis unit

p : Population correlation coefficient

PT : Peak maximum temperature

PWC : Price Waterhouse Coopers

QEMSCAN : Quantitative evaluation of minerals by scanning

qrtz : Quartz

ROM : Run of mine

r : Pearson's correlation coefficient

*R*r : Mean vitrinite random reflectance

Rv_{max} : Mean vitrinite maximum reflectance

S : Sulphur

SACS : South African Committee for Stratigraphy

SANS : South African National Standards

SAWS : South African Weather Services

sc : Secretinite

SEM : Scanning electron microscopy

semifu : Semifusinite

sid : Siderite

TGA : Thermogravimetric Analysis

UJ : University of Johannesburg

v : Vitrinite

VM : Volatile matter

WD : Working distance

WITS : University of the Witwatersrand

wt% : Weight percentage

XRD : X-ray diffraction

XRF : X-ray fluorescence

Chapter 1: Introduction

The rationale and relevance of the study are highlighted in Chapter 1. The phenomenon of coal weathering is introduced with specific reference to the South African context. The problem statement aims, and objectives of the study are also presented.

1.1 Background to the study

Weathering is a natural process that refers to the degradation of rocks by biological, chemical and physical attack (Yatsu, 1988). In the context of coal, weathering primarily results from the chemical process of oxidation which occurs when the coal is exposed to atmospheric conditions that differ from the equilibrium conditions in which the coal was initially preserved through geological time (Hamilton, 1907; Cox and Nelson, 1984; Marchioni, 1983; Cimadevilla *et al*., 2005; Thomas, 2012). Hence, coal seams that are exposed to the atmosphere become susceptible to the weather elements, particularly to excess oxygen, variable temperature conditions and moisture levels, which fluctuate seasonally (Wang *et al*., 2003a). Furthermore, coal seams that are near the Earth's surface may weather when they come into contact with oxygenated ground water (Mc Hugh *et al*., 1991). Mining operations (Figure 1) involve multiple stages of handling and transportation during which coal is often stockpiled outdoors for some time, during which oxidation may lead to self-heating and ultimately spontaneous combustion.

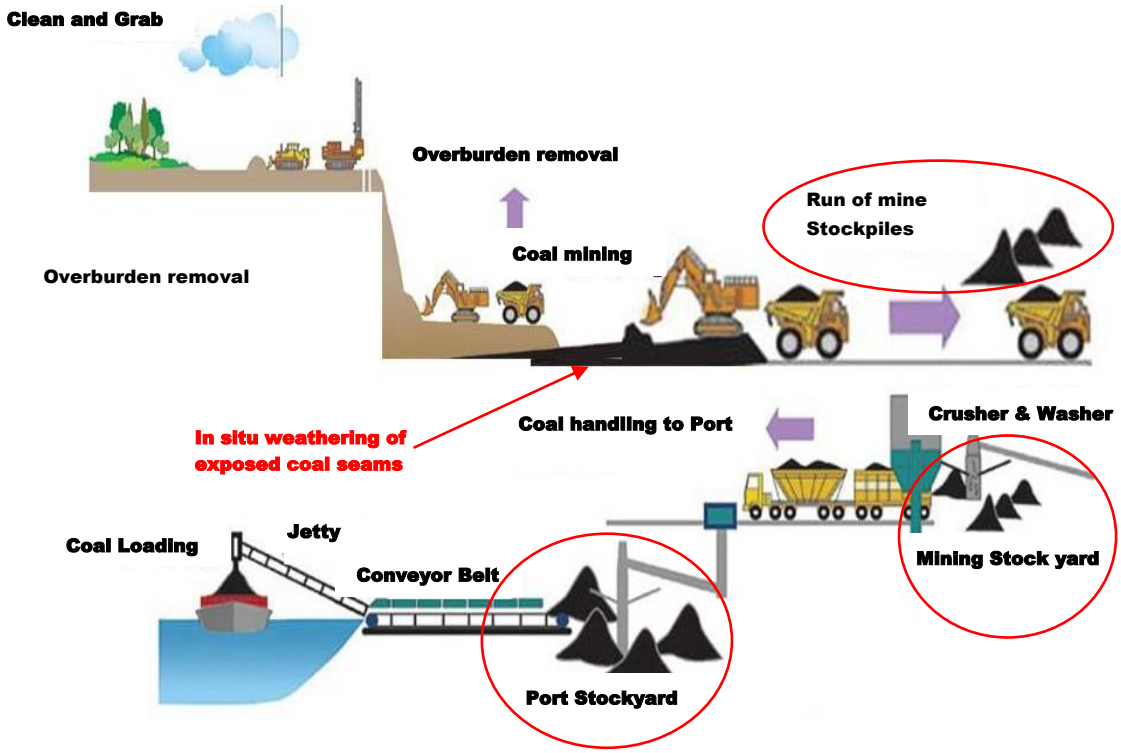


Figure 1. Generalized mining operation showing points (circled in red) at which coal is likely to undergo weathering (Modified after Mangkusubroto, 2010).

The weathering process not only affects exposed coal outcrops, but also coal that is stockpiled. When coal weathers, the initial coal quality changes such that it may not necessarily correspond to the final coal quality received by the end user (Schmidt *et al*., 1936; Marchioni, 1983; Bend *et al*., 1989; Pisupati *et al*., 1993; Ekmann and Le, 2004; Falcon, 2014). Weathered coals pose a risk to the environment because the exothermic heat released during oxidation raises the temperature of the coal (self-heating), and conditions allowing, may cause a fire hazard if the coal to combusts spontaneously (Falcon, 1986; Carras and Young, 1994; Pone *et al*., 2007; Avila *et al*., 2014). Moreover, sulfuric acids released from the oxidised coal can be leached into the ground, causing ground water contamination. The direct economic implication of coal weathering is the reduction in the profitability of mining operations, because weathered outcrops are omitted from resource and reserve estimations. Furthermore, money is forfeited when coal weathers and can no longer be used for its intended purpose (Marchioni, 1983; Thomas, 2012; Aphane and Vermeulen, 2015).

Of particular interest is the impact of weathering on coking and thermal coals. These coals generate significant revenue from both local and export sales, not only in South Africa, but across all global coal producing economies (Baruya, 2014). South Africa's local coal market consumes 70% of all South African coal mined annually, generating a revenue of 56.6 billion Rand in 2015 (Prévost, 2017). Despite the economic challenges facing the South African mining industry in the last five years, coal has competitively remained as the top revenue contributor relative to gold, iron ore, platinum group metals (PGMs) and other metals (PWC, 2017).

South Africa`s northern coalfields (Figure 2), namely the Waterberg, Soutpansberg and Limpopo (Tuli) are unique in that, they host vitrinite-rich coal which differ from the inertinite-rich coals of the central coalfields (Witbank, Highveld and Ermelo) (Snyman, 1998). In the next 20 years, it will become necessary to source more coal from the northern coalfields to meet the growing energy demands of the country, which will no longer be met due to the declining production in the central coalfields (Prévost, 2017). However, a great deal of financial investment will be required to successfully exploit the coal resources of the northern coalfields, which are hosted in complex geological settings. The infrastructure required to prepare the coal for utilization includes more efficient and dry based beneficiation techniques to improve the lower coal grades. Furthermore, an interlinked railway network is necessary to transport the coal from the northern coalfields to the port of Richards Bay coal terminal (Jeffery, 2005; Hancox and Götz, 2014; Prévost, 2017).

The present study is a continuation of an Honours research project titled, "The effects of weathering on coal quality in the Limpopo (Tuli) and Soutpansberg Coalfields (Sebola, 2015)". The aim of the Honours research project was to assess the effect of weathering on stockpiled coals from the Limpopo and Soutpansberg Coalfields. The stockpiles had been stored outdoors for up to two years in the Limpopo Coalfield and five years in the Soutpansberg Coalfield, specifically in the Makhado portion

of the greater Soutpansberg Coalfield. Hence, it was anticipated that the coals had undergone oxidative weathering during the respective periods of outdoor storage. One stockpile was sampled from the Limpopo Coalfield and consisted of coal particles about ±20 mm in size, whereas two stockpiles were sampled from the Makhado Coalfield, namely a run of mine (ROM) stockpile and a processed stockpile also consisting of particles ± 20 mm.

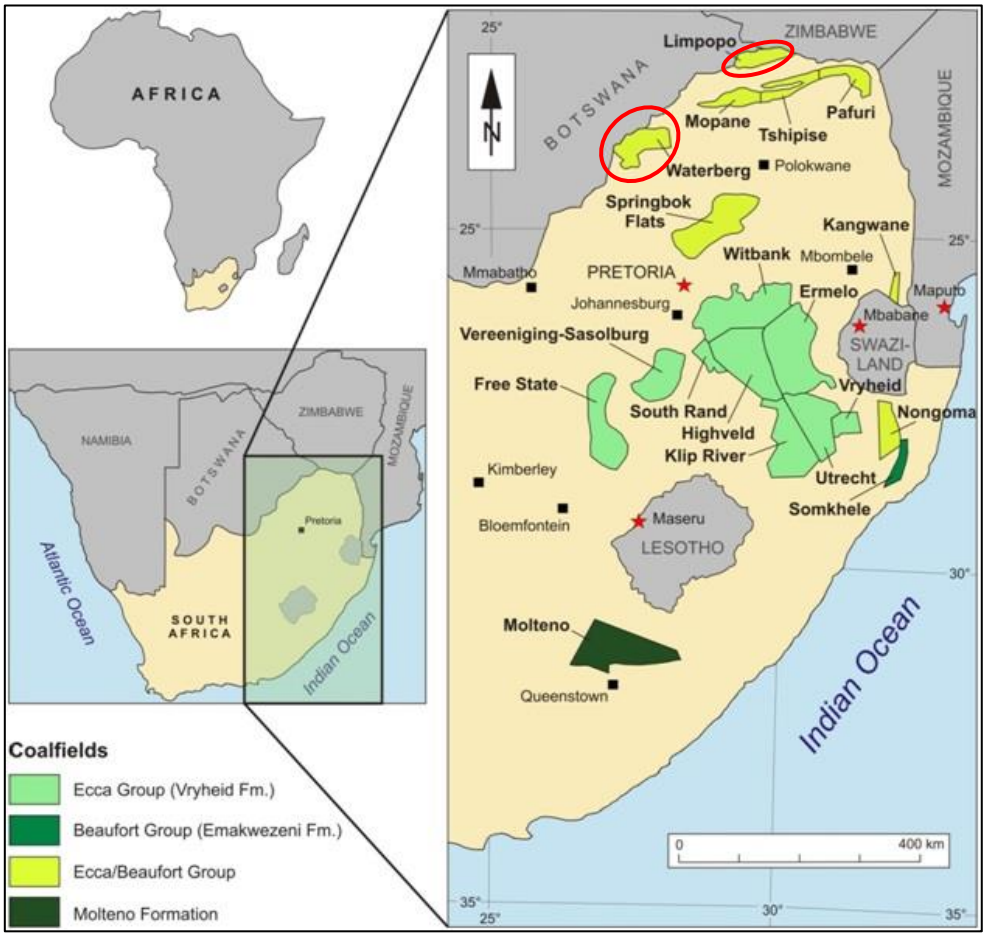


Figure 2. The locations (circled in red) of the Waterberg and Limpopo Coalfields in South Africa (Hancox and Götz, 2014).

Sampling of the stockpiles involved collecting particles from the outermost layer (± 5 cm) and comparing it to material from deeper within the stockpile, which was considered to be fresher compared to the outermost layer that had been directly exposed to the weather elements. The coals were studied using routine coal analyses including proximate analysis, ultimate analysis, free swelling index, calorific value, and petrography. The climatic conditions in the Limpopo and Soutpansberg Coalfields are classified as semi-arid where extreme temperatures greater than 35°C can occur during the summer months. The mean annual rainfall in the Soutpansberg Coalfield varies between 500-800 mm and is higher compared to the Limpopo Coalfield, which receives a mean annual rainfall of only 300 mm (Mpandeli, 2014).

Although some evidence of weathering (Table 1) was detected in the outer layers relative to the fresher inner layers, the extent to which the coals had weathered could be not be constrained relative to a fresh parent coal, which was unfortunately unavailable at the time the study was conducted. Moreover, the various signs of weathering could not be constrained to a particular time from the onset of weathering. It therefore became pertinent to characterize the early stages of coal weathering relative to a fresh parent coal in order to constrain the period in which the various changes occur in coal. This was necessary in order to predict when the technological properties of coal from the northern coalfields would be adversely affected by weathering such that they were no longer suitable for their intended use.

Table 1. Observed signs of weathering due to oxidation in a previous study (Sebola, 2015).

Location	**Duration of exposure to weathering**	**Evidence of weathering relative to inner stockpile for respective stockpiles**
Limpopo Coalfield	Outer layer: 2-year-old stockpile (± 20 mm particles)	Lower calorific value
Soutpansberg Coalfield	Outer layer of 5-year-old ROM stockpile	Lower total carbon and fixed carbon, lower ash, oxygen content, calorific value and free swelling index, fewer fresh macerals, more prevalent cracks of macerals, change in colour on macerals, more altered minerals
	Outer layer of 5-year-old stockpile (± 20 mm particles)	Lower fixed carbon and total carbon, higher ash, volatile matter, oxygen content, lower calorific value, zero free swelling index, higher vitrinite reflectance, change in colour on macerals.

1.2 Progress of coal weathering research in South Africa

Globally, the literature on coal weathering studies dates back to over 150 years ago, covering coals of various ranks and the consequent implications for industry end use (Hamilton; 1907; White, 1909; Schmidt *et al*., 1936; Roy, 1965; Cox and Nelson, 1984; Gethner, 1985; Goodarzi, 1987; Wu *et al*., 1988; Komraus *et al*., 1990; Clemens *et al*., 1990; Bend, and Kosloski, 1993; Martínez and Escobar, 1995; Ndaji and Thomas, 1995; Sarikaya, 1995; Ibarra and Miranda, 1996; Taraba, 1996; Wang *et al*., 2002; Alverez *et al*., 2003; Cimadevilla *et al*., 2005; Sen *et al*., 2009; Baris *et al*., 2012; Miroshnichenko *et al*, 2012a; Ulanovskii, 2012; Butakova *et al*., 2013; Kleshnya *et al*., 2013; Xia and Yang, 2014; Zhang *et al*., 2016; Kus *et al.*, 2017). From these studies it is evident that the vast majority of weathering studies have been conducted on American coals, especially coal from the Illinois and Pennsylvanian

Coalfields (Parr and Hamilton, 1908; Schmidt *et al*., 1936; Jackman *et al*., 1957; Yohe, 1958; Rees *et al*., 1961; Gray *et al*., 1976; Lowenhaupt and Gray, 1980; Malony *et al*., 1982; Teo *et al*., 1982; Liotta *et al*., 1983; Marchioni, 1983; Huffman *et al*., 1985; Ingram and Rimstidt, 1984; Isaacs and Liotta, 1987; Wu *et al*., 1988; Garcia *et al*., 1991; Pisupati *et al.*, 1993; Lo and Cardott, 1995). In stark contrast, fewer weathering studies exist for South African coals (Mendelsohn, 1933; Bird, 1951; Hill, 1986; Itay *et al*., 1989; Wagner, 1999, 2007, 2008; Waanders *et al*., 2003; Mangena and du Cann, 2007; Akinyemi *et al*., 2011). South African coals formed from different plant types and developed under different climatic, and geologic conditions than coal from the northern hemisphere (Falcon and Snyman, 1986; Falcon and Ham, 1988; Kershaw and Taylor, 1992; Cadle *et al*., 1993; Faure, 1996; Cairncross, 2001; Bordy and Catuneanu ,2001; Catuneanu *et al*., 2005).

Coal weathering studies have gradually evolved from merely characterising the macroscopic and sub-microscopic effects of oxidation on coal quality and implications on technological properties, to focusing on constraining the reaction sequence of oxidation and related kinetics at a molecular level as well as delineating the behaviour of functional groups during progressive weathering (Chang and Berner 1998; Wang *et al*., 2003a, b; Sen *et al*., 2009 Miroshnichenko *et al*., 2012a, b). Coal weathering studies can be broadly divided into two main classes namely 1) laboratory-based studies that have specifically dealt with weathering related to spontaneous combustion phenomena; and 2) those that observe and characterise weathering effects on coal and subsequent impacts on utilisation. The present study focuses on the latter because no previous studies have characterized the weathering behaviour of South African coals using fresh parent samples, specifically those from the Waterberg and Limpopo Coalfields. Therefore, a detailed analysis of the chemistry, mineralogy, petrography and technological properties of the coal in response to weathering would provide much needed insight that would be a benefit from a scientific point of view as well as for the coal industry.

Understandably, the available published research on coal weathering in South Africa is focused in the central coalfields (Witbank, Highveld and Ermelo) owing to their economic prominence. Mendelsohn (1933) used routine proximate and ultimate analysis to prove that coal originating from the Witbank and Ermelo Coalfields had undergone oxidation due to poor storage conditions during shipping to London. Bird (1951) investigated the physical weathering of coal in terms of friability and slackening characteristics of coal from the Main Karoo Basin. Wagner (1999) developed a petrographic analysis to identify and quantify weathering features in coals, and subsequently characterised weathered discard stockpiles in the Witbank Coalfield (Wagner, 2007, 2008). de Korte (2001) provides a review on coal weathering with reference to the potential re-mining of weathered pillar coals in the Witbank and Highveld Coalfields. Currently, the importance of characterizing weathered coal is gaining traction in the central coalfields due to the abundance of discarded coal material that has the potential to be reclaimed mainly for electricity generation (Belaid *et al*., 2013). In the future, the characterization of weathered coal will be an important research avenue in the northern coalfields as they are likely to

become the hub of mining in the near future as production dwindles in the central coalfields (Jeffrey, 2005; Prévost, 2017). Furthermore, the diversity of South African coals in the various coalfields necessitates site specific analysis. Hence, the current research aims to contribute to the body of knowledge by documenting the effects of oxidative weathering particularly on coals from the Waterberg and Limpopo Coalfields.

Waanders *et al.* (2003) used Mössbauer spectroscopy to delineate iron minerals in weathered coal from the Witbank Coalfield. Mangena and du Cann (2007) found that weathered pillar coal from the Witbank Coalfield had poor agglomeration properties compared to fresh coal from the Waterberg and Soutpansberg Coalfields. Akinyemi *et al.* (2011) characterised the mineralogy of weathered coal fly ash from an undisclosed power station in the central coalfields. In contrast, fewer oxidation studies exist for coals in the northern coalfields of South Africa, namely the Waterberg, Soutpansberg and Limpopo Coalfields. Itay *et al*. (1989) conducted a kinetic study to investigate the oxidation rate of coal related to spontaneous combustion using fresh middling's coal from Grootegeluk Mine however, detailed chemistry and petrography were not evaluated. Hill (1986) also utilized middling's coal from Grootegeluk Mine to investigate the effect of particle size and moisture on the low temperature oxidation of coal, albeit neither detailed chemistry nor petrography was evaluated. This research aims to address the deficit in the literature by investigating the detailed chemistry and petrography of weathered coals in the northern coalfields.

1.3 Problem statement, Aim and Objectives

Given the importance of the coal industry to South Africa's economy, it is quite surprising that, so few publications exist on the weathering of South African coals, especially since it has been established that weathering due to oxidation has a deleterious effect on coal quality. Moreover, the extent to which freshly mined or exposed coal seams from the Waterberg and Limpopo Coalfields will undergo weathering is poorly understood and requires site specific analysis.

Therefore, the aim of this research was to observe and characterize alteration in the coal particles from the Waterberg and Limpopo Coalfields from the onset of exposure to oxidative weathering.

The **main objectives** of the research are listed together with the *key questions* addressed in the study:

Objective 1: Allow weathering of fresh coal from the Waterberg and Limpopo Coalfields by exposing them to the same atmospheric conditions over a duration of 6 months.

The key question posed in relation to this objective was:

i. *Are the coals more susceptible to weathering under wet or dry conditions when subjected to the same atmospheric conditions?*

Objective 2: Observe the changes that the organic and inorganic coal constituents underwent in response to weathering, relative to a known "fresh" baseline coal quality.

The key questions posed in relation to this objective were:

ii. *Are there quantifiable changes in the organic constituents of the weathered coal relative to the fresh parent samples?*

iii. *Are there quantifiable changes in the inorganic constituents (minerals) of the weathered coal relative to the fresh parent samples?*

Objective 3: Compare the quality changes due to weathering between coalfields using coal from the Waterberg and Limpopo Coalfields.

The key question posed in relation to this objective was:

iv. *Which coals exhibits significant changes in coal quality due to weathering?*

Objective 4: Track, over time, how the changes in the coal constituents affect the future utilization potential of the coals in terms of heating (calorific value and thermogravimetry) and swelling propensity (free swelling index).

The key questions posed in relation to this objective were:

v. *Are the changes in the heating properties as determined by the CV and TGA, likely to negatively affect the performance in a boiler?*

vi. *Are the changes the in the swelling of the coal as determined by the FSI, likely to negatively affect the conversion of the coal into coke?*

The thesis is organized as follows:

Chapter 1: The motivation and background information prompting the study is presented along with the problem statement, aim and objectives.

Chapter 2: The composition of coal is described, as well as the localities and geological history of the northern coals relative to coals of the Main Karoo Basin.

Chapter 3: Relevant literature on coal weathering is discussed.

Chapter 4: The techniques that were followed to collect, prepare and analyse the coals are presented.

Chapter 5: The findings of the research are presented and discussed in relation to similar literature.

Chapter 6: A summary of the body of work and recommendations are made to address the objectives the study.

Chapter 2: Coal geology

This chapter provides a description of the origin of coal and its constituents, including the environment in which the coal forms within the geological context of South Africa. Emphasis is placed on the deposition of the Karoo Supergroup which hosts all South African coals distributed across several basins in the country. The geology of the coal bearing strata in the Waterberg and Limpopo Coalfields are described in relation to the Karoo Supergroup.

2.1 Coal as a sedimentary rock

Sedimentary rocks consisting of a mass and volume exceeding 50% and 70% respectively of carbonaceous material, are referred to as coal (Snyman, 1998). The carbonaceous material is derived from the accumulation of plant matter where disturbance by sedimentation is minimal (Teichmüller, 1989; Thomas, 2012). Factors such as climatic conditions, tectonic activity, plant communities and geochemical parameters prevailing during the time of plant accumulation all contribute to the formation of coal from the initial stages of peatification through to coalification (Falcon and Ham, 1988; Taylor *et al*., 1998; Cairncross, 2001; Malvadkar *et al*., 2004; O'Keefe *et al*., 2013). The characteristics of the resultant coal are determined by the processes alluded to above, which vary in different geological settings and lead to the diversity and unique properties observed in coals throughout the world (Falcon and Ham, 1988; Teichmüller, 1989; Snyman and Botha, 1993). Table 2 provides a summary of the differences between coals from Gondwana and Laurasia.

Table 2. Contrast between coals from Gondwana and Laurasia (Falcon and Ham, 1988; Teichmüller, 1989; Kershaw and Taylor, 1992; Taylor et al., 1998; Malvadkar et al., 2004).

Properties	Gondwana coal	Laurasian coal
Geographic location	Southern hemisphere: South America, Southern Africa, Australia and India.	Northern hemisphere: North America and Europe (including the United Kingdom and Russia).
Age	Deposited during Permian (~280-250 Ma) with fewer deposited in the Triassic (~227-257 Ma).	Deposited during Carboniferous period (~350-290 Ma).
Climate during deposition	Progressive shift in climate from glacial, shallow marine, fluvial to aeolian.	Hot and humid coastal swamps and tropical forests.
Burial depth	Subjected to relatively shallow burial depth therefore, coal seams are less matured, horizontal and easier to mine.	Subjected to great burial depth therefore, coal seams are more matured, inclined and difficult to mine.
Coal rank	Variation in rank due to pockets of intrusions.	More consistent rank due to regional geothermal gradient at greater depth.

Vegetation	Sub-arctic to cold-cool-temperate deciduous forests, to warm savannah like woodlands with reed-infested swamps.	Giant water-loving sub-tropical equatorial types of lycopod horsetails and fleshy-barked trees, with abundant ferns.
Coal seams	Thinner coal seams due to shifting climatic conditions.	Thicker and more developed coal seams due to continuous plant growth under more stable climatic conditions.
Petrographic composition	Inertinite-rich in the main coal bearing basin; vitrinite-rich in subsidiary coal bearing basins.	Vitrinite-rich with low mineral matter.

2.2 Coal forming processes and classification

Coal forms when a substantial amount of various plant materials are rapidly buried and undergo biological, chemical and physical transformation under the influence of geothermal gradients (Figure 3). The initial stages of coal formation involve peatification whereby the deposited plant material is converted into peat by chemical reactions coupled with microbial activity in mildly oxidising to reducing environments (Teichmüller, 1989; Taylor *et al*., 1998; O'Keefe *et al*., 2013). During the peat stage of coal formation, the various plant organs undergo morphological changes to their cell structure, namely the destruction or preservation of cell tissues. Whether the tissues of the various plant organs are preserved or destroyed depends on the oxidising conditions and the processes of decomposition affecting the plant material. Fusinitization and vitrinitization/gelification are the major processes of decomposition controlling the preservation of plant organs in a peat swamp. Fusinitization is the process that forms fusinite and semifusinite macerals and occurs when plant material is preserved in aerobic conditions that cause the plant material to oxidize varying degrees, often leading to the drying out of cell walls or charring in extreme cases. The processes of vitrinitization/gelification occur in anaerobic conditions where the cell structure of plant organs is covered by the secretion of gel-like substances (humic acids), resulting in a gelified homogenous structure. Plant material that is subjected to sub-aerobic conditions in which both fusinitization and vitrinitization/gelification occur, gives rise to reactive semifusinites, a maceral with properties that are transitional between the inertinite and vitrinite maceral groups (Falcon and Snyman, 1986; Teichmüller, 1989; Taylor *et al.*, 1998). During coalification, the burial depth and temperature conditions to which the peat is exposed to cause a change in its chemistry and physical structure (Taylor *et al*., 1998). The chemical changes include the enrichment of elemental carbon whilst hydrogen and oxygen decrease (Malvadkar *et al*., 2004). Physical changes such as the decrease in the coals porosity and the alignment of structural units occur during coalification (Taylor *el al*., 1998). Outside of the coal forming environment, external factors affecting the quality of coal are largely attributed to intrusive bodies (dykes and sills) which cause

devolatilization (loss of volatile matter) or in extreme conditions, burns out the coal completely such that only ash remains (Snyman and Barclay, 1989).

Coal is classified according to its grade, type and rank (Figure 3). The amount of mineral matter in coal determines its grade, whereas coal type is defined by the plant material making up the coal (Gray, 1982; Snyman, 1989; O'Keefe *et al*., 2013). Coal rank describes the maturity of coal and is determined by the temperature and pressure conditions to which the plant material is exposed through geologic time, ranging from lignite to sub-bituminous, bituminous and anthracite, with anthracite being the most mature coal rank characterised by a more highly ordered carbon network (Lett and Ruppel, 2004). Lower rank coals (e.g. lignite) are more susceptible to weathering than coals of higher rank such as anthracite. The coals in this study are medium-rank bituminous C (Kaji *et al*., 1985).

The properties of coal make it a versatile fuel suitable for use in combustion, pyrolysis and coking, gasification and liquefaction (Nowak *et al*., 2004).

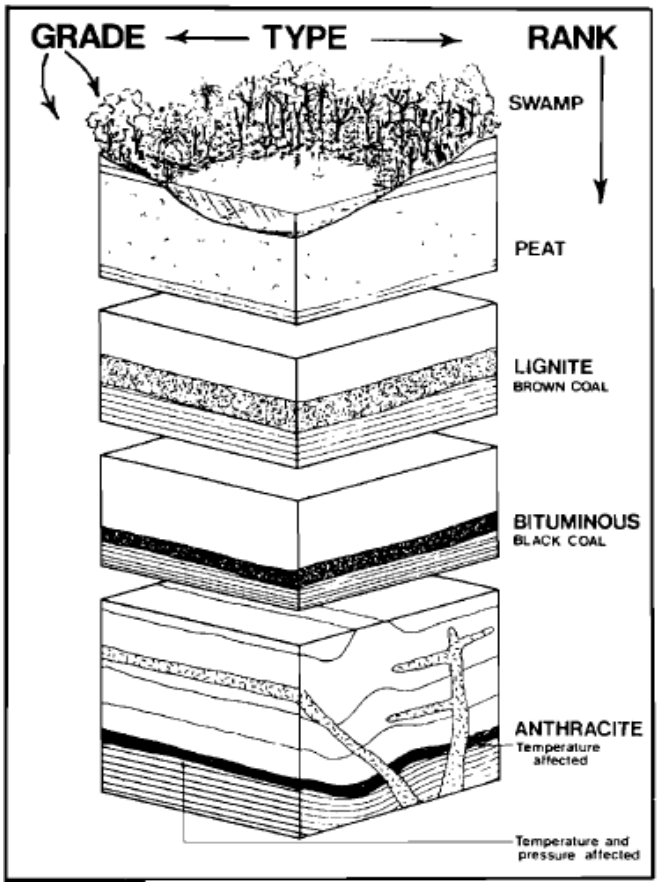


Figure 3. Deposition of coal into the peat swamp followed by an increase in rank with increasing temperature and burial pressure over time, including the subsequent effects of dykes and sills (Falcon and Snyman, 1986).

2.3 The composition of coal

The preserved plant matter, together with mineral matter, make coal a highly heterogenous rock consisting of organic and inorganic constituents which are non-crystalline or crystalline (Vassilev and Vassileva, 1996). Macerals predominantly make up the organic component of coal and are derived from preserved plant material. Minerals make up the inorganic fraction of coal and are derived from various sources such as dissolved salts within the plant material itself, minerals precipitated in the peat swamp or sourced from the influx of sediment during peatification (Falcon and Ham, 1988; Malvadkar *et al*., 2004; O'Keefe *et al*., 2013). Fluid phases, fluid inclusions and gases are also common coal constituents, the latter being vital for the potential extraction of coal bed methane (Vassilev and Vassileva, 1996).

2.3.1 Organic coal constituents: Macerals

Macerals are defined as discrete organic coal constituents that can be arranged into three principal maceral groups namely: vitrinite, liptinite and inertinite (Falcon and Snyman, 1986). Each of these maceral groups are further sub-divided into maceral sub-groups based on the degree of preservation or destruction of the plant material when they are deposited into the peat swamp (Teichmüller, 1989). Individual macerals are therefore distinguished on the basis of their morphology, reflectance level, and/or the degree of gelification (gel-like precipitates/secretions from plant material that can be of chemical or biological origin) during the peatification stage of coal formation (Scott, 2002). Petrographically, macerals are distinguished based on their colour (in reflected and transmitted light), fluorescence, relief and size (Falcon and Snyman, 1986). The classification described herein (Table 3) follows the nomenclature prescribed by the International Committee for Coal and Organic Petrology (ICCP).

For the purpose of the technological applications of coal, the terms “reactive” and “inert” are used to describe the relative ease at which macerals will combust (Falcon and Ham, 1988). Reactive macerals are those that ignite at low temperatures and usually show signs of softening (plasticity) and degassing during carbonization and combustion (Marchioni, 1983), whereas, inert macerals require higher temperatures to combust, burn out slower and have little or no plastic properties (Falcon and Snyman, 1986). Generally, the vitrinite (excluding pseudovitrinite) and liptinite macerals constitute the reactive portion of a coal blend. With the exception of semi-fusinite which is semi-reactive due to its transitional properties, all other inertinite macerals make up the inert portion of coal blends (Thomas, 2012).

Table 3. Maceral classification according to the International Committee for Coal and Organic Petrology (ICCP, 1998; 2001; Pickel et al., 2017).

Maceral Group	Maceral sub-group	Individual Maceral
Vitrinite	Telovitrinite (cell walls)	Telinite
		Collotelinite
	Gelovitrinite (chemical/biological precipitates or secretions)	Corpogelinite
		Gelinite
	Detrovitrinite (detritus)	Vitrodetrinite
		Collodetrinite
Inertinite		Fusinite
		Semifusinite
		Funginite
		Secretinite
		Macrinite
		Micrinite
		Inertodetrinite
Liptinite		Cutinite
		Sporinite
		Algnite
		Resinite
		Liptodetrinite
		Suberinite
		Exsudatinite

2.3.1.1 The vitrinite maceral group

Vitrinite macerals represent preserved cell walls of woody plant material such as branches, twigs, and roots (Falcon and Snyman, 1986; Taylor *et al*., 1998). These woody plant organs were rapidly deposited into the peat swamp, limiting primary oxidation during peatification. It is perhaps for this reason that the effects of oxidative weathering (described in the established literature) are generally limited to vitrinite macerals, because they are only subjected to intense oxidising conditions post coalification (Scott, 2002). The carbon content in vitrinite has been proven to increase consistently with increasing rank, which translates to an increase in the reflectance of vitrinite with increasing rank, when observed microscopically under oil immersion (Taylor *et al*., 1998). Hence, vitrinite is used universally to measure the reflectance levels of coals for the determination of coal rank (Gray *et al*., 1976; Teichmüller, 1989; ICCP, 1998). It is important to note that low rank coals such as lignite (brown coal) and sub-bituminous coal, primarily consist of huminite macerals which are the low rank equivalent of the vitrinite maceral group. Unlike vitrinite, huminite is less mature because it has not undergone

homogenization through the process of geochemical gelification and as such, huminites are the precursors to the vitrinite group macerals (ICCP, 1994; Sýkorová *et al*., 2005; Thomas, 2012).

The vitrinite maceral group is subdivided into telovitrinite, detrovitrinite and gelovitrinite (Table 3). Telinite and collotelinite constitute the telovitrinite sub-group, in which the cell walls of woody plant tissues are either easily identifiable (telinite) or appear homogenous (collotelinite) because they have been extensively covered by gels during peatification and therefore require etching to expose the cell walls (Teichmüller, 1989; Taylor *et al*., 1998). Collotelinite is the most commonly occurring vitrinite maceral in coals worldwide and is used routinely for reflectance measurements due to its smooth and homogenous surface compared to other macerals of the vitrinite group. Telinite is not common in southern African coals (Falcon and Snyman, 1986). The detrovitrinite sub-group consists of vitrinite fragments that occur in isolation (vitrodetrinite) or vitrinite fragments that act as a glue, cementing other macerals (collodetrinite). The gelovitrinite sub-group consists of corpogelinite and gelinite. Corpogelinite are gels that constitute the infillings of cell lumens, especially in telinite, whereas gelinite represents secondary infillings that occur within cleats or microfissures (ICCP, 1998).

Psuedovitrinite is an abnormal vitrinite maceral because it is characterized by a distinctly higher reflectance and relief compared to the other vitrinite macerals and is also characterized by serrations and comma slits on its surface (ICCP, 1998). Furthermore, cell structure may or may not be apparent in pseudovitrinite macerals (Gray, 1982; O'Keefe *et al*., 2013). The origin of pseudovitrinite is still not fully understood. However, it has been suggested that pseudovitrinite is formed as a result of oxidation of the woody cell wall tissues during peatification (Falcon and Snyman, 1986: Kruszewska, 2003). Alternatively, Kaegi (1985) in Taylor *et al*. (1998) propose that pseudovitrinite is intermediate between fresh and weathered vitrinite. The works of Kaegi (1981) and Kaegi *et al*. (1988) in Taylor *et al*. (1998) have noted that comma slits on collotelinite are more common in fresh coals in opencast operations compared to fresh coal from underground coal mines. The thermoplastic properties of pseudovitrinite are lower compared to telinite and collotelinite, thus the presence of pseudovitrinite in coking coals has a negative influence on the burden of the furnace (Crelling, 2008).

2.3.1.2 The liptinite maceral group

The liptinite macerals are derived from hydrogen-rich plant organs, including algae and bacteria, or are the by-products of the decomposition of plants caused by microbial activity (Taylor *et al*., 1998; Pickel *et al*., 2017). Liptinites characteristically exhibit lower reflectance and a higher fluorescence intensity compared to the vitrinite and inertinite maceral groups. Hence, fluorescence microscopy is employed in their identification during routine petrographic analysis (McHugh *et al*., 1991). Liptinite, however, generally constitutes up to 5% in South African coals (Snyman 1989; Kruszewska, 2003).

Cutinite macerals are cuticles that originate either from plants or animals (Scott, 2002; Pickel *et al*., 2017). This maceral is not common in southern African coals. The outer cell walls of spores and pollen grains are the precursors of the sporinite maceral (Teichmüller, 1989). Like cutinite, sporinite macerals are also uncommon in southern African coals because they are prone to biological attack in dry/arid conditions, which prevailed during the latter period of the Ecca Group (Falcon and Snyman, 1986; Johnson *et al*., 2006). Alginite originates from the preservation of individual or colonies of unicellular algae that occur either as discrete elliptical or disc shaped bodies (telalginite), or as lamellae referred to as lamalginite (Pickel *et al*., 2017). The resinite maceral originates from the secretion of resins, balsam, waxes, fats and oils from plant cell walls (Teichmüller, 1989). Resinite commonly occurs in voids such as cavities, microfissures or as droplet shapes. The liptodetrinite maceral incorporates all the small particles of the liptinite maceral group that are not clearly identifiable because they have been reduced in size by mechanical or biochemical degradation, i.e. detrital liptinite macerals (Falcon and Snyman, 1986). Suberinite is derived from suberized cell walls of cork tissue and is further described as "a succession of more or less rectangular, brick-like, or irregularly polygonal 4–6 sided cells" (Pickel *et al*., 2017, p. 40). Exsudatinite is a rare liptinite maceral of secondary origin that forms when hydrogen-rich substances, such as liptinite, expel residue into empty spaces in the coal (Teichmüller, 1989).

2.3.1.3 The inertinite maceral group

As the name suggests, the inertinite macerals are less reactive on combustion compared to the vitrinite and liptinite macerals. Moreover, inertinites have the highest carbon content ranging from 77% to 96% and are distinctly higher reflecting than the other maceral groups (Teichmüller, 1989). According to the ICCP (2001), inertinites exhibit the greatest diversity in terms of their origin and are categorically subdivided into macerals that have plant cell structures (fusinite, semifusinite, and funginite), macerals lacking plant cell wall structures (secretinite, macrinite and micrinite), and fragmented inertinites (inertodetrinite) (Taylor *et al*., 1998; Hower *et al*., 2009). The diversity of the inertinite macerals leaves room for different mechanisms of origin including aerial oxidation, desiccation, fungal activity and charring by fires prior to peatification (Teichmüller, 1989; ICCP, 2001; Scott, 2002; Hower *et al*., 2009). In the case of the inertinites of the Witbank Coalfield, A Nuclear Magnetic Resonance study by Moroeng *et al*. (2018) have found evidence that suggests that these inertinites formed by wild fires and not merely by oxidation, as is widely accepted in the South African context (Falcon and Snyman, 1986; Snyman, 1989). The reader is referred to the publication of Moroeng *et al*. (2018) for more insight into the findings.

Fusinites are highly reflecting and well-preserved cell structures of either parenchyma, sclerenchyma or collenchyma. Semifusinites are macerals that have distinctly intermediate properties between telinite and fusinite macerals within a coal and are derived from the parenchyma and xylem tissues of stems, herbaceous plants and leaves (Falcon and Snyman, 1986). The degree of fusinitization determines

whether the resultant semifusinite is reactive or inert (Falcon and Snyman, 1986; Falcon and Ham, 1988; Snyman, 1989). Funginite represents well preserved cell wall structures that are strictly derived from single or multicellular fungi such as spores, sclerotia and mycelia and occur in various forms including rounded, spindle shaped and tabular (ICCP, 2001). Secretinite represents macerals that are low to highly reflecting, non-cellular and occur as round, vesicular or elongate forms. Macrinite occurs as a highly reflecting amorphous matrix or as discrete inertinite particles displaying no cellular structure. Micrinite is a secondary inertinite maceral, representing very small (<2 microns) aggregates of granular inertinite materials that are derived from the conversion of bituminite into oil (Teichmüller, 1989; Hower *et al*., 2009). Inertodetrinite is of detrital origin, comprising discrete particles of inertinite macerals that are less than 10 microns in size. These particles do not show any cell structure (ICCP, 2001).

2.3.2 Inorganic coal constituents: Mineral matter

Unlike other rocks types, minerals are not the primary constituents in coal, but occur in smaller proportions relative to the organic constituents described in the preceding sections.

The common minerals found in coal worldwide include pyrite, quartz, kaolinite, illite, plagioclase, potassium-feldspar, gypsum, calcite, dolomite, ankerite and siderite (Vassilev and Vassileva, 1996). Minerals are either of intrinsic or extrinsic origin, the former describing minerals that occur within the plants themselves, whereas extrinsic minerals are either introduced into the coal during peatification (washed in, windblown or precipitates) and are referred to as syngenetic minerals. Minerals are of epigenetic origin if they have been introduced into coal during coalification, filling empty voids such as cracks and fissures (Falcon and Snyman, 1986; Taylor *et al*., 1998; Matjie *et al*., 2011).

For technological purposes mineral matter in coal is unwanted as it has been proven to have a deleterious effect on utilisation in terms of emission of pollutants, wear and tear of equipment and lowering operating efficiency (Martinez and Escobar, 1995; Ward, 2002). Furthermore, the presence of mineral matter in coal necessitates processes to separate the mineral matter from the macerals through beneficiation, which is often costly and water intensive. Intrinsic minerals are the most difficult to liberate because they are intimately associated with the valuable organic matter (Falcon and Snyman, 1986). South African coals are typically mineral matter-rich (low grade) and require beneficiation before they can be utilized.

2.4 Overview of the Karoo Supergroup in South Africa

The bulk of South African coals were deposited during the Permian and are hosted in the stratigraphic sequence of the Karoo Supergroup (Catuneanu *et al*., 2005). The Karoo Supergroup was deposited between 300-180 Ma in an extensive retroarc foreland basin referred to as the Main Karoo Basin (MKB) (Catuneanu *et al*., 2002). This basin covers an area of 300 000 km^2 in South Africa and developed in response to compressional tectonics (Smith *et al*., 1993). Figure 4 illustrates the extent of the Karoo deposits across South Africa. Several smaller but geologically related intracratonic basins exist north of the MKB but are characterised by extensional tectonics (Cairncross, 2001; Hancox and Götz, 2014). The Waterberg and Limpopo (Tuli) Coalfields are amongst these subsidiary basins which are essentially located on the back bulge of the MKB (Catuneanu *et al*., 2005). The Waterberg Coalfield developed in the Ellisras Basin whereas the Limpopo Coalfield developed in the Tuli Basin and is sometimes referred to as the Tuli Coalfield (Hancox and Götz, 2014).

The lithostratigraphic units of the Karoo Supergroup consist, from the oldest to the youngest, of the Dwyka Group, Ecca Group, Beaufort Group, Stormberg Group and Lebombo Group. The progression of climate change is evident from the glacial to shallow marine, deltaic to fluvial and finally aeolian type deposits that are characteristic of the Karoo sedimentary sequence (Falcon and Ham, 1988; Catuneanu *et al*., 2002). Deposition of the Dwyka Group began in the late Carboniferous (290 Ma) as a result of glacial melts producing glacial to fluvio-glacial deposits which include diamictities, tillites, dropstones, and conglomerates (Smith *et al*., 1993). This was followed by the deposition of coal associated with organic-rich mudstones, siltstone and sandstone in a shallow marine and pro-delta environment, giving rise to the Ecca Group which is subdivided into the Pietermaritzburg Formation, Vryheid Formation and Volksrust Formation (Cadle *et al*., 1993). Coal deposits of economic importance only occur in the two latter formations.

The Beaufort Group deposits are largely due to meandering rivers that had merged from the deltaic systems of the Ecca period. From the base, the Beaufort Group is subdivided into the Adelaide and Tarkastad sub-groups which consist mainly of sandstone and mudstones (Hancox and Götz, 2014). These are overlain by the Stormberg Group, comprising the Molteno Formation, Elliot Formation and Clarens Formation, which were deposited in semi-arid to arid conditions. The end of Karoo sedimentation is marked by the eruption of the Lebombo Group lavas at ~187 Ma, of which the Drakensberg Mountains is a type locality (Snyman and Barclay, 1989). These voluminous flood basalts have intruded the Karoo strata as dykes and sills and are associated with the breakup of Gondwana (Cadle *et al*., 1993). The lithostratigraphic units of the MKB described above have been correlated to those in the subsidiary basins of South Africa, including the southern and central coalfields of Africa.

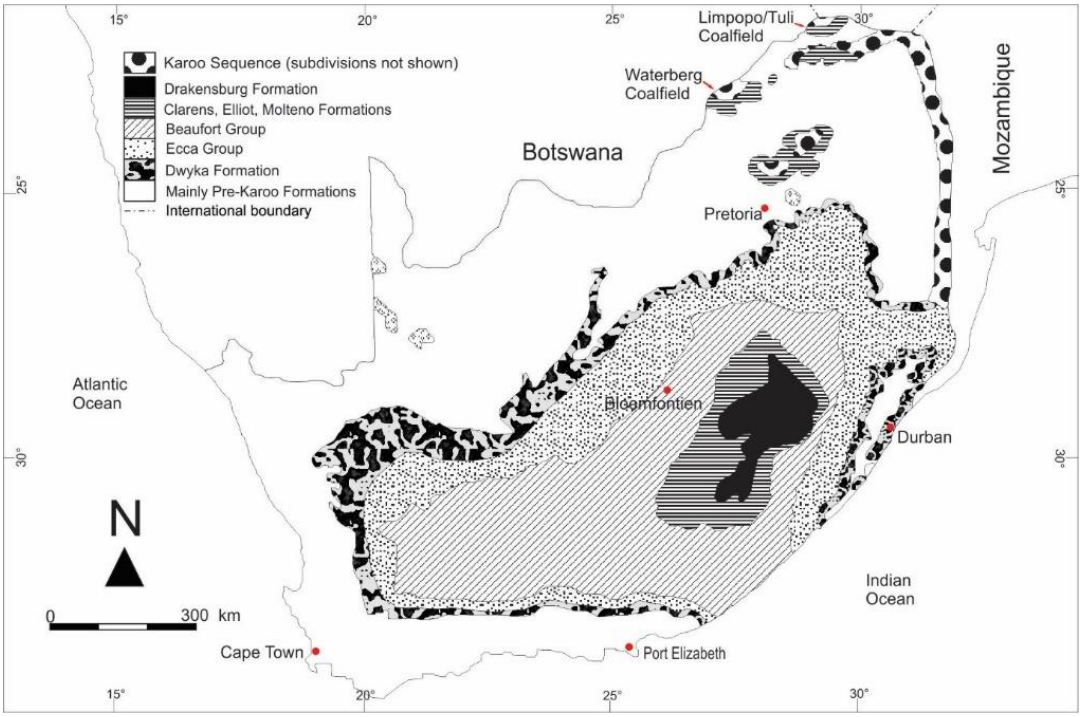


Figure 4. The extent of the Karoo Basin in South Africa (modified after Snyman and Barclay, 1989

2.5 Overview of coalfields in South Africa

A tentative correlation between the stratigraphic units of the MKB, Ellisras Basin (Waterberg Coalfield) and the Tuli Basin (Limpopo Coalfield) is presented in Figure 5.

A total of 19 coalfields exist across the Karoo sequence in South Africa, of which the Witbank, Highveld Ermelo and KwaZulu-Natal Coalfields are the most exploited and geologically understood compared to the northern coalfields (Hancox and Götz, 2014). Coal quality across the coalfields of South Africa is generally characterised by an eastward increase in rank and vitrinite content, whereas the ash content tends to increase westwards (Snyman and Barclay, 1989; Cadle *et al*., 1993). Glossopteris flora gave rise to the coal in the Ecca Group, whereas the Triassic coal of the Molteno Formation was derived mainly from Dicroidium flora and are hosted in the Beaufort Group (Smith *et al*., 1993; Johnson *et al*., 2006; Bamford, 2004). Coals in the MKB are distinctly rich in inertinite, whereas, vitrinite is the major maceral group found in the coals of the northern subsidiary basin, with lesser amounts of inertinite and especially liptinite (Faure *et al*., 1996).

Although the northern coalfields of South Africa have significant coal reserves and are indeed the future of the coal mining industry of the country, challenges such as structural complexities, gaps in the geological knowledge, poor transport infrastructure coupled with the need for more efficient deep mining technology and dry beneficiation techniques, have resulted in the northern coalfields being less exploited (Jeffrey, 2005; Fourie *et al*., 2014).

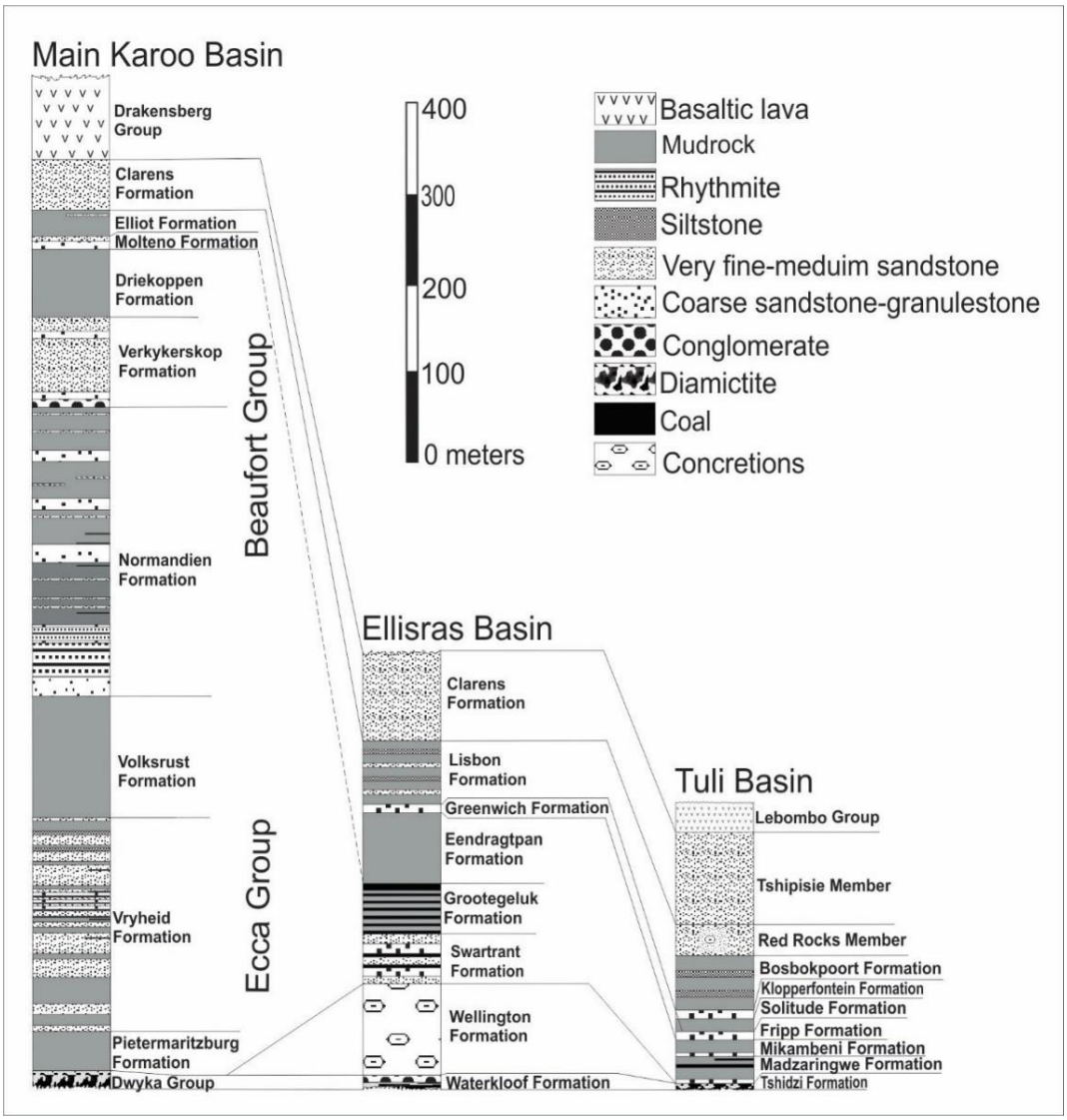


Figure 5. Tentative correlation of stratigraphic units in the Main Karoo Basin, Ellisras Basin and Tuli Basin (modified after Johnson et al., 2006).

2.6 The Waterberg Coalfield

The Waterberg Coalfield is located in the north-western margin of the Limpopo Province and occurs within the Ellisras Basin (Figure 6), which is the South African portion of the larger Kalahari Basin in neighbouring Botswana (Faure *et al*., 1996). The Ellisras Basin covers an area of approximately 3600 km^2 and is confined the by three major faults: the Zoetfontein, Daarby and Eenzaamheid faults, which exert structural control in the basin (Jeffrey, 2005; Fourie *et al*., 2014; Hancox and Götz, 2014). Coal seams in the region have been partitioned into near surface deposits and more deeply buried seams by the Daarby Fault, with the deeply buried coal attracting numerous prospectors for coal bed methane (CBM). The shallower deposits are currently exploited by Exxaro at their Grootegeluk Mine, producing a range of coal products including thermal and metallurgical coal, that are supplied to local and export markets (Fourie *et al*., 2014). Grootegeluk has a total measured coal resource of 4 719Mt (Exxaro, 2018).

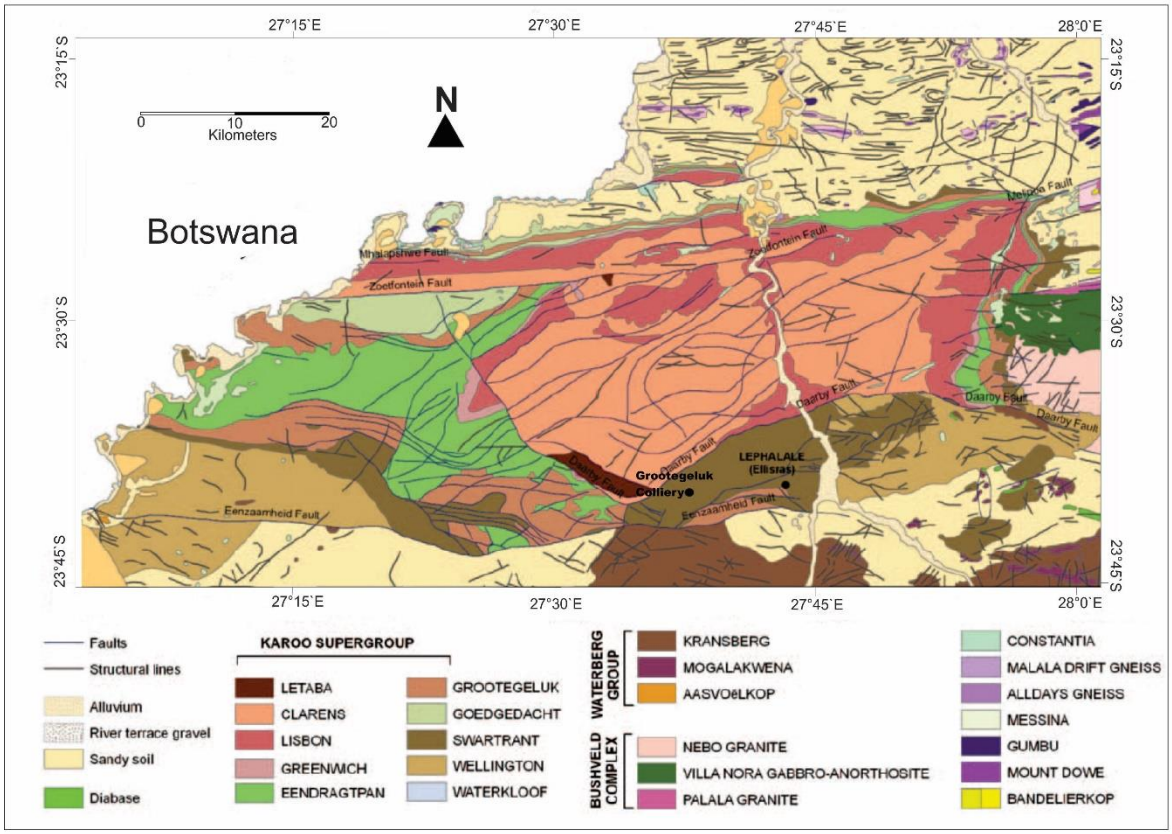


Figure 6. Geology of the Waterberg Coalfield (modified after Fourie et al., 2014).

Similar to the Limpopo Coalfield, the Waterberg Coalfield developed as an intracratonic rift during the late Permian (Cairncross, 2001). This tectonic setting yielded floodplain deposits analogous to those of the MKB. However, the Karoo package in the Waterberg is predominately characterised by carbonaceous mudstones interbedded with coal seams (Smith *et al*., 1993; Snyman and Botha, 1993).

Therefore, the deposits of the Waterberg Coalfield are not to be confused with the Proterozoic rocks of the Waterberg Group nor the Waterberg Basin in Namibia (Johnson *et al*., 2006).

The Waterkloof and Wellington Formations are the lowermost units of the Karoo sequence in the Ellisras Basin and the equivalent of the Dwyka Group in the MKB. The contact between these units with the basement varies laterally such that in the south of the Ellisras Basin, they unconformably overlie the sediments of the Waterberg Group, meta-sediments of the Limpopo Mobile Belt (LMB), Bushveld lavas in the north-eastern margin, and meta-sediments of the LMB in the northern margin (Fourie *et al*., 2014). Above the sequences of the Waterkloof and Wellington Formations, are units corresponding to the Ecca Group in the MKB, namely the Swartrant, Goedgedacht and Grootegeluk Formations. The siltstones and sandstones of the Swartrant Formation, which overlie the Waterkloof and Wellington Formations, are equivalents of the Pietermaritzburg Formation in the MKB.

Eleven economic coal seams are distributed between the Goedgedacht Formation (Vryheid Formation equivalent in the MKB) and Grootegeluk Formation (Volksrust Formation equivalent in the MKB). Of these the Grootegeluk Formation is the principal economic target due to the presence of more well developed (brighter) and thicker coal seams which are interbedded with sandstone and shale, attaining a maximum thickness of 90 m (Faure *et al*., 1996). The Goedgedacht Formation consists of 55 m of coarse sandstones and carbonaceous mudstones interbedded with coal seams of varying thicknesses. The alternating lithologies in the Goedgedacht and Grootegeluk Formations contribute to the high ash content which ranges between 21-62.9 %, necessitating rigorous beneficiation.

Coal deposition in the Waterberg Basin occurred in flood plain settings in which coal in the Goedgedacht Formation was deposited further from the sediment source, in low energy conditions (Botha and Snyman, 1993). Coals in the Goedgedacht Formation are inertinite-rich, for example Wagner and Tlotleng (2012) reported that coal in Bench 11 consisted of 74.7 vol% inertinite. The overlying coal seams of the Grootegeluk Formation are characterized by a high proportion of vitrinite macerals of up to 90 vol% (Faure *et al*., 1996; Hancox and Götz, 2014). These vitrinite rich coals suggest deposition in a low energy environment.

2.7 The Limpopo (Tuli) Coalfield

The Limpopo Coalfield is located at the border between Botswana, South Africa and Zimbabwe and covers an area of 1150 km^2 in South Africa (Figure 7). The coalfield extends into Botswana and Zimbabwe where it is referred to as the Tuli Coalfield or Tuli Basin (Snyman, 1998; Bordy and Catuneanu, 2001).

Coal was discovered in the region well over a century ago, yet it is only recently that detailed geological investigations have been undertaken. The mining company Coal of Africa Limited (CoAL) is the first to attempt to exploit coal resources as of 2011 (De Jager, 1986; Ortlepp, 1986; Snyman, 1998; CoAL, 2016). A total resource of 362.5Mt mineable tonnes in situ (MTIS) has been reported for CoAL`s Vele Colliery which is expected to produce middling's coal, semi-soft coking coal, and thermal coal of export quality (CoAL, 2016). Unlike the Waterberg Coalfield, the South African Committee for Stratigraphy (SACS) have not yet formalised the stratigraphic nomenclature for the Tuli Coalfield. Hence, for the purpose of this research, the nomenclature prescribed by CoAL (2016) at their Vele Colliery is used herein.

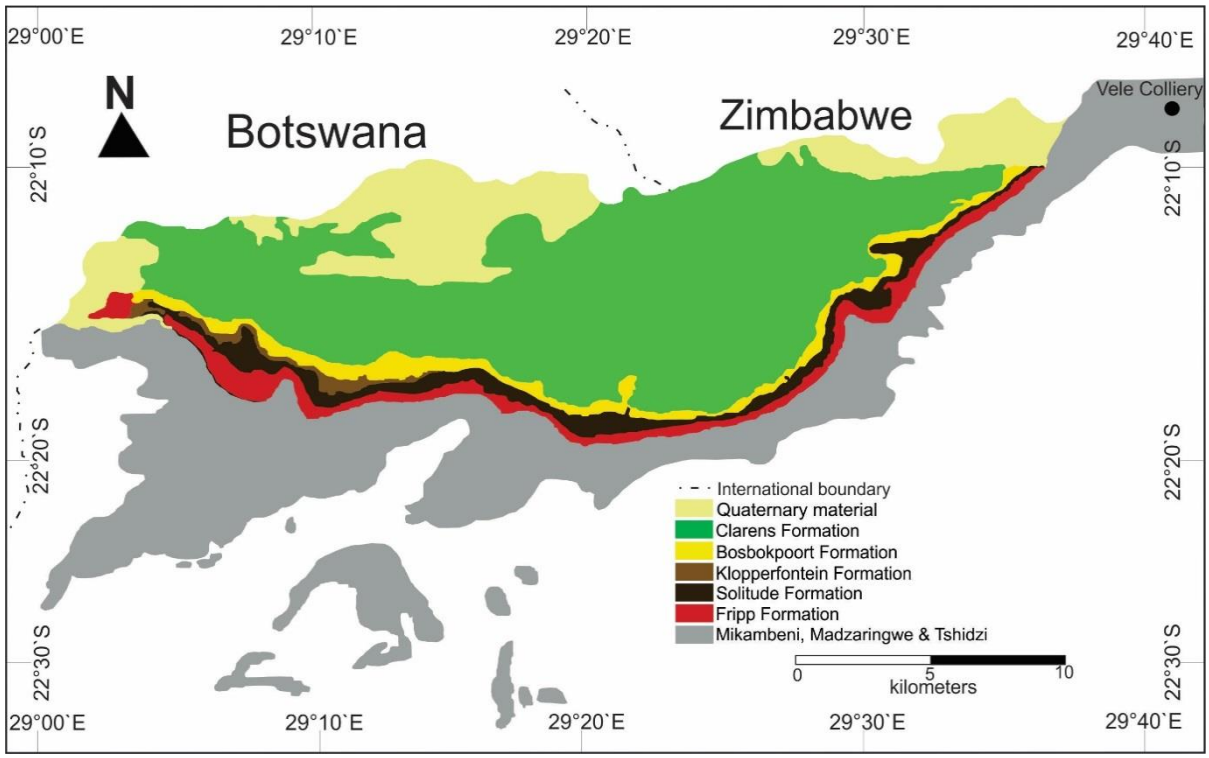


Figure 7. The location of Vele Colliery (top right) on the Geological map of the Limpopo Coalfield (modified after Malaza, 2013).

The Limpopo Mobile Belt (LMB) makes up the pre-Karoo basement on which the diamictites of the Tshidzi Formation are deposited (Bordy and Catuneanu, 2001). These are overlain by the Madzaringwe Formation which is the equivalent of the Ecca Group in the MKB, and consists of siltstone, fine sandstone and economic coal seams. Literature on the depositional environment of coal in the Limpopo Coalfield is sparse. However, the lithologies of the Madzaringwe Formation indicate that coal deposition occurred in a fluvial system, where coal was deposited on the flood plains of meandering rivers (Malaza, 2013).

CoAL (2016) have defined a 15 m thick coal bearing horizon in the Madzaringwe Formation consisting of 6 coal seams: Upper Seam, Middle Seam, Middle Lower Seam, Bottom Upper Seam, Bottom Middle

Seam and Bottom Lower Seam. The Top and Bottom seams are subdivided into Top Lower, Top Middle, Top Upper, Bottom Lower and Bottom Upper units (Hancox and Götz, 2014). Coals from Vele Colliery are generally characterised by an inherent moisture content below 3%, ash content less than 10%, volatile matter between 20-30%, total sulphur less than 1,5% and a free swelling index of 8-9 (Sparrow *et al*., 2013).

Compared to the Waterberg Coalfield where dykes of the Lebombo Group are infrequent, a number of east-west trending dykes have been detected in the Tuli area, causing some devolatilization of nearby seams (Cairncross, 2001; CoAL, 2016). Moreover, Sparrow *et al*. (2013) found that the coking properties of coal located near major fault zones at Vele Colliery were adversely affected because of the hot intrusive fluids that travelled along the fault zones and devolatilized the coal, resulting in a poor coal quality. In other coalfields, such as the Kwazulu Natal Coalfields, it has been reported that the quality of the coal in close proximity to intrusions have been "upgraded" by the heat (Falcon and Ham, 1988; Cadle *et al*., 1993; Cairncross, 2001).

.

Chapter 3: Coal oxidation and weathering

The weathering of coal through the process of oxidation is explained herein, with a discussion on the impact on coal quality in terms of its constituents and subsequent viability for utilization. An overview of the various techniques used to detect weathered coal is also provided.

3.1 Oxidative weathering of coal

Oxidation is recognised as the major chemical process degrading the quality of coal during weathering, expressed by Equation 1 (Marchioni, 1983; Cox and Nelson, 1984; Martinez and Escobar, 1995; ICCP, 2001; Shi *et al*., 2005; Pone *et al*., 2007; Avila *et al*., 2014). There are many reactions involved in the natural oxidation of coal, but it has been widely accepted that it occurs at low temperatures below 100°C and is marked by four principal stages namely: chemisorption, the formation of transitory peroxides, thermal decomposition and the formation of inert humic acids (Itay *et al*., 1989; Martinez and Escobar, 1995; Wang *et al*., 2003b).

$$\textbf{coal oxidation} = \textbf{coal} + \textbf{oxygen} \leftrightarrow \textbf{absorbed oxygen} \rightarrow \textbf{oxycoal} \rightarrow \textbf{CO}, \textbf{CO}_2 \textbf{and } \textbf{H}_2\textbf{O} \qquad \textbf{[Equation 1]}$$

The initial stage of oxidation occurs when oxygen is absorbed through pores on the coal surface (chemisorption), followed by the formation of transitory peroxides (Itay *et al*., 1989; Wang *et al*., 2003b). Due to the nature of the weak single bond, inherent to the peroxide group, they undergo thermal decomposition in which heat and gases (CO, CO_2 and H_2O) are released, and more stable functional groups are formed, viz. carbonyl, carboxylic and phenolic groups (Wang *et al*., 2002; Wang, *et al*., 2003a, b; Avilla *et al*., 2014; Smędowski and Piechaczek, 2016). The final stage of oxidation is characterised by the formation of inert humic acids by the decomposition of the stable functional groups (Garcia *et al*., 1991; Wang *et al*., 2002; Wang *et al*., 2003a). Hence, oxidative coal weathering can be considered as a source of greenhouse gas emissions and contributes to the global carbon cycle (Chang and Berner, 1998; Shi *et al*., 2005, Zhang *et al*., 2016). Although described sequentially, these reactions occur simultaneously and interact with each other during oxidation (Alvarez *et al*., 1998: Cimadevilla *et al*., 2005). In as much as the kinetic steps of coal oxidation are virtually the same for all coals, the response of the coal differs as a function of its composition (Itay *et al*., 1989; Miroshnichenko *et al*., 2012a). The oxidation reaction is generally exponential during the initial stages, progressing until a threshold is reached (Yohe, 1958; Copard *et al*., 2004). If subsequent oxidation events occur at the same temperature, the rate of oxygen adsorption will be minimal and the changes in the chemical and physical structure of the coal will not be as pronounced (Hill, 1986; Pone *et a*l., 2007). However, if oxidation occurs at higher temperatures than preceding oxidation events, new active sites will form on the coal surfaces and allow for further oxidation (Carras and Young, 1994; Pone *et a*l., 2007).

At a molecular level, coal consists of aromatic and aliphatic compounds (Roberts, 1991). Aromaticity, denoted f_a, refers to, "the ratio of carbon atoms that are present in the aromatic rings to those present in aliphatic side chains", within the microstructure of coal (Li *et al*., 2005, p.7178). During the coal forming process, all macerals naturally become more highly reflecting as the aromatic fraction of the coal increases with increasing temperature and pressure conditions (rank advance), resulting in a more highly ordered (i.e. more aromatic) coal (Taylor *et al*., 1998; Gupta, 2007). When coal weathers, the process of oxidation results in a decrease in the aliphatic component, whilst the aromaticity increases (Marchioni, 1983; McHugh *et al*., 1991; Ndaji and Thomas, 1995; Mondragón *et al*., 2002).

In addition to the inherent coal properties, several variables must be taken into consideration during coal oxidation; these may be categorically grouped into internal and external factors (Misz-Kennan and Fabiańska, 2011). Internal factors include the composition and physical properties of coal, the weathering history of the coal, and particle size. External factors include temperature, partial pressure of O_2, and moisture content in the gas medium (Baris *et al*., 2012; Kus *et al.*, 2017). Of these, temperature and coal rank exert the greatest control on the rate of oxidation (Ingram and Rimstidt, 1984). Therefore, it is important that these factors be considered when conducting coal weathering studies. Following this approach for the present study, the inherent properties of the fresh parent coals were analysed prior to weathering to ensure that weathering features were characterized relative a known standard. Furthermore, the temperature conditions affecting the coals were monitored during the study.

Two modes of coal weathering are recognised, namely primary and secondary weathering. Primary weathering of coal occurs while the coal is still in the ground and has not yet been exploited for anthropogenic use, whereas secondary weathering occurs once the coal has been extracted from the ground. Primary weathering occurs *in situ* and may be as a result of high rates of ground water infiltration or when the seam is exposed to varying atmospheric conditions at surface by geological activity or human activity such as tectonic uplift, construction or mine blasting etc. (Taylor *et al*., 1998; Chang and Berner, 1998; Cimadevilla *et al*., 2003; Kus *et al.*, 2017). It should also be noted that primary weathering may also occur during the peat forming stages of coal formation.

Usually the effects of secondary weathering on the quality of the coal are more pronounced than those that occur during primary weathering because the particle size of the coal is reduced after beneficiation, allowing for a faster rate of reaction due to the enhanced surface area (Hamilton, 1907; Taraba, 1996). Understanding the nature of weathered coal involves comparison of a fresh sample relative to its weathered counterpart. For example, weathered coals are known to be marked by elevated oxygen contents, but oxygen is also a major constituent in fresh coals that have not been weathered hence,

knowledge of the initial oxygen content is necessary to ascertain if oxidation has indeed occurred (Marchioni, 1983).

Thus far, the research presented above deals with secondary weathering occurring under natural circumstances which involves several variables. However, scientists have also employed artificial or laboratory oxidation to better understand weathering (Calemma *et al*., 1995; Kus *et al.*, 2017). Natural weathering of coal initiates at low temperatures between ~ 30°-100°C whereas laboratory-based studies may induce oxidation at temperatures as high as 600°C (Ingram and Rimstidt, 1984; Komraus *et al*., 1990; Taylor *et al*., 1998). Consequently, these laboratory studies have been criticised for the use of unrealistic parameters (including exaggerated temperatures and treatment agents) that are not representative of natural oxidation (Chang and Berner, 1998; Casal *et al*., 2003; Gethner; Wu *et al*., 1988; Alvarez *et al*., 2003; Sen *et al*., 2009). It is also evident that laboratory induced studies also inherently lack the influence of micro-organisms, which accelerate the chemical and physical weathering processes during coal oxidation (Marchioni, 1983; Garcia *et al*., 1991; Chang and Berner, 1998; Gethner, 1986; Wu *et al*., 1988; Alvarez *et al*., 2003; Casal *et al*., 2003; Cimadevilla *et al*., 2005). Furthermore, artificial oxidation is a "dry" process in which the effects of moisture is omitted (Marchioni, 1983; Chang and Berner, 1998). For the purpose of this study, artificial oxidation is not considered further.

3.2 Weathering during stockpiling

The life-cycle of coal from the time it is mined may include: processing (beneficiation), transportation and utilisation. In-between these stages, coal is often stored in silos or outdoor stockpiles for some time in which secondary weathering can occur (Rees *et al*., 1961; Marchioni, 1983; Taylor *et al*., 1998; Ekmann and Le, 2004; Falcon, 2014; Vega *et al*., 2017). Figure 8 illustrates how outdoor stockpiles are vulnerable to excess oxygen, wind dispersion, varying temperature and moisture conditions. During primary weathering of *in situ* coal, the coal closest to the surface is oxidised. In stockpiles, the outermost layer weathers significantly compared to the inner contents of the stockpile, which are not directly exposed to atmospheric processes and therefore remain relatively unaffected by weathering. Compacted stockpiles are less affected by weathering because air flow is limited, and the build-up of heat is reduced (Giroux *et al*., 2006; Misz-Kennan and Fabiańska, 2011; Wang and Zhou, 2012). These findings agree with the results of a preceding investigation on stockpiled coal from the Limpopo and Soutpansberg Coalfields (Sebola, 2015). Unless care is taken during this storage period, the quality of the coal could significantly depreciate relative to its initial quality, making it unsuitable for its intended purpose (Gethner, 1985; Banerjee *et al*., 2000; Wagner, 2008).

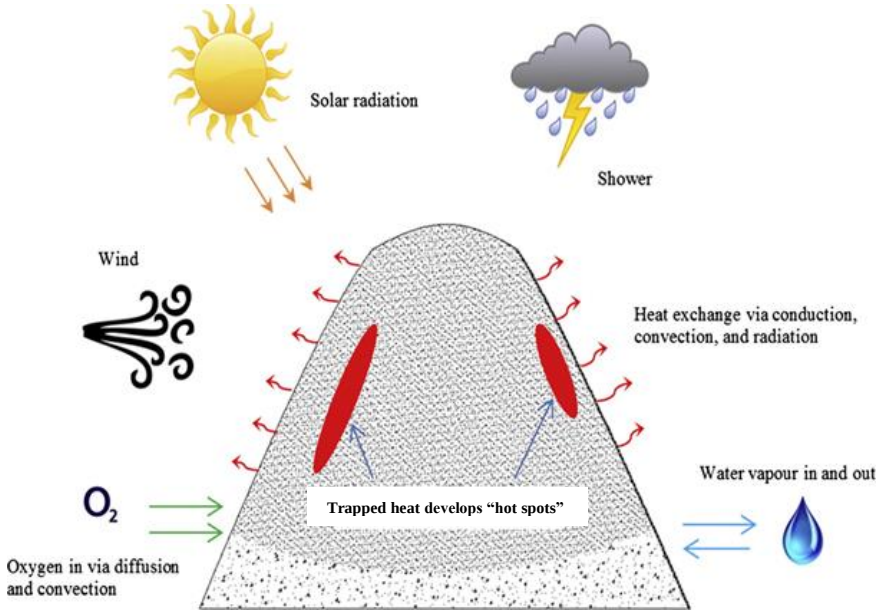


Figure 8. Meteorological parameters driving weathering of a coal stockpile (modified after Zhang et al., 2016).

In order to avoid substantial deterioration in the quality of all Russian coals, storage is restricted to a maximum duration of 60 days in summer and up to 90 days in winter (Miroshnichenko *et al*., 2012a). Jackman *et al*. (1957) determined that the metallurgical coals from Illinois should only be stored for a limited time of 30 days in summer and 6 months in winter. In reality, it is unlikely that coal can strictly be stored according to the recommended time limits mentioned above because of modifying factors such as mine logistics, coal markets, ease of transportation and handling conditions which may serve to either prolong or minimise the duration of storage (Kleshnya *et al*., 2013; Jha *et al*, 2014). The above-mentioned storage restrictions are site specific and may not be applicable on a global scale. This is largely because coals from various regions of the world are diverse in their characteristics. Furthermore, the climatic conditions to which they are exposed to and the particle size at which the coal is stored varies and plays a role in determining viability of the coal quality (Falcon and Ham, 1988; Malvadkar *et al*., 2004; Miroshnichenko *et al*., 2012b).

Outdoor stockpiles are cheap to maintain and easy to manage in terms of reclaiming the coal or increasing the size of the pile on demand. Hence, outdoor stockpiling is the most practiced method of coal storage throughout the global coal industry (Belaid *et al*., 2013). In cases where rigorous environmental regulations have been imposed, coal is stored in enclosed areas or containers such as silos or bunkers, which are expensive to procure and also restrict the quantity of coal that can be stored (Xia and Yang, 2014). Outdoor stockpiles should be conical in shape, with the lee side of the pile facing windward to minimise dispersion of fine particles and to reduce the amount of air infiltrating the pile which may promote oxidation of the coal (Ekmann and Le, 2004). It is also recommended that the particle size should be uniform to reduce the penetration of oxygen into the stockpile (Thomas, 2012).

In addition to compaction, the practice of wetting stockpiled coal minimises the absorption of oxygen on reactive sites because they are blocked off. Furthermore, the build-up of heat (released from the thermal decomposition of peroxides during oxidation) is reduced by the cooling effect of the water (Clement and Matheson, 1996). However, Thomas (2012) and others (Ingram and Rimstidt, 1984; Falcon, 2014) warn that stockpiles should not be watered because the additional moisture releases heat (heat of wetting) upon being absorbed into the coal structure and thereby exacerbating the oxidation reaction. If the presence of additional moisture in coal is below the critical moisture content, the rate of oxidation may be accelerated (Clemens and Matheson, 1996; Butakova *et al*., 2013).

The factors driving coal oxidation in stockpiles may eventually lead to spontaneous combustion. These factors include ambient meteorological conditions (air temperature, wind, rain, solar radiation), coal particle size, surface area exposed, shape of coal pile, coal rank, moisture content, oxygen content, mineral composition (particularly pyrite and carbonate), volatile matter, wetting, storage time, organic matter type (Falcon, 1986; Carras and Young, 1994; Giroux *et al*., 2006; Avila *et al*., 2014; Nádudvari and Fabianska, 2016). The heat released by exothermic reactions during oxidation of organic compounds, including microbial oxidation, pyrite oxidation and heat-of-wetting, causes self-heating whereby "hot spots" develop, which may subsequently trigger spontaneous combustion if the accumulated heat is not reduced through conduction and convection, as depicted in Figure 8 (Clemens and Matheson, 1996; Avila *et al*., 2014; Thomas, 2012; Zhang *et al*., 2016).

3.3 The effect of weathering on coal constituents

When exposed to weathering, the various coal constituents react differently and may affect the subsequent behaviour of the coal in various technological applications.

Although all macerals are affected by weathering, the vitrinite maceral group exhibits the most transformation due to its readily reactive nature compared to the liptinite and inertinite maceral groups (Gray *et al*., 1976; Taylor *et al*., 1998; Suárez-Ruiz and Ward, 2008; Smędowski and Piechaczek, 2016). After vitrinite, liptinite is generally the second most susceptible maceral to oxidative weathering. For example, Roy (1965) observed that the decrease in carbon and hydrogen content, yield of humic acids and weight loss due to oxidation was more pronounced in vitrinite followed by liptinite, whereas similar changes were negligible in fusinite. The following features frequently observed (microscopically) on oxidised vitrinite particles include:

oxidation rims,
micro cracks,
microfissures,
increased reflectance,
discoloration,

high relief, and
rounded edges

These features are far less common on oxidised inertinite and liptinite particles (Gray, 1982; Bend *et al*.,1989; Wagner, 2007; Kus *et al.*, 2017). Perhaps more so for liptinite, which generally occurs in very low proportions in both coals of the Southern and Northern Hemisphere (Falcon and Ham, 1988).

Oxidation rims are zones typically occurring on the edge of vitrinite macerals or along cracks and fissures. Oxidation rims can be either more highly reflecting or of lower reflectance compared to the rest of the vitrinite particle (McHugh, *et al*., 1991; Calemma *et al*., 1995). The dark or lower reflecting oxidation rims indicate that humic acids have formed at temperatures above 150°C, whereas the lighter or more highly reflecting oxidation rims are thermally induced and are common to coals that have been affected by high temperatures from intrusions, self-heating and burning (Ingram and Rimstidt, 1984; McHugh *et al*., 1991; de Korte, 2001; Wang *et al*., 2003a; Wagner, 2007; Misz-Kennan and Fabiańska, 2011; Ribeiro *et al*., 2016). The extent of an oxidation rim on a coal particle not only reflects the length of time it has undergone oxidation, but also the rate of humic acid formation in the case of dark rims, and the intensity of temperature in the case of light oxidation rims (Bend and Kosloski, 1993; Gray *et al*., 1976). The formation of humic acids on the surface of coal reduces the inherent hydrophicity of coal such that it becomes difficult to beneficiate using floatation methods (Ingram and Rimstidt, 1984; Garcia *et al*., 1991; de Korte, 2001). Moreover, the reactivity of the affected coal particle is reduced (Wagner, 2007).

Cox and Nelson (1984) suggest that microfissures on the surface of coal particles are products of physical weathering processes when coal is periodically wetted and dried. Fissures that develop as a result of weathering are distinguishable by their isolation from the natural fissures, and typically occur in a conchoidal pattern (Gray *et al*., 1976).

Vitrinite macerals may become abnormally more highly reflecting following oxidation due to exposure to higher temperatures that increase the aromaticity of the coal (Calemma *et al*., 1995). Changes in the reflectance of coal require temperatures above 150°C (Calemma *et al*., 1995). Some vitrinite particles may develop a dark discoloration due to weathering (Gray, 1982; Wagner, 2008), whilst rounded edges are a product of softening due to heating and have mainly been observed on vitrinite macerals (Misz-Kennan and Fabiańska, 2011).

Pyrite oxidation along with the oxidation of other iron bearing minerals in coal such as siderite and ankerite are the precursor for most of the mineral transformations that occur in coal during weathering (Cole *et al*., 1987; Komraus *et al*., 1990; Waanders *et al*., 2003). Pyrite, in particular, oxidises ten times faster than the macerals in coal and is responsible for most of the inorganic transformations that occur during coal oxidation (Cox and Nelson 1984; Chang and Berner, 1998; Falcon, 2014). This is in agreement with the findings of the investigation by Chandra (1966), who petrographically asserted that

macerals in bituminous coals are more resistant to weathering compared to the mineral matter in coal, and remain, at a petrographic level, relatively unaffected by weathering even after exposure to the atmosphere for up to ten years. When pyrite reacts with oxygen either from air or water, it becomes unstable and oxidises into sulphuric acid (Martinez and Escobar, 1995; Vassilev *et al*., 2010). The sulphuric acid may be neutralized by carbonate minerals in the coal or may react to form gypsum, resulting in a decrease in the carbonate content in the coal whilst the sulphate content increases (Rao and Gluskoter, 1973; Ward, 1989; Garcia *et al*., 1991; Silva *et al*., 2011). According to Ritsema and Groenenberg (1993), the formation of gypsum proceeds as follows:

$$4FeS_{2(s)} + 15O_{2(g)} + 14H_2O = 4Fe(OH)_{3(s)} + 16H^{+}_{(aq)} + 8SO_4^{2-}{}_{(aq)} \qquad \textit{[Equation 2]}$$

$$CaCO_{3(s)} + 2H^{+}_{(aq)} + SO_4^{2-}{}_{(aq)} + H_2O = CaSO_4 \cdot 2H_2O_{(s)} + CO_{2(g)} \qquad \textit{[Equation 3]}$$

Over time, the extensive weathering of pyrite may generate sulphuric acid which can be leached into the surrounding water system, resulting in acid mine drainage (Waanders *et al*., 2003; Aphane and Vermeulen, 2015; Ribeiro *et al*., 2016). The minerals anhydrite, bassinite and jarosite are also associated with the oxidation of pyrite and, to a lesser extent, iron oxide such as goethite, hematite and lepidocrocite have also been identified as alteration minerals in weathered coal owing to pyrite oxidation (Garcia *et al*., 1991; Creelman and Ward, 1996; Waanders *et al*., 2003; Sen *et al*., 2009). Unlike gypsum and jarosite, which have been observed to form during the early stages of pyrite oxidation, goethite and hematite are advanced forms of alteration minerals that develop in the late stages of pyrite oxidation (Huggins *et al*., 1983), and form at high temperatures of up to 347°C in the case of hematite (Komraus *et al*., 1990).

The alteration of clay minerals during coal weathering is primarily due to the addition of moisture in coal which may cause the clay minerals to swell, effectively increasing the volume of the coal, as well as releasing cations such as Al, Na and K which occur in trace amounts in the sulphates formed by pyrite oxidation (Gray, 1982; Huggins *et al*., 1983).

3.4 The effect of weathering on the technological properties of coal

Coal is a versatile fossil fuel that can be used for many applications such as generating electricity through combustion-driven steam turbines, producing coal derived products such as syngas and tars through gasification, and the production of coke for the metallurgical industry (Marchioni, 1983; Schobert and Song, 2002; Schweinfurth, 2009). The coal quality required for the above-mentioned applications is compromised by weathering and results in the weathered coal deviating from its predicted behaviour during utilisation, often causing damage to machinery and ultimately resulting in

end-users incurring financial deficits (Lowenhaupt and Gray, 1980; Giroux *et al*., 2006). The effect of weathering on coal constituents is reflected in the chemistry of the coal, in turn affecting its coking and heating properties. Crelling (2008, p. 174), describes coking coal as, "A coal that, when heated in the absence of air, will melt, vesiculate and harden into a sponge like mass of almost pure carbon." Weathering adversely affects coke quality such that coke stability and the coking rate decrease whereas coke reactivity and the amount of coke breeze generated increases. Moreover, the mechanical strength of the coke is weakened by the increase in the porosity of the coke (Cox and Nelson, 1984; Gray, 1982; Crelling *et al*., 1979; Cimadevilla *et al*., 2005; Miroshnichenko *et al*., 2012a).

It has been proposed that the loss of coking properties during the early stages of weathering is caused by the loss of hydrogen from the hydroaromatic sites in the coal (Yohe,1958; Mondragón *et al*., 2002; Kus *et al.*, 2017). The thermal properties of weathered coals, although reduced to some extent, may still be viable for the generation of electricity (Wagner, 2008). The loss in the heating properties of the coal due to weathering is indicated by a lower than expected calorific value relative to a fresh sample (Hamilton, 1907; Fredericks *et al*., 1983; Wu *et al*., 1988; Pisupati *et al*, 1993; Martinez and Escobar, 1995; Kruszewska and du Cann,1996). Bend *et al.* (1989) observed that the char morphology of oxidized feedstock coal is altered by oxidation such that it becomes more porous and less anisotropic, thereby decreasing the reactivity of the char. In the present study, the heating properties were studied through the calorific value and the coking properties, through the free swelling index which is discussed in the next section.

3.5 Techniques for the detection of weathered coal

A myriad of techniques ranging from chemical-based to petrographic-based techniques have been proposed for the detection of oxidized coal (Chandra, 1966; Gray, 1982; Ingram and Rimstidt, 1984; Huffman *et al*., 1985; Bend *et al*., 1989; Bend and Kosloski, 1993; Mc Hugh *et al*., 1991; Calemma *et al*., 1995; Kruszewska and du Cann, 1996; Sen *et al*., 2009; Desna and Miroshnichenko, 2011; Wagner, 2007). However, most of these techniques are not utilized beyond scientific research.

Conventional coal analysis techniques such as petrography, geochemistry (proximate and ultimate analyses) and thermal tests (thermogravimetry, free swelling index and gieseler plastometry) are the traditional tools employed to investigate coal weathering (Ingram and Rimstidt, 1984; Wu *et al*., 1988: Kruszewska and du Cann, 1996; Casal *et al*., 2003; Sen *et al*., 2009; Jha *et al*., 2015). Other techniques that have been widely used in conjunction with the conventional analyses include solvent extraction tests (Mendelsohn, 1933) and alkaline extraction tests (Lowenhaupt and Gray., 1980), floatation tests (Dey *et al*., 2013), Fourier transform infrared spectroscopy (Martínez and Escobar, 1995; Ibarra and Miranda, 1996), Mössbauer spectroscopy (Waanders *et al*., 2003), scanning electron microscopy, X-ray diffraction and X-ray fluoresce (Liotta *et al*., 1983).

(The identification of weathered coal requires techniques that are quick and easy to implement, especially at the commercial scale for mining houses and production plants (Jha *et al*., 2016). Some techniques have been found to be more useful in the detection of oxidised coal during the early stages of weathering (Wu *et al*., 1988; Jha *et al*., 2014), whereas others were more useful for extremely weathered coals (Wagner, 2007). Moreover, the selection of a suitable technique to detect weathering is also strongly dependant on the coal rank, as low rank coals are more susceptible to oxidation conditions (Kaji *et al*., 1985). Knowledge of the initial or fresh coal quality is necessary to ascertain whether oxidation has occurred and to estimate the extent to which the affected coal has deteriorated. However, this information may not always be available (Gray *et al*., 1976). Due to the heterogeneity of coal, it is best to use the various techniques in combination in order to effectively detect oxidation in coal.

Coal petrography allows for the identification of individual macerals, their interrelationships, as well as their associations with mineral matter (Bend and Kosloski, 1993; Kruszewska and du Cann, 1996). Evidence of weathering on macerals is primarily detected through petrographic observation however, unless coal has undergone significant weathering, signs of oxidation during the early stages of weathering are often poorly developed on the coal particles and require an experienced eye. Furthermore, surface features such as mineral or salt precipitates may be destroyed if not prepared for analysis soon after sampling (Chandra, 1966; Pisupati *et al.*, 1993; Desna and Miroshnichenko, 2011).

Most studies have found that routine bulk chemical analyses such as proximate and ultimate analyses are poor detectors of weathering, especially at the early stages of oxidation or if only mild oxidation has occurred. Thermal and plastic analyses such as calorific value (CV), Gieseler plastometry and free swelling index (FSI) provide for better indicators of weathering (Bend *et al*., 1981; Cox and Nelson, 1984; Wu *et al*., 1988; Casal *et al*., 2003; Vega *et al*., 2017).

The FSI is not considered a useful indicator for the detection of early stage weathering because the analysis is subjective as the swelling number is dependent on the operator comparing the resultant coke button against a standardized diagram. Furthermore, the scale used on the FSI is limited to increments of 0.5, making it difficult to accurately report variations due to weathering (Gray *et al*., 1976; Rees *et al*.,1961; Wu *et al*., 1988; Speight, 2005; Giroux *et al*., 2006; Jha *et al*., 2014). Use of the Gieseler plastometer for the early detection of oxidized coal was found to be effective. Unlike the FSI which only provides an indication of the coke strength, the Gieseler plastometer predicts the actual behaviour of the coal by measuring the initial softening temperature, maximum fluid temperature, solidification temperature and maximum fluidity of the coke (Huffman *et al*., 1985; Gray *et al*., 1976; Alvarez *et al*., 2003; Speight, 2005; Jha *et al*., 2016). In the event that Gieseler plastometery cannot be utilised, the FSI remains a relatively easy and cost-effective technique for the preliminary detection of oxidized coking coal (Gray *et al*., 1976), hence it was utilized in the present study.

An alkali extraction method was developed to detect weathering particularly in coking coals, whereby a transmission spectrophotometer is used to measure the transmittance of coal that has been prepared by boiling it in a solution of sodium hydroxide (NaOH) (Lowenhaupt and Gray, 1980; ASTM D5263-93: 2008). The alkali extraction method is limited to medium rank to high rank coals and cannot be tested on low coal because they are alkali soluble (Gray *et al*., 1976; Marchioni, 1983; ASTM D5263-93: 2008).

Chemical etching and staining of polished coal surfaces was initially used to allow for a better characterization of the vitrinite macerals, as well as to aid in the reconstruction of coal forming environments (Taylor *et al*., 1998). In the context of coal weathering, Gray *et al*. (1976) developed the petrographic staining technique to assist in the identification of weathered coal particles. The procedure involves accentuating the relief of coal components on the surface of a polished coal block by chemical etching, whereby the polished block is immersed in potassium hydroxide. The polished block is then immersed in a solution of safranin-O and ethanol; the safranin-O solution is essentially a red dye that reacts with the aromatic fraction (carboxylic acid groups) in the coal (Lim *et al.*, 1994; Taylor *et al*., 1998). As described in the preceding sections, weathered coals are more aromatic than their fresh counterparts hence, depending on the degree of oxidation, a light green stain will be produced on fresh particles of low rank coals, whereas weathered particles will have a distinctly darker green stain, especially on the particle edges (Marchioni, 1983; Wang and Zhou, 2012). No stains develop on fresh particles of high rank coals however, weathered particles in high rank coals will be marked by light green (mild weathering) to yellow (highly weathered) stains. The extent of weathering is thereafter quantified by petrographically counting the proportion of stained particles relative to those that are unaffected.

The macromolecular structure of weathered macerals in coal has been widely studied using Fourier infrared transform spectroscopy (FTIRS) where changes in the intensities of the infrared bands assigned to the different functional groups occurring in the macerals of coal are studied (Johnson and Cooney, 1983; Ndaji and Thomas, 1995; Ibarra and Miranda, 1996).

When it comes to studying oxidation of the inorganic fraction of coal, electron microscopy, Mossbauer spectroscopy and x-ray diffraction have been used to identify minerals that formed from the oxidation of pyrite and other iron bearing minerals in coal (Huggins *et al*., 1983; Cole *et al*., 1987; Komraus *et al*., 1990; Garcia *et al*., 1991; Waanders *et al*., 2003).

Chapter 4: Materials and methods

Presented in this chapter is the procedure followed during sample selection for the study as well as the various chemical, technological, mineralogy and petrographic methods of analysis that were applied to the coal in order to study the effect of natural weathering on coal particles.

4.1 Sampling and sample preparation

Fresh coal was obtained from the Grootegeluk Mine which is owned by Exxaro, as well as from Vele Colliery which is owned by Coal of Africa Limited, (CoAL). These are open cast mining operations located in the Waterberg and Limpopo Coalfields of South Africa, respectively.

At Grootegeluk Mine, four different coal zones with different qualities and characteristics were sampled, including Benches 3, 5, 9B and 11. The beneficiation process at Grootegeluk Mine operates on the basis that Benches 2, 3 and 4 are mixed to produce a semi-soft coking coal of 10% ash after beneficiation. Bench 5 coal is solely utilised for power generation (thermal coal) due to its high phosphorus content, and Benches 9B and 11 are mixed to produce a metallurgical product (Wagner and Tlotleng, 2012).

When sampling Benches 3, 5 and 9B, a shovel truck extracted approximately 60 tons of fresh coal from a section of an active working face in the pit. The fresh coal was then piled at least 5 m away from the working face, and coal samples for this investigation were handpicked. Each sample weighed approximately 30kg. At Bench 11 fresh coal was sampled from a pile of coal that had been blasted a day prior to sampling.

Due to operational constraints at Vele Colliery, only the Middle Seam could be sampled. Hand shovels were used to expose a section of the Middle Seam coal which was about 5 m away from the main pit wall. Up to 30kg of fresh Middle Seam coal was collected (Figure 9). Given the above sampling procedure and taking into account mine health and safety protocols, it should be noted that the samples collected in this research do not represent the lateral and vertical characteristics of the entire coal seams, but they are considered as representative of different coals from different coalfields. Hill (1986) also acknowledged that the lower rates of reaction observed in his study compared to a similar study by Itay (1983) may have arisen due to variations in the coal qualities since both studies had used middling's coal from the Grootegeluk Mine.

The samples were reduced to fragments of less than 50 mm, 20 mm and 5 mm, using jaw, roll and cone crushers respectively, at the crushing facility located at the University of Johannesburg (UJ) Doornfontein Campus. Replicates that were representative of each bulk sample were obtained by cone

and quartering. From the 1st replicate, the 2nd and 4th quarters were used for the baseline analyses, and the 1st and 3rd quarters were stored. Replicates 2, 3 and 4 were crushed and passed through a -1 mm sieve to ensure that the particle surfaces had maximum exposure to weathering, and to ensure that no further crushing would be necessary for petrography, electron microscopy and Raman spectroscopy. Furthermore, the particle size reduction to -1 mm aided in preventing the mixing and dilution of weathered surfaces with the fresh coal particles.

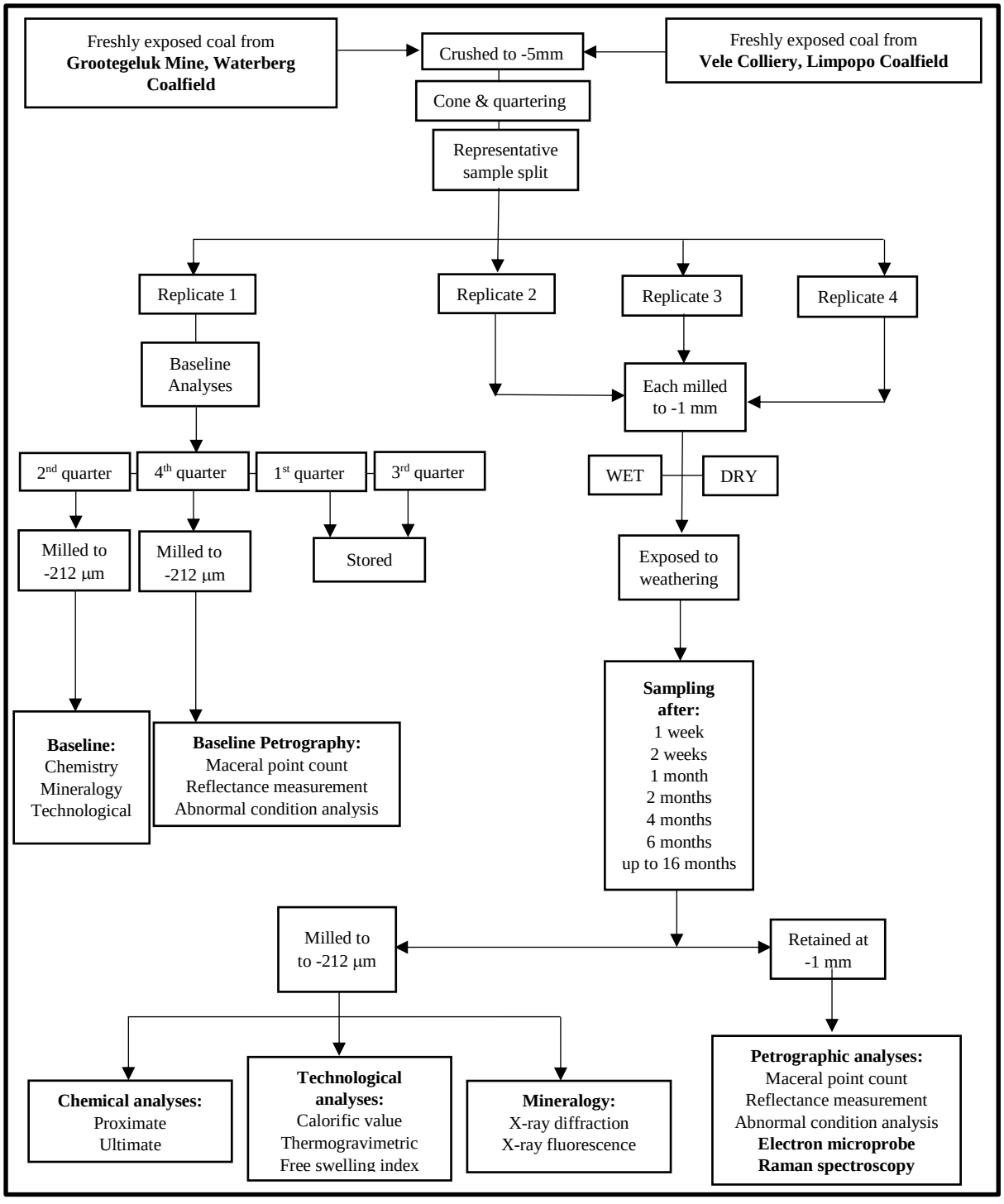


Figure 9. Flow diagram of the sampling, sample preparation and storage procedure.

The standard particle size of -1 mm was used to prepare polished coal blocks for petrographic analysis, electron microprobe analysis, and Raman spectroscopy. For all other chemical (proximate and ultimate analysis), mineralogical (x ray diffraction and x-ray diffraction) and technological analyses (calorific value, thermogravimetric and free swelling index), the -1 mm samples were milled to -212 μm. Each -1 mm sample was split into two one that would be kept dry and the second that would be watered during the weathering experiment.

The -1 mm samples were evenly laid out in clear plastic containers (23 cm x 15 cm x 5 cm) at a maximum thickness of 1.5 cm (Figure 10). All sides of the containers were perforated to allow airflow and the base of the containers was covered with weed guard to allow drainage of any moisture build-up without the loss of fine particles. Furthermore, each container was covered with a lid to prevent particle loss and cross contamination by wind dispersion, thus the effect of natural rainfall was omitted in this study. Instead, the second sample sets were frequently watered with tap water to test the influence of moisture on the weathering process. Tap water was boiled and allowed to cool down to room temperature before use. This was done to reduce the presence of solutes in the water. The biological effect of microbial degradation during natural weathering was also omitted from the study due to the nature of the experimental set up.



Figure 10. Clear plastic containers on the roof of the Bernard Price Building, University of the Witwatersrand.

Wooden pallets were used as an elevated platform on which the samples were placed to prevent waterlogging underneath the containers during rainy weather. The samples were exposed to the weather on the roof of the Bernard Price Building (University of the Witwatersrand) for a duration of six months.

The Bernard Price Building was selected as a suitable location to weather the coals because it is secluded, ensuring that the samples were not tampered with. The samples were set up on the north facing side of the building, ensuring optimum exposure to the sunshine. A weather station recording the climatic conditions was located within 3 m of the samples, ensuring that the measured climatic conditions were representative of those experienced by the samples.

The experiment was initially planned to last 6 months. However, extreme weather conditions (heavy rainfall, hail and strong winds) in the 6th month of the experiment resulted in contamination of some of the samples. For comparative purposes, a few of the contaminated samples were investigated in the 6th month and up to 16 months after sampling according to the official sampling schedule (Table 4) was concluded.

Table 4. Sample nomenclature and sampling intervals.

Dry samples	**Fresh parent sample**	**1 week**	**2 weeks**	**1 month**	**2 months**	**4 months**	**6 months**
Days	**0**	**7**	**14**	**33**	**73**	**125**	**188**
Middle seam	MS B	MS W1	MS W2	MS M1	MS M2	MS M4	MS M6
Bench 3	B3 B	B3 W1	B3 W2	B3 M1	B3 M2	B3 M4	B3 M6
Bench 5	B5 B	B5 W1	B5 W2	B5 M1	B5 M2	B5 M4	B5 M6
Bench 9B	B9 B	B9 W1	B9 W2	B9 M1	B9 M2	B9 M4	B9 M6
Bench 11	B11 B	B11 W1	B11 W2	B11 M1	B11 M2	B11 M4	B11 M6
Wet samples	**Fresh parent sample**	**1 week**	**2 weeks**	**1 month**	**2 months**	**4 months**	**6 months**
Middle seam	MSW B	MSW W1	MSW W2	MSW M1	MSW M2	MSW M4	MS WM6
Bench 3	B3W B	B3W W1	B3W W2	B3W M1	B3W M2	B3W M4	B3W M6
Bench 5	B5W B	B5W W1	B5W W2	B5W M1	B5W M2	B5W M4	B5W M6
Bench 9B	B9W B	B9W W1	B9W W2	B9W M1	B9W M2	B9W M4	B9W M6
Bench 11	B11W B	B11W W1	B11W W2	B11W M1	B11W M2	B11W M4	B11W M6

4.2 Weather Station Assemblage

The ambient meteorological conditions were monitored during the exposure period using a local weather station that was erected 3 m away from the samples. A Davis Vantage Pro2 weather station (Figure 11) was set up on the roof of the Bernard Price Building. The weather station operates using an Integrated Sensor Suite (ISS) which measures and records meteorological data. The meteorological data was remotely monitored from a wireless Vantage Pro2 Console which stores and displays the meteorological data.

The meteorological parameter that was pertinent in this study was the daily average temperature, measured in degrees Celsius (°C). Hence, the samples were placed on the north facing side of the building to ensure maximum sunlight exposure and minimal shade. The meteorological data was transferred from the Vantage Pro2 Console to a computer using a USB data logger. The complimentary WeatherLink 6.0.3 software on the computer was used to analyse the meteorological data.

Data from the South African Weather Services (SAWS) was used to supplement the data from the Davis station. The data provided by SAWS included daily maximum and minimum temperatures (°C) and this data was recorded from station 04758790, located in the Johannesburg Botanical Gardens (-26.1560 27.9990). Station 04758790 is the closest and most reliable alternative from SAWS to the Davis weather station. The temperature measurements from both weather stations were collated and averaged (Appendix A).



Figure 11. Functions of the Davis Vantage Pro2 weather station (Davis, 2016).

4.3 Chemical analyses

Proximate and ultimate analyses are routinely used to characterize coal primarily for use in industrial applications. These analyses were conducted at the coal laboratory in the Council for Geosciences, Pretoria.

4.3.1 Proximate analysis

The behaviour of coal in terms of ash, inherent moisture and volatile matter content are measured by observing the mass that is lost after heating at standardised temperatures. These variables are then easily related to the fixed carbon content by the following equation (Gupta, 2007):

$$\mathbf{C_f = 100\% - (A + M_i + Vm)} \qquad \textit{[Equation 4]}$$

Where A: ash

C_f: fixed carbon

M_i: inherent moisture

Vm: volatile matter

The analyses described below were conducted at the Council for Geosciences in Pretoria, assisted by coal laboratory scientists. Three replicates were averaged for each of the parameters and these results are recorded in Appendix B.

4.3.1.1 Fixed carbon

The fixed carbon content of coal refers to: "the solid, combustible matter left in coal after the lighter, volatile, hydrogen-rich compounds are driven off during coalification" (Schweinfurth, 2009, p. 13). It is determined indirectly by difference, i.e. the sum of the moisture, ash and volatile matter subtracted from one hundred percent (Equation 4). Since the fixed carbon content is initially reported on an air-dried (ad) basis, it is necessary to convert the value to a dry, ash free (daf) basis to ensure that a true representation of the carbon in the coal is reported without the effect of moisture and ash (mineral matter (SANS 10320:2004).

Firstly, the air-dried (ad) value must be converted to dry basis (db) as follows:

$$\mathbf{fixed\ carbon_{db}} = \left(\frac{\mathbf{fixed\ carbon_{ad}}}{\mathbf{100 - moisture_{ad}}}\right) \times \mathbf{100} \qquad \textit{[Equation 5]}$$

Thereafter the dry ash free (daf) value was obtained by:

$$\mathbf{fixed\ carbon_{daf}} = \left(\frac{\mathbf{100}}{\mathbf{100 - ash_{db}}}\right) \times \mathbf{fixed\ carbon_{db}} \qquad \textit{[Equation 6]}$$

4.3.1.2 Moisture content

The inherent moisture refers to the water that is left in the microstructure (pores and capillaries) of coal after the surficial water is dispelled by heating (Falcon and Ham, 1988).

The moisture content was determined according to SANS 5925: 2007. Samples were conditioned to the laboratory atmosphere by laying out the sample in the laboratory for at least two hours prior to the analysis. The mass of a quartz crucible and its lid (m_1) was weighed and recorded. One gram of the sample was measured into the crucible, and the combined mass of the crucible, its lid and sample (m_2)

recorded. The oven temperature was verified with an automated thermocouple to ensure the oven temperature was between 105 and 110°C. The crucibles were then loaded into an oven with their lids ajar to ensure that all the sample moisture was driven off. Three replicates were tested per sample. After two hours and thirty minutes, the crucibles were removed from the oven and tightly closed with their lids to prevent the absorption of moisture. After fifteen to thirty minutes of cooling in the laboratory atmosphere, the crucibles were re-weighed (m_3) and the moisture content was derived as follows:

$$\boldsymbol{inherent\ moisture_{ad} = \left(\frac{m_2 - m_3}{m_2 - m_1}\right) \times 100} \qquad \textit{[Equation 7]}$$

Three replicates were averaged for each sample. The maximum acceptable difference between results obtained were set to a repeatability of 0.10%. Limits for reproducibility have not been established by CGS because results obtained in different laboratories depend on the humidity conditions, which may vary from laboratory to laboratory. An average value was calculated from the replicates.

4.3.1.3 Volatile matter

According to Speight, (2005, p. 212) volatile matter refers to, "hydrogen, carbon monoxide, methane, tar, other hydrocarbons, carbon dioxide, and water obtained on thermal decomposition of coal under prescribed conditions".

The volatile content was determined as per ISO 562: 2010. As with the procedure for moisture, the samples were conditioned to the laboratory atmosphere at least two hours prior to the analysis. The mass of an empty porcelain crucible and its lid (m_1) were measured and recorded. One gram of sample was weighed into the crucible and the combined mass of the crucible, its lid and sample (m_2) recorded. The temperature of the oven was verified using an automated thermocouple to ensure that the temperature was within 900 ± 10°C. The crucibles (closed lids) were loaded into the oven for 7 minutes, after which they were removed and left to cool for fifteen to thirty minutes under laboratory conditions. The crucibles were then re-weighed and the mass recorded (m_3). The volatiles were then calculated using the following equation:

$$\boldsymbol{volatile\ matter_{ad} = \left(\frac{m_2 - m_3}{m_2 - m_1}\right) \times 100 - moisture_{ad}} \qquad \textit{[Equation 8]}$$

The air-dried (ad) value was converted to dry basis as follows:

$$\boldsymbol{volatile\ matter_{db} = \left(\frac{volatile\ matter_{ad}}{100 - moisture_{ad}}\right) \times 100} \qquad \textit{[Equation 9]}$$

Thereafter, the dry ash free (daf) value was obtained by:

$$\textbf{volatile matter}_{\textbf{daf}} = \left(\frac{\mathbf{100}}{\mathbf{100-ash_{db}}}\right) \times \textbf{volatile matter}_{\textbf{db}} \qquad \textit{[Equation 10]}$$

Three replicates were averaged for each sample and an average value was calculated from the replicates. The maximum acceptable difference between results obtained were set to a repeatability of 3% and a reproducibility of 0.5% absolute or 4% of the average result, whichever was greater.

4.3.1.4 Ash content

The residue that is left over when coal has been completely burnt is referred to as ash. The ash consists of oxides which are derived from the mineral matter in the coal (Falcon and Ham, 1988).

The ash content was determined as per ISO 1171: 2003. An empty porcelain crucible was weighed and the mass (m_1) recorded. One gram of sample material was weighed into the crucible and the mass of the crucible and sample recorded (m_2). The crucible was then loaded into an automated oven in which the temperature gradually increased from 500°C to 815 ± 10°C and thereafter gradually decreased. The mass of the crucibles and ash (m_3) were then recorded once the crucibles cooled. The ash content was then calculated as follows on an air-dried basis (SANS 10320: 2004):

$$\boldsymbol{ash_{ad}} = \left(\frac{\boldsymbol{m_2 - m_3}}{\boldsymbol{m_2 - m_1}}\right) \times \mathbf{100} \qquad \textit{[Equation 11]}$$

To exclude the effect of moisture, the air-dried (*ad*) value was converted to dry basis using the following equation (SANS 10320:2004):

$$\boldsymbol{ash_{db}} = \left(\frac{\boldsymbol{ash_{ad}}}{\mathbf{100 - moisture_{ad}}}\right) \times \mathbf{100} \qquad \textit{[Equation 12]}$$

Three replicates were averaged for each sample and an average value was calculated from the replicates. The maximum acceptable difference between results obtained were set to a repeatability of 2.0% of the mean result and a reproducibility of 3.0% of the average result.

4.4.2 Ultimate analysis

Total carbon, hydrogen, nitrogen, oxygen and sulphur are the predominant elements making up coal (Speight, 2005). These elements are either organically or inorganically bound to the macerals and mineral matter in the coal (Ward, 2002). Total carbon encompasses carbon from the organic coal constituents as well as carbon derived from carbon bearing minerals such as carbonates. The hydrogen content includes hydrogen derived from macerals, hydrated minerals and water in the coal structure. The amount of nitrogen present in coal is determined by measuring the nitrogen oxides (NO_x) that are released when coal is burned. Total sulphur includes all the sulphur occurring in the coal in the form of organic sulphur from the organic coal constituents, sulphur from sulphides present in the coal as well as sulphates (Thomas, 2012). The oxygen content present in the minerals and macerals in coal is determined indirectly using the following equation:

$$\%\boldsymbol{Oxygen\ by\ difference} = \mathbf{100} - (\boldsymbol{C} + \boldsymbol{H} + \boldsymbol{S} + \boldsymbol{N}) \qquad \textit{[Equation 13]}$$

Total carbon, hydrogen and nitrogen were determined simultaneously using the Leco CHN 628 organic element analyser, as per ASTM D5373-14: 2004. The sulphur content was determined according to ASTM D4239-14:2015 using the Leco S628 sulphur analyser. A sample mass of ±0. 5000 g was measured into a foil and the mass recorded into the computer. The sample was then loaded into the respective furnaces and analysed by the automated system. Three replicates were analysed per sample and the results were reported as averaged percentages. The samples were analysed on an air-dried basis and thereafter converted to daf to give a true representation of the elemental composition on the organic proportion of the coal, without the effect of moisture and ash (SANS 10320:2004):

$$\%\ \boldsymbol{elemental\ composition_{db}} = \left(\frac{\%\boldsymbol{elemental\ composition_{ad}}}{\mathbf{100} - \boldsymbol{moisture_{ad}}}\right) \times \mathbf{100} \qquad \textit{[Equation 14]}$$

Thereafter, the daf value was obtained by (SANS 10320:2004):

$$\%\boldsymbol{elemental\ composition_{daf}} = \left(\frac{\mathbf{100}}{\mathbf{100} - \boldsymbol{ash_{db}}}\right) \times \%\boldsymbol{elemental\ composition_{db}} \qquad \textit{[Equation 15]}$$

Three replicates were averaged for each sample and an average value calculated from the replicates. This data is available in Appendix C. The maximum acceptable difference between results obtained were set to according to Table 5.

Table 5. Precision of the CHN method used by CGS.

Element	Concentration range (%)	Repeatability limit (r%)	Reproducibility limit (R%)
Carbon	54.9 to 84.7	0.45	1.00
Hydrogen	3.25 to 5.10	0.10	0.25
Nitrogen	0.57 to 1.80	0.05	0.15
Sulphur	0.37 to5.48	$0.053 + 0.019\bar{x}$	$0.125 + 0.053\bar{x}$

Where $\bar{x}$ is the average of two test results.

4.5 Technological analyses

The combustion and coking properties of coal were studied over the duration of the experiment to observe the effects of weathering. Bomb calorimetry, thermogravimetry and the FSI were conducted.

4.5.1 Calorific value (CV)

Calorific value refers to the heat energy given off by coal when it combusts and is directly related to the ash content and total carbon content as a function of the maceral group (Falcon and Snyman, 1986; Suárez-Ruiz and Ward, 2008). This analysis was undertaken at the Council for Geosciences in Pretoria, assisted by coal laboratory scientists.

The gross calorific value was tested according to ISO 1928: 2004 using the Parr 6200 calorimeter and the complimentary Parr 6510 water handling system. The calorimeter consists of a bomb, jacket and water bucket. One gram of sample material was measured into a stainless-steel crucible and firmly placed in the crucible holder of the bomb head. One end of ignition thread was fastened onto the ignition wire and the other end of the thread was placed in contact with the sample in the crucible to ensure that the sample was ignited. The bomb was then tightly sealed and pressurised with oxygen. The pressurized bomb was then placed in the jacket containing water in a bucket filled with 200 ml of distilled water derived from the water handling system. Once submerged in the water, anodes were connected to the bomb head and the analysis was initiated through the automated system.

Three replicates were conducted per sample and the heat values were recorded to two decimal places in units of MJ/kg. The maximum acceptable difference between results obtained were set to a repeatability of 0.12 MJ/kg and a reproducibility of 0.3MJ/kg. An average value was calculated from the replicates (Appendix D).

4.5.2 Thermogravimetric analysis (TGA)

Thermogravimetry is a common technique employed to predict the behaviour of coal during combustion in commercial plants, by measuring the coals initial/ignition temperature (IT), fixed carbon ignition temperature (IT_{FC}), peak maximum temperature (PT) and burnout temperature (BT) (Li *et al*., 2005; Sen *et al*., 2009; Joshi *et al*., 2013). The data is recorded as a burning profile (Figure 12) which illustrates the relationship between the evolution of a coals mass as a function of temperature, under constant heating conditions (Morgan *et al*., 1986). The first derivative is calculated from the weight loss curve and indicates the rate (%/min) at which weight is lost during combustion; hence, the profile is referred to as a derivative thermogravimetric curve (DTG).

Cumming and McLaughlin (1982) observed that an initial decrease in weight (positive DTG curve) occurs at temperatures below 100 °C and translates to a loss in the inherent moisture. However, this phenomenon is not usually reported on standard burning profiles and is dependent on the moisture level and rank of the coal. Thereafter, the derivative curve becomes negative as the sample mass increases due to oxidation between 270-310 °C (Crelling *et al*., 1992). After oxidation, the rate of weight loss increases (i.e. positive derivative curve) indicating the loss of volatile matter (IT_{VM}). The fixed carbon ignition temperature (IT_{FC}) indicates the point at which the devolatilization of inorganic matter is complete and the organic matter begins to burn (Li *et al*., 2005). The peak maximum temperature (PT) represents the point where the burning rate is at its maximum and maximum weight loss has occurred. The temperature at which complete oxidation occurs just before the reaction stops is the burnout temperature (BT) (Norton, 1993).

Coal from Bench 5 in the Waterberg Coalfield was selected for thermogravimetric analysis because it is specifically used to generate electricity. Hence, changes in its combustion behaviour as a result of weathering were monitored by observing variations in the thermal profiles over the duration of the experiment.

The instrument (TA Q600 TGA) used to conduct the analysis is housed in the Clean Coal Technology Research (CCTR) laboratory in the School of Chemical and Metallurgical Engineering, University of the Witwatersrand. The analysis was conducted under the supervision of the senior technician of the CCTR.

For each sample, an aluminium crucible was cleaned, and its mass tarred in the instrument. Thereafter 0.010 g of sample material was measured into the crucible and loaded into the instrument. The samples were heated from 0 to 900ºC at a constant rate of 10°C/min^{-1} in an oxygen atmosphere at a purge rate of 50cm^3 min^{-1}. A slow heating rate of 10°C/min^{-1} was selected so as to obtain a high resolution of the various stages of combustion described above. Nitrogen was used to purge the chamber at a rate of 50cm^3 min^{-1}.

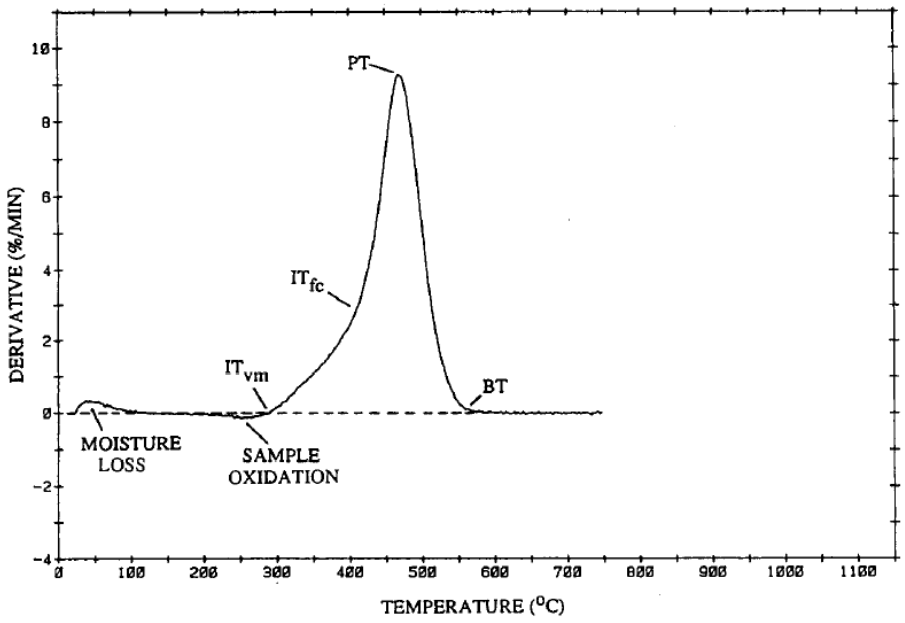


Figure 12. Parameters on a burning profile determined by thermogravimetry (Norton, 1993).

4.5.3 Free swelling index (FSI)

The FSI measures the extent to which coal swells into a carbon-rich mass on a scale of 0 to 9, zero signifying no swell (Speight, 2005). This thermoplastic property is important in the metallurgical industry where coking coals are used as a reductant in the conversion of iron ore (Suárez-Ruiz and Ward, 2008). The swelling values of the coking the coals obtained for this study, i.e. the Middle Seam (MS) and Bench 3 (B3) were tested according to the ISO 501: 2012 standard described below. These samples were chosen because the parent coal exhibited swelling, and they are mined for the purpose of producing coke. This analysis was undertaken at the Council for Geosciences in Pretoria, assisted by coal laboratory scientists.

The samples were milled to -212 µm and analysed on the same day of sampling and milling to avoid further oxidation of the coal which would lead to erroneous results. One gram of the sample was weighed into a silica crucible and levelled to ensure that the resulting coke would correspond, as best as possible, to the standard swell profiles depicted in Figure 13. The crucibles were closed with lids that have a small (6 mm) circular opening at their centre to allow volatiles to escape during heating. The crucibles were then placed on the triangle of the burner and heated for one minute and thirty seconds. During this time the initially orange flame later turned blue, signalling the release of volatiles. Once all the volatiles were driven off, the flame turned orange and the burner was switched off. After the crucible had cooled, the residue was compared to the standard swell profiles (Figure 13) to determine the swelling number (ISO 501: 2012).

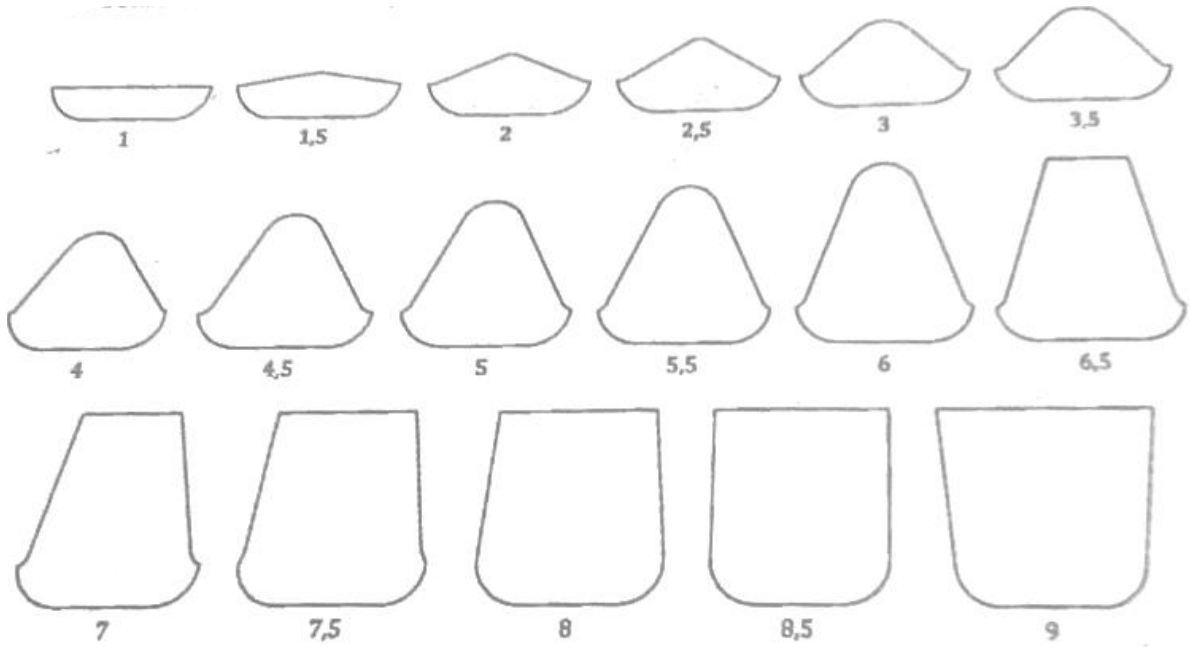


Figure 13. Button profiles according to ISO 501:2012

4.6 Petrography

Coal petrography is a routine coal analysis tool that utilises a petrographic microscope to optically classify coal constituents and identify their associations on a qualitative and quantitative basis (Richards *et al*., 2013). The analysis was conducted under the supervision of Professor Nicola Wagner at the Department of Geology, located at the Kingsway Campus of the University of Johannesburg.

A Zeiss Axio Imager M2M petrographic microscope, equipped with a Hilgers Fossil system which enables routine coal analysis (vitrinite reflectance, maceral point count) and high-resolution imaging of samples using the monochromatic and colour cameras, was used for analysing representative samples.

The petrography blocks were prepared by mixing coal of a particle size of -1mm with 7g of epoxy resin and 1g of hardener. The mixture was left to harden overnight, followed by several rounds of grinding and polishing using the Streurs TegraPol-11 to produce a smooth surface suitable for optical analysis. This procedure was followed according to SANS 7404-2: 2015.

4.6.1 Maceral point count

The maceral point count was conducted to identify and quantify the proportion of the various types of macerals present in the fresh parent coal samples, including the mineral matter present in the samples. The fresh parent coals are samples: MSB, B3B, B5B, B9B and B11B. The macerals and minerals that are pertinent to coals from the Waterberg and Limpopo Coalfields are listed in Table 6. The macerals were counted at a magnification of x500 under oil immersion. Up to 500 points were analysed as the

automated stage traversed across on the polished block. This procedure was followed according to SANS 7404-3: 2016, and the results were quantified on a mineral matter free (mmf) basis, as well as including mineral matter (incl. mm).

Table 6. Macerals and mineral matter analysed in the study.

Vitrinite	**Inertinite**	**Liptinite**	**Mineral matter**
Telinite	Fusinite	Cutinite	Pyrite
Collotelinite	Semifusinite	Sporinite	Calcite
Vitrodetrinite	Funginite	Algnite	Quartz
Collodetrinite	Secretinite	Resinite	Clay minerals
Corpogelinite	Macrinite	Liptodetrinite	
Gelinite	Micrinite	Suberinite	
	Inertodetrinite	Exsudatinite	

The maceral point count was only conducted on the fresh parent samples because it was assumed that the maceral composition would not vary during the early stages of weathering.

4.6.2 Vitrinite reflectance

The intensity of coal reflectance is directly proportional to its carbon content, which increases with increasing coal rank during coalification, particularly in collotelinite (Teichmüller, 1989). Hence, reflectance measurements are conducted on collotelinite macerals, which are characterised by a smooth surface on which the cell wall structure is not clearly identifiable due to extreme gelification (ICCP, 1998).

The monochrome camera was used to conduct the mean random reflectance (Rr) measurements on 100 points of collotelinite present in each sample under reflected light using a 50x oil objective. Measurements were taken as the automated stage of the microscope moved in a predetermined raster pattern across the surface of the coal block. Prior to each sample run, the system was calibrated to measure an intensity of reflected light at 0.90 %, using a yttrium-aluminium-garnet (YAG) standard. This procedure was followed according to SANS 7404-5: 1994.

The results were presented as a histogram and the mean value of reflectance and the standard deviation were produced for each sample analysed. The mean reflectance values were used to determine the rank of the coal according to the classification scheme in Table 7, and to detect any changes in the reflectance due to weathering.

Table 7. Coal rank classification using SANS 10320: 2004.

Coal rank	Rank parameter
Low-rank coals	
Low-rank C (Lignite C)	Rr < 0,4 % and bed moisture > 35 % and < 75 %, ash-free basis
Low-rank B (Lignite B)	Rr < 0,4 % and bed moisture < 35 %, ash-free basis
Low-rank A (Sub-bituminous coal)	0.4 % ≤ *R*r < 0.5 %
Medium-rank coals (bituminous coals)	
Medium-rank D (Bituminous D)	0.5 % ≤*R*r < 0.6
Medium-rank C (Bituminous C)	0.6 % ≤*R*r < 1.0 %
Medium-rank B (Bituminous B)	1.0 % ≤Rr < 1.4 %
Medium-rank A (Bituminous A)	1.4 % ≤*R*r < 2.0 %
High-rank coals (anthracites)	
High-rank C (Anthracite C)	2.0 % <*R*r < 3.0 %
High-rank B (Anthracite B)	3.0 % <*R*r < 4.0 %
High-rank A (Anthracite A)	4.0 % <*R*r < 6.0 % (or *R*v max < 8.0)

4.6.3 Abnormal Condition Analysis (ACA)

The abnormal condition analysis (ACA) was developed by Wagner (1999), for the purpose of quantifying abnormal features in coal using a petrographic microscope. As with the procedure outlined for the maceral point count, the ACA was conducted by identifying abnormal features at 500 points on a polished block as the automated point counter traversed across the coal block. The abnormal features considered in this study include the presence of alteration minerals, oxidation rims, cracks, fissures and devolatilization pores (Wagner, 1999; 2008).

4.7 Mineralogy

Weathering alters the minerals present in coal and therefore, x-ray diffraction, x-ray fluorescence, electron microscopy, and Raman spectroscopy were used to identify the original minerals present in the fresh (parent) coals and thereafter to identify new or alteration minerals that formed in the weathered samples. Due to the compositional complexity of coal and the fact that every analytical technique is to some extent flawed by some limitation, the integrated use of several techniques was necessary to compensate for these limitations and to increase the confidence of the results reported here.

The petrographic analysis facilitated the selection of samples with observed weathered minerals and alteration products that were assessed using electron microscopy and Raman spectroscopy.

4.7.1 X-ray diffraction (XRD)

The mineral phases present in the fresh parent coals were identified using non-destructive testing of polycrystalline and amorphous materials using XRD. Thereafter, each weathered sample was analysed at the various sampling intervals to detect the formation of new minerals and alteration due to weathering. The samples were milled to -212 μm and sent to the XRD laboratory situated at the Council for Geosciences in Pretoria.

The XRD measurements were performed on a Bruker D8 Advance instrument with 2.2kW Cu long fine focus tube (Cu Kα, λ=1.54060) and 90 position sample changer. The system is equipped with a LynxEye detector with 3.7º active area. Samples are scanned from 2 to 70° 2θ $Cu_{K\alpha}$ at a speed of 0.02° 2θ steps size/3 sec, and generator settings of 40 kV and 40mA.

Phase concentrations were determined as semi-quantitative estimates, using relative peak heights/areas proportions (Brime, 1985).

4.7.2 X-ray Fluorescence (XRF)

The bulk major oxide composition of the samples was determined at the various sampling intervals to detect whether changes in composition occurred due to weathering. Samples were milled to -212 μm and sent to the XRF laboratory situated at the Council for Geosciences in Pretoria.

4.7.3 Electron microprobe analysis (EMPA)

In addition to the identification of weathered minerals and newly formed alteration minerals, the purpose of utilising electron microscopy in this study was to determine whether the chemical composition of minerals in the weathered coals differed from those in the fresh parent coal sample. The mineral of interest was calcite because it reacts to form gypsum as described in the literature review. A Cameca SX-5FE electron microprobe equipped with 5 WDS spectrometers was used. The instrument is housed at the MMU (Microscopy and Microanalysis Unit) of the University of the Witwatersrand.

Sample preparation for EMPA involved coating the polished blocks with carbon to ensure conductivity on the surface of the samples. Analytical conditions were set to an acceleration voltage of 15 kV and a 20 nA beam current. Natural and synthetic standards were used for calibration. A 10 μm diameter

electron beam was used during quantitative analysis. Counting times were 10 seconds on the peak, and 5 seconds total on the background for all elements.

Carbonate analyses were standardized for Ca on calcite, Mg on dolomite, Mn on rhodonite and Fe on almandine. The data were collected with CAMECA software. An automated X-PHI matrix algorithm was applied to correct for differential matrix effects. Oxygen was calculated by stoichiometry. Due to the carbonaceous nature of the samples negatively affecting the vacuum of the instrument, the analysis could only be conducted over a short duration on a limited number of samples and therefore a limited number of individual mineral grains. Furthermore, this instrument was unavailable due to technical issued hence alternative techniques such as field scanning electron microscopy (FE-SEM) and Raman spectroscopy were used to supplement the data.

4.7.4 Field scanning electron microscopy (FE-SEM)

Due to the setbacks encountered in utilising the electron microprobe, the Zeiss high vacuum FE-SEM was used to supplement the compositional data of selected altered calcite minerals. The FE-SEM housed at the pyrometallurgy unit of the School of Metallurgical and Chemical Engineering (Richard Ward Building) at the University of the Witwatersrand was used.

Back-scattered electron (BSE) images, energy dispersive x-ray spectroscopy (EDS) and compositional maps were measured on selected red calcite grains that showed signs of alteration. The samples analysed had been left to weather for up to 16 months. Polished coal blocks were prepared according to the procedure described in Section 4.6 and coated with gold/palladium to induce conductivity under the electron beam. The extra high tension (EHT) voltage was adjusted depending on the conductivity of the surface and ranged between 15-20 kV. The samples were imaged at a magnification of 199-751x using a working distance (WD) ranging between 7.7-9.1 mm. The analysis was conducted by the instrument technician.

4.7.5 Raman Spectroscopy

During this research there were some technical constraints associated with EMPA analyses. Due to financial constraints, the EMPA could not be conducted at commercial laboratories. Therefore, EMPA data was supplemented by carrying out Raman spectroscopy at the microscopy and microanalysis unit. After a preliminary petrographic analysis of each sample, Raman spectroscopy was used to identify alteration minerals present in the coal when the EMPA was out of service for technical reasons.

The Horiba Jobin Yvon LabRAM HR Raman spectrometer was used to carry out the analysis. The spectrometer is equipped with an argon ion laser which was used to emit green monochromatic light at

a wave length of 514.5 nm. All analyses were conducted using a dry air lens 100x objective. The analysis was conducted by the instrument technician.

4.8 Statistical analyses

To determine if there were any relationships between the variables investigated in this study, and whether the relationships are significant, linear regression and correlation coefficients were conducted.

Linear regression is a statistical evaluation of how well a set of data points (y) can be predicted using the straight-line (Equation 16). The data points are depicted on a scatter plot where points that lie near the regression line are considered as accurate predictions of the equation, whereas points that lie further away from the line are poorly defined by the equation (Underhill and Bradfield, 2013; StatSoft, 2018).

$$\boldsymbol{y = mx + c} \qquad \textit{[Equation 16]}$$

where: y = predicted or dependant variable

m = gradient

x = explanatory independent variable

c = y intercept

The correlation of determination (R^2) gives an indication of the strength of the relationship between the x and y variables (Equation 17). When R^2 is equal to zero or close to zero, no relationship or a weak relationship exists between x and y, whereas a perfect or strong relationship exists between x and y when R^2 is equal to one or close to one (Underhill and Bradfield, 2013; StatSoft, 2018).

$$\boldsymbol{R^2 = \frac{b(\sum xy - \frac{\sum x \sum y}{n})}{\sum y^2 - (\frac{\sum y}{n})^2}} \qquad \textit{[Equation 17]}$$

Pearson's correlation coefficient (r) and the population correlation coefficient (p) are used to determine whether the relationship between x and y is statistically significant. The correlation coefficient (Equation 18) always occurs between +1 and -1 where positive r values describe a positive slope on the regression line on which x and y are both increasing. Negative r values describe a negative slope on the regression line on which the y values decreases while the x values increase (Underhill and Bradfield, 2013; StatSoft, 2018).

$$\mathbf{r = \frac{\sum(x_i - \bar{x})(y_i - \bar{y})}{\sqrt{\sum(x_i - \bar{x}) - ((y_i - \bar{y})}}} \qquad \textit{[Equation 18]}$$

The values of the population correlation coefficient (p) are derived from tabulated probability levels (Appendix E) which are dependent on the degree of freedom (d.f) (Equation 19) for the correlation coefficient. When the value of the correlation coefficient is greater than the p, the relationship between x and y is said to be statistically significant (Underhill and Bradfield, 2013; StatSoft, 2018).

$$\boldsymbol{d.f = n - 2} \qquad \textit{[Equation 19]}$$

where n = number of x and y pairs

Chapter 5: Results and discussion

The results of the various analyses that were undertaken are presented and discussed in this chapter with the aim of assessing the extent to which the coals have weathered over time. Firstly, the temperature data collected from the weather stations are presented to provide insight on the external temperature conditions impacting on the coals during the study. Secondly, the changes in the chemical composition of the coal is assessed in terms of the proximate and ultimate analyses, followed by the impact on the combustion properties (CV and TGA) and coking properties (FSI). Lastly, the data from the mineralogical (XRF, XRD, Raman spectroscopy, EMPA and FE-SEM) and petrographic analyses are presented to discuss the effect of weathering on the organic and inorganic constituents of the coals.

5.1 Temperature measurements

As discussed in the literature review, temperature is one of the major factors controlling the extent to which coal will weather by oxidation (Itay *et al*., 1989; Wang, *et al*., 2003b). The collated average daily temperature measurements from the Davis weather station and the SAWS station are reported in Appendix A. The summary of this temperature data is presented as monthly averages in Table 8.

The temperature data covers the period from 2 August 2016 to 6 February 2017, during which the samples were exposed to weathering on the roof. This period marked the transition from winter during August 2016 to spring (September and October) to summer (November, December and January) and finally waning summer conditions in February 2017. Initially, the samples experienced the lowest temperature conditions in August 2016, in which the average minimum temperature was 9.40°C. Thereafter, the samples experienced increasing temperature conditions which peaked in December 2016, reaching an average maximum of 27.46°C. The range in temperature conditions (9.40 - 27.23 °C) to which the samples were subjected to is similar to those reported by Cimadevilla *et al* (2005) and can be described as mild oxidation conditions.

Table 8. Summary of monthly average temperatures from 2 August 2016 to 6 February 2017.

Month	Average temperature (°C)	Average maximum temperature (°C)	Average minimum temperature (°C)
August 2016	14.85	21.41	9.40
September 2016	17.92	23.36	12.83
October 2016	19.87	26.58	13.13
November 2016	19.36	24.71	14.98
December 2016	21.46	27.46	15.84
January 2017	19.85	24.46	15.77
February 2017	20.47	24.97	16.38

5.2 Chemical analyses

5.2.1 Proximate results

The results of the proximate analysis are illustrated in Figure 14 for the dry and wet samples in terms of their inherent moisture content, volatile matter (daf), ash content (db) and fixed carbon content (daf). The statistical significance of the trends is discussed with respect to the correlation coefficient (r) and population correlation coefficient (p) which are recorded in Table 9.

Prior to weathering, the fresh parent sample of B3 is characterized by slightly higher inherent moisture, volatile matter and ash compared to the MS. Whereas the parent sample of B9 has slightly higher inherent moisture, ash and fixed carbon content than B11. The parent sample of B5 is characterized by the highest ash content (35.13 %) of all the samples and the second highest volatile matter (42.55%) after B3 (43.74%).

With increasing exposure to weathering, the moisture content increased in all the samples, with the wet samples (except for B11W) having the fastest rates of increase due to the additional moisture they received when they were watered regularly throughout the experiment. The increase in the moisture content is statistically significant for all the samples, excluding B3, B3W, B5 and B5W, where it was insignificant (Table 9). The volatile matter also decreased in all the samples apart from B9, but the decrease in the volatiles was only significant in samples B3W and B11. The ash content only increased in samples MS, MSW and B11W whereas in all the other samples, the ash content decreased. The changes in the ash content are only significant in the MS, MSW and B11 samples. The fixed carbon content only decreased in the MSW, B9, B9W, B11 and B11W whilst all other samples appeared to increase in fixed carbon with weathering time. None of the changes in the fixed carbon content are significant.

The increase in the moisture content as a result of weathering is consistent with the findings of Fredericks *et al* (1983), and Martinez and Escobar (1995). In the case of the dry samples, the increase in the moisture content is likely due to the combination of moisture expelled during oxidation (Equation 1) and moisture derived from the humidity build up in the containers. The decrease in the volatile matter indicates that the coals have undergone minor devolatilization in response to the mild temperature conditions (Kus *et al.*, 2017) described in Section 5.1. In agreement with these observed changes, varied responses have been reported in the literature for the behaviour of the moisture, volatile matter, ash and fixed carbon (Fredericks *et al*. 1983; Pisupati *et al*., 1991; Kus *et al*., 2017), primarily as a function of the type coal and conditions in which it weathered (Yohe, 1958).

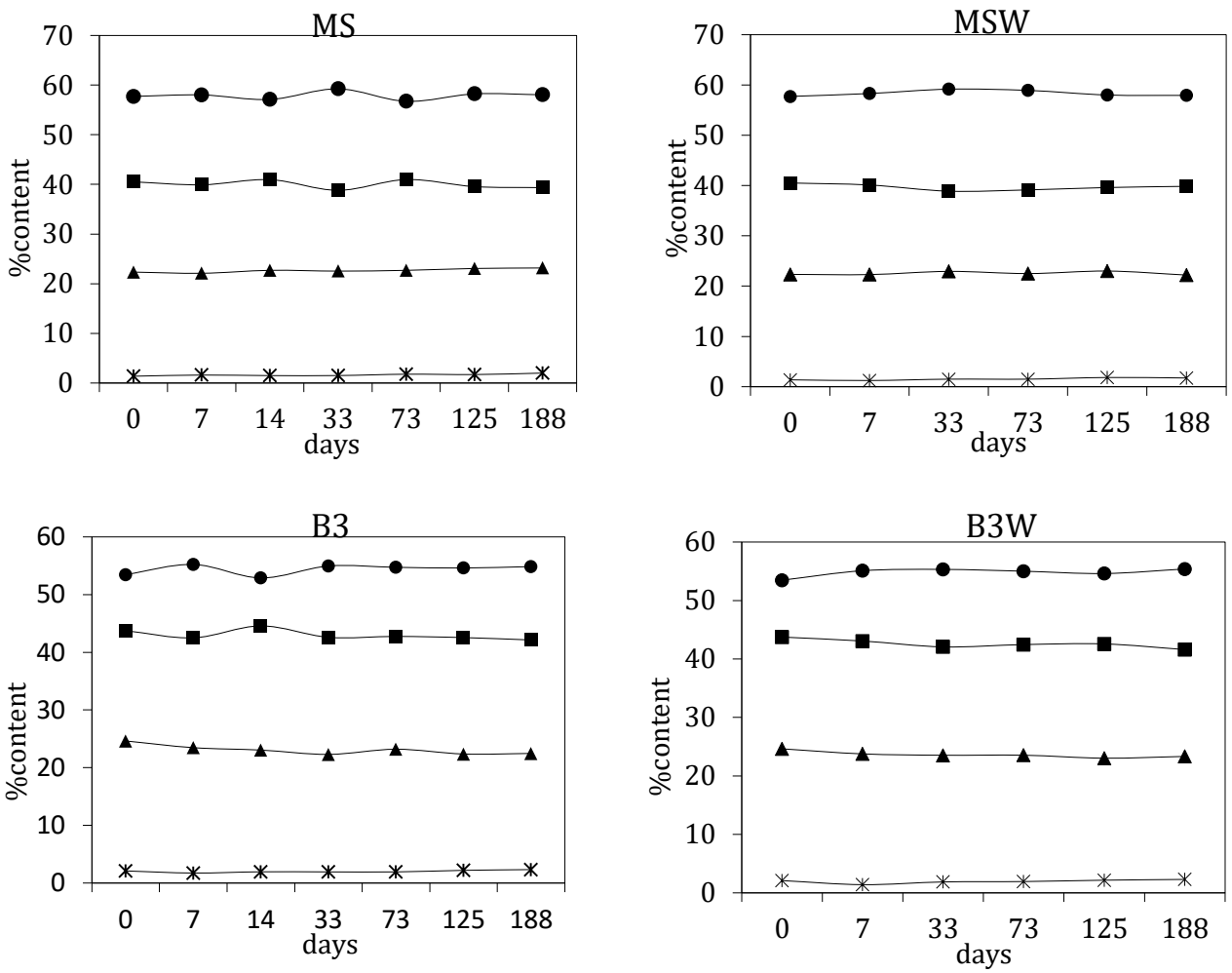


Figure 14. Proximate results of the dry samples and their wet counterparts. * Inherent moisture content, ■ volatile matter (daf), ▲ ash content (db) and ●fixed carbon content (daf).

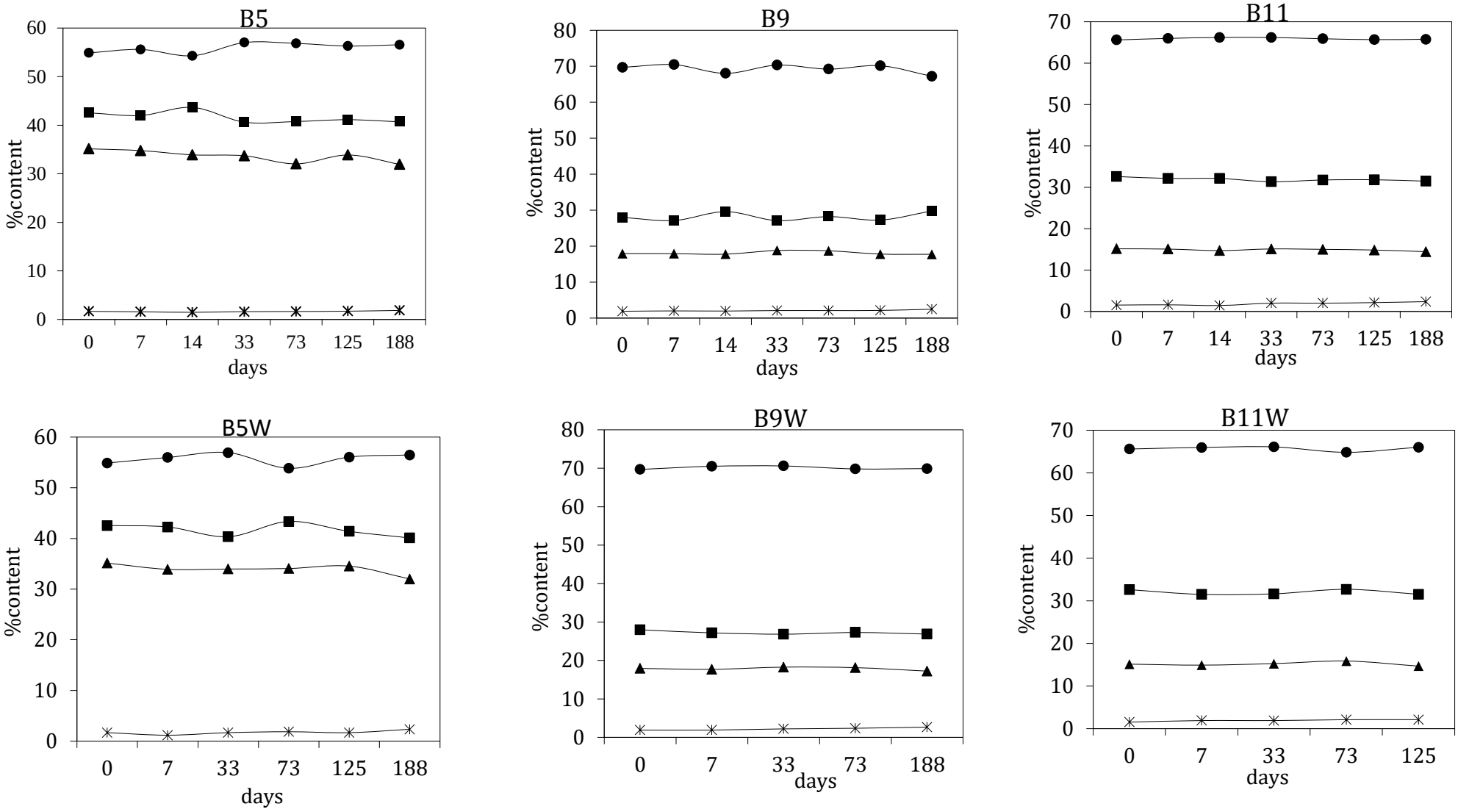


Figure 14 continued. Proximate results of the dry samples and their wet counterparts. * Inherent moisture content, ■ volatile matter (daf), ▲ ash content (db) and ● fixed carbon content (daf).

Table 9. Statistical analysis of the proximate results

Middle seam (MS)					Middle seam wet (MSW)				
Days	**Inherent moisture%**	**Volatile matter% (daf)**	**Ash% (db)**	**Fixed carbon% (daf)**	**Days**	**Inherent moisture%**	**Volatile matter% (daf)**	**Ash% (db)**	**Fixed carbon% (daf)**
0	1.37	40.52	22.33	57.73	**0**	1.37	40.52	22.33	57.73
7	1.60	39.92	22.10	58.02	**7**	1.23	40.11	22.30	58.30
14	1.49	40.96	22.69	57.11	**33**	1.50	38.88	22.93	59.17
33	1.50	38.81	22.53	59.25	**73**	1.50	39.14	22.50	58.92
73	1.77	40.98	22.69	56.73	**125**	1.83	39.61	23.00	58.01
125	1.70	39.56	23.07	58.23	**188**	1.73	39.85	22.20	57.93
188	2.00	39.35	23.17	58.05	**Equation**	y = 0.1038x + 1.1644	y = -0.1313x + 40.144	y = 0.0286x + 22.444	y = -0.0034x + 58.354
Equation	y = 0.085x + 1.2924	y = -0.1502x + 40.614	y = 0.1583x + 22.021	y = 0.0361x + 57.73	**rate (% /day)**	0.1038	-0.1313	0.0286	-0.0034
rate (% /day)	0.085	-0.1502	0.1583	0.0361	**Coefficient of determination (R^2)**	0.7549	0.1406	0.0245	0.0001
Coefficient of determination (R^2)	0.7546	0.1515	0.8162	0.0091	**Pearson's correlation coefficient (r)**	0.8688	0.3750	0.1565	0.0100
Pearson's correlation coefficient (r)	0.8687	0.3892	0.9034	0.0954	**Population correlation coefficient (ρ)**	0.8114			
Population correlation coefficient (ρ)	0.7545				**n= 6-2**	4			
n= 7-2	5				**Comment**	significant	insignificant	insignificant	insignificant
Comment	significant	insignificant	significant	insignificant					

Table 9 continued. Statistical analysis of the proximate results

Bench 3 (B3)					Bench 3 wet (B3W)				
Days	**Inherent moisture%**	**Volatile matter% (daf)**	**Ash% (db)**	**Fixed carbon% (daf)**	**Days**	**Inherent moisture%**	**Volatile matter% (daf)**	**Ash% (db)**	**Fixed carbon% (daf)**
0	2.10	43.74	24.63	53.47	**0**	2.10	43.74	24.63	53.47
7	1.73	42.51	23.47	55.23	**7**	1.40	43.07	23.77	55.09
14	1.95	44.57	23.05	52.89	**33**	1.87	42.07	23.53	55.32
33	1.93	42.60	22.30	54.95	**73**	1.93	42.46	23.54	55.01
73	1.93	42.75	23.20	54.73	**125**	2.17	42.57	23.03	54.61
125	2.20	42.55	22.37	54.62	**188**	2.30	41.61	23.33	55.39
188	2.33	42.13	22.47	54.86	**Equation**	y = 0.0962x + 1.6244	y = -0.336x + 43.763	y = -0.2484x + 24.509	y = 0.2241x + 54.032
Equation	y = 0.0577x + 1.7952	y = -0.2345x + 43.918	y = -0.3054x + 24.29	y = 0.1706x + 53.71	**rate (% /day)**	0.0962	-0.336	-0.2484	0.2241
rate (% /day)	0.0577	-0.2345	-0.3054	0.1706	**Coefficient of determination (R^2)**	0.3232	0.703	0.7264	0.3452
Coefficient of determination (R^2)	0.3909	0.3465	0.6414	0.1813	**Pearson's correlation coefficient (r)**	0.5685	0.8385	0.8523	0.5875
Pearson's correlation coefficient (r)	0.6252	0.5886	0.8009	0.4258	**Population correlation coefficient (ρ)**	0.8114			
Population correlation coefficient (ρ)	0.7545				**n= 6-2**	4			
n= 7-2	5				**Comment**	insignificant	significant	significant	significant
Comment	insignificant	insignificant	significant	insignificant					

able 9 continued. Statistical analysis of the proximate results

Bench 5 (B5)					Bench 5 wet (B5W)				
Days	**Inherent moisture%**	**Volatile matter% (daf)**	**Ash% (db)**	**Fixed carbon% (daf)**	**Days**	**Inherent moisture%**	**Volatile matter% (daf)**	**Ash% (db)**	**Fixed carbon% (daf)**
0	1.67	42.55	35.13	54.88	**0**	1.67	42.55	35.13	54.88
7	1.57	42.00	34.77	55.60	**7**	1.17	42.26	33.90	55.98
14	1.47	43.67	33.89	54.29	**33**	1.67	40.33	33.97	56.94
33	1.60	40.62	33.70	57.01	**73**	1.85	43.35	34.06	53.84
73	1.63	40.76	32.03	56.84	**125**	1.67	41.40	34.53	56.06
125	1.70	41.13	33.87	56.30	**188**	2.33	40.10	32.00	56.47
188	1.87	40.70	31.93	56.56	**Equation**	y = 0.1433x + 1.2233	y = -0.3378x + 42.847	y = -0.3907x + 35.3	y = 0.1454x + 55.185
Equation	y = 0.0368x + 1.4962	y = -0.3651x + 43.092	y = -0.4735x + 35.511	y = 0.3216x + 54.64	**rate (% /day)**	0.1433	-0.3378	-0.3907	0.1454
rate (% /day)	0.0368	-0.3651	-0.4735	0.3216	**Coefficient of determination (R^2)**	0.5081	0.2409	0.4807	0.0571
Coefficient of determination (R^2)	0.4139	0.4639	0.6891	0.4491	**Pearson's correlation coefficient (r)**	0.7128	0.4908	0.6933	0.2390
Pearson's correlation coefficient (r)	0.6434	0.6811	0.8301	0.6701	**Population correlation coefficient (ρ)**	0.8114			
Population correlation coefficient (ρ)	0.7545				**n= 6-2**	4			
n= 7-2	5				**Comment**	**insignificant**	**insignificant**	**insignificant**	**insignificant**
Comment	insignificant	insignificant	significant	insignificant					

Table 9 continued. Statistical analysis of the proximate results

Bench 9B (B9)					Bench 9B wet (B9W)				
Days	**Inherent moisture%**	**Volatile matter% (daf)**	**Ash% (db)**	**Fixed carbon% (daf)**	**Days**	**Inherent moisture%**	**Volatile matter% (daf)**	**Ash% (db)**	**Fixed carbon% (daf)**
0	1.90	27.99	17.93	69.70	**0**	1.90	27.99	17.93	69.70
7	2.00	27.12	17.90	70.44	**7**	1.90	27.18	17.70	70.51
14	1.96	29.59	17.77	68.03	**33**	2.20	26.84	18.27	70.60
33	2.10	27.09	18.80	70.32	**73**	2.37	27.28	18.13	69.83
73	2.10	28.21	18.70	69.21	**188**	2.67	26.86	17.23	69.92
125	2.13	27.25	17.80	70.15	**Equation**	y = 0.2x + 1.6067	y = -0.2142x + 27.871	y = -0.0967x + 18.143	y = -0.0253x + 70.187
188	2.47	29.78	17.73	67.22	**rate (% /day)**	0.2	-0.2142	-0.0967	-0.0253
Equation	y = 0.0752x + 1.7933	y = 0.1524x + 27.537	y = 0.0046x + 18.072	y = -0.2441x + 70.273	**Coefficient of determination (R^2)**	0.9404	0.5295	0.1408	0.0094
rate (% /day)	0.0752	0.1524	0.0046	-0.2441	**Pearson's correlation coefficient (r)**	0.9697	0.7277	0.3752	0.0970
Coefficient of determination (R^2)	0.7735	0.084	0.0005	0.1816	**Population correlation coefficient (ρ)**	0.8783			
Pearson's correlation coefficient (r)	0.8795	0.2898	0.0224	0.4261	**n= 5-2**	3			
Population correlation coefficient (ρ)	0.7545				**Comment**	significant	insignificant	insignificant	insignificant
n= 7-2	5								
Comment	significant	insignificant	insignificant	insignificant					

Table 9 continued. Statistical analysis of the proximate results

Bench 11 (B11)					Bench wet (B11W)				
Days	**Inherent moisture%**	**Volatile matter% (daf)**	**Ash% (db)**	**Fixed carbon% (daf)**	**Days**	**Inherent moisture%**	**Volatile matter% (daf)**	**Ash% (db)**	**Fixed carbon% (daf)**
0	1.53	32.60	15.13	65.59	**0**	1.53	32.60	15.13	65.59
7	1.60	32.14	15.07	65.97	**7**	1.90	31.49	14.90	65.96
14	1.43	32.12	14.70	66.20	**33**	1.90	31.63	15.27	66.09
33	2.00	31.33	15.10	66.20	**73**	2.10	32.69	15.87	64.82
73	2.00	31.76	15.00	65.88	**125**	2.10	31.52	14.67	66.02
125	2.13	31.82	14.83	65.68	**Equation**	y = 0.1333x + 1.5067	y = -0.096x + 32.274	y = 0.0033x + 15.157	y = -0.0299x + 65.785
188	2.37	31.48	14.43	65.76	**rate (% /day)**	0.1333	-0.096	0.0033	-0.0299
Equation	y = 0.1476x + 1.2762	y = -0.1562x + 32.519	y = -0.081x + 15.219	y = -0.0149x + 65.956	**Coefficient of determination (R^2)**	0.8299	0.0634	0.0001	0.008
rate (% /day)	0.1476	-0.1562	-0.081	-0.0149	**Pearson's correlation coefficient (r)**	0.9110	0.2518	0.0100	0.0894
Coefficient of determination (R^2)	0.8397	0.6068	0.4654	0.018	**Population correlation coefficient (ρ)**	0.8783			
Pearson's correlation coefficient (r)	0.9164	0.7790	0.6822	0.1342	**n= 5-2**	3			
Population correlation coefficient (ρ)	0.7545				**Comment**	**significant**	**insignificant**	**insignificant**	**insignificant**
n= 5-2	5								
Comment	significant	significant	nearly significant	insignificant					

5.2.2 Ultimate analysis

The behaviour of the elemental components (total carbon, hydrogen, total sulphur and oxygen) of the coal samples in response to weathering are reported in this section. The minor constituents: hydrogen, nitrogen and sulphur content are discussed first, followed by the major constituents: total carbon and oxygen content. Lastly, the hydrogen to carbon ratio (H/C) and oxygen to carbon (O/C) ratios are discussed.

5.2.2.1 Behaviour of hydrogen, nitrogen and total sulphur content over time

The trend of the hydrogen, nitrogen and total sulphur content in the dry samples and their wet counterparts are illustrated in Figure 15. The statistical significance of the trends is discussed with respect to the correlation coefficient (r) and population correlation coefficient (P) which are recorded in Table 10.

The hydrogen content is highest in the fresh parent sample of B5 (6.29%), whereas B9 (4.06%) and B11 (3.91%) have lower proportions. B3 (5.44%) has a slightly higher hydrogen content compared to the MS (5.24%). The nitrogen content is similar for the parent samples of B5 (1.76%) and B9 (1.72%), but lower in B11 (1.66%). B3 (1.52%) has a higher nitrogen content compared to the MS (1.46%). The total sulphur content is highest in B5 (3.50%) followed by B3 (3.02%), the MS (2.9%), B11 (0.61%) and B9 (0.63%).

The samples underwent minor changes in their elemental composition over the six-month period of weathering. All the samples apart from MSW and B11W, displayed decreasing hydrogen trends, however, only MSW has a significant correlation. An increasing nitrogen trend was observed for all the samples, with only B11W having a significant trend. The total sulphur trend in all the samples but B3W, increased but only samples MS, B3, B5 and B11W reported significant correlations.

The hydrogen fraction of coal tends to decrease with weathering and corresponds to a decreasing H/C ratio as discussed in Section 5.2.2.3 (in agreement with Fredericks *et al*., 1983; Liotta *et al.*, 1983; Wu *et al*., 1988; Pisupati *et al.*, 1991, 1993; Miroshnichenko *et al*., 2012b; Wang and Zhou, 2012). Some studies (Fredericks *et al*., 1983; Huffman *et al*., 1985) have reported a decrease of nitrogen in response to weathering, while Isaacs and Liotta (1987) noted that there were no apparent trends in the nitrogen content as a function of weathering. The total sulphur content, specifically the pyritic form, has generally been reported to decrease due to pyrite oxidation and the subsequent formation of sulphates (Huffman *et al*., 1985; Pisupati *et al*, 1993). Hence, the total content may show an increasing trend due to the development of sulphates (Wu *et al*.,1988). The effect of weathering on sulphur in the pyritic and sulphate form is further discussed in Section 5.6.

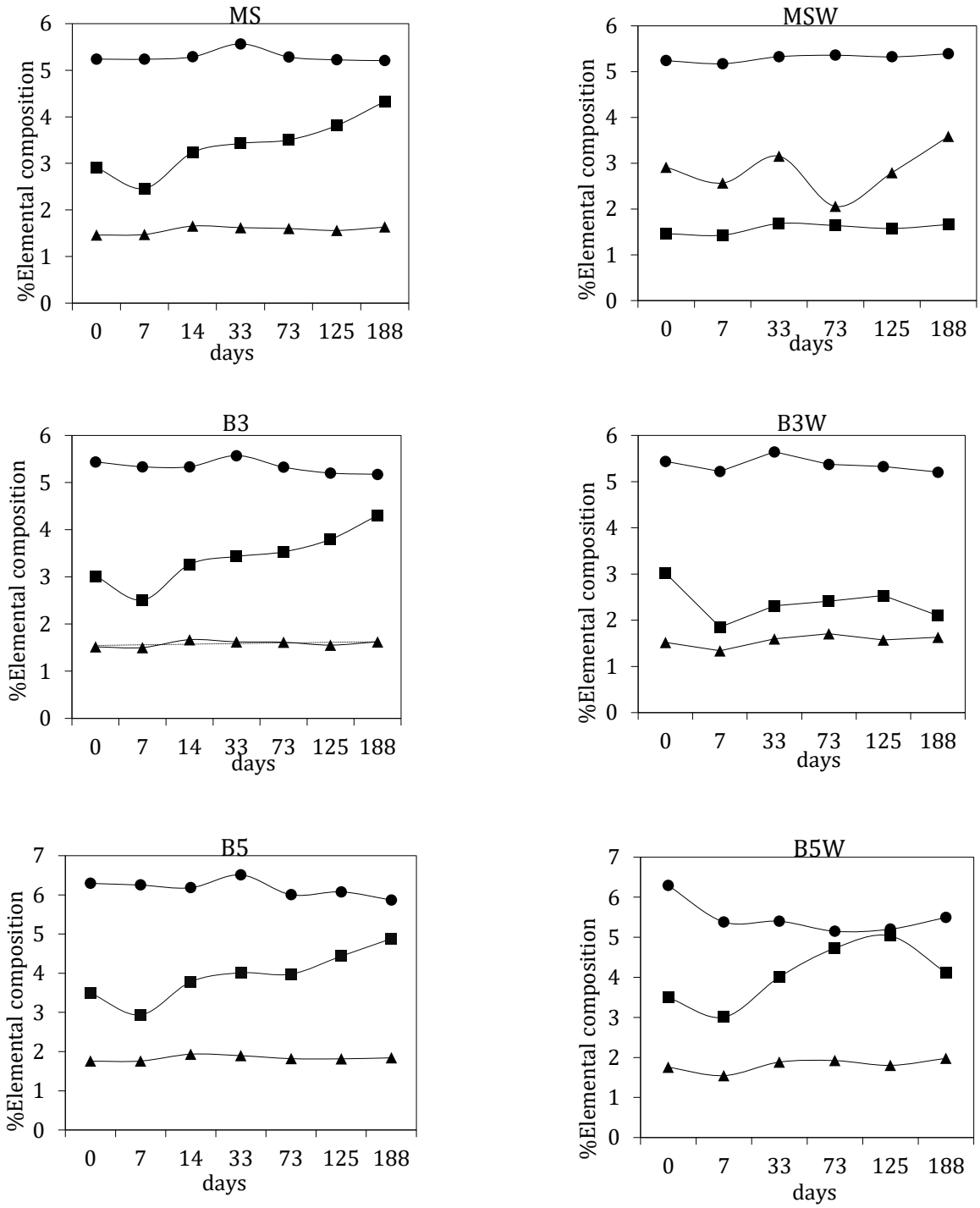


Figure 15. Ultimate results for the dry samples and their wet counterparts. ●hydrogen, ■ total sulphur and ▲nitrogen.

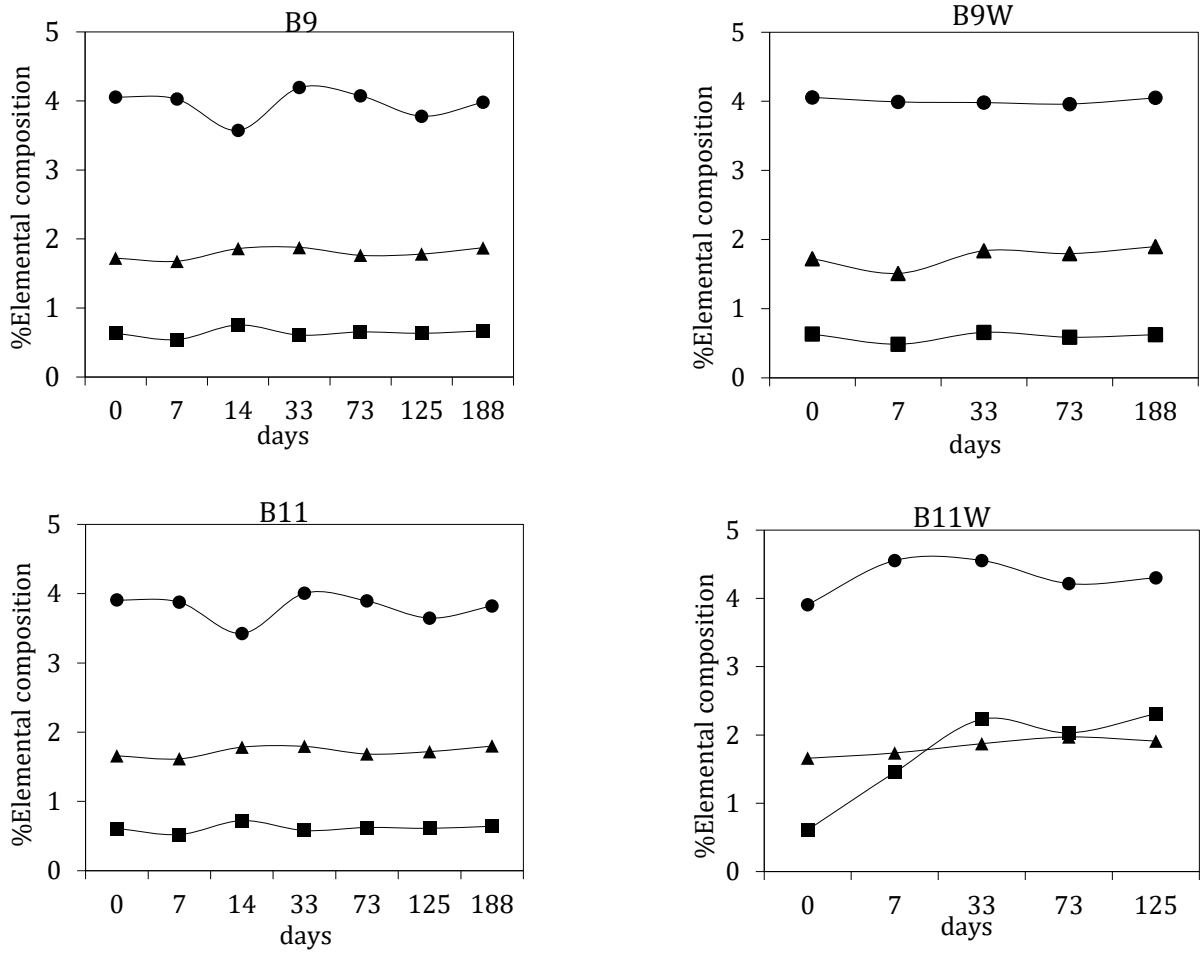


Figure 15 continued. ***Ultimate results for the dry samples and their wet counterparts. ●hydrogen, ■ total sulphur and ▲nitrogen.***

Table 10. Statistical analysis of the ultimate results

Middle Seam (MS)						**Middle Seam wet (MSW)**					
Days	**C%**	**H%**	**N%**	**S%**	**O%**	**Days**	**C%**	**H%**	**N%**	**S%**	**O%**
0	86.11	5.24	1.46	2.91	4.28	**0**	86.11	5.24	1.46	2.91	4.28
7	86.58	5.24	1.47	2.46	4.25	**7**	85.87	5.17	1.43	2.57	4.96
14	88.04	5.29	1.65	3.23	1.79	**33**	86.68	5.33	1.68	3.15	3.16
33	*89.42*	5.57	1.62	3.43	0.04	**73**	85.00	5.36	1.64	2.06	5.94
73	88.97	5.28	1.60	3.50	0.64	**125**	86.17	5.32	1.57	2.79	4.14
125	86.17	5.22	1.56	3.81	3.23	**188**	87.34	5.39	1.66	3.58	2.03
188	85.99	5.21	1.63	4.33	2.84	**Equation**	y = 0.1523x + 85.663	y = 0.0351x + 5.1783	y = 0.084x + 2.5497	y = 0.0396x + 1.4356	y = -0.3111x + 5.1737
Equation	y = -0.0086x + 87.361	y = -0.0045x + 5.3097	y = 0.0227x + 1.4818	y = 0.2581x + 2.3506	y = -0.2676x + 3.5075	**rate (% /day)**	0.1523	0.0351	0.0840	0.0396	-0.3111
rate (% /day)	-0.0086	-0.0045	0.0227	0.2581	-0.2676	**Coefficient of determination (R^2)**	0.132	0.6698	0.0918	0.484	0.1813
Coefficient of determination (R^2)	0.0002	0.0061	0.4031	0.8511	0.1188	**Pearson's correlation coefficient (r)**	0.3637	0.8184	0.3030	0.6957	0.4258
Pearson's correlation coefficient (r)	0.0141	0.0781	0.6349	0.9226	0.3447	**Population correlation coefficient (ρ)**	0.8114				
Population correlation coefficient (ρ)	0.7545					**n= 6-2**	4				
n= 7-2	5					**Comment**	insignificant	significant	insignificant	insignificant	insignificant
Comment	insignificant	insignificant	insignificant	significant	insignificant						

Table 10 continued. Statistical analysis of the ultimate results

Bench 3 (B3)						Bench 3 wet (B3W)					
Days	**C%**	**H%**	**N%**	**S%**	**O%**	**Days**	**C%**	**H%**	**N%**	**S%**	**O%**
0	89.41	5.44	1.52	3.02	0.62	**0**	89.41	5.44	1.52	3.02	0.62
7	88.25	5.34	1.50	2.51	2.41	**7**	83.42	5.22	1.34	1.85	8.18
14	88.86	5.34	1.67	3.26	0.87	**14**	84.62	5.65	1.60	2.31	5.82
33	89.55	5.57	1.62	3.43	0.18	**33**	85.66	5.37	1.71	2.41	4.84
73	89.71	5.33	1.62	3.53	0.19	**73**	82.87	5.33	1.57	2.54	7.69
125	85.83	5.20	1.55	3.80	3.62	**125**	83.54	5.21	1.63	2.10	7.52
188	85.51	5.18	1.62	4.31	3.39	**Equation**	y= -0.8552x + 87.912	y = -0.0315x + 5.4797	y = 0.0395x + 1.4233	y = -0.0698x + 2.6164	y = 0.917x + 2.569
Equation	y = -0.5598x + 90.398	y = -0.038x + 5.4939	y = 0.0131x + 1.5342	y = 0.239x + 2.453	y = 0.3591x + 0.1716	**rate (% /day)**	-0.8552	-0.0315	0.0395	-0.0698	0.9170
rate (% /day)	-0.5598	-0.038	0.0131	0.239	0.3591	**Coefficient of determination (R^2)**	0.4393	0.1319	0.3443	0.1063	0.3681
Coefficient of determination (R^2)	0.4655	0.3676	0.2068	0.8202	0.2688	**Pearson's correlation coefficient (r)**	0.6628	0.3632	0.5868	0.3260	0.6067
Pearson's correlation coefficient (r)	0.6823	0.6063	0.4548	0.9056	0.5185	**Population correlation coefficient (ρ)**	0.8114				
Population correlation coefficient (ρ)	0.7545					**n= 6-2**	4				
n= 7-2	5					**Comment**	insignificant	insignificant	insignificant	insignificant	insignificant
Comment	insignificant	insignificant	insignificant	significant	insignificant						

Table 10 continued. Statistical analysis of the ultimate results

Bench 5 (B5)						Bench 5 wet (B5W)					
Days	**C%**	**H%**	**N%**	**S%**	**O%**	**Days**	**C%**	**H%**	**N%**	**S%**	**O%**
0	86.54	6.29	1.76	3.50	1.92	**0**	86.54	6.29	1.76	3.50	1.92
7	84.41	6.25	1.76	2.94	4.64	**7**	84.34	5.38	1.55	3.01	5.72
14	83.49	6.18	1.93	3.78	4.61	**33**	84.75	5.40	1.88	4.01	3.95
33	81.81	6.51	1.90	4.01	5.78	**73**	83.03	5.15	1.92	4.73	5.17
73	84.18	6.00	1.82	3.98	4.02	**125**	80.78	5.20	1.80	5.03	7.19
125	82.45	6.08	1.82	4.44	5.22	**188**	84.57	5.50	1.98	4.12	3.84
188	81.74	5.87	1.84	4.88	5.67	**Equation**	y = -0.6362x + 86.229	y = -0.1362x + 5.9644	y = 0.0547x + 1.6231	y = 0.2828x + 3.0746	y = 0.4349x + 3.1089
Equation	y = -0.6294x + 86.034	y = -0.0642x + 6.4254	y = 0.009x + 1.7956	y = 0.2623x + 2.8824	y = 0.4222x + 2.8625	**rate (% /day)**	-0.6362	-0.1362	0.0547	0.2828	0.4349
rate (% /day)	-0.6294	-0.0642	0.009	0.2623	0.4222	**Coefficient of determination (R^2)**	0.3768	0.3777	0.4414	0.4949	0.201
Coefficient of determination (R^2)	0.6305	0.4366	0.0876	0.8157	0.478	**Pearson's correlation coefficient (r)**	0.6138	0.6146	0.6644	0.7035	0.4483
Pearson's correlation coefficient (r)	0.7940	0.6608	0.2960	0.9032	0.6914	**Population correlation coefficient (ρ)**	0.8114				
Population correlation coefficient (ρ)	0.7545					**n= 6-2**	4				
n= 7-2	5					**Comment**	insignificant	insignificant	insignificant	insignificant	insignificant
Comment	significant	insignificant	insignificant	significant	insignificant						

Table 10 continued. Statistical analysis of the ultimate results

Bench 9B (B9)						Bench 9B wet (B9W)					
Days	**C%**	**H%**	**N%**	**S%**	**O%**	**Days**	**C%**	**H%**	**N%**	**S%**	**O%**
0	86.16	4,06	1,72	0,63	7,42	**0**	86,16	4,06	1,72	0,63	7,42
7	86.71	4,03	1,68	0,54	7,04	**7**	86,37	3,99	1,51	0,49	7,64
33	87.93	3,57	1,86	0,75	5,88	**33**	86,95	3,98	1,84	0,66	6,57
73	89.48	4,19	1,88	0,61	3,84	**73**	88,16	3,96	1,80	0,59	5,49
125	88.32	4,07	1,76	0,65	5,18	**188**	89,21	4,05	1,90	0,62	4,22
188	85.56	3,78	1,78	0,63	8,24	**Equation**	y = 0,7885x + 85,005	y = -0,0044x + 4,0223	y = 0,064x + 1,5618	y = 0,0083x + 0,5734	y = -0,8564x + 8,8379
Equation	y = 0.1457x + 86.893	y = -0,0081x + 3,9872	y = 0,0201x + 1,7135	y = 0,0067x + 0,6154	y = -0,1644x + 6,7914	**rate (% /day)**	0,7885	-0,0044	0,064	0,0083	-0,8564
rate (% /day)	0.1457	-0.0081	0.0201	0.0067	-0.1644	**Coefficient of determination (R^2)**	0,935	0,0266	0,454	0,039	0,903
Coefficient of determination (R^2)	0.0523	0.0069	0.3017	0.0508	0.0548	**Pearson's correlation coefficient (r)**	0,9672	0,1631	0,6738	0,1965	0,9503
Pearson's correlation coefficient (r)	0.2287	0.0831	0.5493	0.2254	0.2341	**Population correlation coefficient (ρ)**	0,8783				
Population correlation coefficient (ρ)	0.7545					**n= 5-2**	3				
n= 7-2	5					**Comment**	significant	insignificant	insignificant	insignificant	significant
Comment	insignificant	insignificant	insignificant	insignificant	insignificant						

Table 10 continued. Statistical analysis of the ultimate results

Bench 11 (B11)						Bench 11 wet (B11W)					
Days	**C%**	**H%**	**N%**	**S%**	**O%**	**Days**	**C%**	**H%**	**N%**	**S%**	**O%**
0	85.36	3.91	1.66	0.61	8.46	**0**	85.36	3.91	1.66	0.61	8.46
7	85.71	3.88	1.62	0.52	8.27	**7**	86.09	4.56	1.74	1.45	6.17
14	86.39	3.43	1.78	0.72	7.68	**33**	85.54	4.56	1.87	2.23	5.81
33	87.50	4.01	1.79	0.58	6.12	**73**	88.60	4.22	1.97	2.03	3.18
73	85.39	3.89	1.68	0.62	8.40	**125**	86.80	4.30	1.91	2.31	4.68
125	85.58	3.65	1.72	0.61	8.44	**Equation**	y = 0.5389x + 84.86	y = 0.0445x + 4.1741	y = 0.0738x + 1.6089	y = 0.3978x + 0.5336	y = -1.055x + 8.8235
188	87.21	3.82	1.80	0.64	6.52	**Rate (% /day)**	0.5389	0.0445	0.0738	0.3978	-1.055
Equation	y = 0.1537x + 85.55	y = -0.009x + 3.8331	y = 0.0189x + 1.6468	y = 0.0063x + 0.5914	y = -0.1699x + 8.3787	**Coefficient of determination (R^2)**	0.4213	0.0684	0.8239	0.7883	0.7310
rate (% /day)	0.1537	-0.009	0.0189	0.0063	-0.1699	**Pearson's correlation coefficient (r)**	0.6491	0.2615	0.9077	0.8879	0.8550
Coefficient of determination (R^2)	0.1404	0.0096	0.3144	0.0494	0.1387	**Population correlation coefficient (ρ)**	0.8783				
Pearson's correlation coefficient (r)	0.3747	0.0980	0.5607	0.2223	0.3724	**n= 5-2**	3				
Population correlation coefficient (ρ)	0.7545					**Comment**	insignificant	insignificant	significant	significant	insignificant
n= 7-2	5										
Comment	insignificant	insignificant	insignificant	insignificant	insignificant						

5.2.2.2 Behaviour of total carbon and oxygen content over time

A simple rule of thumb in the diagnosis of weathered coal is to determine whether the carbon content has decreased with an accompanying increase in the oxygen content (Wu *et al*., 1988; Mc Hugh *et al*., 1993; Miroshnichenko *et al*., 2012a; Wang and Zhou, 2012). Figure 16 illustrates the response of the total carbon and oxygen due to weathering.

All the parent coals are characterized by a total carbon content ranging between 85%-89.41%. The oxygen content is more variable, with B11 (8.46%) and B9 (7.42%) having the highest proportions. The MS (4.28%) has a much higher oxygen content than B3 (0.62%). B5 consists of 1.92% oxygen.

The total carbon content decreased in samples MS, B3, B3W, B5 and B5W, whereas the remaining samples have increasing total carbon trends. Figure 16 shows that the weathering trends for the carbon content in the MS (0.12%) and B9 (0.55%) are very similar in that they decreased slightly by 0.12% and 0.55%, respectively. Notably, the carbon content in B3W decreased to greater extent (5.87%) compared to its dry counterpart B3 (3.9%). Despite these observations, only samples B5 and B9W have significant carbon trends (Table 10). The overall shape of the bar graph for B5 suggests an exponential decrease in total carbon, and an exponential decrease for B9W. Mirroring, the carbon content, the oxygen content only increased in B3, B3W, B5 and B5W, albeit statistically insignificant. Only sample B9W has a statistically significant oxygen trend with weathering time.

The samples which showed trends contrary to those observed in the literature, i.e. increasing carbon and decreasing oxygen, suggests that oxidation was quite minimal in those samples. For example, Isaacs and Liotta (1987) observed that the carbon content fluctuated within 156 days of weathering, whereby carbon decreased from an initial value of 68.4% to 66.9% after 2 weeks, and thereafter increased to 68.3%. Similarly, the decrease in the fixed carbon content is quite marginal in samples MS, B3, B3W, B5 and B5W. These samples do not correspond to those with decreasing fixed carbon trends i.e. MSW, B9, B9W and B11W.

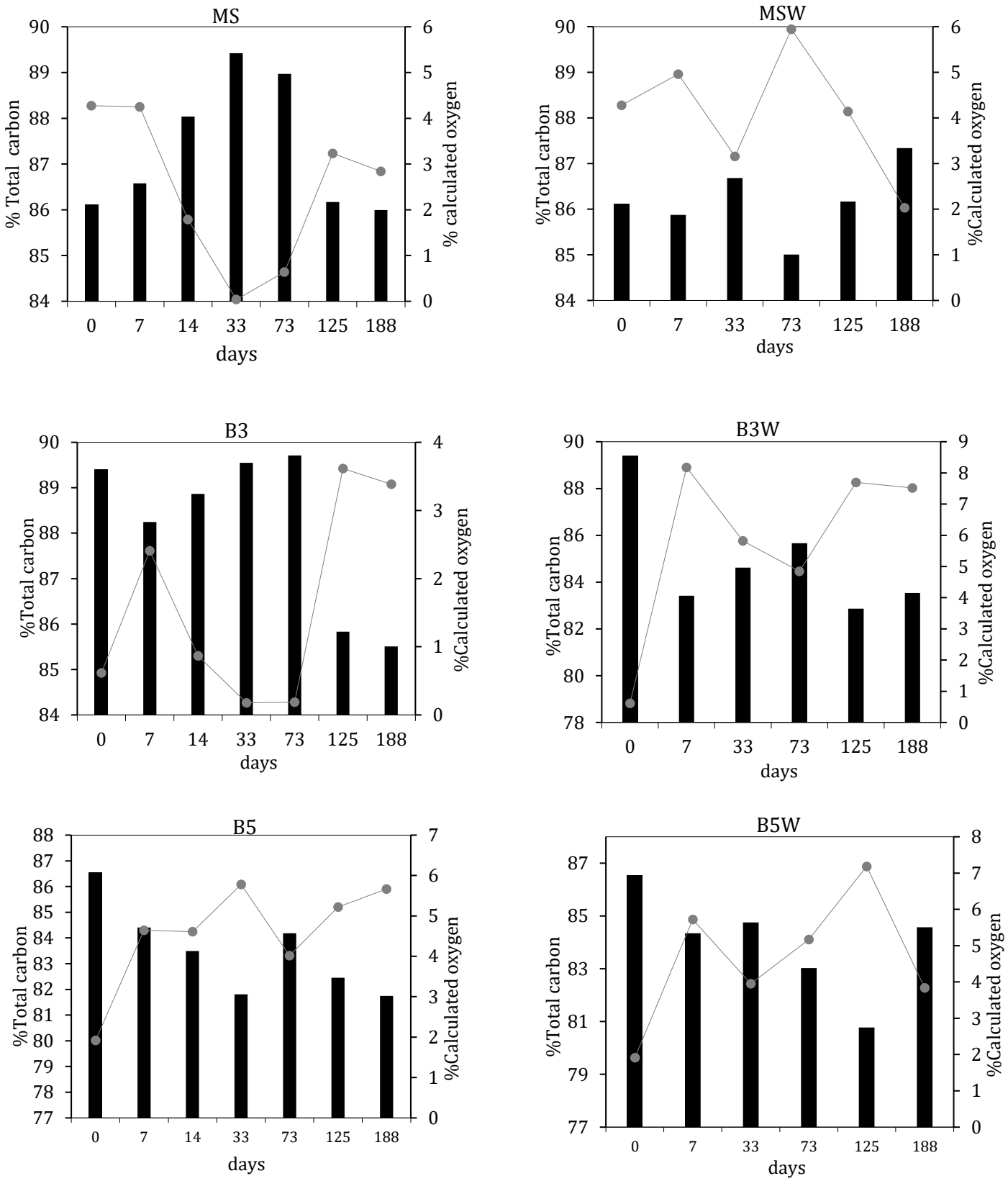


Figure 16. Total carbon (bar graph) and calculated oxygen (line graph) for the dry samples and their wet counterparts.

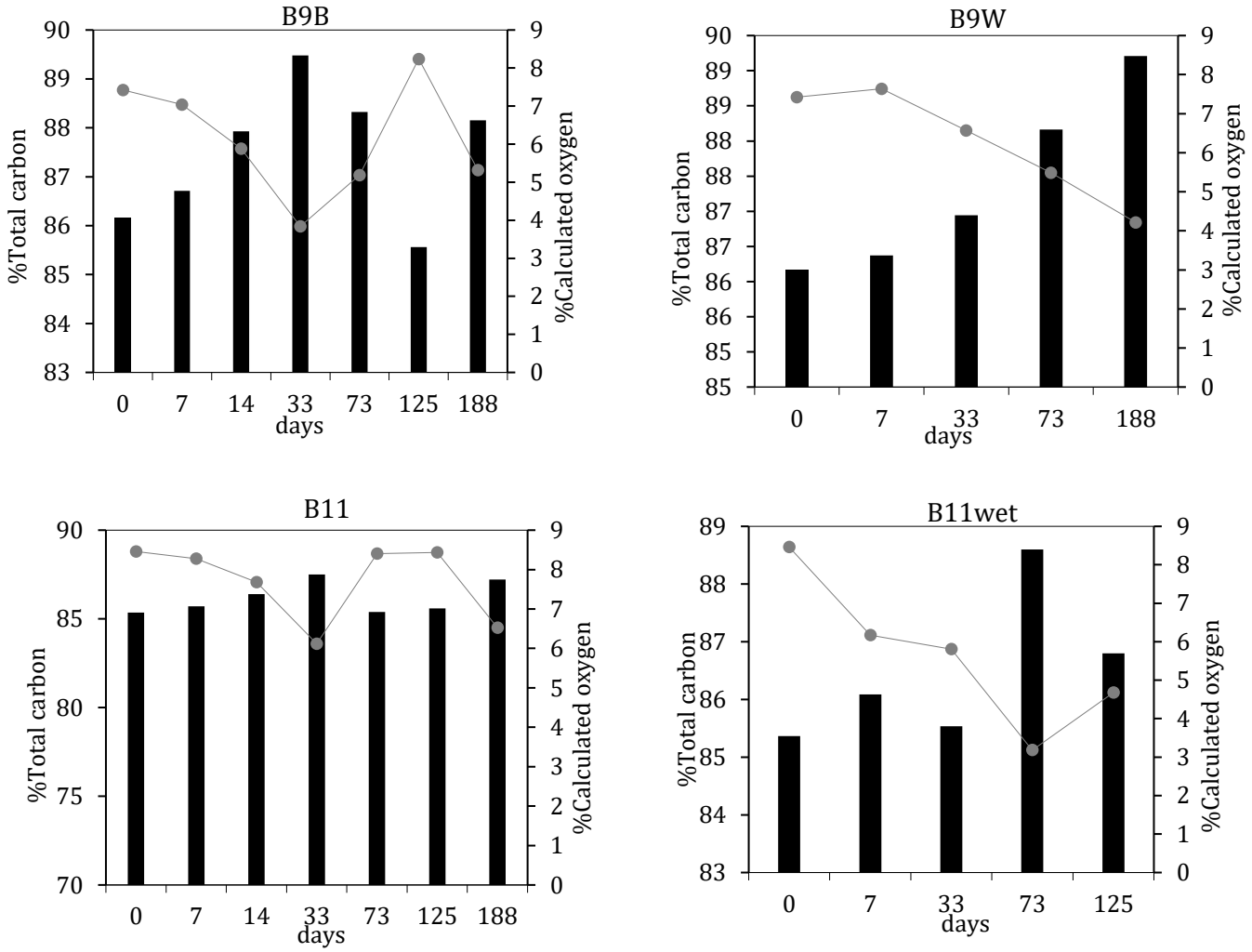


Figure 16 continued. Total carbon (bar graph) and calculated oxygen (line graph) for the dry samples and their wet counterparts

5.2.2.3 Hydrogen to carbon ratio (H/C) vs oxygen to carbon (O/C) ratio with weathering time

The trends of the H/C ratio and the O/C ratio have long been used as indicators of weathering in coals in relation to decreasing carbon, hydrogen and oxygen (Fredericks *et al*., 1983; Kus *et al.*, 2017). Figure 17 illustrates the trends in the behaviour of the H/C ratio and O/C during the weathering period.

Most of the samples, dry and wet, displayed decreasing trends in the H/C ratio, whereas samples MSW, B3W and B11W displayed increasing H/C trends. However, the trends are also characterized by a distinct peak that occurred between 14-73 days of weathering. This is true for the dry and wet counterparts of coking coals MS and B3 which show peaks in the H/C content. This trend was also observed in samples B5, B11 and B11W, although not as pronounced in samples B11 and B11W. The period between 14-73 days of the experiment marks the onset of increasing temperature conditions in spring whereby the average maximum temperature conditions increased from 21.41°C to 26.58°C and the average minimum temperature increased from 9.40°C to 13.13°C. These conditions, along with the trends in hydrogen and total carbon (Section 5.2.2.1 and Section 5.2.2.2, respectively) may have contributed to the H/C peaks, but the peak average maximum temperature at four months (27.46°C) did not coincide with any peak in the H/C content.

The increasing H/C trends indicates that those samples remained relatively unaffected by weathering, compared to those with a decreasing H/C trend. The H/C ratio is directly related to the aromaticity in the coals hence, it can be inferred that samples with a decreasing trend in the H/C reflect increasing aromaticity and therefore oxidation of the coal (Liotta *et al*., 1983; McHugh *et al*., 1991; ICCP, 1998). Only samples B3, B3W, B5 and B5W displayed increasing O/C trends, consistent with the findings in the literature mentioned above however the rest of the samples (MS, MSW, B9, B9W, B11 and B11W) displayed decreasing trends which are consistent with the fact that the oxygen content displayed a decreasing trend. It is unlikely that the additional moisture received by B3W and B5W resulted in and increasing O/C trend since the other wet samples did not behave in a similar manner. A further example is B9W which shows a near linear decrease in both the H/C and O/C ratios compared to its dry counterpart B9. This difference is likely due to its inherent properties, i.e. the exponential increase in the total carbon with increasing exposure to weathering, accompanied by decreasing oxygen as described in Section 5.2.2.2.

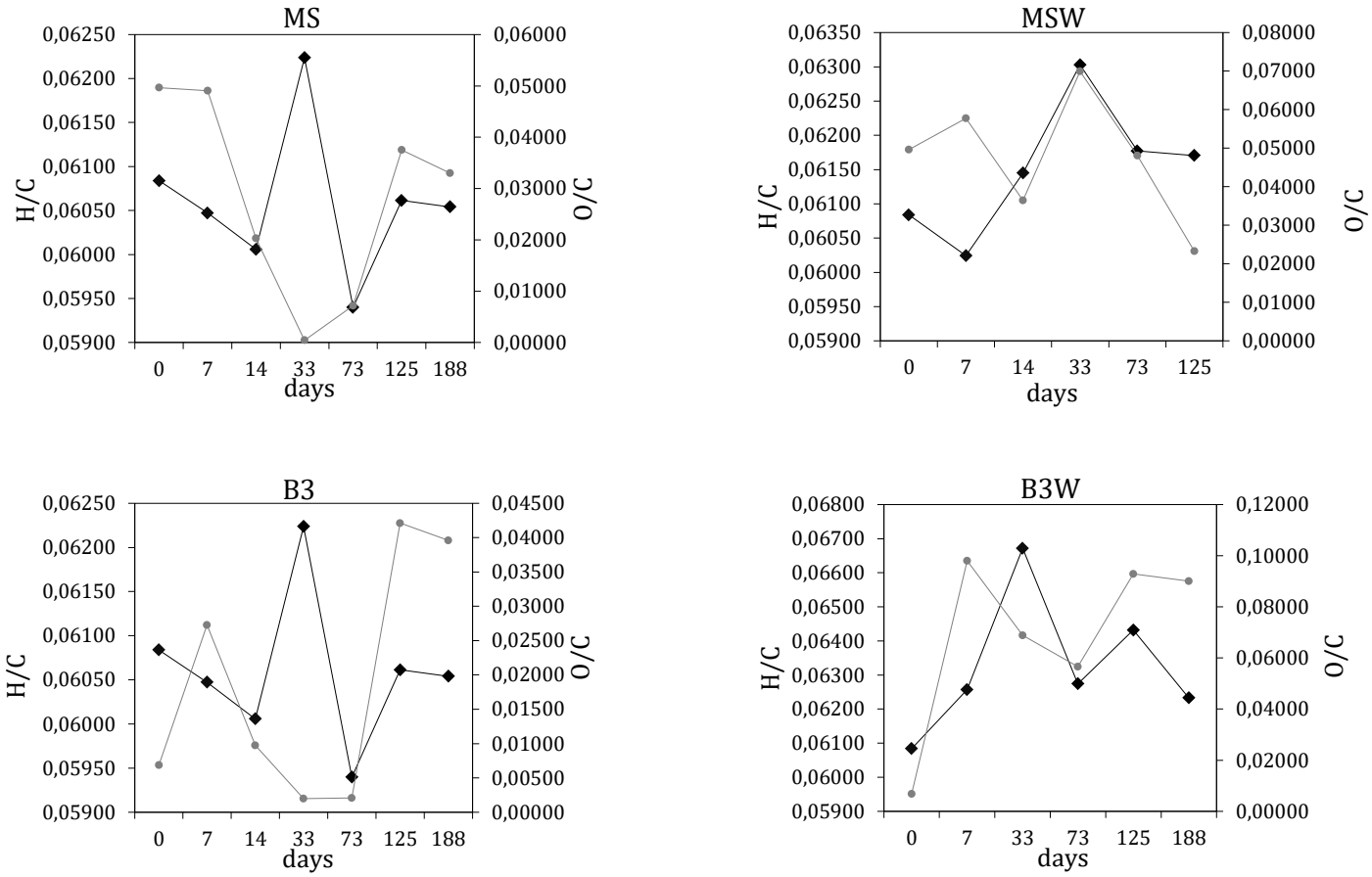
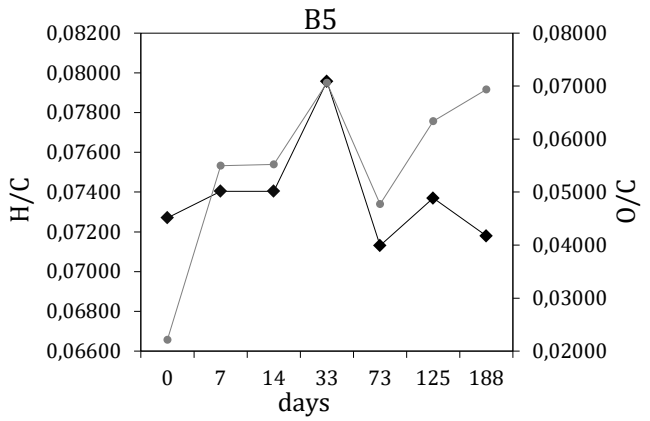
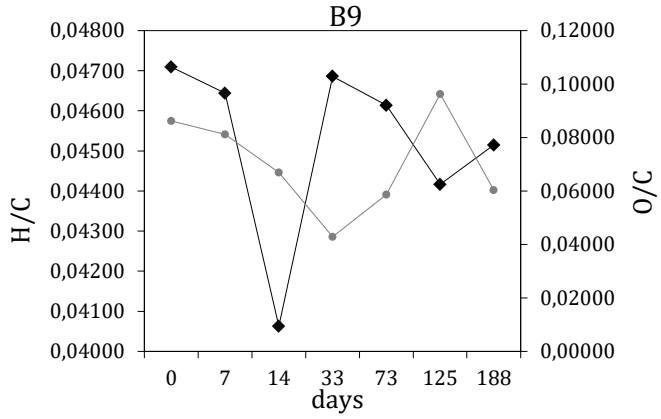
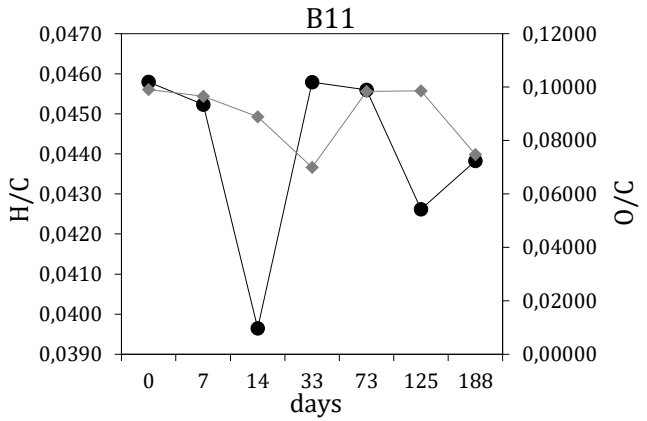
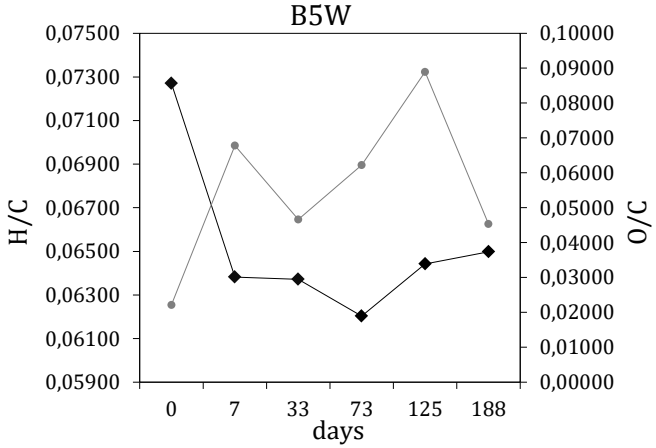


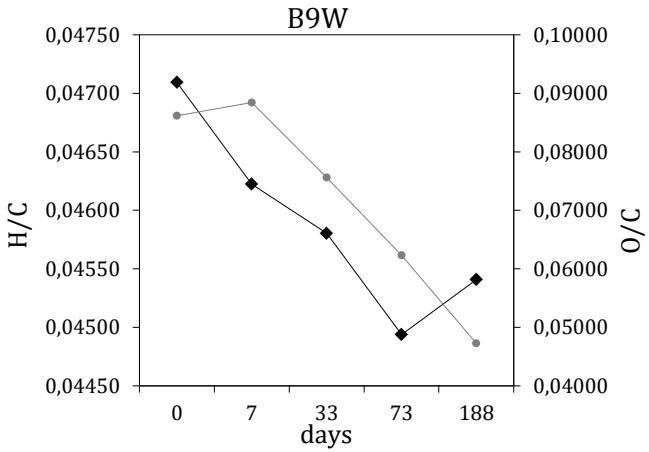
Figure 17. The H/C ratio (♦) and the O/C ratio (●) for the dry samples and their wet counterparts.











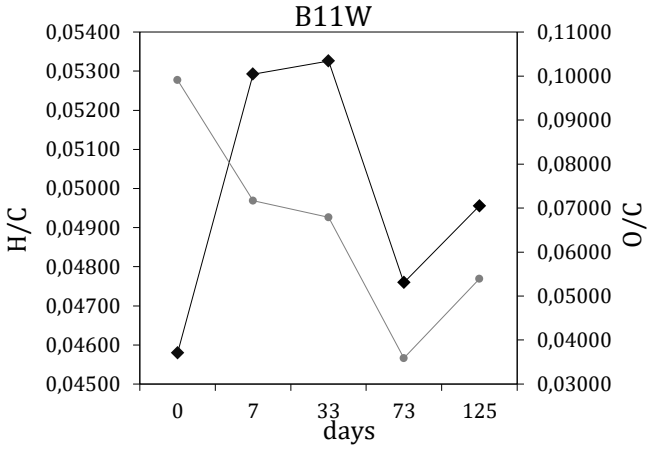


Figure 17 continued. The H/C ratio (♦) and the O/C ratio (●) for the dry samples and their wet counterparts.

5.3 Calorific Value (CV)

The trends in the calorific value are illustrated in Figure 18 for each sample over the duration of the study. The statistical significance of the trends is discussed with respect to the correlation coefficient (r) and population correlation coefficient (P) which are recorded in Table 11.

The calorific value slightly decreased in all the wet and dry coals (excluding sample B5). The decreases were however, only significant in samples the MS, B9, B9W, B11 and B11W (Table 11). Furthermore, the decrease in the calorific values were predominantly higher in the dry samples. The samples that show significant decreases in the CV are characterized by almost linear graphs, whereas the samples that have insignificant CV trends appear to have oscillating line graphs.

Rees *et al* (1961), in Kus *et al.* (2017), reported that the calorific value decreased by 5% from the original value after 25 years of weathering. In the present study the highest decrease (1.21 MJ/kg) occurred in MS and the lowest decrease (0.1 MJ/kg) occurred in B3. The decrease in the calorific value of coal due to oxidation has also been noted by many authors (Hamilton, 1907; Fredericks *et al*., 1983; Isaacs and Liotta, 1987; Wu *et al*., 1988; Pisupati *et al*, 1993; Martinez and Escobar, 1995; Kruszewska and du Cann, 1996; Kus *et al.*, 2017). Hamilton (1907) noted that the CV tends to decrease when coal is exposed to high temperatures. Compared to other technological properties the CV is the most resilient property in coals as it can take a number of years of exposure to natural weathering before the CV decreases significantly. This is especially true in discarded coal in that even after years of weathering, the CV of the discards may still be suitable for combustion when blended with fresh coal (Falcon, 1986; Wagner, 2008; Kus *et al.*, 2017).

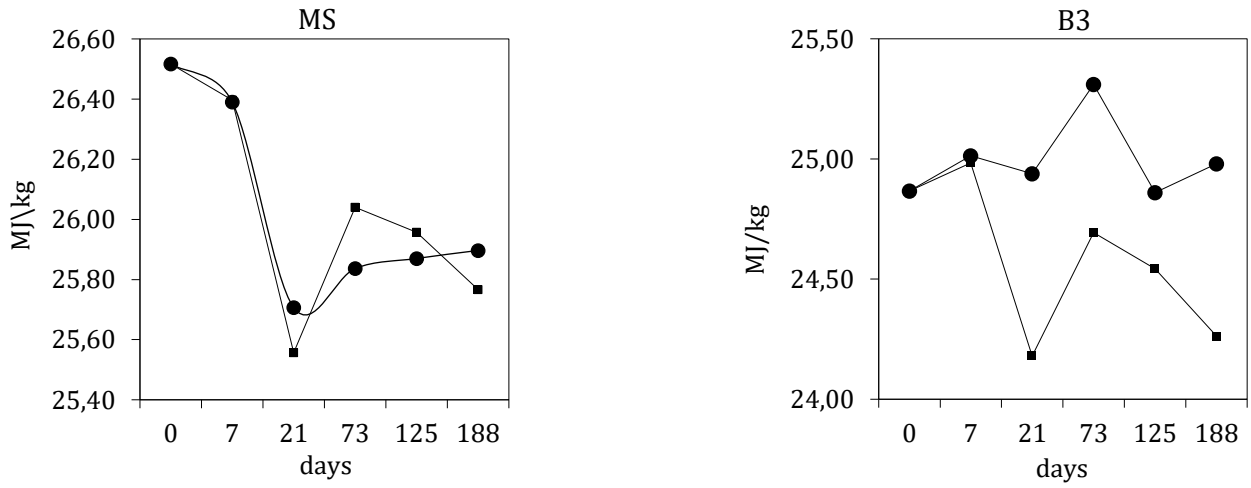


Figure 18. The behaviour of the calorific value for the dry samples (●) and their wet counterparts (■).

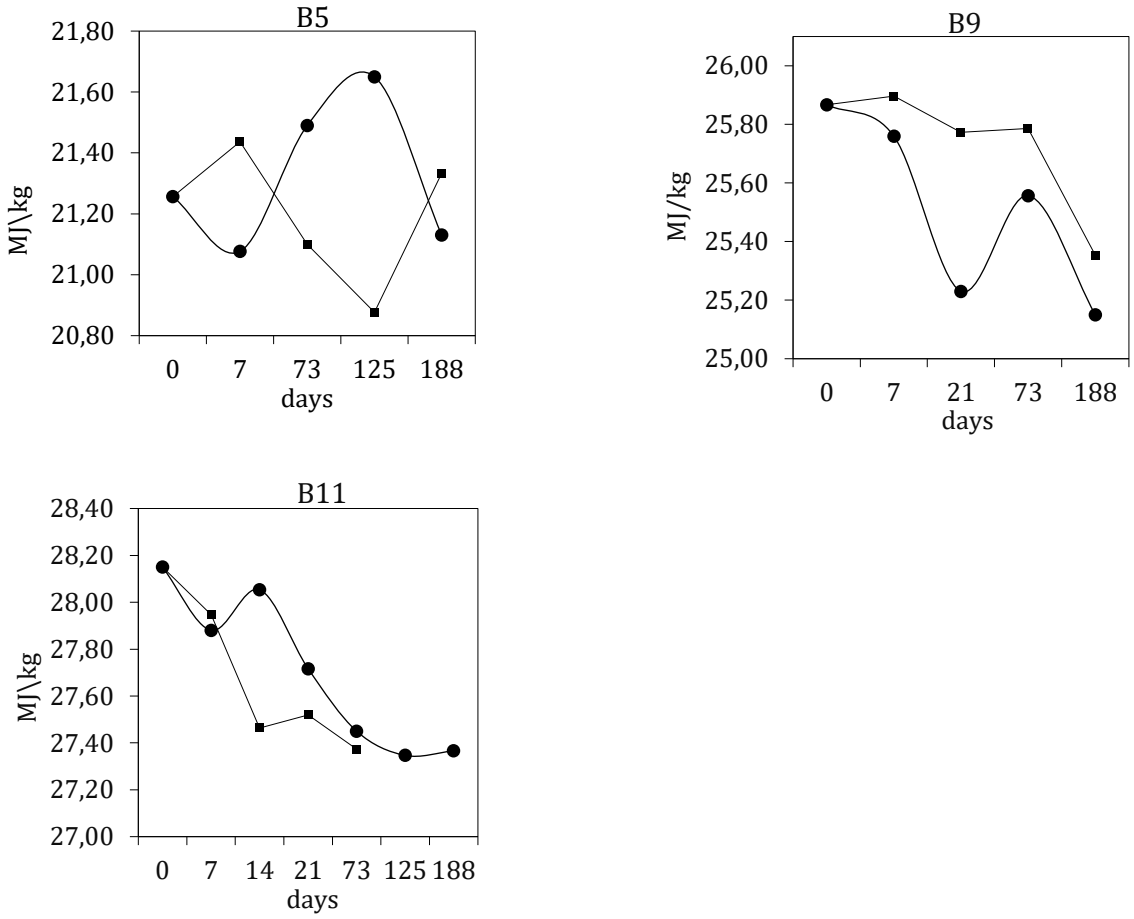


Figure 18 continued19. The behaviour of the calorific value for the dry samples (●) and their wet

Table 11. Statistical analysis of the calorific value

Days	MS	B3	B5	B9	B11	Days	MSW	B3W	B5W	B9W	B11W
0	26.52	24.87	21.26	25.87	28.15	**0**	26.52	24.87	21.26	25.87	28.15
7	26.39	25.01	21.08	25.76	27.88	**7**	26.40	24.98	21.44	25.90	27.95
14	25.71	24.94	21.49	25.23	28.05	**21**	25.56	24.18	21.39	25.77	27.46
21	25.84	25.31	21.65	25.56	27.72	**73**	26.04	24.69	21.10	25.79	27.52
73	25.87	24.86	21.13	25.15	27.45	**125**	25.96	24.54	20.88	-	27.37
125	25.90	24.98	20.39	25.48	27.35	**188**	25.77	24.26	21.33	25.35	28.15
188	25.31	24.86	-	25.09	27.37	**Equation**	y = -0.131x + 26.498	y = -0.0937x + 24.934	y = -0.0452x + 21.39	y = -0.1137x + 26.076	y = -0.198x + 28.285
Equation	y = -0.1583x + 26.566	y = -0.0059x + 24.999	y = 0.0301x + 20.639	y = -0.106x + 25.872	y = -0.1436x + 28.283	**Rate (MJ/kg per day)**	-0.131	-0.0937	-0.0452	-0.1137	-0.198
Rate (MJ/kg per day)	-0.1583	-0.0059	0.0301	-0.106	-0.1436	**Coefficient of determination (R^2)**	0.4488	0.2237	0.1625	0.6685	0.8559
Coefficient of determination (R^2)	0.7024	0.0064	0.0032	0.5728	0.8774	**Pearson's correlation coefficient (r)**	0.6699	0.4730	0.4031	0.8176	0.9251
Pearson's correlation coefficient (r)	0.8381	0.0800	0.0566	0.7568	0.9367	**Population correlation coefficient (ρ)**	0.8114				
Population correlation coefficient (ρ)	0.7545					**n= 6-2**	4				
n= 7-2	5					**Comment**	insignificant	insignificant	insignificant	significant	significant
Comment	significant	insignificant	insignificant	significant	significant						

5.4 Thermogravimetric analysis (TGA)

The derivative thermogravimetric curves (DTG) for selected dry and wet counterparts of Bench 5 are plotted in Figure 20. This coal was selected for TGA because it is a thermal coal utilized for power generation; hence the results of this analysis provides insight into its performance during combustion. The limits of the parameters on the burning profiles were determined according to those proposed by Pisupati (1996), whereby the initial temperature (IT) is defined as the temperature at which the rate of weight loss exceeds 0.1 min^{-1} after the initial moisture loss peak. The peak temperature (PT) is defined as the temperature at which the rate of weight loss was maximum and the burnout temperature (BT) is the temperature at which the rate of weight loss decreased to 1.0 min^{-1}. The complete data set is tabulated in Appendix F and is summarized in Table 12.

The initial temperature of the fresh sample is 290.73 °C and thereafter increased to 344,74°C and 345,43°C after 6 months of weathering in the dry and wet samples respectively. On the one hand, Pisupati *et al*. (1991) observed that weathered coals ignite at lower temperatures relative to their fresh counterparts. On the other hand, Banerjee *et al*., (2000) observed that weathered coals ignite at higher temperatures compared to their weathered counterparts.

All the dry and wet subsets of Bench 5 underwent increases in mass, especially at higher temperatures which, according to literature, is indicative of multiple stages of oxidation. (Crelling *et al*., 1992). The percentage of the sample weight in the current investigation increased by an average of 0.38 wt % and thus it is argued that this increase was due to oxygen adsorption. The oxidation stages typically occurred between temperature intervals of 35.46-53.79°C and 129.03-284.86°C. Pisupati (1996) reported a higher weight change of up to 3 wt % for laboratory oxidised coals that had been oxidised for up to 72 hours.

Devolatilization in the wet and dry samples commenced at lower temperatures with increasing exposure to weathering. The fresh sample initially devolatilized at 284.84°C, and thereafter progressively decreased such that the wet sample devolatilized at 281.75 °C after 6 months of weathering. Similarly, the onset of devolatilization in the dry sample occurred at 282.63°C after six months of weathering. This is in agreement with Pisupati *et al* (1991) and Banerjee *et al* (2000) who also reported that weathered coals readily lose their volatiles at lower temperatures.

The peak temperature of both the dry and wet samples appeared to increase slightly with weathering time from 431.46 to 438.34°C after four months of weathering in the dry samples, and also increased from 431.46 to 446.97°C in the wet samples after six months of weathering. However, the peak temperature of the dry six-month sample occurred at a lower temperature (423.79°C) compared to the fresh sample. According to Norton (1993), coals that combust at higher peak temperatures burn slower

and at higher temperatures, whereas coals that combust at lower peak temperatures ignite and burn more easily.

Overall, the dry and wet samples burned out at lower temperatures with increasing exposure to weathering. After six months of weathering, the burn out temperature decreased from 524.50°C to 521.42°C in the dry samples and from 524.50°C to 522.15°C in the wet samples. In contrast, Banerjee *et al* (2000) observed that weathered coals burn out at higher temperatures compared to their fresh counterparts.

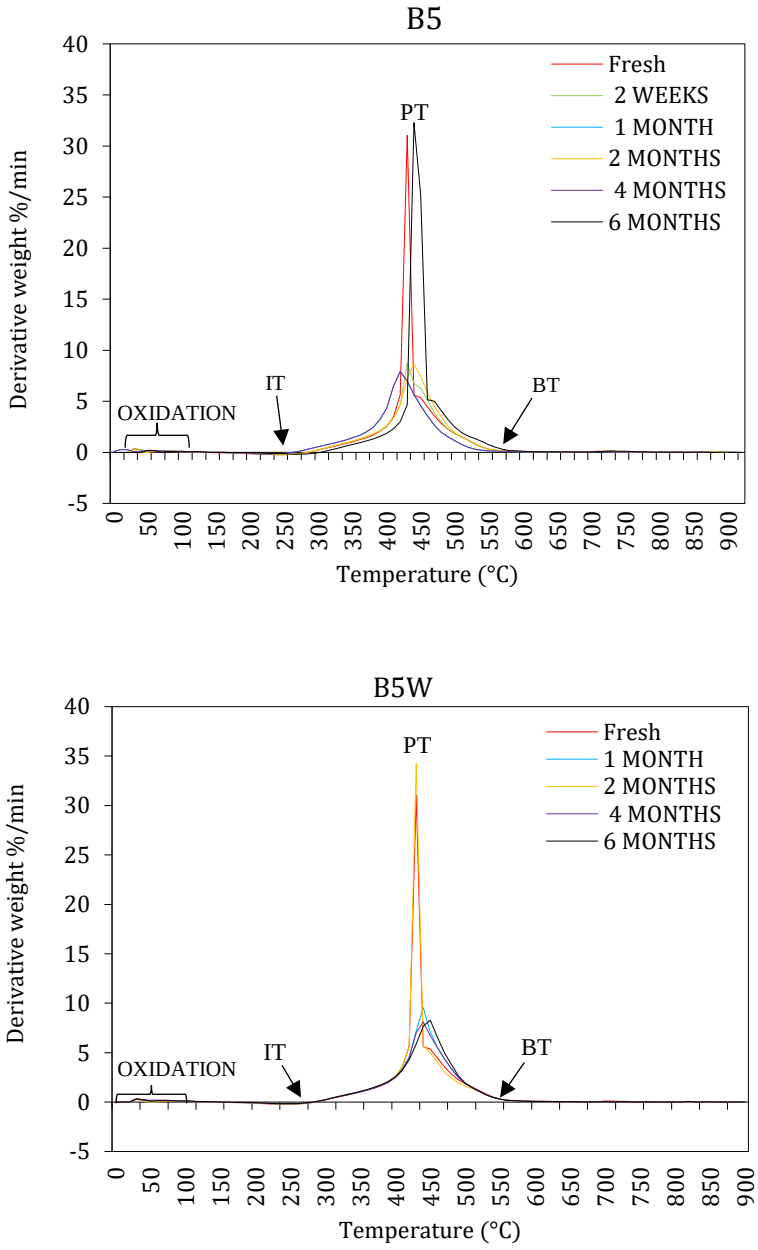


Figure 20. DTG curves for B5 and its wet counterpart B5W showing temperature (x-axis) vs rate of mass loss 1 % min^{-1} (y-axis).

To summarize, both the dry and wet samples of Bench 5 ignited at higher temperatures compared to the fresh parent sample and were characterized by higher peak temperatures, whereas devolatilization and complete combustion (BT) commenced at lower temperatures. Notably the changes in the initial temperature, devolatilization temperature and peak temperature were slightly more pronounced in the wet sample compared to its dry counterpart. This suggests that the reactivity of the wet sample was slightly more impaired compared to the samples that oxidised under relatively dry conditions. Hence, it can be inferred that as weathering progresses, the affected particles will be rapidly consumed in the furnace at lower temperatures compared to the fresh particles, which may in turn necessitate greater quantities of coal to compensate the rapid combustion. Further investigation is necessary to better understand the ramifications of combustion with coals that have undergone dry versus wet oxidation.

Table 12. Summary of thermogravimetric analysis results

Sample	**Devolatilization Temperature °C**	**Initial Temperature °C**	**Peak Temperature °C**	**Burn out Temperature °C**	
B5B	284.84	292.15	431.46	524.50	
B5 W2	284.77	344.01	436.09	523.81	
B5 M1	284.55	347.62	437.56	524.58	
B5 M2	283.78	344.65	437.04	523.81	
B5 M4	283.07	349.01	438.34	523.23	
B5 M6	282.63	344.74	423.79	521.42	
B5W M1	283.98	345.56	438.81	523.65	
B5W M2	283.50	346.89	432.99	521.43	
B5W M4	283.14	349.18	436.65	522.37	
B5W M6	281.75	345.43	446.97	522.15	
Sample	**Start of oxidation Temperature °C**	**End of oxidation Temperature °C**	**Sample**	**Start of oxidation Temperature °C**	**End of oxidation Temperature °C**
B5B	36.06	36.03	**B5 M6**	35.65	49.51
	35.46	48.13		138.18	138.6
	132.75	284.76		144.29	144.8
B5 W2	35.52	45.39		149.74	150.5
	140.08	284.68		151.17	152.43
B5 M1	35.61	145.89		154.10	157.21
	147.32	284.47		158.12	181.58
B5 M2	36.50	36.44	**B5W M1**	36.80	36.75
	35.79	52.27		35.83	52.18
	140.01	140.68		134.16	134.99
	141.85	143.02		137.94	140.28
	143.95	145.87		140.62	142.21
	147.12	148.04		143.05	283.89
	148.96	283.7	**B5W M2**	36.18	36.17
B5 M4	35.52	45.65		35.93	35.9
	153.60			35.82	53.79
	155.69	156.2		141.90	283.41
	158.80	161.9	**B5W M4**	150.68	151.1
	163.24	282.99		154.11	283.05
			B5W M6	35.46	44.18
				159.00	160.26
				162.44	281.67

5.5 Free Swelling Index (FSI)

The plasticity of coking coals MS and B3 is discussed in terms of the FSI, which, on a scale of 0 to 9, gives an indication of how well the coal will swell. The statistical significance of the trends is discussed with respect to the correlation coefficient (r) and population correlation coefficient (P) which are recorded in Table 13.

The MS and B3 samples initially had swelling values of 3 and 1.5 respectively, corresponding to a medium caking and weakly caking strength according to Speight (2005). After the first week of weathering, both MS and MSW increased in their FSI, followed by a progressive decrease over the remainder of the experiment (Figure 21). Notably the increase in the FSI for MSW was higher than its dry counterpart MS, however both samples had the same FSI value of 0.5 at the end of the experiment. MSW displayed the fastest decrease in the FSI at a significant rate ($r = 0.8607$; $\rho = 0.8114$) of -0.6286 per day compared to the MS which decreased by -0.59 units per day which is significant ($r = 0.9460$; $\rho = 0.8114$). The rate in the decrease of the FSI for B3 was lower relative to the wet and dry samples of the Middle Seam. B3 decreased significantly ($r = 0.6770$; $\rho = 0.8114$) at a rate of -0.1964 per day, similarly, the FSI of B3W also decreased significantly ($r = 0.9249$; $\rho = 0.8114$) at a rate of -0.33 per day.

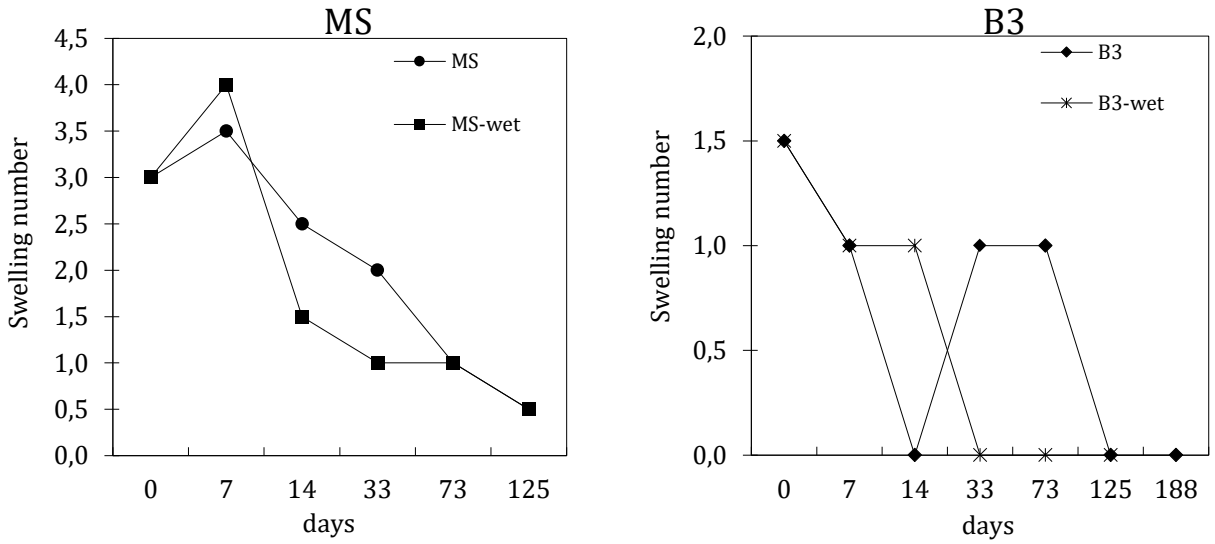


***Figure 21*. Trends in the free swelling index for coking coals the from the Middle Seam (MS) and Bench 3 (B3).**

In summary, the FSI decreased in a similar manner to the study conducted by Jha *et al* (2014), where the FSI of two Indian coking coals decreased from an initial value of 3 to 1.5 and from 1.5 to 1 after just two months of weathering in a similar experimental set up to the present study. Jha *et al* (2016) noted that the FSI of prime quality coking coal (FSI = 5.5) decreased significantly during the first few weeks of weathering, and then levelled off for the remainder of the experiment. The slight increase in the swelling of coking coals MS and MSW after one week of weathering is in agreement with the findings of Alvarez *et al* (1998), who noted that mild oxidation conditions may serve to improve the

strength of coking coals, especially those of higher rank. Although it has been reported that the hydrogen content of coal is highly susceptible to low temperature oxidation, which translates to a rapid decrease in the coals swelling propensity during weathering (Yohe,1958; Mondragón *et al*., 2002; Kus *et al.*, 2017), the hydrogen content in the present study decreased marginally despite the FSI decreasing to zero after 6 months of weathering. Huffman *et al*., (1985) observed that coking coals with high initial FSI values such as Pittsburgh coke (FSI =8.5) and Pocahontas no 3. coke (FSI = 7.5) were not severely impaired as the FSI was reduced to values of 8 and 4.5 respectively, after 436 days of weathering outdoors.

Table 13. Statistical analyses of coking coals MS and B3.

MS		**MSW**	
Days	**FSI**	**Days**	**FSI**
0	3.0	**0**	3.0
7	3.5	**7**	4.0
14	2.5	**33**	1.5
33	2.0	**73**	1.0
125	1.0	**125**	1.0
188	0.5	**188**	0.5
Equation	y = -0.5857x + 4.1333	**Equation**	y = -0.6286x + 4.0333
Rate	-0.59	**Rate**	-0.6286
Coefficient of determination (R^2)	0.8949	**Coefficient of determination (R^2)**	0.7408
Pearson's correlation coefficient (r)	0.9460	**Pearson's correlation coefficient (r)**	0.8607
Population correlation coefficient (ρ)	0.8114	**Population correlation coefficient (ρ)**	0.8114
n= 6-2	4	**n= 6-2**	4
Comment	significant	**Comment**	significant
B3		**B3W**	
Days	**FSI**	**Days**	**FSI**
0	1.5	**0**	1.5
7	1.0	**7**	1.0
33	0.5	**33**	1.0
73	1.0	**73**	0.5
125	1.0	**125**	0.0
188	0.0	**188**	0.0
Equation	y = -0.1964x + 1.4286	**Equation**	y = -0.3286x + 1.7333
Rate	-0.1964	**Rate**	-0.3286
Coefficient of determination (R^2)	0.4583	**Coefficient of determination (R^2)**	0.8555
Pearson's correlation coefficient (r)	0.6770	**Pearson's correlation coefficient (r)**	0.9249
Population correlation coefficient (ρ)	0.8114	**Population correlation coefficient (ρ)**	0.8114
n= 6-2	4	**n= 6-2**	4
Comment	significant	Comment	significant

5.6 Mineralogy

The inorganic (mineral) composition of the coal is discussed using the results obtained from XRD, XRF, electron microprobe analysis, and Raman spectroscopy.

5.6.1 Inorganic (mineral) composition of the coal

The mineralogy of the fresh parent samples was determined on a weight percentage (wt%) basis using XRD and are recorded in Table 14.

The silicate phases detected are quartz, kaolinite, illite, smectite, mica and palygorskite. Calcite and dolomite are the carbonate phases, while the phosphates detected are fluorapatite, goyazite and gorceixite. Pyrite is the only sulphide detected in all the coals. Of these minerals, quartz and kaolinite are the major minerals detected in all the samples, comprising proportions greater than 20 wt%. Calcite, dolomite, pyrite, mica and smectite each constituted usually less than 15 wt% of the samples. Goyazite/gorceixite was only detected in samples B9B and B9W whereas, fluorapatite was detected in all the coals excluding samples B11 and B11W. Fluorapatite, goyazite/gorceixite and palygorskite are considered accessory minerals due to their relatively small proportions (generally less than 7 wt%).

After a month of weathering, white precipitates were observed on the surfaces of samples B3W and B5W. The identity of this precipitate was confirmed in samples B5W and B11W as gypsum. Previously gypsum had been omitted from the analysis due to the high background of the samples. Speight (2005) noted that extremely weathered coals are characterised by a high sulphate content exceeding 0.1 wt%, however, 0.1 wt% was below the detection limit of the XRD instrument indicating that only minor oxidation had occurred in the samples. Furthermore, gypsum of up to 3 wt% was only detected in samples B5, B5W and B11W by XRD. This indicates that XRD is not a suitable tool for the detection of mineral alteration during the early stages of weathering due to low detection limits. Gupta (2007) and others (Sen *et al*., 2009; Matjie *et al*., 2011) suggest the integrated use of conventional analyses with advanced techniques such as EMPA, Raman Spectroscopy and QEMSCAN for mineralogical investigations. A similar approach was followed to assist in the detection of mineral transformations during the early stages of weathering by utilizing, EMPA, Raman, and FE-SEM.

Table 14. Mineralogy of coal samples as determined by XRD (wt%).

Minerals (wt%)	$CaCO_3$	$CaMg(CO_3)_2$	FeS_2	SiO_2	$Al_2Si_2O_5(OH)_4$	$KAl_2(AlSi_3O_{10})(F,OH\ v)2$	$Na_{0.33}(Al_{1.67}Mg_{0.33})Si_4O_{10}(OH)_2$	$(Mg,Al)_2Si_4O_{10}(OH)\cdot4(H_2O)$	$BaAl_3(PO_4)(PO_3OH)(OH)_6$.	$Ca_5(PO_4)_3F$	$CaSO_4\cdot2H_2O$
Time	**Calcite**	**Dolomite**	**Pyrite**	**Quartz**	**Kaolinite**	**Mica**	**Smectite**	**Palygorskite I/S**	**Goyazite/Gorceixite**	**Fluorapatite**	**Gypsum**
Middle Seam (MS)											
0 days	10.00	2.00	10.00	34.00	34.00	7.00	3.00	-	-	-	-
1 week	15.00	2.00	5.00	36.00	31.00	7.00	2.00	2.00	-	-	-
2 weeks	16.00	2.00	7.00	38.00	33.00	-	-	4.00	-	-	-
1 Month	18.00	2.00	9.00	34.00	33.00	-	2.00	2.00	-	-	-
2 Months	14.00	3.00	9.00	32.00	31.00	7.00	-	-	-	-	-
4 Months	15.00	-	8.00	37.00	30.00	-	3.00	7.00	-	-	-
Middle Seam wet (MSW)											
6 Months	12.00	2.00	11.00	31.00	30.00	8.00	-	-	-	2.00	-
0 days	10.00	2.00	10.00	34.00	34.00	7.00	3.00	-	-	-	-
1 week	15.00	2.00	5.00	36.00	31.00	7.00	2.00	2.00	-	-	-
1 Month	10.00	2.00	9.00	42.00	34.00	-	-	3.00	-	-	-
2 Months	11.00	3.00	7.00	33.00	32.00	9.00	-	-	-	-	-
4 Months	10.00	2.00	6.00	39.00	36.00	-	-	5.00	-	2.00	-
6 Months	12.00	3.00	7.00	34.00	29.00	9.00	-	-	-	3.00	-
Bench 3 (B3)											
0 days	-	4.00	3.00	38.00	50.00	4.00	1.00	-	-	-	-
1 week	-	8.00	5.00	40.00	43.00	4.00	-	-	-	-	-
2 weeks	1.00	9.00	5.00	36.00	46.00	3.00	-	-	-	-	-
1 Month	-	5.00	4.00	40.00	46.00	5.00	-	-	-	-	-
2 Months	-	7.00	5.00	37.00	45.00	5.00	-	-	-	3.00	-
4 Months	-	10.00	4.00	40.00	41.00	5.00	-	-	-	-	-
6 Months	-	10.00	5.00	39.00	41.00	5.00	-	-	-	-	-
Bench 3 wet (B3W)											
0 days	-	4.00	3.00	38.00	50.00	4.00	1.00	-	-	-	-
1 week	-	8.00	4.00	43.00	42.00	3.00	-	-	-	-	-
1 Month	-	7.00	4.00	38.00	46.00	5.00	-	-	-	-	-
2 Months	5.00	-	9.00	21.00	51.00	4.00	-	-	-	9.00	-
4 Months	-	9.00	6.00	40.00	42.00	3.00	-	-	-	-	-
6 Months	9.00	-	8.00	41.00	35.00	7.00	-	-	-	-	-
Bench 5 (B5)											
0 days	5.00	-	9.00	21.00	52.00	5.00	1.00	-	-	7.00	-
1 week	11.00	-	3.00	22.00	55.00	3.00	-	-	-	6.00	-
2 weeks	3.00	-	8.00	23.00	55.00	3.00	-	-	-	8.00	-
1 Month	3.00	-	11.00	23.00	53.00	4.00	-	-	-	6.00	-
2 Months	-	5.00	5.00	33.00	48.00	5.00	-	-	-	3.00	-
4 Months	5.00	-	7.00	21.00	54.00	5.00	1.00	2.00	-	5.00	-
6 Months	5.00	-	8.00	21.00	54.00	4.00	-	-	-	7.00	1.00
Bench 5 wet (B5W)											
0 days	5.00	-	9.00	21.00	52.00	5.00	1.00	-	-	7.00	-
1 week	2.00	-	3.00	26.00	58.00	4.00	-	2.00	-	7.00	-
1 Month	2.00	-	8.00	24.00	56.00	4.00	-	-	-	6.00	-
2 Months	4.00	-	7.00	20.00	53.00	5.00	-	-	-	11.00	-
4 Months	2.00	-	10.00	21.00	54.00	4.00	-	-	-	6.00	3.00
6 Months	2.00	-	7.00	21.00	56.00	5.00	-	-	-	8.00	2.00

Bench 9B (B9)											
0 days	14.00	12.00	1.00	3.00	61.00	-	3.00	2.00	3.00	1.00	-
1 week	15.00	13.00	-	-	64.00	-	2.00	2.00	2.00	2.00	-
2 weeks	16.00	13.00	1.00	-	63.00	-	-	2.00	3.00	2.00	-
1 Month	20.00	12.00	-	-	62.00	-	1.00	1.00	3.00	1.00	-
2 Months	15.00	13.00	-	-	62.00	-	-	-	2.00	4.00	-
4 Months	17.00	16.00	-	-	55.00	-	3.00	2.00	5.00	2.00	-
6 Months	15.00	12.00	-	-	59.00	2.00	-	-	4.00	3.00	-
Bench 9B wet (B9W)											
0 days	14.00	12.00	1.00	3.00	61.00	-	3.00	2.00	3.00	1.00	-
1 week	17.00	11.00	-	-	64.00	-	1.00	2.00	3.00	2.00	-
1 Month	18.00	13.00	-	-	62.00	-	1.00	1.00	3.00	2.00	-
2 Months	14.00	12.00	-	-	68.00	-	-	-	3.00	-	-
4 Months	-	12.00	7.00	10.00	67.00	-	2.00	2.00	-	-	-
6 Months	13.00	12.00	-	-	61.00	2.00	-	-	6.00	4.00	-
Bench 11 (B11)											
0 days	-	15.00	7.00	7.00	66.00	2.00	3.00	-	-	-	-
1 week	-	18.00	4.00	9.00	67.00	7.00	2.00	2.00	-	-	-
2 weeks	-	18.00	5.00	9.00	66.00	-	-	2.00	-	-	-
1 Month	-	15.00	6.00	9.00	68.00	-	1.00	1.00	-	-	-
2 Months	-	19.00	7.00	7.00	62.00	-	-	-	-	-	-
4 Months	-	23.00	4.00	8.00	60.00	-	3.00	2.00	-	-	-
6 Months	-	18.00	4.00	8.00	64.00	2.00			-	-	-
Bench B11 wet (B11W)											
0 days	-	15.00	7.00	7.00	66.00	2.00	3.00	-	-	-	-
1 week	-	19.00	8.00	8.00	64.00	-	1.00	-	-	-	-
1 Month	-	16.00	6.00	18.00	58.00	-	1.00	1.00	-	-	-
2 Months	-	18.00	5.00	6.00	67.00	-	-	-	-	-	-
4 Months	-	16.00	5.00	9.00	63.00	-	4.00	2.00	-	-	3.00
6 Months	-	6.00	5.00	37.00	46.00	-	4.00	2.00	-	-	-

5.6.2 Mineral transformations due to weathering

As discussed in the preceding section, gypsum was identified as an alteration mineral due to weathering. Figure 22 illustrates the extent of gypsum precipitation after the dry samples, which had been kept dry throughout the experiment, were contaminated by rainwater. As described in Section 3.3, the presence of gypsum on the wet samples indicates that pyrite grains had oxidised and produced sulphuric acid, which reacted with calcite or dolomite to form gypsum (Rao and Gluskoter, 1973; Ward, 1989; Lett and Ruppel, 2004; Silva *et al*., 2011). No gypsum precipitates nor red calcite grains were observed in any of the dry samples after 6 months of weathering.

It is plausible that some of the sulphuric acid was neutralized by the carbonates (calcite and dolomite) present in the samples and therefore produced fewer gypsum precipitates (Figure 22A) in the wet samples that had not been contaminated by rainwater, whereas additional sulphuric acid in the contaminated samples may have been derived from the acidic nature of the rainwater and may therefore account for the extreme precipitation of gypsum as observed in Figure 22B. Under natural weathering conditions in which microbial activity accelerates the weathering process, more oxidation of pyrite might have occurred, resulting in a greater yield in gypsum precipitation, albeit the experimental parameters in the present study excluded both the microbial and rainfall aspect affecting coal weathering (Hercod *et al*., 1998).

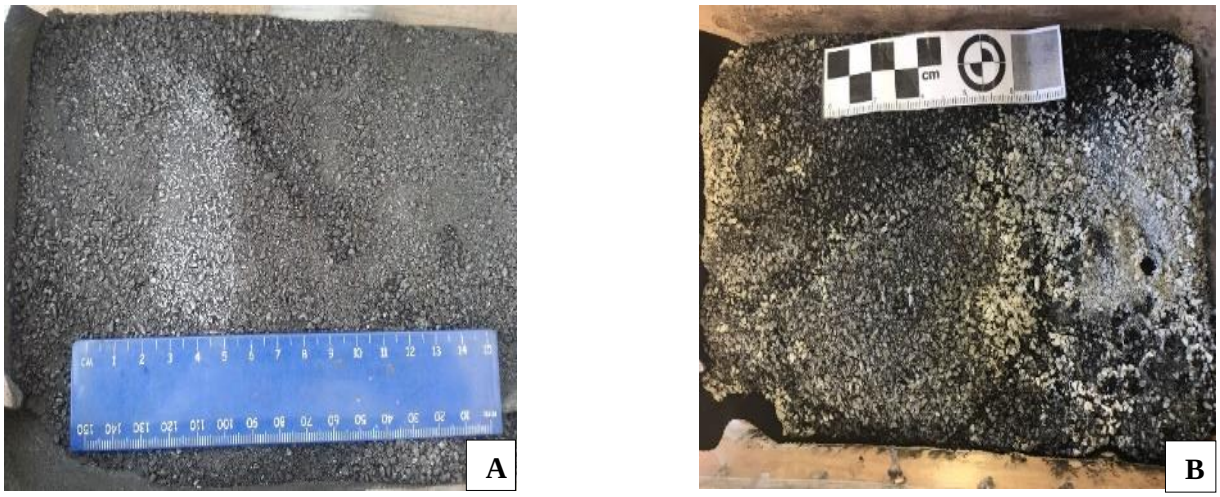


Figure 22. Example of the small extent of gypsum precipitated on the surface of B5W [A] compared to B5 after contamination by rainwater [B].

Another mineralogical change observed during the experiment was the appearance of some red platy grains in the samples that had been watered for the duration of the study (Figure 23A). These red minerals were unusual because they had not been previously observed in any of the fresh samples. The red calcite grains were initially observed in B5W after four months of water treatment and in all other wet samples subsequently thereafter.

It was suspected that these red minerals were products of weathering, i.e. alteration minerals because their red colour relative to the clear calcite grains suggested that the grains had become enriched in Fe^{2+} by the oxidation of pyrite. However, the chemical composition (measured in weight percentage by electron microscopy) indicates that this assumption is not always true of the fresh and weathered calcite grains (Figure 23B). The average weight percentage of iron oxide (FeO, 0.24 wt%) in a fresh, clear calcite grain of the parent sample B5B is similar to the FeO content of a weathered red calcite grain in sample B5W M6 (FeO, 0.25 wt%) that had been contaminated by rainwater at six months of weathering (Figure 23B). However, the concentration of magnesium oxide and manganese oxide is slightly lower in the rainwater contaminated sample, B5M6 (MgO, 0.12 wt%; MnO, 0.13 wt%), relative to the unweathered clear calcite grain in B5B (MgO, 0.19 wt%; MnO, 0.24 wt%). The clear, weathered calcite grain in B5WM6 is distinctly characterised by very low levels of iron oxide (FeO, 0.02 wt%), and manganese oxide (MnO; 0.03 wt%), and it also has the highest level of magnesium (MgO, 0.34 wt%) compared to the fresh and weathered calcite grains in samples B5B and B5M6.

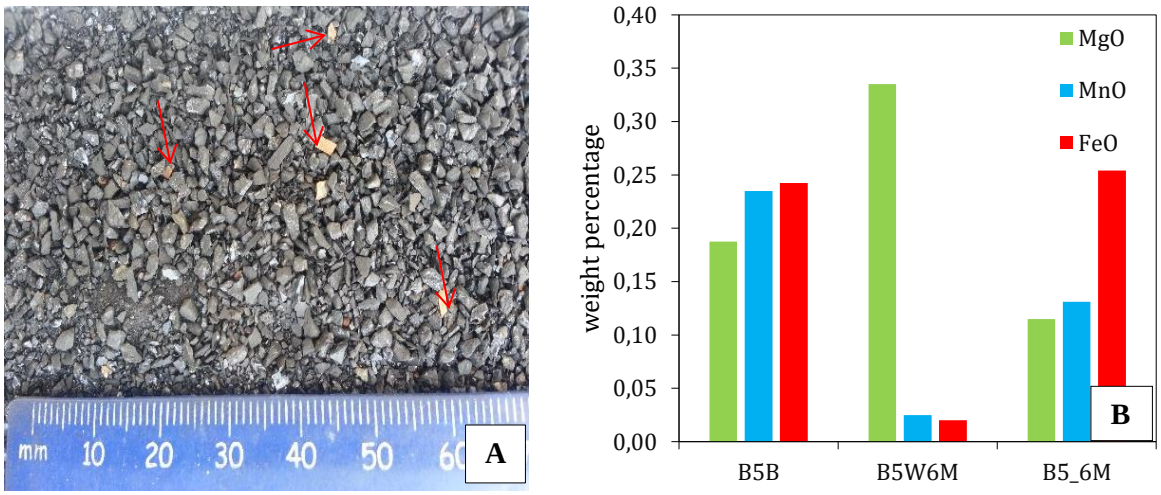


Figure 23. [A] Platy red calcite grains in sample B5W. [B]. The average chemical composition of fresh clear calcite in sample B5B compared to weathered clear calcite in B5W 6M and weathered red calcite grains in a rainwater contaminated sample B56M.

The red calcite grains that were observed in the wet samples were typically characterized by a smooth texture and platy form. Furthermore, these calcite grains appeared red in colour, both to the naked eye and under oil immersion during petrographic analyses (Section 5.7.3). In contrast, the texture of the weathered calcite grain in Figure 24A was rough and uneven. Although this calcite grain was identified by its red colour, the grain appeared dark grey under oil immersion, and only appeared red along its grain boundary. This indicates that the red colouration alone does not specifically equate to weathering since other red grains that were investigated (Appendix G) had very similar compositions to the red calcite grains. In Figure 24, two distinct zones can be observed along the grain boundary of calcite. That is, a black rim and white rim (Figure 24B). The white rim was positively confirmed to be siderite by

EMPA analysis, whereas the black rim was confirmed to be calcite despite the red colour as observed in the photomicrograph (Figure 24A).

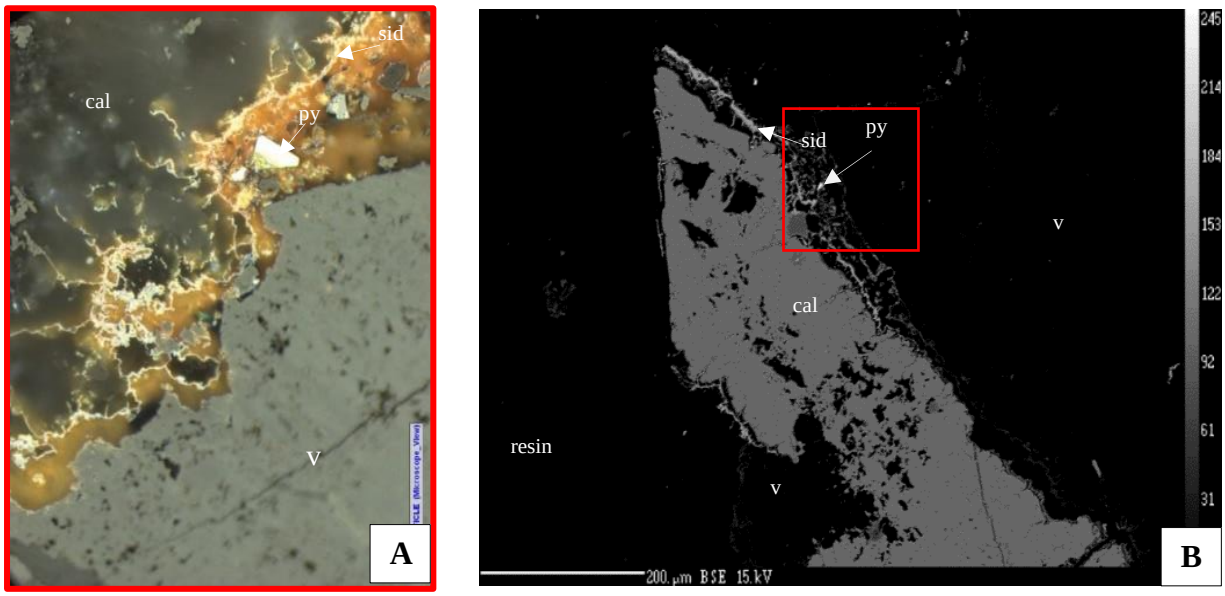


Figure 24. Calcite (cal), pyrite (py) and siderite (sid) occurring with vitrinite (v) in sample B5W after six months of weathering, under oil immersion at x10 magnification [A] and electron microprobe back-scattered image at 200 µm [B].

Due to the setbacks encountered in using the EMPA, additional compositional data was supplemented using field scanning electron microscopy (FE-SEM). Back-scattered electron (BSE) images, energy dispersive spectra (EDS) and compositional maps were measured on selected red calcite grains that showed signs of alteration. The samples that were analysed had been left to weather for up to 16 months and had been contaminated by rainwater.

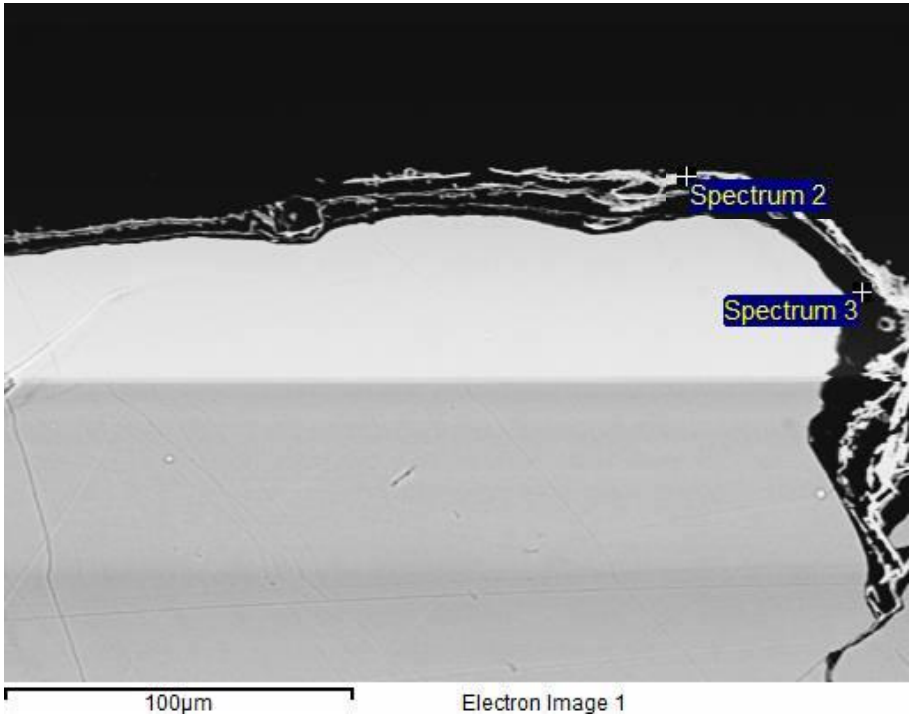
The selected calcite grains are characterized by the presence of growth rims or zones along the grain boundaries. This distinct zonation is clearly visible on the SEM images (Figure 25-29). Two types of distinct growth rims/zones can be seen on the BSE images (Figure 25-29), namely a black rim and a bright white rim/zone. In agreement with the Raman spectroscopy (Appendix H) and EMPA, the EDS also confirms that the red grains are calcite, despite the characteristic red colour. In Figure 25 the black rim (spectrum 3) contains carbon (67.07 wt%) and oxygen (31.69 wt%), with minor amounts of iron (1 wt%) and calcium (0.24 wt%). Adjacent to the black rim is the bright white rim (spectrum 2) which comprises lower carbon (59.12 wt%), but higher oxygen (38.21 wt%), iron (2.30 wt%) and calcium (0.37 wt%). These observations are also true of the EDS spectrum in Figure 25 and 27 which show that the black rims are carbon rich with slightly lower oxygen compared to the white rim which typically has iron associated with it. Unlike the electron microprobe analysis, magnesium, and manganese were not detected. Furthermore, no sulphur was detected in association with the alteration growth rims.

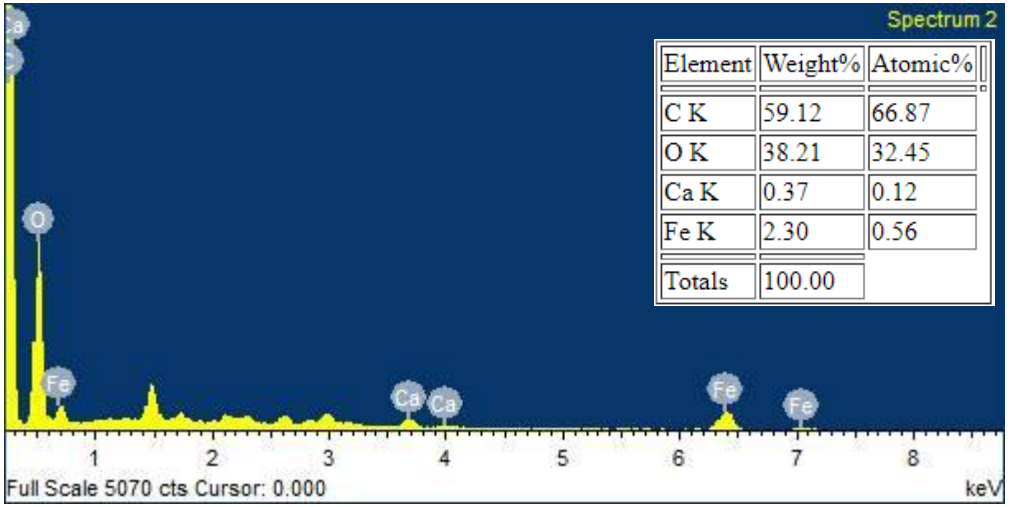
As expected for calcite, the compositional maps (Figure 26 and 29) indicate that the whole grain is calcium rich. The growth rims have very low calcium concentrations in the black rim (0,24 wt%) which appears to have lower calcium compared to the white outer rim (0.37 wt%). In Figure 26 the outline of the white rim is clearly defined by some iron enrichment (2.30 wt%) relative to the calcite grain itself and the adjacent black rim (1 wt%). However, the distribution of iron in Figure 29 is not as clearly defined, as it appears to be disseminated within both black and white rims. The EDS of the white rims (spectrum 2 in Figure 25, spectrum 2 and 4 in Figure 27, and spectrum 4 in Figure 28) suggest the formation of siderite. This observation is in line with the results of the EMPA in which the white rim was positively identified as siderite. The compositional maps (Figure 26 and 29) also show that the black rims are more enriched in carbon and have lower oxygen content compared to the white rims.

To summarize, gypsum precipitates were observed in small quantities on the surface of the watered samples which was confirmed by XRD analyses. However, the results from Raman spectroscopy, EMPA and FE-SEM do not prove that the growth rims/zones are gypsum because no sulphur was detected in the compositional analyses of the grain in Figure 26. The sulphur detected in the grain depicted in Figure 29 occurs in trace amounts and is disseminated. Therefore, there is no clear evidence that the detected sulphur is associated with the growth rims. Furthermore, the rims are both characterized by carbon, oxygen and lower proportions of calcium and iron. Based on these facts it can be concluded that the rims/zones formed by the dissolution of calcite because of frequent watering whereas the black rims most likely represent a transitory zone in which calcium is leached out. The white rims are characterized by traces of iron and therefore represents the early development of siderite.

Although reference has been made to calcite in the oxidation of pyrite, alteration features of calcite similar to those observed in the present study, are rare in the literature (Wagner, 2007; Falcon, 2014). Moreover, mention has rarely been made of siderite precipitating as a by-product of the oxidation of pyrite, where the reaction of iron and dissolved carbon dioxide produces the precipitation of siderite (Ward, 1989; Silva *et al*., 2011). In most cases, siderite is reported as the source of iron for the subsequent formation of iron sulphates during oxidation (Cole *et al*., 1987; Rao and Gluskoter, 1973; Komraus *et al*., 1990; Garcia *et al*., 1991; Ritsema and Groenenberg, 1993; Martinez and Escobar, 1995; Waanders *et al*., 2003; Vassilev *et al*., 2010).

In the case of coal oxidation during outdoor storage, the iron and carbon dioxide necessary to form siderite would be derived from the oxidation of the organic matter (Equation 1) and pyrite oxidation (Equation 2 and 3). Further research into the mechanism of siderite precipitation during the oxidation of stored coals is necessary.





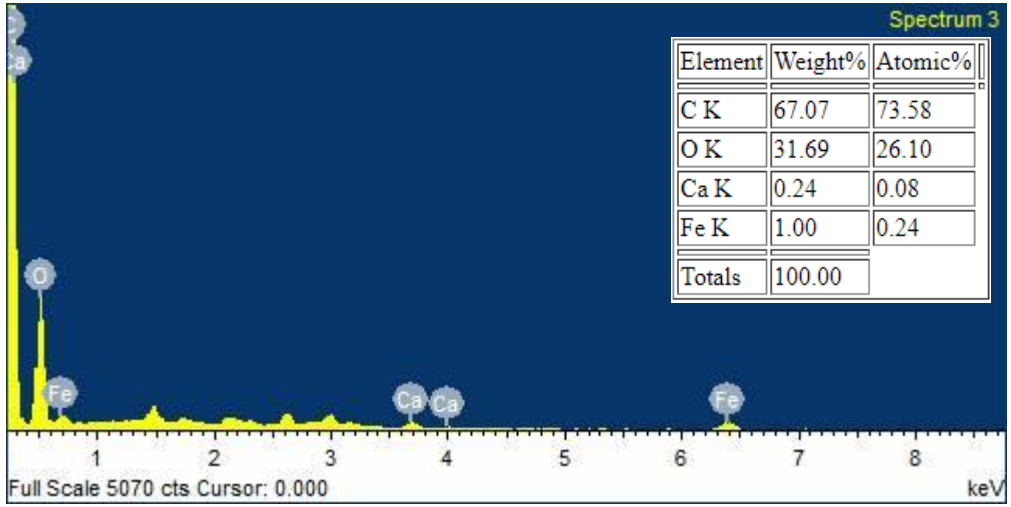


Figure 25. SEM back-scattered electron images and selected EDS data in coal sampled after 16 months of weathering.

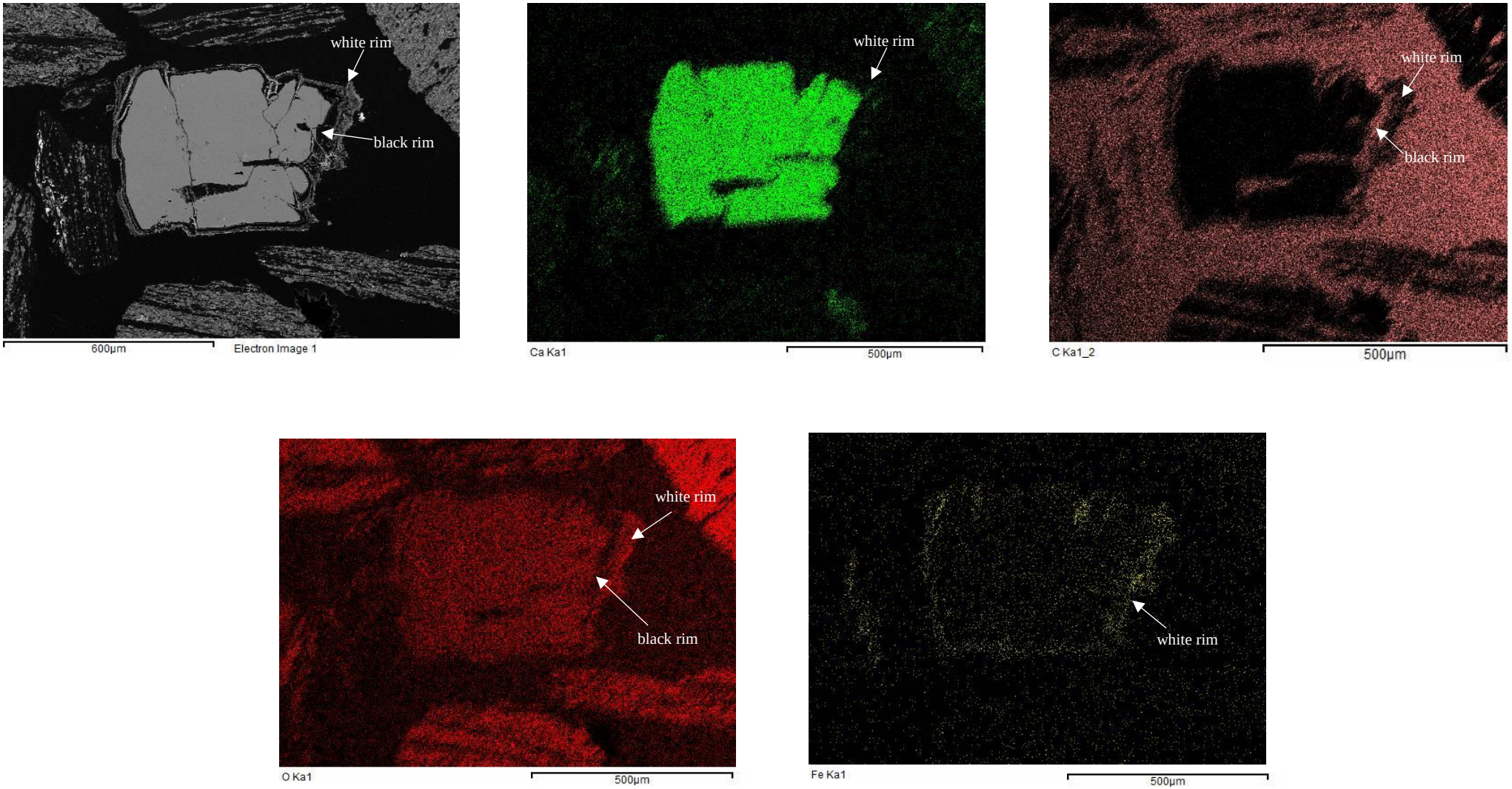
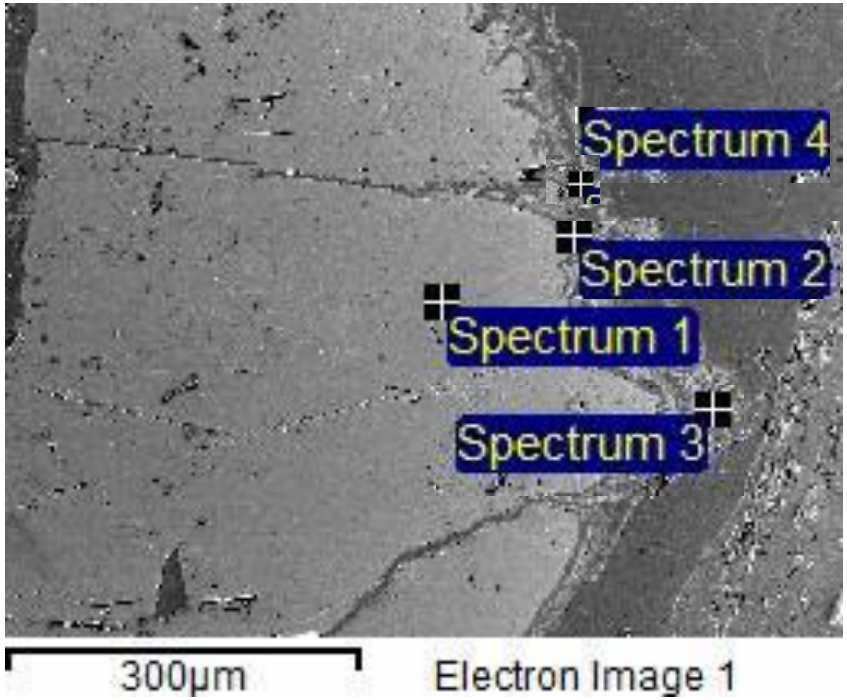
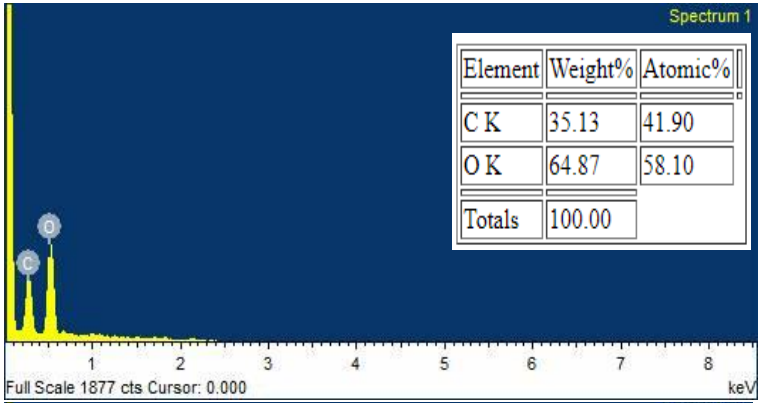
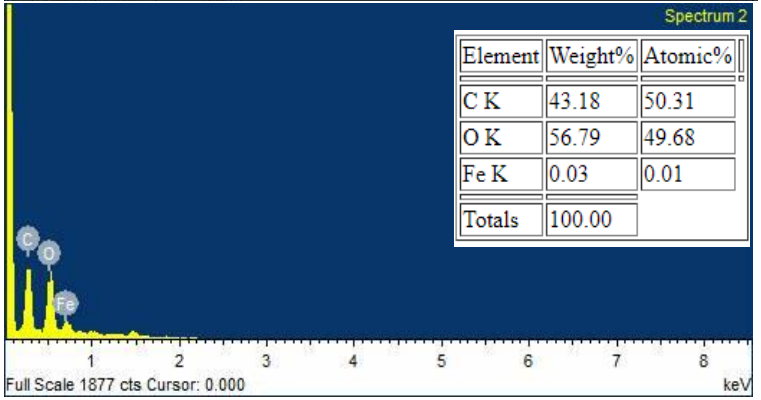
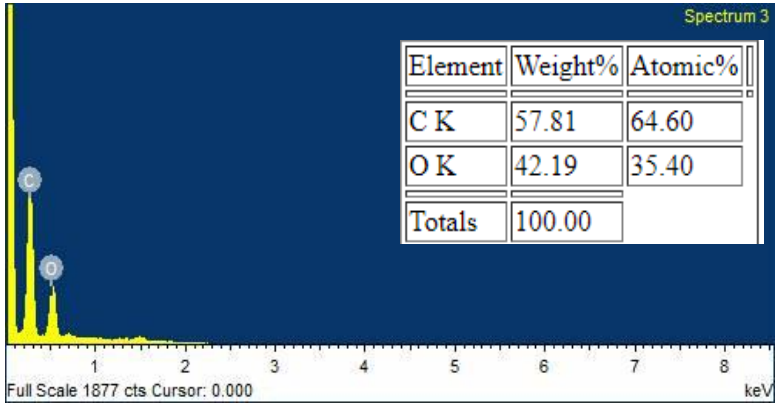


Figure 26. SEM-EDS elemental maps of altered calcite grain after 16 months of weathering









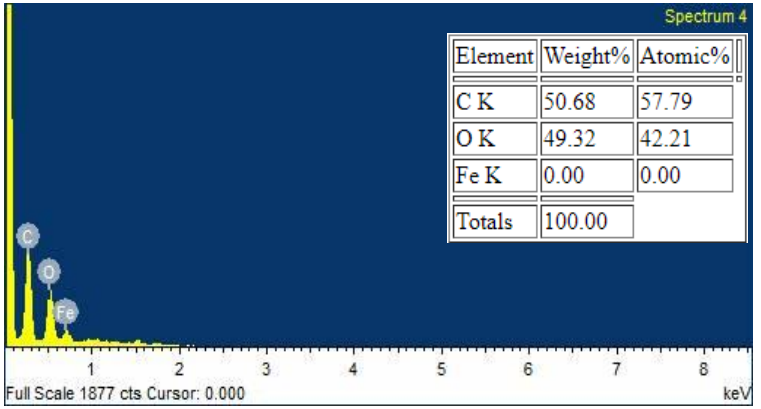
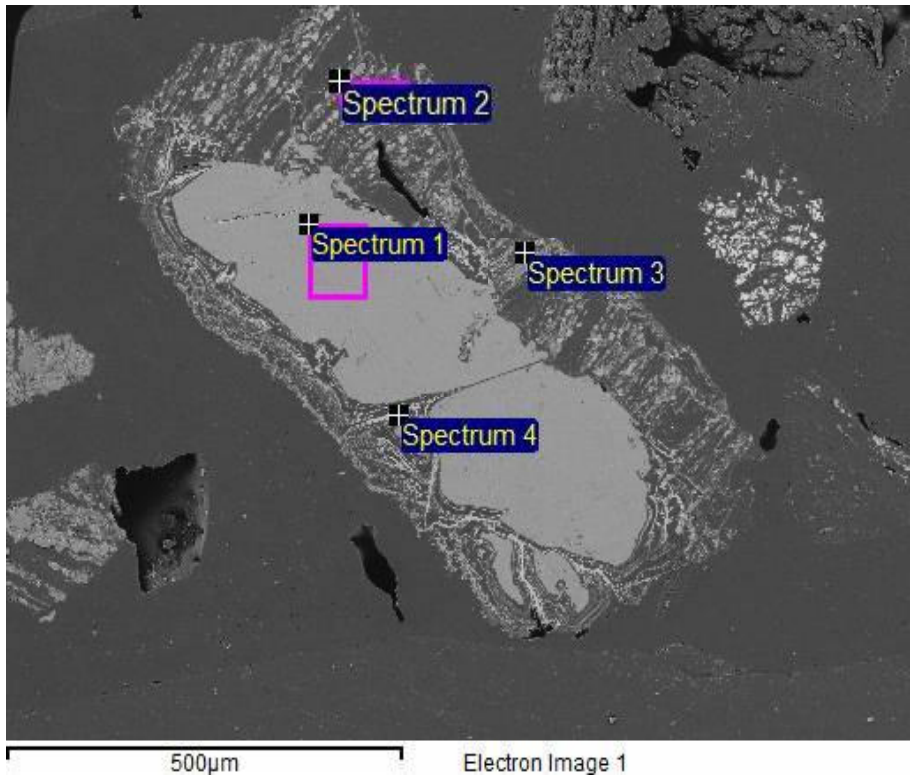
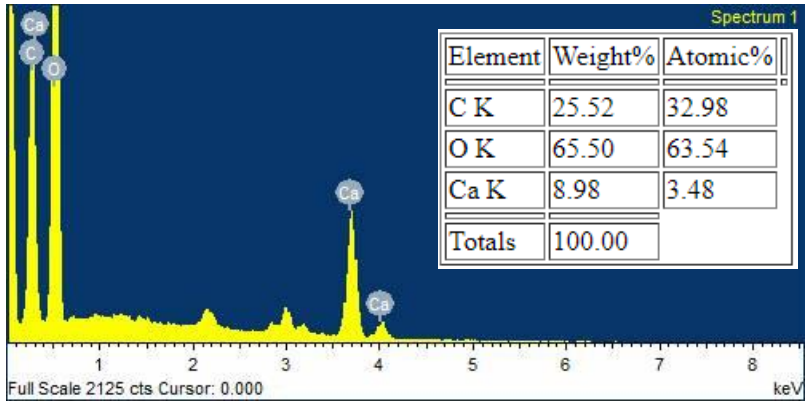
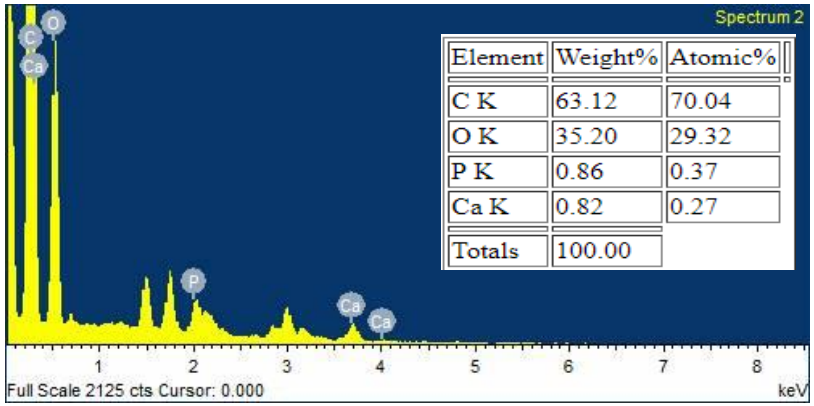
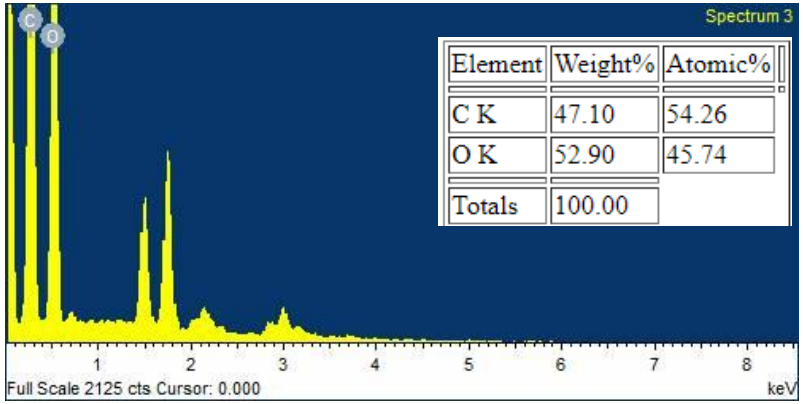


Figure 27. SEM back-scattered electron images and selected EDS data in coal sampled after 16 months of weathering.









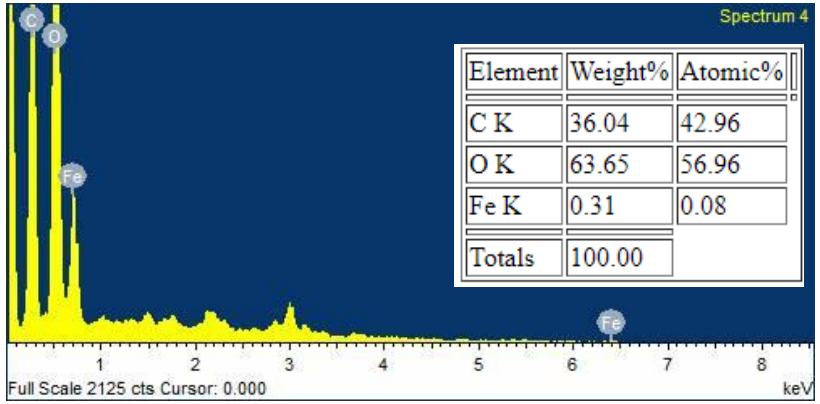


Figure 28. SEM back-scattered electron images and selected EDS data in coal sampled after 16 months of weathering.

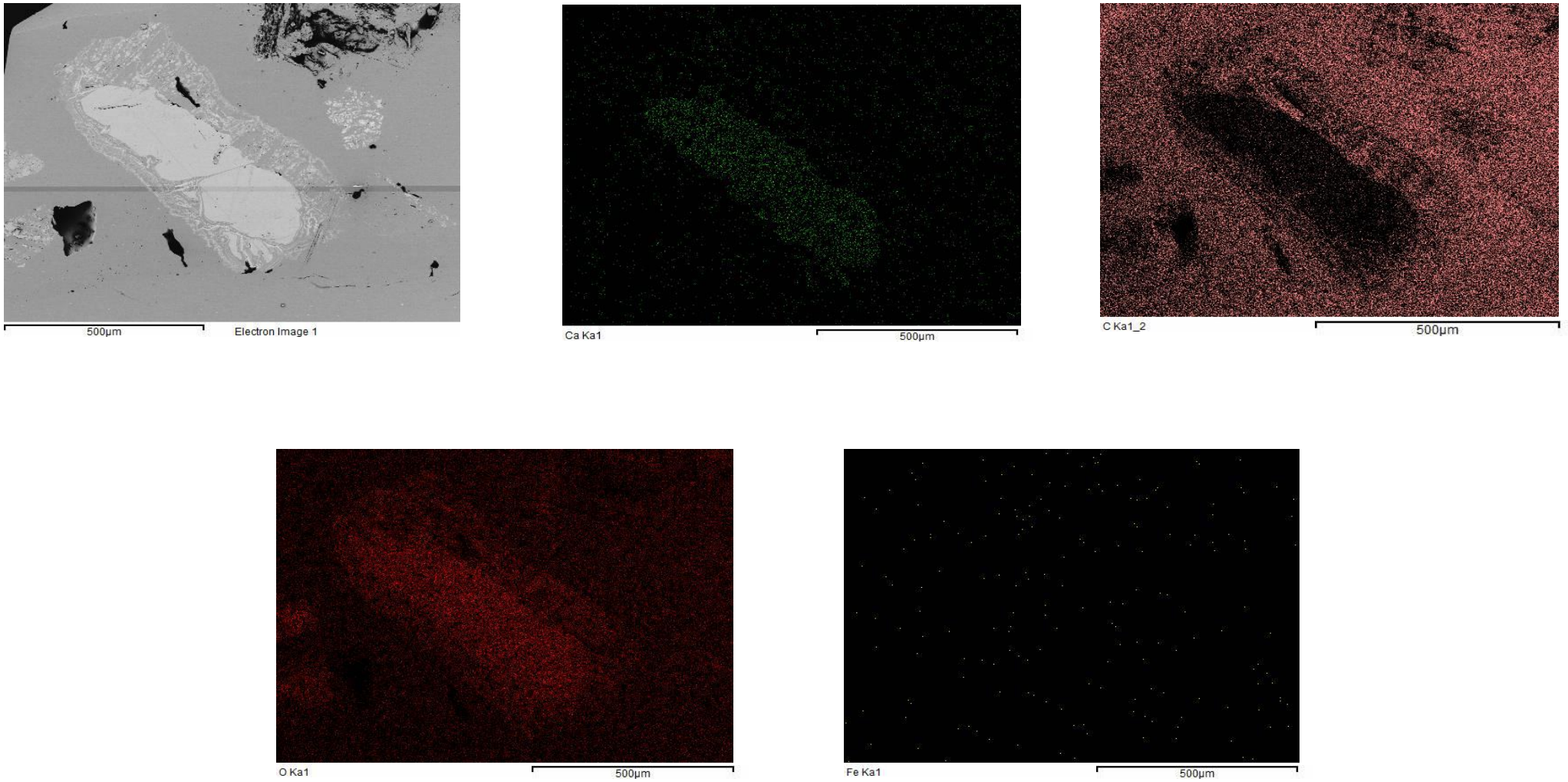


Figure 29. SEM-EDS elemental maps of altered calcite grain after 16 months of weathering

5.6.3 Major oxide composition of coal ash

The major oxide compositions of the dry and wet samples were determined using XRF and are presented on a weight percentage (wt%) basis. Consistent with the XRD data, SiO_2, Al_2O_3, $Fe_2O_{3\,(t)}$ and CaO are the most abundant oxides in all the samples, while MgO, TiO_2, K_2O, Na_2O, MnO, P_2O_5 and Cr_2O_3 occur in minor concentrations (Appendix I). Since the oxidation of sulphur and the subsequent reaction with carbonates is the major cause of mineral transformation in coal, as discussed in the preceding sections, the behaviour of the $Fe_2O_{3\,(t)}$ and CaO content will be discussed in this section. The statistical significance of the trends is discussed with respect to the correlation coefficient (r) and population correlation coefficient (p) which are recorded in Table 15.

The $Fe_2O_{3\,(t)}$ and CaO content varied from sample to sample and illustrated different trends. After 188 days of weathering the $Fe_2O_{3\,(t)}$ content decreased in samples B3, B5, B5W, B9, B11and B11W but appeared to increase in samples MS, MSW, B3W and B9W. Of these, only sample MS has a significant trend. The CaO increased in samples MS and B3W whereas all other samples had a decreasing CaO trend. The CaO was only significant in sample B11W.

In general, most of the samples displayed decreasing $Fe_2O_{3\,(t)}$ trends which were mirrored by a decreasing CaO trend. This observation is consistent with Fredericks *et al* (1983) who noted that the $Fe_2O_{3\,(t)}$ and CaO content was generally lower in low to highly weathered high volatile bituminous coals from Australia. The decrease in the $Fe_2O_{3\,(t)}$ and CaO content may be due to the loss of iron and calcium ions during the oxidation of pyrite and dissolution of calcite, respectively. In contrast, Pisupati *et al* (1993) reported both increases and decreases in the $Fe_2O_{3\,(t)}$ and CaO of weathered Pennsylvanian coals relative to their fresh counterparts. Liotta *et al* (1983) observed that $Fe_2O_{3\,(t)}$ and CaO increased in the Illinois No.6 coal after 35 days of weathering due to pyrite oxidation.

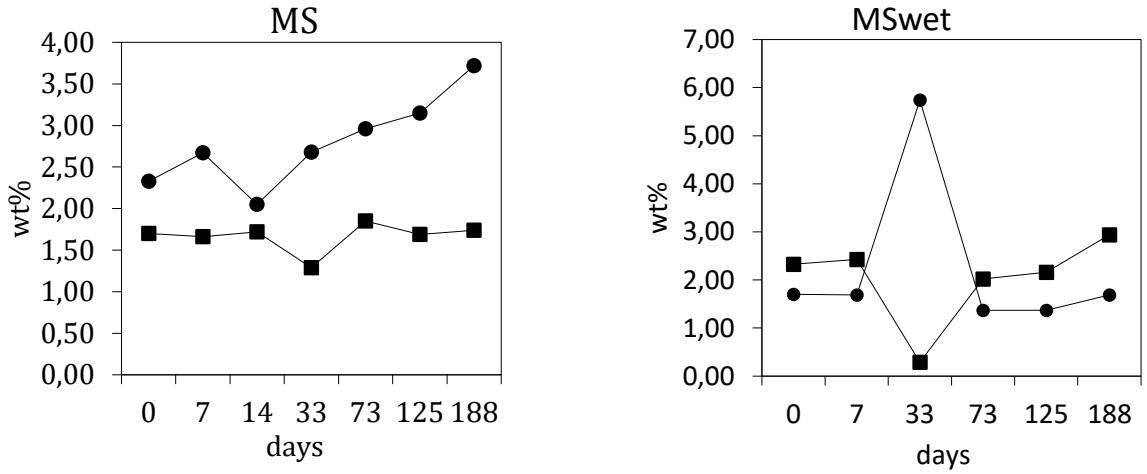


Figure 30. $Fe_2O_{3\,(t)}$ (●) and CaO (■) trends for the dry samples and their wet counterparts

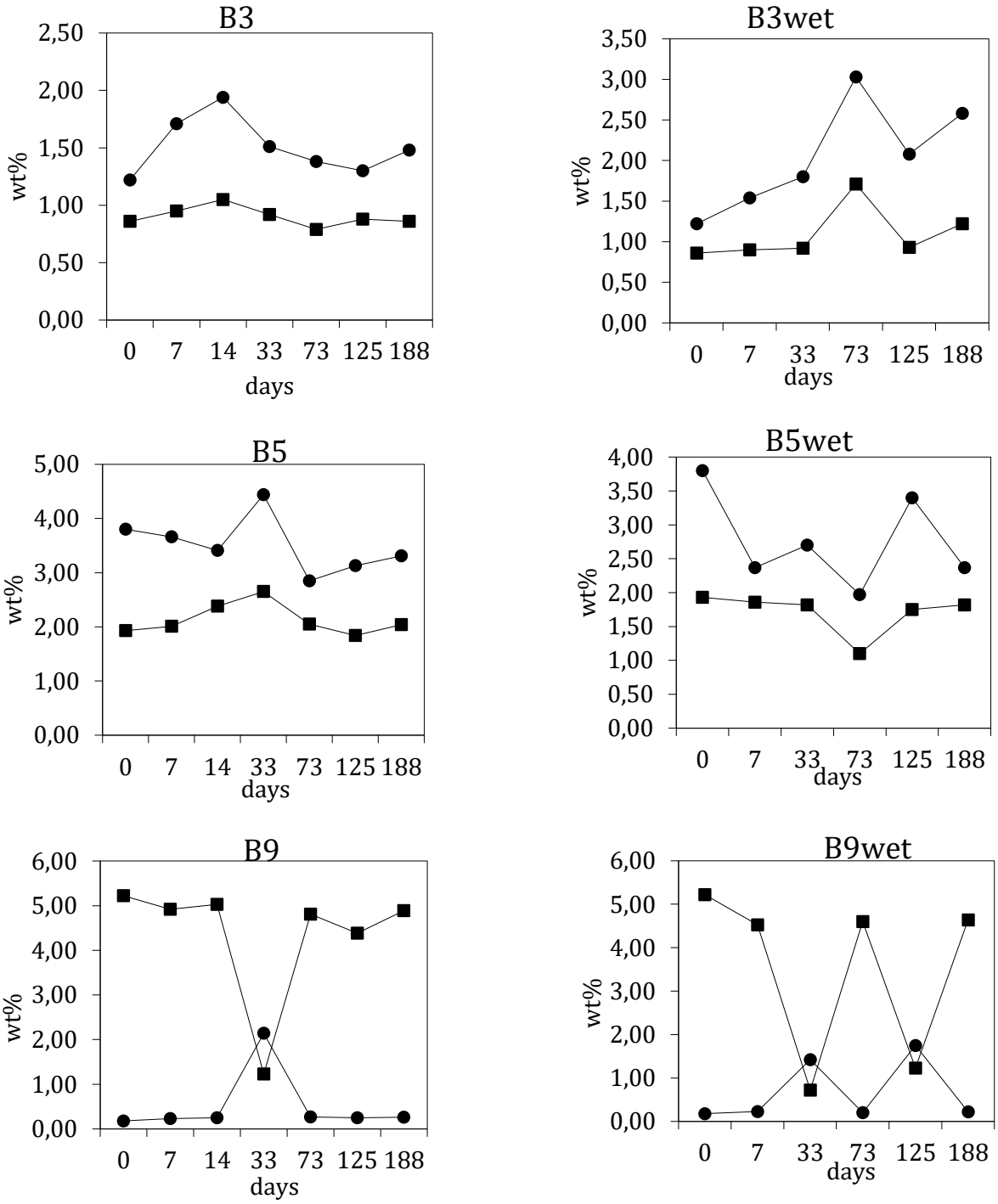


Figure 29 continued. $Fe_2O_{3\,(t)}$ (●) and CaO (■) trends for the dry samples and their wet counterparts

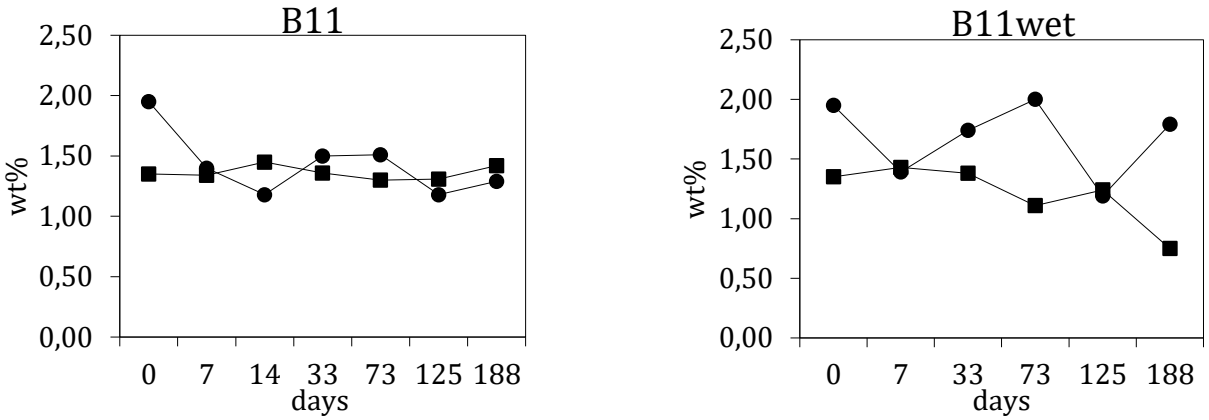


Figure 29 continued. $Fe_2O_{3\,(t)}$ (●) and CaO (■) trends for the dry samples and their wet counterparts

Table 15. Statistical analyses of the total iron content ($Fe_2O_{3\,(t)}$) and calcium oxide (CaO).

Sample	**Middle Seam (MS)**		**Bench 3 (B3)**		**Bench 5 (B5)**		**Bench 9B (B9)**		**Bench 11 (B11)**	
Days	**$Fe_2O_{3\,(t)}$**	**CaO**	**$Fe_2O_{3\,(t)}$**	**CaO**	**$Fe_2O_{3\,(t)}$**	**CaO**	**$Fe_2O_{3\,(t)}$**	**CaO**	**$Fe_2O_{3\,(t)}$**	**CaO**
0	2.33	1.70	1.22	0.86	3.80	1.93	0.18	5.22	1.95	1.35
7	2.67	1.66	1.71	0.95	3.66	2.01	0.23	4.92	1.40	1.34
14	2.05	1.72	1.94	1.05	3.41	2.38	0.25	5.03	1.18	1.45
21	2.68	1.29	1.51	0.92	4.44	2.65	2.14	1.23	1.50	1.36
73	2.96	1.85	1.38	0.79	2.85	2.05	0.27	4.81	1.51	1.30
125	3.15	1.69	1.30	0.88	3.13	1.84	0.25	4.38	1.18	1.31
188	3.72	1.74	1.48	0.86	3.31	2.04	0.26	4.89	1.29	1.42
Equation	y = 0.2157x + 1.9314	y = 0.0111x + 1.62	y = -0.0214x + 1.5914	y = -0.0143x + 0.9586	y=-0.1104x + 3.9557	y=-0.0121x + 21771	y = 0.0107x + 0.4686	y = x + 4.6814	y = -0.0746x + 1.7286	y = -1x10^{-16} +1.3614
Rate (wt%/ day)	0.2157	0.0111	-0.0214	-0.0143	-0.1104	-0.0121	0.0107	-0.0818	-0.0746	-3x10^{-16}
Coefficient of determination (R^2)	0.7203	0.0185	0.0347	0.1391	0.2129	0.0085	0.001	0.0159	0.3652	1x10^{-28}
Pearson's correlation coefficient (r)	0.8487	0.1360	0.1863	0.3730	0.4614	0.0922	0.03162	0.1261	0.6043	1x10^{-14}
Population correlation coefficient (ρ)	0.7545									
n= 7-2	5									
Comment	significant	insignificant	insignificant	insignificant	insignificant	insignificant	insignificant	insignificant	insignificant	insignificant

Table 15 continued. Statistical analyses of the total iron content (Fe2O3 (t)) and calcium oxide(CaO)

Sample	**Middle Seam wet (MSW)**		**Bench 3 wet (B3W)**		**Bench 5 wet (B5W)**		**Bench 9B wet (B9W)**		**Bench 11 wet (B11W)**	
Days	**$Fe_2O_{3\,(t)}$**	**CaO**	**$Fe_2O_{3\,(t)}$**	**CaO**	**$Fe_2O_{3\,(t)}$**	**CaO**	**$Fe_2O_{3\,(t)}$**	**CaO**	**$Fe_2O_{3\,(t)}$**	**CaO**
0	2.33	1.70	1.22	0.86	3.8	1.93	0.18	5.22	1.95	1.35
7	2.43	1.69	1.54	0.90	2.37	1.86	0.23	4.53	1.39	1.43
33	0.29	5.74	1.80	0.92	2.70	1.82	1.42	0.72	1.74	1.38
73	2.02	1.37	3.03	1.71	1.97	1.10	0.20	4.60	2.00	1.11
125	2.16	1.37	2.08	0.93	3.40	1.75	1.75	1.23	1.19	1.24
188	2.94	1.69	2.58	1.22	2.37	1.82	0.22	4.64	1.79	0.75
Equation	y = 0.1134x + 1.6313	y = -0.1537x + 2.798	y=0.2757x + 1.0767	y= 0.0766x + 0.822	y = -0.1369x + 3.2473	y = -0.0457x + 1.8733	y = 0.1011x + 0.3127	y = -0.2549x + 4.382	y = -0.0326x + 1.7907	y = -0.1097x + 1.594
Rate (wt%/ day)	0.1134	-0.1537	0.2757	0.0766	-0.1369	-0.0457	0.1011	-0.2549	-0.0326	-0.1097
Coefficient of determination (R^2)	0.0546	0.0282	0.5904	0.1883	0.1353	0.078	0.0692	0.0586	0.036	0.6595
Pearson's correlation coefficient (r)	0.2337	0.1679	0.7684	0.4339	0.3678	0.2793	0.2631	0.2421	0.1897	0.8121
Population correlation coefficient (ρ)	0.8114									
n= 6-2	4									
Comment	insignificant	insignificant	insignificant	insignificant	insignificant	insignificant	insignificant	insignificant	insignificant	significant

5.7 Petrography

The petrographic analysis enabled characterization of the weathered coals relative to the fresh parent coals on a microscopic level. The associations of the organic (macerals) and inorganic (mineral matter) constituents are discussed here with reference to the impact of weathering.

5.7.1 Maceral point count

The organic and inorganic composition of the fresh parent coals are recorded in Table 16 and are quantified including mineral matter (inc. mm), as well as on a mineral matter free (mmf) basis. The maceral point count was conducted to identify and quantify the proportion of the various types of macerals (Figure 31) and minerals (Figure 32) present in the fresh parent coals (MSB, B3B, B5B, B9B and B11B).

Samples MSB, B3B and B5B are characterized by the predominance of the vitrinite macerals (46.7-70.6 vol%), particularly collotelinite (30.4-50.7 vol%). Pseudovitrinite is also present in these samples, generally occurring in proportions less than 2 vol%. Samples B9B and B11B consist largely of inertinite (60.4-75.8 vol%), of which inert semifusinite, inert inertodetrinite and fusinite are the major inertinite macerals. Liptinite occurs in the lowest proportions in all the samples mainly in the form of sporinite and to a lesser extent cutinite. Notably, the petrographic composition of coking coals MSB from the Limpopo Coalfield and B3B from the Waterberg Coalfield are very similar. However, B3B has lower proportions of telinite, corpogelinite, inert inertodetrinite, quartz and pyrite relative to MSB, but higher proportions of fusinite, semifusinite (both inert and reactive), secretinite, suberinite and clay minerals. The commonly observed macerals are presented in Figure 31.

As discussed in Section 5.6.1, mineral matter in the coals is present in the form of silicates, sulphides and carbonates. Mineral matter is highest in sample B5B (27 vol%) and lowest in B11B (6.9 vol%). The proportion of clay minerals is highest in B5B (7.7 vol%) and B3B (6.8 vol%), whereas MSB, B9B and B11B have considerably less clay minerals (0-3 vol%). B9B has the highest amount of carbonate minerals (9.9 vol%) which are mainly calcite and dolomite. In all other samples, carbonates only constitute 1.0-1.8 vol% of the coal composition. The commonly observed minerals are presented in Figure 32.

Quartz is often disseminated within carbonates or clay minerals (Figure 32A). The clay minerals also tend to be finely disseminated within the macerals (Figure 32A and B). Calcite occurs as elongated laths and cleat infillings or as veins crosscutting the macerals (Figure 32C and D). Pyrite veins (Figure 32E) and massive pyrite grains (Figure 32F) are common, as well as framboids of varying sizes (Figure 32G and H).

Table 16.Maceral constituents including mineral matter (inc. mm) and mineral matter free (mmf) basis

Sample identification		**MSB**		**B3B**		**B5B**		**B9B**		**B11B**	
		inc. mm	**mmf**	**inc. mm**	**mmf**	**inc. mm**	**mmf**	**inc. mm**	**mmf**	**inc. mm**	**mmf**
MACERAL GROUP	**MACERAL (vol%)**	**vol%**	**vol%**	**vol%**	**vol%**	**vol%**	**vol%**	**vol%**	**vol%**	**vol%**	**vol%**
Vitrinite	**telinite**	1.8	2.1	0.4	0.5	6.7	9.2	0.0	0.0	0.4	0.4
	collotelinite	50.7	60.1	50.2	56.8	30.4	41.6	4.4	5.0	21.7	23.3
	vitrodetrinite	0.0	0.0	0.0	0.0	0.0	0.0	0.0	0.0	0.0	0.0
	collodetrinite	7.4	8.8	9.2	10.4	7.3	10.0	3.6	4.1	6.1	6.6
	corpogelinite	9.0	10.7	3.2	3.6	2.4	3.2	0.0	0.0	1.0	1.1
	gelinite	0.0	0.0	0.0	0.0	0.0	0.0	1.2	1.4	0.8	0.8
	pseudovitrinite	1.8	2.1	1.2	1.4	0.0	0.0	0.0	0.0	0.2	0.2
Inertinite	**fusinite**	7.6	9.0	13.4	15.2	6.7	9.2	7.9	9.1	19.5	20.9
	reactive semifusinite	0.8	0.9	1.4	1.6	1.4	1.9	5.9	6.8	4.1	4.4
	inert semifusinite	1.8	2.1	4.2	4.8	6.3	8.6	30.9	35.5	18.5	19.9
	micrinite	0.0	0.0	0.0	0.0	0.0	0.0	0.2	0.2	0.2	0.2
	macrinite	0.0	0.0	0.2	0.2	0.0	0.0	0.0	0.0	0.2	0.2
	secretinite	0.2	0.2	0.4	0.5	2.4	3.2	3.2	3.6	4.7	5.1
	funginite	0.0	0.0	0.0	0.0	0.0	0.0	0.0	0.0	0.0	0.0
	inertodetrinite R	0.0	0.0	0.0	0.0	0.0	0.0	2.6	3.0	1.4	1.5
	inertodetrinite I	0.8	0.9	0.4	0.5	3.2	4.3	25.1	28.9	11.8	12.7
Liptinite	**sporinite**	2.3	2.8	2.2	2.5	5.7	7.8	2.2	2.5	2.6	2.7
	cutinite	0.2	0.2	1.6	1.8	0.4	0.5	0.0	0.0	0.0	0.0
	resinite	0.0	0.0	0.0	0.0	0.2	0.3	0.0	0.0	0.0	0.0
	alginite	0.0	0.0	0.0	0.0	0.0	0.0	0.0	0.0	0.0	0.0
	liptodetrinite	0.0	0.0	0.0	0.0	0.0	0.0	0.0	0.0	0.0	0.0
	suberinite	0.0	0.0	0.4	0.5	0.0	0.0	0.0	0.0	0.0	0.0
	exsudatinite	0.0	0.0	0.0	0.0	0.0	0.0	0.0	0.0	0.0	0.0
Mineral matter	**clay**	3.5		6.8		7.7		0.0		0.2	
	quartz	6.3		2.8		12.6		2.8		3.5	
	pyrite	4.9		0.8		5.7		0.2		1.4	
	carbonate	1.0		1.2		1.0		9.9		1.8	
	other	0		0.0		0.0		0.0		0.0	
SUMMARY TABLE											
MACERAL GROUP	**VITRINITE**	70.6	83.8	64.2	72.6	46.7	64.1	9.1	10.5	30.1	32.3
TOTALS (vol%)	**INERTINITE**	11.2	13.2	20.0	22.6	19.9	27.3	75.8	87.0	60.4	64.9
	LIPTINITE	2.5	3.0	4.2	4.8	6.3	8.6	2.2	2.5	2.6	2.7
	MINERAL MATTER	15.7		11.6		27.0		12.9		6.9	
	TOTAL INERTINITE	11.2	13.2	20.0	22.6	19.9	27.3	75.8	87.0	60.4	64.9
	TOTAL REACTIVE MACERALS	74.0	87.7	69.8	79.0	54.4	74.6	19.8	22.7	38.2	41.0

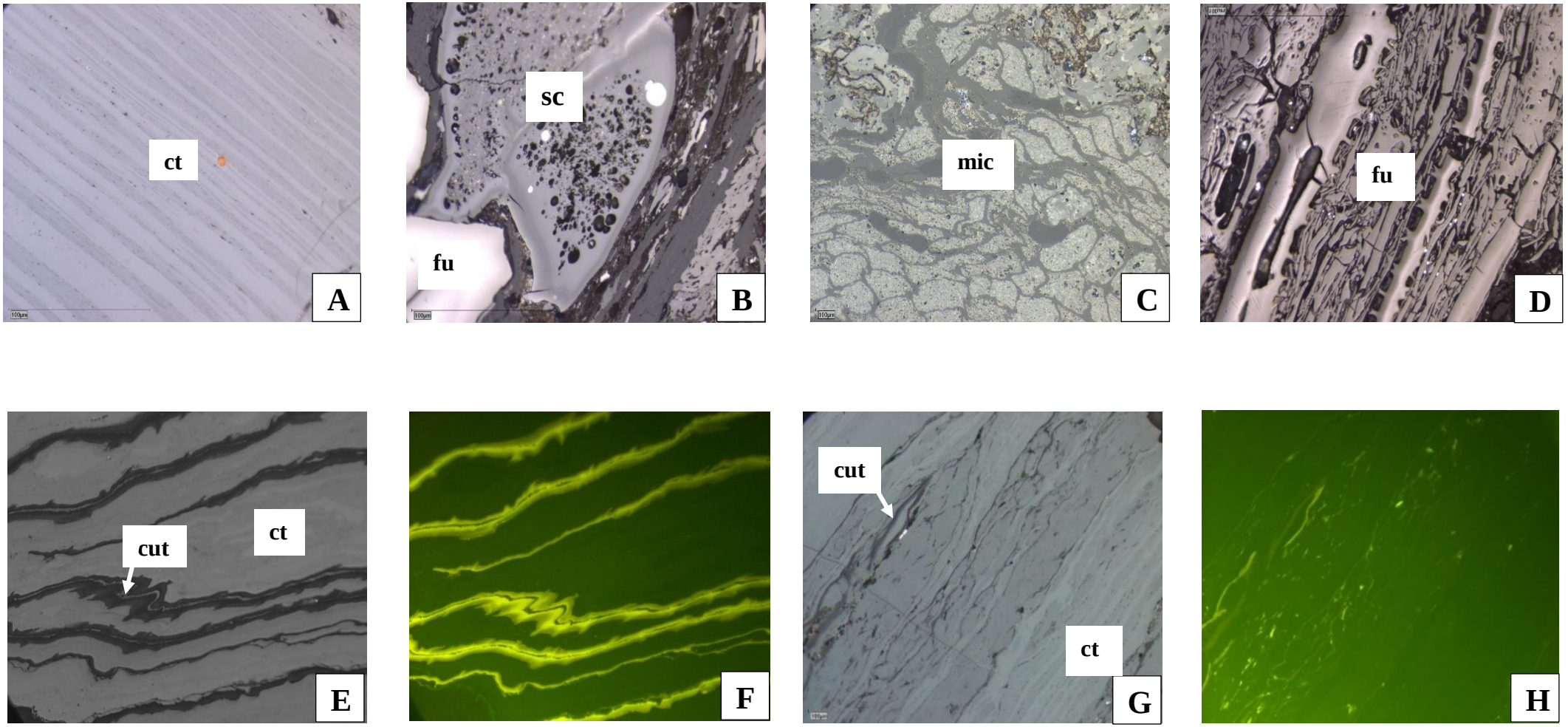


Figure 31. Photomicrograph of fresh macerals. Alternating bands of collotelinite in MSW M4 [A], Secretinite and fusinite in B11W M6 [B], Micrinite in B9 M4 [C], Fusinite in MS M4 [D], Cutinite and colloteliite in B5W M2 [E], Cutinite and collotelinite under fluorescent light in B5W M2 [F], Cutinite and collotelinite in B3W M6 [G], Cutinite and collotelinite under fluorescent light in B3W M6 [H]. ct= collotelinite, cut= cutinite, fu= fusinite, mic= micrinite, sc= secretinite. (Oil immersion at x500μm magnification).

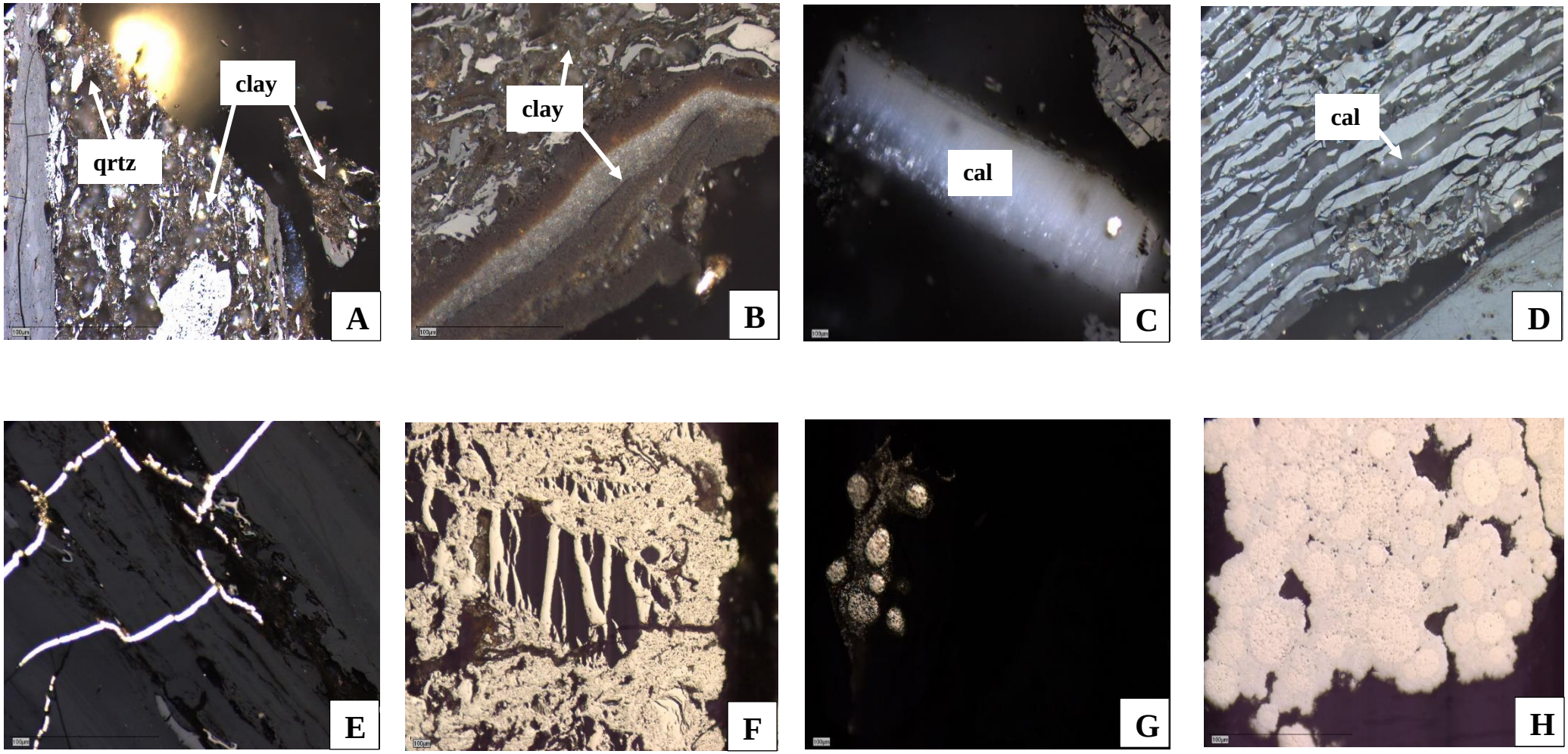


Figure 32. Photomicrographs of fresh minerals as per the maceral point count. Quartz grains with clay minerals in B3 M6 [A], Clay minerals in B5 M4 [B], Calcite lath in B9W M6 [C], Calcite veins impregnating vitrinite in B3B [D], Pyrite veins crosscutting vitrinite in B3 M6 [E], Massive pyrite in B5 M2 [F], Pyrite nodules in B3W M2 [G] and MS M4 [H]. qrtz= quartz, clay= clay minerals, cal= calcite, py= pyrite. (Oil immersion at x500μm magnification).

5.7.2 Vitrinite reflectance

The random reflectance (Rr%) measurements on vitrinite for the dry samples and their wet counterparts are recorded in Table 17. Based on the reflectance measurements, all the samples are ranked as medium-rank bituminous C according to the guidelines the SANS 10320: 2004 (Table 7).

The reflectance of both the dry and wet counterparts of all the samples appeared relatively constant and therefore unaffected by weathering, but the reflectance in the wet sample MSW and B11W, decreased slightly. No clear trend was observed for the dry sample of B3, however its wet counterpart (B3W) suggests some increase in the vitrinite reflectance due to weathering. Notably B3W had a significant decrease in its volatile matter content as discussed in Section 5.2.1. This is in line with Wagner (2007) who observed that an increase in the vitrinite reflectance of discarded coals was accompanied by a loss of volatiles during weathering. The reflectance in both the dry and wet samples of B5 decreased with weathering time. No trend was observed for the dry samples of B9 but the reflectance of the wet samples (B9W) appeared to decrease. Similar to the MS, the reflectance of vitrinite in B11 remained relatively constant and does not appear to have been affected by weathering, but the reflectance in the wet sample (B11W) does appear to have decreased as a result of weathering.

Overall, the changes in the reflectance of vitrinite during the early stages of weathering are quite minimal and are consistent with the literature. For example, Kruszewska and du Cann (1996) reported that there was no significant change in vitrinite reflectance after 938 days of exposure to weathering. Similarly, Chandra (1966) observed no significant change in the vitrinite reflectance of coals that had weathered for up to 10 years. An increase in the reflectance of vitrinite particles has commonly been observed in coals that have undergone self-heating due to the build-up of heat such as those in coal waste dumps (Misz-Kennan and Fabiańska, 2011; Ribeiro *et al* (2016). It can therefore be concluded that apart from the wet samples of B3 which showed an increasing reflectance trend due to weathering, the reflectance of all other samples remained unaffected by early stage weathering.

Table 17. Random reflectance (Rr%) measurements for medium-rank C bituminous coal.

Days	0	73	125	188	Days	0	73	125	188
MS	0.77	0.77	0.76	*	**MSW**	0.77	0.76	0.75	0.75
B3	0.62	0.66	0.65	0.61	**B3W**	0.62	0.62	0.75	0.72
B5	0.71	0.68	0.67	*	**B5W**	0.71	0.64	0.66	*
B9	0.79	0.83	0.77	0.81	**B9W**	0.79	0.80	0.75	0.75
B11	0.73	0.71	0.73	0.72	**B11W**	0.73	0.70	0.71	0.62

*****Samples were not suitable for analysis due to EMPA coating.

5.7.3 Abnormal condition analysis (ACA)

The abnormal condition analysis was conducted to petrographically quantify the degree of weathering. The findings of this analysis are recorded in Table 18 as volume weight percentage (vol%).

The ACA reveals that fresh macerals and minerals are the major constituents (84-98 vol%) making up the coals, indicating that the petrographic make-up of the samples was not greatly affected by early stage weathering (Table 18). On the one hand, the proportion of fresh particles appears to be slightly decreasing in most of the dry samples (MS, B3, B5 and B9). The wet samples on the other hand show no clear trend. Tell-tale signs of weathering could only be deduced from the very small proportion of constituents that are characterized by cracks, fissures and mineral alteration (Table 18). Other petrographic features indicating intense weathering such as secondary oxidation rims, heat affected particles, leached particles and porous fusinite were not observed. Bench 3 had the highest proportion (3-6 vol%) of desiccation cracks in the form of pseudovitrinite, which are likely to be of primary origin (Taylor *et al*.,1998).

Lower reflecting oxidation rims were mostly observed on secretinite, fusinite and occasionally on corpogelinite (Figure 33). These low reflecting oxidation rims are primary weathering features that typically develop on inertinite macerals during the coal forming process and differ from those that form as a result of weathering (Wagner, 2007; Kus *et al.*, 2017). During coal weathering, oxidation rims tend to develop on vitrinite macerals (McHugh, *et al*., 1991; Calemma *et al*., 1995). No oxidation rims were observed on the vitrinite particles during this experiment. This is likely as a result of the low ambient temperature conditions that the samples were subjected to compared to laboratory studies in which oxidation rims can be induced in short periods of time at higher temperatures (Bend and Kosloski, 1993).

Cracks and fissures were sighted in a few particles of vitrinite in each of the samples, and generally constituted 1-6 vol% of the coal composition. The cracks and fissures commonly originate from the centre of the particles and radiate outwards (Figure 34). The extent of cracking and fissuring varied in terms of whole particles that were affected or particular areas on the particles.

The altered calcite minerals occurred in proportions of 1-5 vol% and were predominantly observed in the wet samples. However, some (1 vol%) altered calcite was observed in the dry samples B5 M2 and B3 M6 (Table 18). This suggests that the process of calcite alteration was more rapid in the wet samples due to the additional moisture. As described in Section 5.6, calcite alteration was visually detected by means of the red coloured calcite particles compared to clear calcite particles (Figure 35). This red colour was also petrographically observed and is distinct from the colour of the fresh calcite particles which tends to be dark grey (Figure 32 C and D). As discussed in Section 5.6.2, growth rims were observed on some of the altered calcite particles, indicating that calcite dissolution and leaching of ions

had occurred. The edges of the altered calcite minerals are often accompanied by a bright white rim which was well developed in sample B3W (Figure 35E). Although Wagner (2007) also observed similar alteration minerals to the red calcite grains, identity and composition were not determined. Furthermore, similar photomicrographs of calcite alteration have rarely been reported elsewhere in the available literature on coal weathering (Wagner, 2007; Falcon, 2014).

Smedowski and Piechaczek (2016) did not find any evidence of weathering on the macerals that had been exposed to ambient air temperatures below 50°C. Similarly, Kruszewska and du Cann (1996) did not detect any weathering features on coals that had weathered for 938 days, in their petrographic investigations. Hence the ambient air temperature conditions that the coals in this study were subjected to (9.40°C -26.58°C) were not sufficient to induce extensive oxidation of both the organic and inorganic coal constituents in great proportions, nor cause intense weathering features which could otherwise affect the coals combustion and carbonising properties.

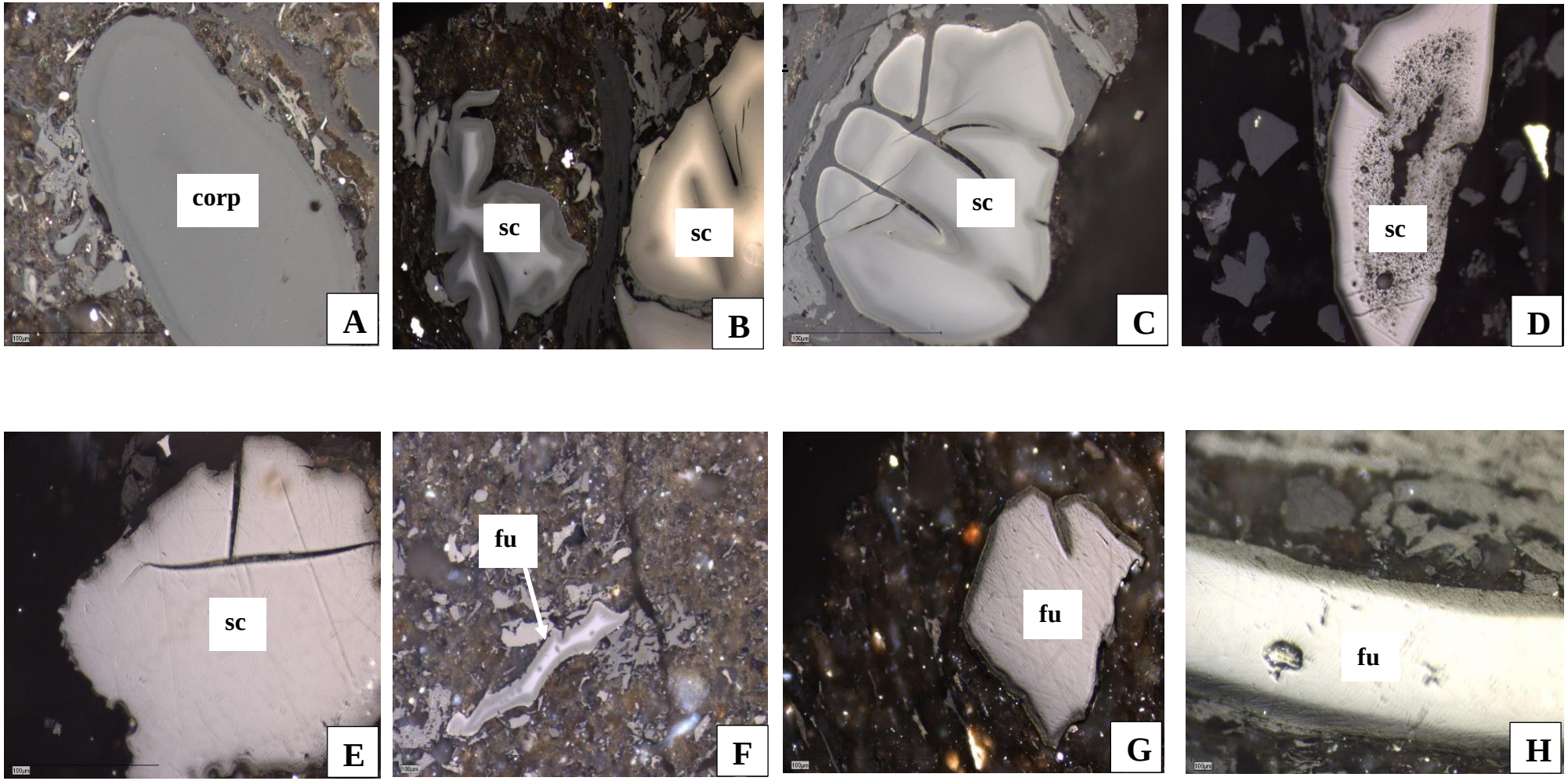


Figure 33. Photomicrographs of inherent oxidation rims occurring on fresh macerals in samples B5 M2 [A], B5W M4 [B], B5 M2 [C], and MS 4M [D], B3W M4 [E], B11W M6 [F], and after 16 months of weathering [G] and [H]. corp= corpogellinite, fu= fusinite, sc= secretinite. Oil immersion at x500μm magnification.

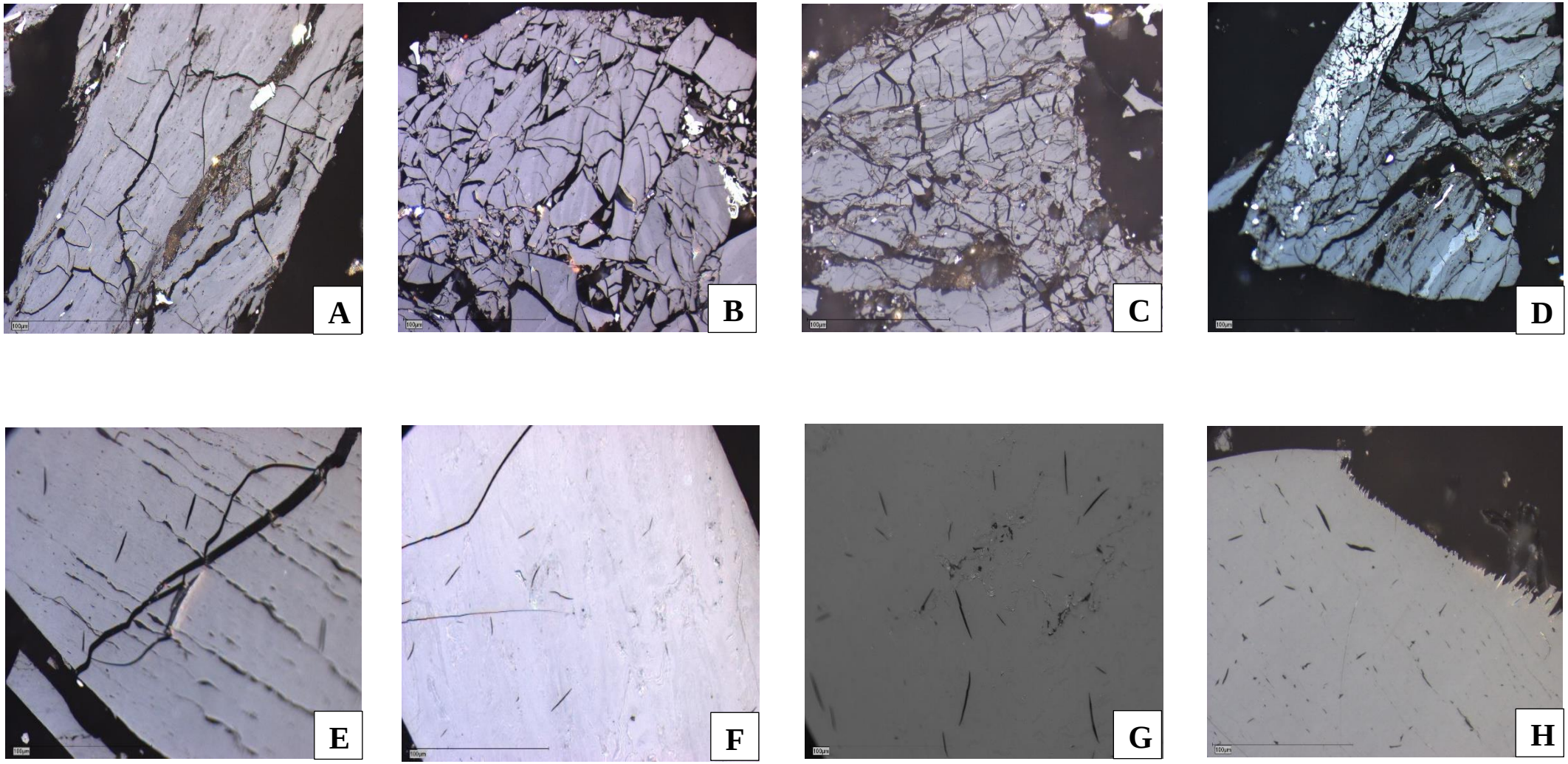


Figure 34.Photomicrographs of cracks and fissures in samples B3W M4 [A], MSW M2 [B], MS M2 [C] and B3W M2 [D]; Examples of pseudovitrinite (primary origin) in samples B3W M4 [E], B3W M4 [F], B11 M6 [G], and B5W M4 [H]. Oil immersion at x500μm magnification.

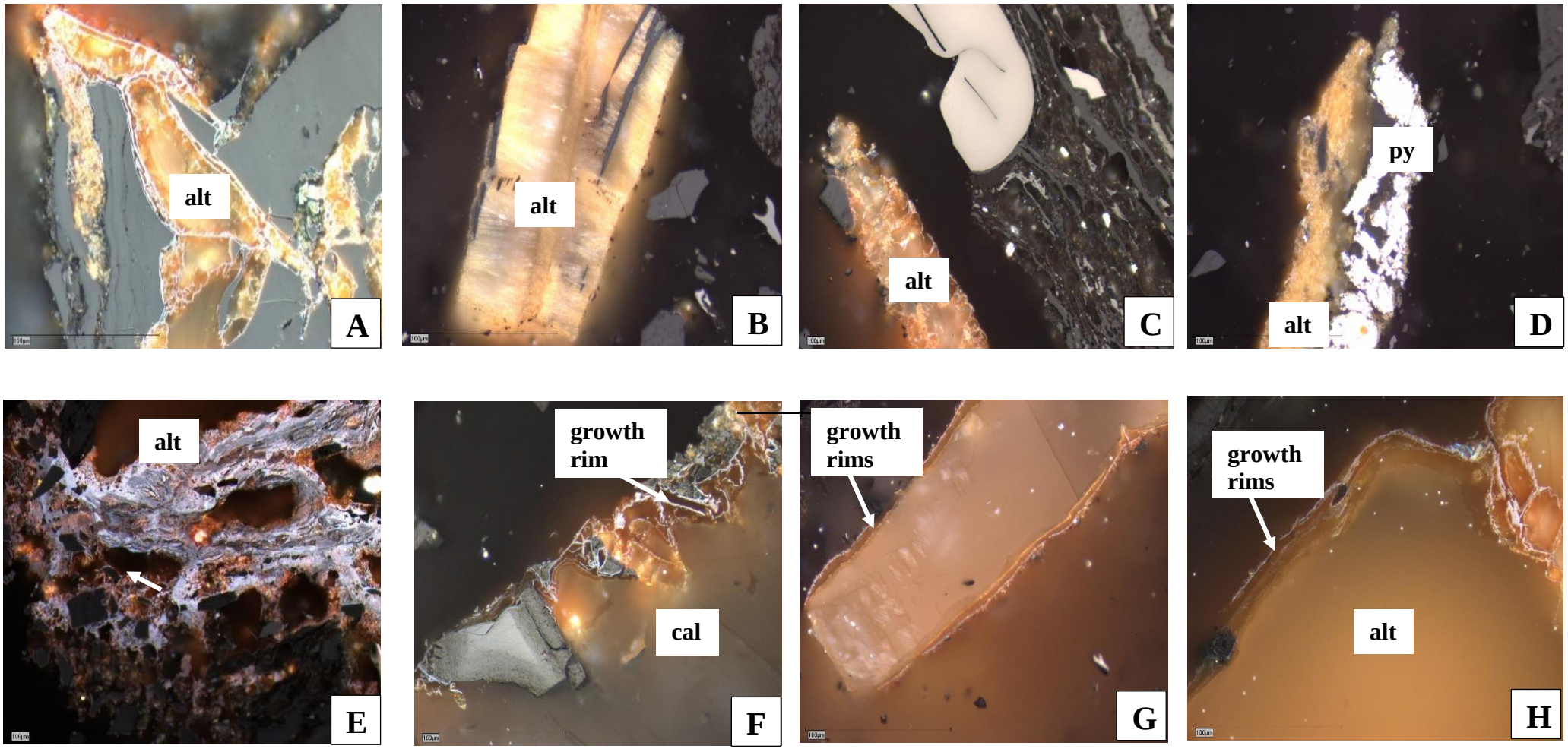


Figure 35. Photomicrographs of various forms of altered calcite (bright red). Altered calcite veins in B3W M6 [A], Altered calcite lath in B11W M6 [B] and in B5W M4 [C], Altered calcite adjacent to pyrite in B11W M6 [D], Extensive alteration (white zone) associated with red altered calcite B3W M4 [E], Growth rims on the edge of calcite grain in sample collected after 16 months of weathering [F], Growth zones along the edge of altered calcite lath in B3W and sample collected after 16 months of weathering [H]. alt= alteration of calcite, py= pyrite, oxy rim= oxidation rim. Oil immersion at x500μm magnification.

Table 18. Proportion of weathered vs fresh coal constituents as determined by the ACA (vol %)

Sample	**MS W1**	**MS M2**	**MS M4**	***MS M6**	**MSW M2**	**MSW M4**	**MSW M6**
Fresh	97	94	91	-	92	89	97
Fissures few	2	1	6	-	1	3	1
Fissures many	1	0	0	-	0	0	1
Cracks few	0	3	1	-	3	3	0
Cracks extensive	0	2	2	-	2	3	0
Cracks desiccation	0	0	0	-	0	0	0
Discolouration dark zones	0	0	0	-	0	0	0
Discolouration light zones	0	0	0	-	0	0	0
Alteration minerals	0	0	0	-	2	2	1
Sample	**B3B**	**B3 M2**	**B3 M4**	**B3 M6**	**B3W M2**	**B3W M4**	**B3W M6**
Fresh	95	93	89	92	92	92	91
Fissures few	2	0	4	0	1	0	0
Fissures many	0	0	0	0	0	0	0
Cracks few	0	2	1	1	1	2	2
Cracks extensive	0	0	0	0	1	1	4
Cracks desiccation	3	5	6	6	5	5	3
Discolouration dark zones	0	0	0	0	0	0	0
Discolouration light zones	0	0	0	0	0	0	0
Alteration minerals	0	0	0	1	0	0	0
Sample	**B5 W1**	**B5 M2**	**B5 M4**	***B5 M6**	**B5W M2**	**B5W M4**	***B5W M6**
Fresh	98	96	96	-	92	92	-
Fissures few	1	2	2	-	4	3	-
Fissures many	0	0	0	-	1	1	-
Cracks few	1	0	0	-	0	0	-
Cracks extensive	0	1	0	-	0	0	-
Cracks desiccation	0	0	1	-	0	0	-
Discolouration dark zones	0	0	0	-	0	0	-
Discolouration light zones	0	0	1	-	1	1	-
Alteration minerals	0	1	0	-	2	3	-
Sample	**B9B**	**B9 M2**	**B9 M4**	**B9 M6**	**B9W M2**	**B9W M4**	**B9W M6**
Fresh	98	98	97	95	97	92	92
Fissures few	0	0	1	1	0	0	2
Fissures many	0	0	0	1	0	0	0
Cracks few	1	2	2	1	2	5	4
Cracks extensive	1	0	0	2	1	1	2
Cracks desiccation	0	0	0	0	0	1	0
Discolouration dark zones	0	0	0	0	0	0	0
Discolouration light zones	0	0	0	0	0	1	0
Alteration minerals	0	0	0	0	0	0	0
Sample	**B11B**	**B11 M2**	**B11 M4**	**B11 M6**	**B11W M2**	**B11W M4**	**B11W M6**
Fresh	95	88	91	96	95	88	84
Fissures few	0	5	4	2	2	4	5
Fissures many	0	2	0	0	0	1	0
Cracks few	2	2	1	0	0	0	2
Cracks extensive	1	2	1	0	1	1	2
Cracks desiccation	2	0	2	2	1	5	2
Discolouration dark zones	0	0	0	0	0	0	0
Discolouration light zones	0	1	1	0	1	1	0
Alteration minerals	0	0	0	0	0	0	5

*Samples were not suitable for analysis due to EMPA coating.

Chapter 6: Conclusions and recommendations

6.1 Summary

The purpose of this research was to observe how coal particles from the Waterberg and Limpopo Coalfields weathered under dry and wet conditions over a duration of 6 months. Fresh coal milled to a particle size of -1 mm was placed in perforated containers and left to weather outdoors. The samples were subjected to weathering under mild ambient air temperatures in the range 9.4-27.23°C. One set of the samples was repeatedly watered, the other not. Samples were taken at intervals of 1 week, 2 weeks, 1 month, 2 months, 4 months and 6 months, and analysed to monitor changes in the coal quality due to oxidative weathering.

6.2 Conclusions

The findings from the integrated use of the chemical, technological, mineralogical and petrographic analyses reveal that most of the changes that occurred during the early stages of oxidative weathering are minimal.

The key findings from this study are interpreted, discussed and conclusions drawn in relation to the specific objectives and the research questions posed under each objective for the study:

Objective 1: Allow weathering of fresh coal from the Waterberg and Limpopo Coalfields by exposing them to the same atmospheric conditions over a duration of 6 months.

The key question posed in relation to this objective was:

vii. Are the coals more susceptible to weathering under wet or dry conditions when subjected to the same atmospheric conditions?

The statistical analyses proved that the rate of change for the majority of the wet samples from both coalfields were more pronounced for certain coal properties such as the inherent moisture, volatile matter, ash, fixed carbon, total carbon, hydrogen, nitrogen, total sulphur, oxygen, CV, $Fe_2O_{(t)}$ and CaO content. However, a rapid change in the above-mentioned properties did not necessarily equate to weathering, because some of the reported rates of change were not consistent with the expected indicators for weathered coals as described in the literature. For example, despite the wet samples MSW, B9W and B11W showing faster rates of change in terms of their total carbon content relative to their dry counterparts, the trends in the total carbon content for those wet samples increased over time. Hence, they cannot be considered as being weathered. The statistical analysis of the swelling properties clearly

shows that the FSI of the wet samples of the MS and B3 diminished more rapidly compared to their dry counterparts. Similarly, the decrease in CV was generally more pronounced in the dry samples compared to the wet samples.

Given these findings, it can be concluded that coal as a whole does not weather uniformly because the different coal properties are more susceptible to weathering under either wet or dry conditions.

Objective 2: Observe the changes that the organic and inorganic coal constituents underwent in response to weathering, relative to a known "fresh" baseline coal quality.

The key questions posed in relation to this objective were:

viii. *Are there quantifiable changes in the organic constituents of the weathered coal relative to the fresh parent samples?*

The ACA petrographic analysis confirmed that 84-98 vol% of the particles were fresh. Petrographic indicators of weathering after 6 months were limited to the presence of altered calcite grains (1-5 vol%), cracks (1-3 vol%) and fissures (1-5 vol%) in rare particles.

ix. *Are there quantifiable changes in the inorganic constituents (minerals) of the weathered coal relative to the fresh parent samples?*

As described in the XRD, EMPA, FE-SEM and petrographic sections, four definite signs of changes in the inorganic constituents were observed. That is, 1) The appearance red calcite grains, 2) rare calcite alteration showing growth rims, 3) precipitation of siderite associated with the calcite growth rims, as well as 4) periodic precipitation of gypsum. These changes occurred in very small quantities (1-5 wt%) and were generally observed in the samples that had been watered throughout the experiment. However, the occurrence of the red calcite grains in a few of the dry samples that were not contaminated indicates that there was a greater extent of mineral alteration when coal weathers under wet conditions. The presence of these alteration minerals indicates that they formed as by-products of pyrite oxidation and the dissolution of calcite. No signs of weathering were observed on the other minerals present in the samples.

Objective 3: Compare the quality changes due to weathering between coalfields using coal from the Waterberg and Limpopo Coalfields.

The key question posed in relation to this objective was:

x. Which coals exhibits significant changes in coal quality due to weathering?

Unless proved to be statistically significant, all obsereved changes in the coal quality that were in line with the literature, were considered as apparent and could not be confirmed with certainty. The statistical analyses show that the properties of coal were not affected to the same degree despite being subjected to the same ambient temperature conditions during wet and dry treatment. Although more samples showed changes consistent with those reported in the literature, fewer coal properties were found to be statistically significant (Table 19), and therefore more reliant indicators of the weathering during the early stages.

Table 19. Statistically significant changes in the coal properties of the samples studied

Sample	Increased consistent with the literature	Decreased consistent with the literature
Middle seam (MS)	moisture, ash, total sulphur	FSI, CV
Bench 3 (B3)	total sulphur	FSI
Bench 5 (B5)	total sulphur	total carbon,
Bench 9B (B9)	moisture	CV
Bench 11 (B11)	moisture, ash	volatile matter, CV
Middle seam wet (MSW)	moisture, ash	FSI, hydrogen
Bench 3 wet (B3W)	-	FSI, volatile matter
Bench 5 wet (B5W)	-	-
Bench 9B wet (B9W)	Moisture	-
Bench 11 wet (B11W)	total sulphur	CV

Objective 4: Track, over time, how the changes in the coal constituents affect the future utilization potential of the coals in terms of heating (calorific value and thermogravimetry) and swelling propensity (free swelling index).

The key questions posed in relation to this objective were:

xi. Are the changes in the heating properties as determined by the CV and TGA, likely to negatively affect the performance in a boiler?

The thermogravimetric analysis indicates that with increasing exposure to weathering, the dry and wet samples of bench 5 (Waterberg Coalfield) ignited at higher temperatures, combusted at higher peak temperatures and burned out at lower temperatures. Thus, indicating that the reactivity of the coal decreased with increasing exposure to weathering. Compared to the dry subset of Bench 5, the wet samples combusted at higher ignition, devolatilization and peak temperatures. Despite the above-mentioned observations, the CV results of Bench 5 did not show a decreasing trend. So, the results are inconclusive in terms of the impact of weathering on the heating properties of the coal.

xii. Are the changes the in the swelling of the coal as determined by the FSI, likely to negatively affect the conversion of the coal into coke?

The propensity of the coals to swell was severely reduced in both coking coals from the Waterberg and Limpopo Coalfields, more so for the wet samples compared to their dry counterparts. It was also evident that the Waterberg coking coal weathered rapidly compared the Limpopo coking coal. Based on this finding it is likely that early stage weathering under mild temperature conditions with render the coals ineffective for coking.

Overall, the samples followed similar weathering trends as reported in the literature for other coals around the world in terms of minimal chemical, mineral and petrographic changes during early stage weathering under mild temperature conditions. However, the mineralogical alteration of calcite as observed in this study, together with the variabilities in the chemical and technological properties, indicates that coals from different regions require site-specific analysis in terms of understanding their weathering behaviour. For example, in the present study, coal weathering under wet conditions generally resulted in a greater deterioration of the coals coking properties and caused more mineral alteration compared to the samples that weathered under dry conditions. This finding may not necessarily be true for all coals, even within the same coalfield as the weathering behaviour depends on the inherent coal properties and environmental conditions to which it is subjected. Given that the coal in this study was weathered at small particle size (-1 mm) and under relatively controlled environmental conditions, it is unlikely (apart from the mineral transformations) that the changes observed in the organic composition of the coal would detrimentally affect coal quality at a commercial scale; i.e. coal stored at larger particle sizes under limited air exposure. However coking coals, which are prone to weather rapidly in terms of their swelling properties, should be utilized within the 4-6-month period, especially those with weakly caking properties such as those used this study. Furthermore, caution should be taken to limit self-heating and ultimately spontaneous combustion, which are a common phenomenon in stockpiled coals at various points of mining operations. Although oxidation is virtually impossible to prevent once coal has been extracted, the preventative measures discussed in Section 3.2 should be used to reduce the risk of self-heating and spontaneous combustion.

6.3 Recommendations

For the advancement of coal weathering research on South African coals, it is recommended that follow-up studies be conducted in terms of:

- Investigation into the alteration of calcite during coal storage by means of a detailed reaction kinetics and mineral composition.

- A weathering study that considers more meteorological parameters such as rainfall, humidity and solar radiation intensity affecting the coal during weathering.

- Incorporate the Saffranin-O staining technique (Gray *et al*. 1976) into the ACA to allow for better petrographic characterization of oxidized macerals at the early stages of weathering.

- The preceding recommendations should be applied to studies where coal is weathered for longer than 6 months.

References

Akinyemi, S. A., Akinlua, A., Gitari, W. M., Akinyeye, R. O., Petrik, L. F. (2011). A geochemical analytical scheme for the appraisal of partitioning and mobility of major elements in weathered dry disposed coal fly ash. Energy Science and Technology, 2, 13-25.

Alvarez, R., Barriocanal, C., Casal, M. D., Diez, M. A., Cimadevilla, J. L. G., Pis, J. J., Canga, C. S. (1998). Weathering Study of an Industrial Coal Blend Used in Cokemaking. ISIJ international, 38, 1332-1338.

Alvarez, R., Cimadevilla, J. L. G., Barriocanal, C., Casal, M. D., Diez, M. A., Pis, J. J., Canga, C. S. (2003). Influence of coal weathering on coke quality. Ironmaking and steelmaking, 30, 307-312.

Aphane, V., and Vermeulen, P. D. (2015). Acid mine drainage and its potential impact on the water resources in the Waterberg Coalfield, South Africa. South African Journal of Geology, 118, 55-70.

ASTM D4239-14: 2015. Standard Test Method for Sulphur in the Analysis Sample of Coal and Coke Using High-Temperature Tube Furnace Combustion. American Society for Testing and Materials (ASTM).

ASTM D5263-93: 2008. Standard Test Method for Determining the Relative Degree of Oxidation in Bituminous Coal by Alkali Extraction, ASTM International, West Conshohocken, PA, 2008, www.astm.org.

ASTM D5373-14: 2004. Standard Test Methods for Instrumental Determination of Carbon, Hydrogen, and Nitrogen in Laboratory Samples of Coal and Coke. American Society for Testing and Materials (ASTM).

Avila, C., Wu, T., Lester, E. (2014). Estimating the spontaneous combustion potential of coals using thermogravimetric analysis. Energy and Fuels, 28, 1765-1773.

Bamford, M. K. (2004). Diversity of the woody vegetation of Gondwanan Southern Africa. Gondwana Research, 7, 153-164.

Banerjee, D., Hirani, M., Sanyal, S.K. (2000). Coal-quality deterioration in a coal stack of a power station. Applied Energy, 66, 267-275.

Baris, K., Kizgut, S., Didari, V. (2012). Low-temperature oxidation of some Turkish coals. Fuel, 93, 423-432.

Baruya, P. (2014). Coal reserves in a carbon constrained future. IEA Clean Coal Centre, 81pp.

Belaid, M., Falcon, R.M.S., Vainikka, P., Patsa, K. V. (2013). Potential and technical basis for utilising coal beneficiation discards in power generation by applying circulating fluidised bed boilers. International Conference on Chemical, Ecology and Environmental Sciences (ICEES'2013).

Bend, S. L., and Kosloski, D. M. (1993). A petrographic examination of coal oxidation. International Journal of Coal Geology, 24, 233-243.

Bend, S. L., Edwards, I. A. S., Marsh, H. (1989). The effects of oxidation and weathering on coal combustion. American Chemical Society. 34, 923-930.

Bird, C. E. (1951). The friability and weathering characteristics of South African coals. Journal of the Southern African Institute of Mining and Metallurgy, 51, 329-342.

Bordy, E. M., and Catuneanu, O. (2001). Sedimentology of the upper Karoo fluvial strata in the Tuli Basin, South Africa. Journal of African Earth Sciences, 33, 605-629.

Brime, C. (1985). The accuracy of X-ray diffraction methods for determining mineral mixtures. Mineralogical Magazine, 49, 531-538.

Butakova, V. I., Popov, V. K., Posokhov, Y. M., Kuznetsova, N. P. (2013). Initial stage in the low-temperature oxidation of coal in air. Coke and Chemistry, 56, 225-234.

Cadle, A. B., Cairncross, B., Christie, A. D. M., Roberts, D. L. (1993). The Karoo Basin of South Africa: type basin for the coal-bearing deposits of southern Africa. International Journal of Coal Geology, 23, 117-157.

Cairncross, B. (2001). An overview of the Permian (Karoo) coal deposits of southern Africa. Journal of African Earth Sciences, 33, 529-562.

Calemma, V., Del Piero, G., Rausa, R., Girardi, E. (1995). Changes in optical properties of coals during air oxidation at moderate temperature. Fuel, 74, 383-388.

Carras, J. N., and Young, B. C. (1994). Self-heating of coal and related materials: models, application and test methods. Progress in Energy and Combustion Science, 20, 1-15.

Casal, M. D., Gonzalez, A. I., Canga, C. S., Barriocanal, C., Pis, J. J., Alvarez, R., Dıez, M. A. (2003). Modifications of coking coal and metallurgical coke properties induced by coal weathering. Fuel Processing Technology, 84, 47-62.

Catuneanu, O., Hancox, P. J., Cairncross, B., Rubidge, B. S. (2002). Foredeep submarine fans and forebulge deltas: orogenic off-loading in the underfilled Karoo Basin. Journal of African Earth Sciences, 35, 489-502.

Catuneanu, O., Wopfner, H., Eriksson, P. G., Cairncross, B., Rubidge, B. S., Smith, R. M. H., Hancox, P. J. (2005). The Karoo basins of south-central Africa. Journal of African Earth Sciences, 43, 211-253.

Chandra, D. (1966). Effect of storage of coals on reflectance and petrological composition. Economic Geology, 61, 754-759.

Chang, S., and Berner, R. A. (1998). Humic substance formation via the oxidative weathering of coal. Environmental Science and Technology, 32, 2883-2886.

Cimadevilla, J. L. G., Alvarez, R., Pis, J. J. (2003). Photoacoustic FT-IR study of weathered stockpiled coking coals. Vibrational spectroscopy, 31, 133-141.

Cimadevilla, J. L. G., Alvarez, R., Pis, J. J. (2005). Effect of coal weathering on technological properties of cokes produced at different scales. Fuel Processing Technology, 86, 809-830.

Clemens, A. H., and Matheson, T. W. (1996). The role of moisture in the self-heating of low-rank coals. Fuel, 75, 891-895.

Clemens, A. H., Matheson, T. W., Rogers, D. E. (1990). DTA studies of the low temperature oxidation of low rank coals. Fuel, 69, 255-256.

CoAL (2016). Mineral Resources and Ore Reserves Update 2016.Coal of Africa Limited, 118pp.

Cole, D. A., Simmons, G. W., Herman, R. G., Klier, K., Czakó-Nagy, I. (1987). Transformations of iron minerals during coal oxidation. Fuel, 66, 1240-1248.

Copard, Y., Disnar, J. R., Becq-Giraudon, J. F., Laggoun-Défarge, F. (2004). Erroneous coal maturity assessment caused by low temperature oxidation. International Journal of Coal geology, 58, 171-180.

Cox, J. L., and Nelson, C. R. (1984). Coal weathering: causes, effects and implications. American Chemical Society., Division of Fuel Chem., Preprints, 29, 102-107.

Creelman, R. A., and Ward, C. R. (1996). A scanning electron microscope method for automated, quantitative analysis of mineral matter in coal. International Journal of Coal Geology, 30, 249-269.

Crelling, J. C. (2008). Coal carbonization. In: Suárez-Ruiz, I., and Crelling, J. C. (Eds.). Applied coal petrology: the role of petrology in coal utilization. Academic Press.173-192.

Crelling, J. C., Hippo, E. J., Woerner, B. A., West, D. P. (1992). Combustion characteristics of selected whole coals and macerals. Fuel, 71, 151-158.

Crelling, J.C., Schrader, R.H., Benedict, L.G. (1979). Effects of weathered coal on coking properties and coke quality. Fuel, 58, 542-546.

Cumming, J. W., and McLaughlin, J. (1982). The thermogravimetric behaviour of coal. Thermochimica Acta, 57, 253-272.

Davis (2016). Vantage-Pro2. https://www.davisnet.com/solution/vantage-pro2/. [Accessed 6 August 2016].

De Jager, F.S.J., 1986. Coal occurrences of the central, north-western, northern and eastern Transvaal. In: Anhaeusser, C.R., Maske, S. (Eds.), Mineral Deposits of Southern Africa. Geological Society of South Africa, 2047–2055.

de Korte, G.J. (2001). Beneficiation of Weathered Coal. Coaltech Report 2020-4.6.2. p. 20.

Desna, N. A., and Miroshnichenko, D. V. (2011). Oxidized coal in coking: A review. Coke and Chemistry, 54, 139.

Dey, S., Paul, G. M., and Pani, S. (2013). Flotation behaviour of weathered coal in mechanical and column flotation cell. Powder Technology, 246, 689-694.

Ekmann, J. M., and Le, P. H. (2004). Coal storage and transportation. Encyclopaedia of Energy. Elsevier, New York, 551-580.

Exxaro (2018). Grootegeluk.http://www.exxaro.com/index.php/where-we-operate/coal/grootegeluk/ [Accessed, 16 February 2018].

Falcon, R. M.S. (1986). Spontaneous combustion of the organic matter in discards from the Witbank Coalfield. Journal of the Southern African Institute of Mining and Metallurgy, 86, 243-250.

Falcon, R.M.S, and Ham, A. J. (1988). The characteristics of Southern African coals. Journal of the South African Institute of Mining and Metallurgy, 88, 145-161.

Falcon, R.M.S. (2014). Causes of self-heating and spontaneous combustion in coal. Power point presentation pp 64. http://www.fossilfuel.co.za/conferences/2014/SponCombustion130214/IntroandCausesofSponCom-RF.pdf [Accessed 13 February 2018].

Falcon, R.M.S. and Snyman, C.P. (1986). An Introduction to Coal Petrography: Atlas of Petrographic Constituents in the Bituminous Coals of Southern Africa. Geological Society of Southern Africa, Johannesburg. 27pp.

Faure, K., Willis, J. P., Dreyer, J. C. (1996). The Grootegeluk Formation in the Waterberg Coalfield, South Africa: facies, palaeoenvironment and thermal history-evidence from organic and clastic matter. International Journal of Coal geology, 29, 147-186.

Fourie, C. J. S., Henry, G., Mare, L. P. (2014). The structure of the Karoo-age Ellisras Basin in Limpopo province, South Africa, in the light of new airborne geophysical data. South African Journal of Geology, 117, 193-210.

Fredericks, P. M., Warbrooke, P., Wilson, M. A. (1983). Chemical changes during natural oxidation of a high volatile bituminous coal. Organic Geochemistry, 5, 89-97.

Frezzotti, M. L., Tecce, F., Casagli, A. (2012). Raman spectroscopy for fluid inclusion analysis. Journal of Geochemical Exploration, 112, 1-20.

Garcia, A. B., Moinelo, S. R., Martinez-Tarazona, M. R., Tascón, J. M. (1991). Influence of weathering process on the flotation response of coal. Fuel, 70, 1391-1397.

Gethner, J. S. (1985). Thermal and oxidation chemistry of coal at low temperatures. Fuel, 64, 1443-1446.

Gethner, J. S. (1986). Coal oxidation and thermal chemistry. Preprint Paper., American Chemical Society, Division of Fuel Chemistry (United States), 31(CONF-860911).

Giroux, L., Kolijn, C. J., Pichler, F. S. (2006). Storage of small samples of coking coal for thermal rheological tests. Fuel Processing Technology, 87, 547-561.

Goodarzi, F. (1987). Comparison of elemental distribution in fresh and weathered samples of selected coals in the Jurassic-Cretaceous Kootenay Group, British Columbia, Canada. Chemical geology, 63, 21-28.

Gray, R. J. (1982). A petrologic method of analysis of nonmaceral microstructures in coal. International Journal of Coal Geology, 2, 79-97.

Gray, R. J., Rhoades, A. H., King, D. T. (1976). Detection of oxidized coal and the effect of oxidation on the technological properties. Transactions of the Society of Mining Engineers. AIME; (United States), 260, 2-31.

Gupta, R. (2007). Advanced coal characterization: a review. Energy and Fuels, 21, 451-460.

Hamilton, N.D. (1907). Weathering of coal. MSc, College of Science, University of Illinois. 37pp.

Hancox, P. J., and Götz, A. E. (2014). South Africa's Coalfields—A 2014 perspective. International Journal of Coal Geology, 132, 170-254.

Hercod, D. J., Brady, P. V., Gregory, R. T. (1998). Catchment-scale coupling between pyrite oxidation and calcite weathering. Chemical Geology, 151, 259-276.

Hill, C.R. (1986). Particle size and moisture effects in the low-temperature oxidation of coal. Unpublished MSc, University of the Witwatersrand, 130pp.

Hower, J.C., O'Keefe, J.M., Watt, M.A., Pratt, T.J., Eble, C.F., Stucker, J.D., Richardson, A.R. and Kostova, I.J. (2009). Notes on the origin of inertinite macerals in coals: observations on the importance of fungi in the origin of macrinite. International Journal of Coal Geology, 80, 135-143.

Huffman, G. P., Huggins, F. E., Dunmyre, G. R., Pignocco, A. J., Lin, M. C. (1985). Comparative sensitivity of various analytical techniques to the low-temperature oxidation of coal. Fuel, 64, 849-856.

Huggins, F. E., Huffman, G. P., Lin, M. C. (1983). Observations on low-temperature oxidation of minerals in bituminous coals. International Journal of Coal Geology, 3, 157-182.

Ibarra, J. V., and Miranda, J. L. (1996). Detection of weathering in stockpiled coals by Fourier transform infrared spectroscopy. Vibrational spectroscopy, 10, 311-318.

ICCP (1998). The new vitrinite classification (ICCP Systems 1994). International Committee for Coal and Organic Petrology (ICCP). Fuel, 80, 349-358.

ICCP (2001). The new inertinite classification (ICCP System 1994). International Committee for Coal and Organic Petrology (ICCP). Fuel, 80, 459-471.

Ingram, G.R., and Rimstidt, J.D., (1984). Natural weathering of coal. Fuel 63, 292–296.

Isaacs, J. J., and Liotta, R. (1987). Oxidative weathering of Powder River basin coal. Energy and Fuels, 1, 349-351.

ISO 1171: 2003. Determination of Ash. International Organization for Standardization (ISO), Geneva, Switzerland.

ISO 1928: 2004. Determination of Gross Calorific Value and Calculation of Net Calorific Value, International Organization for Standardization (ISO), Geneva, Switzerland.

ISO 501: 2012. Hard Coal-Determination of the crucible swelling number. International Organization for Standardization (ISO), Geneva, Switzerland.

ISO 562: 2010. Hard coal and coke-Determination of volatile matter. International Organization for Standardization (ISO), Geneva, Switzerland.

Itay, M. (1983). The low temperature oxidation of coal: Its kinetics and implication for spontaneous combustion. Unpublished PhD, University of the Witwatersrand, 262pp.

Itay, M., Hill, C. R., Glasser, D. (1989). A study of the low temperature oxidation of coal. Fuel Processing Technology, 21, 81-97.

Jackman, H. W., Eissler, R. L., and Reed, F. H. (1957). Weathering of Illinois coals during storage. Illinois State Geological Survey, Circular no. 227.

Jeffrey, L. (2005). Challenges associated with further development of the Waterberg Coalfield. Journal of the Southern African Institute of Mining and Metallurgy, 105, 453-457.

Jha, P. K., Das, T. K., Prasad, B. N., Soni, A. B. (2015). Determination of Weathering of Coal Using pH Values of the Coal Slurry. International Journal of Coal Preparation and Utilization, 35, 25-30.

Jha, P. K., Das, T. K., Soni, A. B. (2014). Effect of Weathering on Coal Quality. International Proceedings of Economics Development and Research, 75, 155.

Jha, P. K., Das, T. K., Soni, A. B. (2016). Study the Effect of Weathering on Coal and Coke Quality. International Journal of Coal Preparation and Utilization, 1-10.

Johnson, M.R., Van Vuuren, C.J., Visser, J.N.J., Cole, D.I., Wickens, H., de, V., Christie, A.D.M., Roberts, D.L., Brandl, G. (2006). Sedimentary rocks of the Karoo Supergroup. In: Johnson, M.R., Anhaeusser, C.R., Thomas, R.J. (Eds.), The Geology of South Africa, Geological Society of South Africa, Johannesburg/Council for Geoscience, Pretoria, pp. 461–499.

Johnson, R. A., and Cooney, R. P. (1983). The effect of weathering on the 1600 cm-1 band of bituminous coal. Australian Journal of Chemistry, 36, 2549-2554.

Joshi, K., Raghavan, V., Rangwala, A. S. (2013). Effect of weathering of coal and organic dusts on their spontaneous ignition. Fire Technology, 49, 843-856.

Kaegi, D. D. (1981). Predicting coke stability from coal petrographic analyses. In Proceedings of Ironmaking Conference, United States,40, No. CONF-8103154-). Inland Steel Research Labs., East Chicago, IN.

Kaegi, D. D. (1985). On the identification and origin of pseudovitrinite. International Journal of Coal Geology, 4, 309-319.

Kaegi, D. D., Valia, H. S., Harrison, C. H. (1988). Maceral behaviour and coal carbonization. In 47th Ironmaking Conference, 339-349 pp.

Kaji, R., Hishinuma, Y., and Nakamura, Y. (1985). Low temperature oxidation of coals: effects of pore structure and coal composition. Fuel, 64, 297-302.

Kershaw, J. R., and Taylor, G. H. (1992). Properties of Gondwana coals with emphasis on the Permian coals of Australia and South Africa. Fuel Processing Technology, 31, 127-168.

Kleshnya, G. G., Lavrova, O. Y., Revenko, N. M., Drozdnik, I. D., Miroshnichenko, D. V., Desna, N. A., Ivanova, E. V. (2013). Determining the degree of coal oxidation at PAO AKKhZ. Coke and Chemistry, 56, 398-404.

Komraus, J. L., Popiel, E. S., Mocek, R. (1990). Chemical transformations of ferruginous minerals during the process of oxidation of hard coal. Hyperfine Interactions, 58, 2589-2592.

Kruszewska, K. J. (2003). Fluorescing macerals in South African coals. International Journal of Coal Geology, 54, 79-94.

Kruszewska, K. J., and du Cann, V. M. (1996). Detection of the incipient oxidation of coal by petrographic techniques. Fuel, 75, 769-774.

Kus, J., Misz-Kennan, M., ICCP (2017). Coal weathering and laboratory (artificial) coal oxidation. International Journal of Coal Geology, 171, 12-36.

Lett, R.G. and Ruppel, T.C. (2004). Coal, Chemical and Physical Properties. Encyclopaedia of Energy. Elsevier, New York, 411-423.

Li, S., Whitely, N., Xu, W., Pan, W.P. (2005). Characterization of Coal by Thermal Analysis Methods. In: Ramon D.A. (Ed.), Fundamentals and Applications to Material Characterization. Universidade da Coruña, Servicio de Publicaciones,111-120pp.

Lim, S. C., Rathbone, R. F., Rubel, A. M., Givens, E. N., Derbyshire, F. J. (1994). Carbon Monoxide Pretreatment of Subbituminous Coals. Energy and Fuels, 8, 294-300.

Liotta, R., Brons, G., Isaacs, J. (1983). Oxidative weathering of Illinois No. 6 coal. Fuel, 62, 781-791.

Lo, H. B., and Cardott, B. J. (1995). Detection of natural weathering of Upper McAlester coal and Woodford Shale, Oklahoma, USA. Organic Geochemistry, 22, 73-83.

Lowenhaupt, D. E., and Gray, R. J. (1980). The alkali-extraction test as a reliable method of detecting oxidized metallurgical coal. International Journal of Coal Geology, 1, 63-73.

Malaza, N. (2013). Basin Analysis of the Soutpansberg and Tuli Coalfields, Limpopo Province of South Africa. Unpublished PhD Thesis, University of Fort Hare, 270pp.

Maloney, D. J., Jenkins, R. G., Walker Jr, P. L. (1982). Low-temperature air oxidation of caking coals. 2. Effect on swelling and softening properties. Fuel, 61, 175-181.

Malvadkar, S.B., Forbes, S., McGurl, G.V. (2004). Coal resources, formation of. Encyclopaedia of energy, 1, 529-550.

Mangena, S. J., and du Cann, V. M. (2007). Binderless briquetting of some selected South African prime coking, blend coking and weathered bituminous coals and the effect of coal properties on binderless briquetting. International Journal of Coal Geology, 71, 303-312.

Mangkusubroto, P. (2010). Coal is mined by two methods – surface or 'opencast' mining and underground or 'deep' mining. [WWW]. http://prasindo.blogspot.co.za/2010/09/coal-is-mined-by-two-methods-surface-or.html. (November 25th, 2017).

Marchioni, D. L. (1983). The detection of weathering in coal by petrographic, rheologic and chemical methods. International Journal of Coal Geology, 2, 231-259.

Martínez, M., and Escobar, M. (1995). Effect of coal weathering on some geochemical parameters. Organic Geochemistry, 23, 253-261.

Matjie, R. H., French, D., Ward, C. R., Pistorius, P. C., Li, Z. (2011). Behaviour of coal mineral matter in sintering and slagging of ash during the gasification process. Fuel Processing Technology, 92, 1426-1433.

McHugh, E. A., Diessel, C. F., Kutzner, R. (1991). Use of fluorescence microscopy in the detection of low level oxidation in bituminous coals. Fuel, 70, 647-653.

Mendelsohn, J. (1933). Solvent extraction as a method of detecting the oxidation of coal. Journal of the Southern African Institute of Mining and Metallurgy, 33, 285-290.

Miroshnichenko, D. V., Drozdnik, I. D., Kaftan, Y. S., Bidolenko, N. B., Desna, N. A. (2012a). Coking of coal batch with different content of oxidized coal. Coke and Chemistry, 55, 155-164.

Miroshnichenko, D. V., Drozdnik, I. D., Kaftan, Yu. S., Ivanova, E. V., Sirokotyaga, K. N., Desna N. A. (2012b). Kinetic Characteristics of Coal Oxidation. Coke and Chemistry, 55, 87–96.

Misz-Kennan, M., and Fabiańska, M. J. (2011). Application of organic petrology and geochemistry to coal waste studies. International Journal of Coal Geology, 88, 1-23.v

Mondragón, F., Ruíz, W., Santamaría, A. (2002). Effect of early stages of coal oxidation on its reaction with elemental sulphur. Fuel, 81, 381-388.

Morgan, P.A. Robertson, S.D. Unsworth, J.F. (1986). Combustion studies by thermogravimetric analysis. 1. Coal oxidation. Fuel, 65, 1546-1551.

Moroeng, O. M., Wagner, N. J., Brand, D. J., Roberts, R. J. (2018). A Nuclear Magnetic Resonance study: Implications for coal formation in the Witbank Coalfield, South Africa. International Journal of Coal Geology, 188, 145-155.

Mpandeli, S. (2014). Managing Climate Risks Using Seasonal Climate Forecast Information in Vhembe District in Limpopo Province, South Africa. Journal of Sustainable Development, 7, pp 68.

Nádudvari, Á., and Fabiańska, M. J. (2016). The impact of water-washing, biodegradation and self-heating processes on coal waste dumps in the Rybnik Industrial Region (Poland). International Journal of Coal Geology, 154, 286-299.

Ndaji, F. E., and Thomas, K. M. (1995). The effects of oxidation on the macromolecular structure of coal. Fuel, 74, 932-937.

Norton, G.A. (1993). A review of the derivative thermogravimetric technique (burning profile) for fuel combustion studies. Thermochimica Acta, 214, 171-182.

Nowak, M. A., Paul, A. D., Srivastava, R. D., Radios, A. (2004). Coal conversion. Encyclopaedia of Energy, 1, 425-434.

O'Keefe, J. M., Bechtel, A., Christanis, K., Dai, S., DiMichele, W. A., Eble, C. F., Esterle, J.S., Mastalerz, M., Raymond, A.L., Valentim, B.V., Wagner, N.J., Ward C.R., Hower,. J.C. (2013). On the fundamental difference between coal rank and coal type. International Journal of Coal Geology, 118, 58-87.

Ortlepp, G.J., (1986). Limpopo Coalfield. In: Anhaeusser, C.R., Maske, S. (Eds.), Mineral Deposits of Southern Africa, vol. II. Geological Society of South Africa, Johannesburg, 2057–2061.

Parr, S. W., and Hamilton, N. D. (1908). The Weathering of Coal. Naval Engineers Journal, 20, 469-470.

Pickel, W., Kus, J., Flores, D., Kalaitzidis, S., Christanis, K., Cardott, B. J., M. Misz-Kennan, S. Rodrigues, A. Henschel, M. Hamor-Vido, Crosdale, P. Wagner, N.J., ICCP (2017). Classification of liptinite–ICCP System 1994. International Journal of Coal Geology, 169, 40-61.

Pisupati, S. V. (1996). An examination of burning profiles as a tool to predict combustion behaviour of coals (No. CONF-960376--). American Chemical Society, Washington, DC (United States).

Pisupati, S. V., Scaroni, A. W., Hatcher, P. G. (1993). Devolatilization behaviour of naturally weathered and laboratory oxidized bituminous coals. Fuel, 72, 165-173.

Pisupati, S. V., Scaroni, A. W., Stoessner, R. D. (1991). Combustion characteristics of naturally weathered (in situ) bituminous coals. Fuel Processing Technology, 28, 49-66.

Pone, J. D. N., Hein, K. A., Stracher, G. B., Annegarn, H. J., Finkleman, R. B., Blake, D. R., McCormack, J.K., Schroeder, P. (2007). The spontaneous combustion of coal and its by-products in the Witbank and Sasolburg Coalfields of South Africa. International Journal of Coal Geology, 72, 124-140.

Prévost, X. (2017). Coal's powerful role. Inside Mining, 10, 12-13 pp.

PWC. (2017). Highlighting trends in the South African mining industry. SA mine 9th edition. PricewaterhouseCoopers (PWC), 83pp.

Rao, C. P., and Gluskoter, H. J. (1973). Occurrence and distribution of minerals in Illinois coals. Circular no. 476.

Rees, O. W., Coolican, F. C., Pierron, E. D., Beeler, C. W. (1961). Effects of outdoor storage on Illinois steam coals. Champaign, Ill.: Illinois State Geological Survey, Prairie Research Institute.

Ribeiro, J., Suárez-Ruiz, I., Ward, C. R., Flores, D. (2016). Petrography and mineralogy of self-burning coal wastes from anthracite mining in the El Bierzo Coalfield (NW Spain). International Journal of Coal Geology, 154, 92-106.

Richards, J. M., Naude, G., Theron, S. J., McCullum, M. (2013). Petrological characterization of coal: an evolving science. Journal of the Southern African Institute of Mining and Metallurgy, 113, 865-875.

Ritsema, C. J., and Groenenberg, J. E. (1993). Pyrite oxidation, carbonate weathering, and gypsum formation in a drained potential acid sulphate soil. Soil Science Society of America Journal, 57, 968-976.

Roberts, D. L. (1991). The inherent moisture content of South African Permian coals. International Journal of Coal Geology, 17, 297-311.

Roy, M. M. (1965). Studies on coal macerals; Part 3, Aerial oxidation of macerals. Economic Geology, 60, 1213-1217.

SANS 10320:2004. South African guide to the systematic evaluation of coal resources and coal reserves. South African National Standard (SANS).

SANS 5925:2007. Moisture Content of coal samples intended for general analysis (Air-Oven Method): second edition; South African National Standard (SANS).

SANS 7404-2:2015 Methods for the petrographic analysis of coals - Part 2: Method of preparing coal samples. South African National Standard (SANS).

SANS 7404-3:2016. Methods for the petrographic analysis of coals Part 3: Method of determining maceral group composition. South African National Standard (SANS).

SANS 7404-5:1994 Methods for the petrographic analysis of coals - Part 5: Method of determining microscopically the reflectance of vitrinite. South African National Standard (SANS).

Sarikaya, M. (1995). Flotation test as a method for studying coal weathering. International Journal of Mineral Processing, 43, 31-35.

Schmidt, L., Elder, J., Davis, J. (1936). Oxidation of Coal at Storage Temperatures Effect on Carbonizing Properties. Industrial and Engineering Chemistry, 28, 1346-1353.

Schobert, H. H., and Song, C. (2002). Chemicals and materials from coal in the 21st century. Fuel, 81, 15-32.

Schweinfurth, S. P. (2009). An introduction to coal quality. The National Coal Resource Assessment Overview: US Geological Survey Professional Paper.

Scott, A. C. (2002). Coal petrology and the origin of coal macerals: a way ahead? International Journal of Coal Geology, 50, 119-134.

Sebola, M.T. (2015). The effects of weathering on coal in the Limpopo and Soutpansberg Coalfields. Unpublished Honours Research project, University of the Witwatersrand, 60pp.

Sen, R., Srivastava, S. K., Singh, M. M. (2009). Aerial oxidation of coal-analytical methods, instrumental techniques and test methods: A survey. Indian Journal of Chemical Technology (2009), 103-135.

Shi, T., Wang, X., Deng, J., Wen, Z. (2005). The mechanism at the initial stage of the room-temperature oxidation of coal. Combustion and Flame, 140, 332-345.

Silva, L. F. O., Querol, X., Da Boit, K. M., de Vallejuelo, S. F. O., Madariaga, J. M. (2011). Brazilian coal mining residues and sulphide oxidation by Fenton's reaction: an accelerated weathering procedure to evaluate possible environmental impact. Journal of Hazardous Materials, 186, 516-525.

Smędowski, Ł., and Piechaczek, M. (2016). Impact of weathering on coal properties and evolution of coke quality described by optical and mechanical parameters. International Journal of Coal Geology, 168, 119-130.

Smith, R. M. H., Eriksson, P. G., Botha, W. J. (1993). A review of the stratigraphy and sedimentary environments of the Karoo-aged basins of Southern Africa. Journal of African Earth Sciences (and the Middle East), 16, 143-169.

Snyman, C. P. (1989). The role of coal petrography in understanding the properties of South African coal. International Journal of Coal Geology, 14, 83-101.

Snyman, C. P., and Barclay, J. (1989). The coalification of South African coal. International Journal of Coal Geology, 13, 375-390.

Snyman, C. P., and Botha, W. J. (1993). Coal in south Africa. Journal of African Earth Sciences (and the Middle East), 16, 171-180.

Snyman, C.P. (1998). Coal. In: Wilson, M.G.C., Anhaeusser, C.R. (Eds.), The Mineral Resources of South Africa. Handbook, 16. Council for Geoscience, South Africa, pp. 136–205. South African Committee.

Sparrow, J., Wagner, N., Falcon, R.M.S. (2013). The effect of geological structures in the exploration for Prime Coking Coal. Presentation at the FFF 2nd Limpopo Coalfields Conference (October 2013).

Speight, J. G. (2005). Handbook of coal analysis. John Wiley and Sons, New Jersey, 212pp.

StatSoft, I. (2018). Electronic statistics textbook. Tulsa, OK: Electronic Statistics Textbook. http://www.statsoft.com/Textbook.

Sua´rez-Ruiz, I., and Ward, C.R. (2008). Basic Factors Controlling Coal Quality and Technological Behaviour of Coal. In: Suárez-Ruiz, I., and Crelling, J. C. (Eds.). Applied coal petrology: the role of petrology in coal utilization. Academic Press.173-192.

Sýkorová, I., Pickel, W., Christanis, K., Wolf, M., Taylor, G. H., Flores, D. (2005). Classification of huminite—ICCP System 1994. International Journal of Coal Geology, 62, 85-106.

Taraba, B. (1996). Analysis of the factors affecting natural oxidation of coal matter. In: Křibek B. (Ed.), Weathering of fossil organic matter: proceedings of the Czech Working Group meeting, Prague, November 26-27, 1996: international geological correlation programme, project 357, organics and mineral deposits. Czech Geological Survey, Czech Republic, 9-19.

Taylor, G. H., Teichmüller, M., Davis, A. C. F. K., Diessel, C. F. K., Littke, R., Robert, P. (1998). Organic Petrology. Gebruder Borntraeger, Berlin, 704 pp.

Teichmüller, M. (1989). The genesis of coal from the viewpoint of coal petrology. International Journal of Coal Geology, 12, 1-87.

Teo, K. C., Finora, S., Leja, J. (1982). Oxidation states in surface and buried coal from the Fording River Deposit. Fuel, 61, 71-76.

Thomas, L. (2012). Coal Geology- second edition John. Wiley and Sons Ltd, 444pp.

Ulanovskii, M. L. (2012). Kinetic research on coal oxidation: A review, Coke and Chemistry, 55, 256-260.

Underhill, L., and Bradfield, D. (2013). INTROSTAT (Statistics textbook). Doctoral dissertation, University of Cape Town, 337pp. http://open.uct.ac.za/bitstream/handle/11427/4150/INTROSTAT_ebook.pdf?sequence=1

Vassilev, S. V., and Vassileva, C. G. (1996). Occurrence, abundance and origin of minerals in coals and coal ashes. Fuel Processing Technology, 48, 85-106.

Vassilev, S. V., Vassileva, C. G., Baxter, D., Andersen, L. K. (2010). Relationships between chemical and mineral composition of coal and their potential applications as genetic indicators. Part 2. Mineral classes, groups and species. Geologica Balcanica, 39, 43-67.

Vega, M. F., Fernández, A. M., Díaz-Faes, E., Barriocanal, C. (2017). Improving the properties of high volatile coking coals by controlled mild oxidation. Fuel, 191, 574-582.

Waanders, F. B., Vinken, E., Mans, A., Mulaba-Bafubiandi, A. F. (2003). Iron minerals in coal, weathered coal and coal ash–SEM and Mössbauer results. Hyperfine Interactions, 148, 21-29.

Wagner, N. J. (1999). The effect of weathering on stored discard coals and the impact on combustion. PhD dissertation, University of the Witwatersrand.

Wagner, N. J. (2007). The Abnormal Condition Analysis used to characterize weathered discard coals. International Journal of Coal Geology, 72, 177-186.

Wagner, N. J. (2008). The characterization of weathered discard coals and their behaviour during combustion. Fuel, 88, 1687-1697.

Wagner, N. J., and Tlotleng, M. T. (2012). Distribution of selected trace elements in density fractionated Waterberg coals from South Africa. International Journal of Coal Geology, 94, 225-237.

Wang, G., and Zhou, A. (2012). Time evolution of coal structure during low temperature air oxidation. International Journal of Mining Science and Technology, 22, 517-521.

Wang, H., Dlugogorski, B. Z., Kennedy, E. M. (2002). Thermal decomposition of solid oxygenated complexes formed by coal oxidation at low temperatures. Fuel, 81, 1913-1923.

Wang, H., Dlugogorski, B. Z., Kennedy, E. M. (2003a). Analysis of the mechanism of the low-temperature oxidation of coal. Combustion and Flame, 134, 107-117.

Wang, H., Dlugogorski, B. Z., Kennedy, E. M. (2003b). Coal oxidation at low temperatures: oxygen consumption, oxidation products, reaction mechanism and kinetic modelling. Progress in Energy and Combustion Science, 29, 487-513.

Ward, C. R. (1989). Minerals in bituminous coals of the Sydney Basin (Australia) and the Illinois Basin (USA). International Journal of Coal Geology, 13, 455-479.

Ward, C. R. (2002). Analysis and significance of mineral matter in coal seams. International Journal of Coal Geology, 50, 135-168.

White, D. (1909). The effect of oxygen in coal (Vol. 382). US Government United States Geological. Survey. Bull., 382, 71pp.

Wu, M. M., Robbins, G. A., Winschel, R. A., Burke, F. P. (1988). Low-temperature coal weathering: its chemical nature and effects on coal properties. Energy and Fuels, 2, 150-157.

Xia, W., and Yang, J. (2014). Changes in surface properties of anthracite coal before and after inside/outside weathering processes. Applied Surface Science,313, 320-324.

Yatsu, E. (1988). The Nature of Weathering: An Introduction. SOZOSHA, Tokyo, 624pp.

Yohe, G.R. (1958). Oxidation of coal. Illinois State Geological Survey Rep. Invest., 207, 51pp.

Zhang, J., Ren, T., Liang, Y., Wang, Z. (2016). A review on numerical solutions to self-heating of coal stockpile: Mechanism, theoretical basis, and variable study. Fuel, 182, 80-109.

Appendices

Appendix A. Ambient temperature measurements over the duration of the experiment.

Day	Month	Average Temperature (°C)	Maximum Temperature (°C)	Minimum Temperature (°C)
1	02 August 2016	11.50	20.30	2.70
2	03 August 2016	11.55	19.70	3.40
3	04 August 2016	9.55	17.10	2.00
4	05 August 2016	10.95	21.30	0.60
5	06 August 2016	13.40	24.70	2.10
6	07 August 2016	14.60	25.40	3.80
7	08 August 2016	15.35	24.70	6.00
8	09 August 2016	12.70	21.50	3.90
9	10 August 2016	16.43	21.50	11.00
10	11 August 2016	15.78	21.10	10.80
11	12 August 2016	15.50	20.20	11.80
12	13 August 2016	14.45	18.90	10.10
13	14 August 2016	16.55	21.20	12.60
14	15 August 2016	17.52	22.10	14.20
15	16 August 2016	13.33	17.80	9.60
16	17 August 2016	13.10	17.90	9.20
17	18 August 2016	12.89	17.80	8.20
18	19 August 2016	13.81	18.90	9.00
19	20 August 2016	16.57	21.70	12.70
20	21 August 2016	16.59	22.90	11.30
21	22 August 2016	12.51	16.90	7.30
22	23 August 2016	10.38	17.30	10.38
23	24 August 2016	13.60	21.30	7.10
24	25 August 2016	17.52	23.30	12.30
25	26 August 2016	18.55	24.80	13.40
26	27 August 2016	16.38	22.60	10.40

27	28 August 2016	17.90	24.00	12.60
28	29 August 2016	19.11	25.80	14.00
29	30 August 2016	19.66	25.60	15.70
30	31 August 2016	17.67	23.90	13.10
31	01 September 2016	16.65	22.70	11.40
32	02 September 2016	17.27	23.10	11.60
33	03 September 2016	18.51	25.50	12.40
34	04 September 2016	18.43	23.80	12.40
35	05 September 2016	18.23	23.50	13.10
36	06 September 2016	20.08	24.60	15.90
37	07 September 2016	20.29	25.30	15.10
38	08 September 2016	22.28	27.20	17.20
39	09 September 2016	21.31	26.80	15.90
40	10 September 2016	20.75	25.30	15.80
41	11 September 2016	15.73	21.70	10.10
42	12 September 2016	17.15	22.30	11.60
43	13 September 2016	19.96	24.90	15.20
44	14 September 2016	14.16	17.70	11.20
45	15 September 2016	17.35	23.70	11.50
46	16 September 2016	20.09	25.20	15.30
47	17 September 2016	14.84	21.10	9.70
48	18 September 2016	7.18	9.50	4.70
49	19 September 2016	11.48	18.20	5.60
50	20 September 2016	14.93	21.10	9.90
51	21 September 2016	18.82	24.80	13.80
52	22 September 2016	21.22	26.10	16.40
53	23 September 2016	21.75	27.40	15.50
54	24 September 2016	19.83	25.90	14.90
55	25 September 2016	20.46	26.30	15.70
56	26 September 2016	17.95	23.30	12.90
57	27 September 2016	18.84	23.60	14.80

58	28 September 2016	16.76	22.10	12.30
59	29 September 2016	16.84	24.10	11.10
60	30 September 2016	18.31	23.90	11.80
61	01 October 2016	20.32	25.40	15.40
62	02 October 2016	16.63	22.20	10.30
63	03 October 2016	11.32	17.90	4.80
64	04 October 2016	10.93	18.00	4.60
65	05 October 2016	15.62	23.30	8.30
66	06 October 2016	21.93	28.30	15.50
67	07 October 2016	23.64	28.80	17.40
68	08 October 2016	19.30	24.80	13.70
69	09 October 2016	16.54	22.20	13.20
70	10 October 2016	17.08	24.40	8.30
71	11 October 2016	21.31	28.50	13.50
72	12 October 2016	23.55	28.90	17.80
73	13 October 2016	19.81	25.60	14.90
74	14 October 2016	17.68	23.60	11.60
75	15 October 2016	19.20	26.40	11.90
76	16 October 2016	20.84	26.80	15.80
77	17 October 2016	20.70	26.30	14.40
78	18 October 2016	14.94	20.30	10.70
79	19 October 2016	14.23	17.90	11.80
80	20 October 2016	16.70	21.90	11.80
81	21 October 2016	19.45	25.10	13.80
82	22 October 2016	21.15	29.90	12.40
83	23 October 2016	21.20	29.60	12.80
84	24 October 2016	22.70	29.70	15.70
85	25 October 2016	22.50	30.50	14.50
86	26 October 2016	22.20	29.20	15.20
87	27 October 2016	22.95	32.30	13.60
88	28 October 2016	24.20	32.60	15.80

89	29 October 2016	24.90	33.90	15.90
90	30 October 2016	26.35	34.30	18.40
91	31 October 2016	26.15	35.30	17.00
92	01 November 2016	23.00	27.60	19.80
93	02 November 2016	19.42	25.90	15.50
94	03 November 2016	19.31	25.10	13.60
95	04 November 2016	22.51	28.50	16.70
96	05 November 2016	20.75	23.30	18.10
97	06 November 2016	21.65	26.20	18.20
98	07 November 2016	19.74	22.60	17.20
99	08 November 2016	19.37	25.60	15.60
100	09 November 2016	19.41	26.00	15.30
101	10 November 2016	19.83	26.70	15.90
102	11 November 2016	15.02	19.50	11.30
103	12 November 2016	17.22	23.70	11.70
104	13 November 2016	20.47	26.20	14.70
105	14 November 2016	19.50	25.10	14.30
106	15 November 2016	16.39	21.50	12.40
107	16 November 2016	16.79	21.80	12.60
108	17 November 2016	20.98	27.30	14.00
109	18 November 2016	21.63	27.30	16.40
110	19 November 2016	15.01	19.30	11.80
111	20 November 2016	17.38	24.30	12.40
112	21 November 2016	17.02	21.60	13.00
113	22 November 2016	20.63	27.00	16.30
114	23 November 2016	19.22	24.50	16.10
115	24 November 2016	16.46	17.70	15.10
116	25 November 2016	16.68	22.70	13.20
117	26 November 2016	17.47	22.40	12.20
118	27 November 2016	17.73	23.20	13.10
119	28 November 2016	21.63	29.20	14.40

120	29 November 2016	24.55	29.40	19.60
121	30 November 2016	23.91	30.00	18.90
122	01 December 2016	23.49	29.30	16.70
123	02 December 2016	20.93	27.40	13.80
124	03 December 2016	20.55	27.10	14.00
125	04 December 2016	22.75	30.20	16.00
126	05 December 2016	20.82	25.30	16.70
127	06 December 2016	19.95	24.20	15.70
128	07 December 2016	21.04	26.40	18.40
129	08 December 2016	21.99	27.80	17.10
130	09 December 2016	22.12	26.80	16.80
131	10 December 2016	24.45	30.90	18.00
132	11 December 2016	21.55	27.80	15.30
133	12 December 2016	20.35	25.60	15.10
134	13 December 2016	20.10	26.30	13.90
135	14 December 2016	20.90	25.40	16.40
136	15 December 2016	21.30	27.30	15.30
137	16 December 2016	23.20	29.80	16.60
138	17 December 2016	23.00	30.10	15.90
139	18 December 2016	23.00	29.80	16.20
140	19 December 2016	23.75	31.70	15.80
141	20 December 2016	23.20	31.70	14.70
142	21 December 2016	23.65	30.80	16.50
143	22 December 2016	24.15	32.20	16.10
144	23 December 2016	25.45	32.70	18.20
145	24 December 2016	22.45	26.80	18.10
146	25 December 2016	17.20	20.50	13.90
147	26 December 2016	16.40	19.70	13.10
148	27 December 2016	19.17	22.90	16.10
149	28 December 2016	17.98	21.70	14.70
150	29 December 2016	19.87	24.70	16.90

151	30 December 2016	19.35	24.40	15.10
152	31 December 2016	21.30	26.70	16.10
153	01 January 2017	23.83	29.10	17.80
154	02 January 2017	23.29	28.10	17.60
155	03 January 2017	22.65	27.60	18.20
156	04 January 2017	18.00	20.50	14.70
157	05 January 2017	18.91	23.40	14.20
158	06 January 2017	20.20	25.10	15.60
159	07 January 2017	16.92	17.70	16.30
160	08 January 2017	16.04	16.90	14.60
161	09 January 2017	17.63	21.90	14.70
162	10 January 2017	19.80	24.30	15.70
163	11 January 2017	19.62	24.40	15.30
164	12 January 2017	20.96	24.80	16.50
165	13 January 2017	19.64	25.70	16.60
166	14 January 2017	20.88	25.80	16.40
167	15 January 2017	20.38	26.30	15.60
168	16 January 2017	20.51	26.20	15.20
169	17 January 2017	16.46	22.60	11.10
170	18 January 2017	17.64	25.30	9.20
171	19 January 2017	22.25	28.60	16.50
172	20 January 2017	21.71	27.30	17.70
173	21 January 2017	20.68	27.10	17.20
174	22 January 2017	20.26	25.30	15.90
175	23 January 2017	20.86	26.40	16.10
176	24 January 2017	21.55	26.40	17.10
177	25 January 2017	20.09	24.50	16.90
178	26 January 2017	18.95	21.40	16.90
179	27 January 2017	17.26	20.10	14.90
180	28 January 2017	19.38	24.20	16.40
181	29 January 2017	21.71	27.50	16.80

182	30 January 2017	17.47	19.20	15.30
183	31 January 2017	19.94	24.70	15.90
184	01 February 2017	21.17	26.90	15.90
185	02 February 2017	21.23	26.60	17.10
186	03 February 2017	20.42	24.80	15.40
187	04 February 2017	19.46	23.20	15.90
188	05 February 2017	19.78	24.10	16.90
189	06 February 2017	20.73	24.20	17.10

Appendix B. Replicate (R) runs for the proximate analysis

	Inherent moisture %				Volatile matter % (db)				Ash % (db)				Calculated fixed carbon %			
Sample	**R1**	**R2**	**R3**	**Average**	**R1**	**R2**	**R3**	**Average**	**R1**	**R2**	**R3**	**Average**	**R1**	**R2**	**R3**	**Average**
MSB	1.50	1.30	1.30	1.37	31.50	31.30	31.60	31.47	22.20	22.40	22.40	22.33	44.80	45.00	44.70	44.83
B3B	2.10	2.00	2.20	2.10	32.90	33.00	33.00	32.97	24.70	24.60	24.60	24.63	40.30	40.40	40.20	40.30
B5B	1.70	1.60	1.70	1.67	27.60	27.60	27.60	27.60	35.00	35.20	35.20	35.13	35.70	35.60	35.50	35.60
B9B	1.90	1.90	1.90	1.90	22.90	23.00	23.00	22.97	17.80	18.00	18.00	17.93	57.40	57.10	57.10	57.20
B11 B	1.70	1.50	1.40	1.53	27.60	27.70	27.70	27.67	15.20	15.10	15.10	15.13	55.50	55.70	55.80	55.67
Sample	**R1**	**R2**	**R3**	**Average**	**R1**	**R2**	**R3**	**Average**	**R1**	**R2**	**R3**	**Average**	**R1**	**R2**	**R3**	**Average**
MS W1	1.60	1.60	1.60	1.60	31.00	31.20	31.10	31.10	22.00	22.30	22.00	22.10	45.40	44.90	45.30	45.20
B3 W1	1.80	1.80	1.60	1.73	32.70	32.50	32.40	32.53	23.50	23.50	23.40	23.47	42.00	42.20	42.60	42.27
B5 W1	1.60	1.60	1.50	1.57	27.90	27.30	27.00	27.40	34.80	34.80	34.70	34.77	35.70	36.30	36.80	36.27
B9 W1	1.90	2.10	2.00	2.00	22.30	22.10	22.40	22.27	18.00	17.80	17.90	17.90	57.80	58.00	57.70	57.83
B11 W1	1.60	1.60	1.60	1.60	27.00	27.30	27.60	27.30	15.00	15.10	15.10	15.07	56.40	56.00	55.70	56.03
MSW W1	1.30	1.20	1.20	1.23	31.20	31.10	31.20	31.17	22.30	22.30	22.30	22.30	45.20	45.40	45.30	45.30
B3W W1	1.50	1.30	1.40	1.40	32.80	32.90	32.80	32.83	23.80	23.70	23.80	23.77	41.90	42.10	42.00	42.00
B5W W1	1.10	1.20	1.20	1.17	28.10	27.80	27.90	27.93	33.90	33.90	33.90	33.90	36.90	37.10	37.00	37.00
B9W W1	1.90	1.90	1.90	1.90	22.40	22.30	22.40	22.37	17.80	17.70	17.60	17.70	57.90	58.10	58.10	58.03
B11W W1	1.90	1.90	1.90	1.90	27.10	27.20	26.90	27.07	14.90	14.90	14.90	14.90	56.10	56.00	56.30	56.13
Sample	**R1**	**R2**	**R3**	**Average**	**R1**	**R2**	**R3**	**Average**	**R1**	**R2**	**R3**	**Average**	**R1**	**R2**	**R3**	**Average**
MS W2	1.50	1.48	1.51	1.49	31.62	31.55	31.82	31.66	22.70	22.60	22.70	22.69	44.15	44.34	43.97	44.15
B3 W2	1.91	2.02	1.92	1.95	34.55	34.08	34.28	34.30	23.05	23.08	23.01	23.05	40.49	40.82	40.80	40.70
B5 W2	1.48	1.498	1.43	1.47	28.64	28.61	29.36	28.87	33.69	33.74	33.89	33.77	36.20	36.15	35.32	35.89
B9 W2	1.93	1.98	1.96	1.96	24.29	24.42	24.28	24.33	17.78	17.75	17.79	17.77	56.00	55.85	55.97	55.94
B11 W2	1.40	1.50	1.40	1.43	27.40	27.40	27.40	27.40	14.70	14.70	14.70	14.70	56.50	56.40	56.50	56.47
Sample	**R1**	**R2**	**R3**	**Average**	**R1**	**R2**	**R3**	**Average**	**R1**	**R2**	**R3**	**Average**	**R1**	**R2**	**R3**	**Average**
MS M1	1.50	1.50	1.50	1.50	30.00	30.20	30.00	30.07	22.50	22.50	22.60	22.53	46.00	45.80	45.90	45.90
B3 M1	2.00	1.90	1.90	1.93	33.00	33.20	33.10	33.10	22.20	22.40	22.30	22.30	42.80	42.50	42.70	42.67
B5 M1	1.60	1.60	1.60	1.60	26.90	27.00	26.90	26.93	33.70	33.70	33.70	33.70	37.80	37.70	37.80	37.77
B9 M1	2.10	2.10	2.10	2.10	22.10	21.90	22.00	22.00	18.90	18.70	18.80	18.80	56.90	57.30	57.10	57.10
B11 M1	2.00	2.00	2.00	2.00	26.70	26.50	26.60	26.60	15.20	14.90	15.20	15.10	56.10	56.60	56.20	56.30
MSW M1	1.50	1.50	1.50	1.50	29.90	30.00	30.00	29.97	23.00	22.90	22.90	22.93	45.60	45.60	45.60	45.60
B3W M1	1.80	1.90	1.90	1.87	32.20	32.10	32.20	32.17	23.50	23.50	23.60	23.53	42.50	42.50	42.30	42.43
B5W M1	1.60	1.70	1.70	1.67	26.60	26.70	26.60	26.63	33.90	33.90	34.10	33.97	37.90	37.70	37.60	37.73
B9W M1	2.20	2.20	2.20	2.20	22.10	21.80	21.90	21.93	18.30	18.30	18.20	18.27	57.40	57.70	57.70	57.60
B11W M1	1.90	1.90	1.90	1.90	26.80	26.80	26.80	26.80	15.30	15.20	15.30	15.27	56.00	56.10	56.00	56.03
Sample	**R1**	**R2**	**R3**	**Average**	**R1**	**R2**	**R3**	**Average**	**R1**	**R2**	**R3**	**Average**	**R1**	**R2**	**R3**	**Average**
MS M2	1.76	1.75	1.79	1.77	31.74	31.88	31.42	31.68	22.76	22.60	22.71	22.69	43.74	43.77	44.08	43.86
B3 M2	1.90	1.90	2.00	1.93	32.70	32.90	32.90	32.83	23.30	23.20	23.10	23.20	42.10	42.00	42.00	42.03
B5 M2	1.70	1.60	1.60	1.63	27.80	27.70	27.60	27.70	32.10	32.00	32.00	32.03	38.40	38.70	38.80	38.63
B9 M2	2.10	2.10	2.10	2.10	22.90	23.00	22.90	22.93	18.70	18.70	18.70	18.70	56.30	56.20	56.30	56.27
B11 M2	2.00	2.00	2.00	2.00	27.10	27.00	26.90	27.00	15.30	14.30	15.40	15.00	55.60	56.70	55.70	56.00
MSW M2	1.50	1.50	1.50	1.50	30.10	30.40	30.50	30.33	22.50	22.50	22.50	22.50	45.90	45.60	45.50	45.67
B3W M2	2.00	1.90	1.90	1.93	32.40	32.40	32.60	32.47	23.54	23.54	23.54	23.54	42.06	42.16	41.96	42.06
B5W M2	1.82	1.88	1.856	1.85	28.64	28.45	28.67	28.59	34.15	34.02	34.02	34.06	35.39	35.65	35.45	35.50
B9W M2	2.40	2.30	2.40	2.37	22.20	22.20	22.60	22.33	18.10	18.20	18.10	18.13	57.30	57.30	56.90	57.17
B11W M2	2.20	2.20	1.90	2.10	27.80	27.40	27.30	27.50	15.80	15.80	16.00	15.87	54.20	54.60	54.80	54.53
Sample	**R1**	**R2**	**R3**	**Average**	**R1**	**R2**	**R3**	**Average**	**R1**	**R2**	**R3**	**Average**	**R1**	**R2**	**R3**	**Average**
MS M4	1.70	1.70	1.70	1.70	30.20	30.60	30.50	30.43	23.00	23.10	23.10	23.07	45.10	44.60	44.70	44.80
B3 M4	2.20	2.20	2.20	2.20	32.80	33.10	33.20	33.03	22.30	22.40	22.40	22.37	42.70	42.30	42.20	42.40
B5 M4	1.70	1.70	1.70	1.70	27.20	27.30	27.10	27.20	33.90	33.90	33.80	33.87	37.20	37.10	37.40	37.23
B9 M4	2.20	2.10	2.10	2.13	22.50	22.40	22.30	22.40	17.80	17.80	17.80	17.80	57.50	57.70	57.80	57.67
B11 M4	2.20	2.10	2.10	2.13	27.20	27.00	27.10	27.10	14.80	14.80	14.90	14.83	55.80	56.10	55.90	55.93
MSW M4	1.80	1.90	1.80	1.83	30.50	30.30	30.70	30.50	23.00	23.00	23.00	23.00	44.70	44.80	44.50	44.67
B3W M4	2.10	2.20	2.20	2.17	32.70	32.80	32.80	32.77	22.90	23.00	23.20	23.03	42.30	42.00	41.80	42.03
B5W M4	1.60	1.70	1.70	1.67	27.10	27.20	27.00	27.10	34.60	34.50	34.50	34.53	36.70	36.60	36.80	36.70
B9W M4	2.00	2.00	2.00	2.00	26.40	26.50	26.30	26.40	15.50	15.40	15.40	15.43	56.10	56.10	56.30	56.17
B11W M4	2.10	2.10	2.10	2.10	27.00	26.50	27.20	26.90	14.70	14.70	14.60	14.67	56.20	56.70	56.10	56.33
Sample	**R1**	**R2**	**R3**	**Average**	**R1**	**R2**	**R3**	**Average**	**R1**	**R2**	**R3**	**Average**	**R1**	**R2**	**R3**	**Average**
MS M6	2.00	2.00	2.00	2.00	30.00	30.30	30.40	30.23	23.10	23.20	23.20	23.17	44.90	44.50	44.40	44.60
B3 M6	2.30	2.30	2.40	2.33	32.80	32.60	32.60	32.67	22.50	22.50	22.40	22.47	42.40	42.60	42.60	42.53
B5 M6	1.80	1.90	1.90	1.87	27.80	27.60	27.70	27.70	31.80	32.50	31.50	31.93	38.60	38.00	38.90	38.50
B9 M6	2.40	2.60	2.40	2.47	24.30	24.30	24.90	24.50	17.70	17.70	17.80	17.73	55.60	55.40	54.90	55.30
B11 M6	2.40	2.40	2.30	2.37	27.10	27.00	26.70	26.93	14.60	14.30	14.40	14.43	55.90	56.30	56.60	56.27
MSW M6	1.80	1.60	1.80	1.73	31.00	31.00	31.00	31.00	22.20	22.20	22.20	22.20	45.00	45.20	45.00	45.07
B3W M6	2.20	2.30	2.40	2.30	31.80	31.90	32.00	31.90	23.30	23.40	23.30	23.33	42.70	42.40	42.30	42.47
B5W M6	2.30	2.40	2.30	2.33	27.20	27.10	27.50	27.27	32.00	32.00	32.00	32.00	38.50	38.50	38.20	38.40
B9W M6	2.70	2.60	2.70	2.67	22.10	22.40	22.20	22.23	17.30	17.10	17.30	17.23	57.90	57.90	57.80	57.87
B11W M6	2.20	2.30	2.40	2.30	31.80	31.90	32.00	31.90	23.30	23.40	23.30	23.33	42.70	42.40	42.30	42.47

Appendix C. Replicate (R) runs for the ultimate analysis

	Total carbon %				Hydrogen % (db)				Nitrogen % (db)				Total sulphur %				Calculated oxygen %			
Sample	**R1**	**R2**	**R3**	**Average**	**R1**	**R2**	**R3**	**Average**	**R1**	**R2**	**R3**	**Average**	**R1**	**R2**	**R3**	**Average**	**R1**	**R2**	**R3**	**Average**
MSB	66.10	65.90	65.90	65.97	4.04	3.97	4.03	4.01	1.12	1.12	1.12	1.12	2.28	2.13	2.28	2.23	26.46	26.88	26.67	26.67
B3B	63.10	62.80	62.80	62.90	4.08	4.01	3.99	4.03	1.13	1.12	1.15	1.13	1.35	1.30	1.36	1.34	30.34	30.77	30.70	30.60
B5B	55.10	55.20	55.30	55.20	3.64	3.67	3.62	3.64	1.21	1.22	1.22	1.22	3.77	3.76	3.66	3.73	36.28	36.15	36.20	36.21
B9B	69.30	69.40	69.40	69.37	3.26	3.27	3.27	3.27	1.39	1.39	1.38	1.39	0.52	0.52	0.49	0.51	25.53	25.42	25.46	25.47
B11 B	71.40	71.40	71.20	71.33	3.76	3.74	3.75	3.75	1.48	1.49	1.49	1.49	1.87	1.85	1.86	1.86	21.49	21.52	21.70	21.57
Sample	**R1**	**R2**	**R3**	**Average**	**R1**	**R2**	**R3**	**Average**	**R1**	**R2**	**R3**	**Average**	**R1**	**R2**	**R3**	**Average**	**R1**	**R2**	**R3**	**Average**
MS W1	66.40	66.50	66.20	66.37	4.03	3.98	4.03	4.01	1.13	1.13	1.13	1.13	1.91	1.94	1.81	1.89	26.53	26.45	26.83	26.60
B3 W1	63.40	63.50	63.60	63.50	3.96	3.97	3.99	3.97	1.11	1.12	1.11	1.11	1.50	1.46	1.49	1.48	30.03	29.95	29.81	29.93
B5 W1	54.30	54.40	53.90	54.20	3.43	3.45	3.40	3.43	1.10	1.10	1.09	1.10	2.94	2.97	2.89	2.93	38.23	38.08	38.72	38.34
B9 W1	69.90	69.60	69.80	69.77	3.26	3.22	3.24	3.24	1.36	1.35	1.34	1.35	0.44	0.43	0.44	0.44	25.04	25.40	25.18	25.21
B11 W1	71.50	71.50	71.90	71.63	3.80	3.74	3.81	3.78	1.34	1.31	1.20	1.28	1.29	1.36	1.36	1.34	22.07	22.09	21.73	21.96
MSW W1	65.80	65.90	66.00	65.90	3.91	4.04	3.96	3.97	1.36	1.16	0.77	1.10	1.97	1.96	1.98	1.97	26.96	26.94	27.29	27.06
B3W W1	63.30	62.70	62.10	62.70	3.94	3.92	3.91	3.92	1.10	0.96	0.96	1.01	1.35	1.43	1.39	1.39	30.31	30.99	31.64	30.98
B5W W1	55.50	54.40	55.40	55.10	3.54	3.49	3.52	3.52	1.20	0.80	1.03	1.01	1.90	1.98	2.01	1.96	37.86	39.33	38.04	38.41
B9W W1	69.70	69.60	69.90	69.73	3.20	3.23	3.24	3.22	1.04	1.29	1.33	1.22	0.39	0.39	0.40	0.39	25.67	25.49	25.13	25.43
B11W W1	71.80	72.00	71.80	71.87	3.82	3.82	3.77	3.80	1.46	1.45	1.44	1.45	1.18	1.15	1.31	1.21	21.74	21.58	21.68	21.67
Sample	**R1**	**R2**	**R3**	**Average**	**R1**	**R2**	**R3**	**Average**	**R1**	**R2**	**R3**	**Average**	**R1**	**R2**	**R3**	**Average**	**R1**	**R2**	**R3**	**Average**
MS W2	67.01	67.06	67.07	67.05	4.05	4.02	4.01	4.03	1.26	1.25	1.27	1.26	2.46	2.46	2.47	2.46	25.22	25.21	25.18	25.20
B3 W2	67.08	66.90	65.78	66.59	4.00	3.94	4.11	4.02	1.26	1.27	1.30	1.28	1.69	1.68	1.70	1.69	25.97	26.21	27.11	26.43
B5 W2	54.51	54.40	54.24	54.38	3.43	3.38	3.36	3.39	1.28	1.27	1.26	1.27	3.02	3.03	3.02	3.02	37.76	37.92	38.12	37.93
B9 W2	70.94	70.28	71.44	70.89	2.79	2.91	2.94	2.88	1.50	1.49	1.51	1.50	0.61	0.61	0.61	0.61	24.16	24.71	23.50	24.13
B11 W2	72.60	72.90	72.40	72.63	3.89	3.90	3.21	3.67	1.61	1.61	1.63	1.62	1.70	1.69	1.71	1.70	20.20	19.90	21.05	20.38
Sample	**R1**	**R2**	**R3**	**Average**	**R1**	**R2**	**R3**	**Average**	**R1**	**R2**	**R3**	**Average**	**R1**	**R2**	**R3**	**Average**	**R1**	**R2**	**R3**	**Average**
MS M1	67.00	67.80	67.90	67.57	4.02	4.01	4.01	4.01	1.24	1.20	1.21	1.22	2.61	2.65	2.72	2.66	25.13	24.34	24.16	24.54
B3 M1	65.50	65.40	65.10	65.33	4.09	4.10	4.14	4.11	1.24	1.24	1.24	1.24	1.56	1.53	1.56	1.55	27.61	27.73	27.96	27.77
B5 M1	60.00	59.70	60.00	59.90	3.66	3.66	3.65	3.66	1.26	1.25	1.26	1.26	3.23	3.36	3.36	3.32	31.85	32.03	31.73	31.87
B9 M1	70.00	70.50	70.40	70.30	3.22	3.26	3.25	3.24	1.42	1.40	1.39	1.40	0.52	0.50	0.54	0.52	24.84	24.34	24.42	24.53
B11 M1	71.20	70.80	71.40	71.13	3.76	3.73	3.77	3.75	1.58	1.57	1.58	1.58	1.78	1.86	1.83	1.82	21.68	22.04	21.42	21.71
MSW M1	66.00	65.70	65.70	65.80	4.04	4.03	4.06	4.04	1.30	1.27	1.26	1.28	2.37	2.38	2.43	2.39	26.29	26.62	26.55	26.49
B3W M1	64.07	64.11	64.23	64.14	3.89	3.96	4.03	3.96	1.28	1.27	1.28	1.28	1.85	1.86	1.81	1.84	28.91	28.80	28.65	28.79
B5W M1	53.92	53.46	53.83	53.74	3.37	3.34	3.29	3.33	1.25	1.24	1.24	1.24	3.05	3.07	3.06	3.06	38.41	38.89	38.58	38.63
B9W M1	70.20	70.40	70.80	70.47	3.18	3.17	3.15	3.17	1.42	1.46	1.43	1.44	0.47	0.46	0.48	0.47	24.73	24.51	24.14	24.46
B11W M1	72.40	71.80	72.70	72.30	3.79	3.84	3.83	3.82	1.59	1.59	1.56	1.58	1.66	1.64	1.63	1.64	20.56	21.13	20.28	20.66
Sample	**R1**	**R2**	**R3**	**Average**	**R1**	**R2**	**R3**	**Average**	**R1**	**R2**	**R3**	**Average**	**R1**	**R2**	**R3**	**Average**	**R1**	**R2**	**R3**	**Average**
MS M2	67.00	67.80	67.90	67.57	4.02	4.01	4.01	4.01	1.24	1.20	1.21	1.22	2.61	2.65	2.72	2.66	25.13	24.34	24.16	24.54
B3 M2	65.50	65.40	65.10	65.33	4.09	4.10	4.14	4.11	1.24	1.24	1.24	1.24	1.56	1.53	1.56	1.55	27.61	27.73	27.96	27.77
B5 M2	59.40	59.60	59.30	59.43	3.55	3.54	3.52	3.54	1.29	1.27	1.28	1.28	2.46	2.57	2.59	2.54	33.30	33.02	33.31	33.21
B9 M2	70.00	70.50	70.40	70.30	3.22	3.26	3.25	3.24	1.42	1.40	1.39	1.40	0.52	0.50	0.54	0.52	24.84	24.34	24.42	24.53
B11 M2	71.20	70.80	71.40	71.13	3.76	3.73	3.77	3.75	1.58	1.57	1.58	1.58	1.78	1.86	1.83	1.82	21.68	22.04	21.42	21.71
MSW M2	67.90	67.40	67.10	67.47	4.10	4.09	4.08	4.09	1.23	1.24	1.23	1.23	2.05	2.06	2.14	2.08	24.72	25.21	25.45	25.13
B3W M2	64.07	64.11	64.23	64.14	3.89	3.96	4.03	3.96	1.28	1.27	1.28	1.28	1.85	1.86	1.81	1.84	28.91	28.80	28.65	28.79

B5W M2	53.92	53.46	53.83	53.74	3.37	3.34	3.29	3.33	1.25	1.24	1.24	1.24	3.05	3.07	3.06	3.06	38.41	38.89	38.58	38.63
B9W M2	70.20	70.40	70.80	70.47	3.18	3.17	3.15	3.17	1.42	1.46	1.43	1.44	0.47	0.46	0.48	0.47	24.73	24.51	24.14	24.46
B11W M2	72.40	71.80	72.70	72.30	3.79	3.84	3.83	3.82	1.59	1.59	1.56	1.58	1.66	1.64	1.63	1.64	20.56	21.13	20.28	20.66
Sample	**R1**	**R2**	**R3**	**Average**	**R1**	**R2**	**R3**	**Average**	**R1**	**R2**	**R3**	**Average**	**R1**	**R2**	**R3**	**Average**	**R1**	**R2**	**R3**	**Average**
MS M4	65.10	65.30	65.10	65.17	3.90	4.00	3.95	3.95	1.18	1.18	1.18	1.18	2.87	2.87	2.91	2.88	26.95	26.65	26.86	26.82
B3 M4	63.60	63.80	63.60	63.67	4.06	4.08	4.03	4.06	1.19	1.18	1.18	1.18	1.52	1.54	1.53	1.53	29.63	29.40	29.66	29.56
B5 M4	53.70	54.00	53.10	53.60	3.41	3.42	3.27	3.37	1.18	1.18	1.13	1.16	3.09	3.10	3.16	3.12	38.62	38.30	39.34	38.75
B9 M4	68.80	68.80	68.90	68.83	3.04	3.06	3.03	3.04	1.49	1.42	1.39	1.43	0.61	0.61	0.61	0.61	26.06	26.11	26.07	26.08
B11 M4	70.90	71.40	71.70	71.33	3.72	3.75	3.70	3.72	1.50	1.54	1.56	1.53	1.56	1.55	1.57	1.56	22.32	21.76	21.47	21.85
MSW M4	64.90	65.40	65.10	65.13	4.00	4.05	4.02	4.02	1.18	1.19	1.20	1.19	2.12	2.08	2.13	2.11	27.80	27.28	27.55	27.54
B3W M4	62.60	62.40	62.20	62.40	4.00	4.00	4.04	4.01	1.18	1.18	1.19	1.18	2.04	2.08	2.11	2.08	30.18	30.34	30.46	30.33
B5W M4	52.50	51.60	51.90	52.00	3.41	3.31	3.33	3.35	1.17	1.15	1.16	1.16	3.21	3.28	3.23	3.24	39.71	40.66	40.38	40.25
B9W M4	70.90	70.70	70.70	70.77	3.71	3.66	3.72	3.70	1.54	1.53	1.53	1.53	2.07	2.06	2.03	2.05	21.78	22.05	22.02	21.95
B11W M4	72.63	72.60	72.31	72.51	3.62	3.64	3.52	3.59	1.61	1.60	1.58	1.60	1.86	1.99	1.94	1.93	20.28	20.17	20.65	20.37
Sample	**R1**	**R2**	**R3**	**Average**	**R1**	**R2**	**R3**	**Average**	**R1**	**R2**	**R3**	**Average**	**R1**	**R2**	**R3**	**Average**	**R1**	**R2**	**R3**	**Average**
MS M6	65.30	64.30	65.40	65.00	4.22	4.09	4.18	4.16	1.37	1.36	1.38	1.37	3.37	3.50	3.50	3.46	25.74	26.75	25.54	26.01
B3 M6	64.40	64.40	64.30	64.37	4.15	4.13	4.16	4.15	1.28	1.27	1.28	1.28	1.58	1.59	1.63	1.60	28.59	28.61	28.63	28.61
B5 M6	54.60	55.10	54.10	54.60	3.56	3.58	3.56	3.57	1.28	1.27	1.28	1.28	3.19	3.10	3.18	3.16	37.37	36.95	37.88	37.40
B9 M6	70.50	71.00	70.70	70.73	3.19	3.19	3.20	3.19	1.50	1.51	1.50	1.50	0.51	0.54	0.56	0.54	24.30	23.76	24.04	24.03
B11 M6	74.10	73.90	73.90	73.97	3.89	3.90	3.89	3.89	1.64	1.64	1.63	1.64	1.65	1.56	1.61	1.61	18.72	19.00	18.97	18.90
MSW M6	66.50	67.30	67.30	67.03	4.12	4.11	4.14	4.12	1.26	1.27	1.28	1.27	3.18	3.25	3.23	3.22	24.94	24.07	24.05	24.35
B3W M6	73.20	73.30	72.80	73.10	3.82	3.83	3.82	3.82	1.58	1.59	1.60	1.59	1.71	1.71	1.72	1.71	19.69	19.57	20.06	19.77
B5W M6	55.90	56.20	56.40	56.17	3.62	3.65	3.68	3.65	1.30	1.32	1.32	1.31	2.77	2.71	2.72	2.73	36.41	36.12	35.88	36.14
B9W M6	71.80	71.90	71.90	71.87	3.27	3.28	3.24	3.26	1.53	1.53	1.53	1.53	0.54	0.49	0.48	0.50	22.86	22.80	22.85	22.84
B11W M6	64.60	64.70	65.00	64.77	4.18	4.13	4.20	4.17	1.29	1.35	1.31	1.32	1.96	1.98	2.01	1.98	27.97	27.84	27.48	27.76

Appendix D. Replicate (R) runs for the calorific value (MJ/kg)

Sample	R1	R2	R3	Average
MSB	26.55	26.49	26.51	26.52
B3B	24.85	24.88	24.87	24.87
B5B	21.22	21.30	21.25	21.26
B9B	25.88	25.85	25.87	25.87
B11 B	28.22	28.09	28.14	28.15
Sample	**R1**	**R2**	**R3**	**Average**
MS W1	26.41	26.39	26.37	26.39
B3 W1	25.02	25.02	25.00	25.01
B5 W1	21.07	21.07	21.09	21.08
B9 W1	25.74	25.74	25.80	25.76
B11 W1	27.86	27.90	27.88	27.88
MSW W1	26.30	26.48	26.41	26.40
B3W W1	24.99	24.93	25.03	24.98
B5W W1	21.43	21.47	21.41	21.44
B9W W1	25.82	25.91	25.96	25.90
B11W W1	27.97	27.91	27.96	27.95
Sample	**R1**	**R2**	**R3**	**Average**
MS W2	25.70	25.69	25.73	25.71
B3 W2	21.31	21.27	21.31	21.30
B5 W2	26.36	26.27	26.29	26.31
B9 W2	25.20	25.24	25.25	25.23
B11 W2	28.04	28.07	28.05	28.05
Sample	**R1**	**R2**	**R3**	**Average**
MS M1	25.89	25.82	25.80	25.84
B3 M1	25.31	25.30	25.32	25.31
B5 M1	21.49	21.52	21.46	21.49
B9 M1	25.59	25.51	25.57	25.56
B11 M1	27.66	27.74	27.75	27.72
MSW M1	25.61	25.50	25.56	25.56
B3W M1	24.10	24.21	24.23	24.18
B5W M1	21.43	21.41	21.32	21.39
B9W M1	25.70	25.83	25.79	25.77
B11W M1	27.40	27.48	27.51	27.46
Sample	**R1**	**R2**	**R3**	**Average**
MS M2	25.86	25.82	25.93	25.87
B3 M2	24.84	24.91	24.83	24.86
B5 M2	21.64	21.63	21.68	21.65
B9 M2	25.10	25.20	25.15	25.15
B11 M2	27.42	27.42	27.51	27.45
MSW M2	26.05	26.09	25.98	26.04
B3W M2	24.66	24.72	24.70	24.69
B5W M2	21.10	21.11	21.09	21.10
B9W M2	25.75	25.77	25.84	25.79
B11W M2	27.47	27.53	27.56	27.52
Sample	**R1**	**R2**	**R3**	**Average**
MS M4	25.85	25.94	25.90	25.90
B3 M4	24.94	25.01	24.99	24.98
B5 M4	21.31	21.30	20.78	21.13
B9 M4	25.45	25.46	25.53	25.48
B11 M4	27.38	27.34	27.32	27.35
MSW M4	25.98	25.88	26.01	25.96
B3W M4	24.49	24.51	24.63	24.54
B5W M4	20.84	20.84	20.95	20.88
B9W M4	27.43	27.39	27.53	27.45
B11W M4	27.38	27.33	27.41	27.37
Sample	**R1**	**R2**	**R3**	**Average**
MS M6	25.29	25.34	25.31	25.31
B3 M6	24.81	24.90	24.87	24.86
B5 M6	20.42	20.32	20.44	20.39
B9 M6	24.40	24.50	24.60	24.50
B11 M6	25.12	25.08	25.06	25.09
MSW M6	25.78	25.81	25.71	25.77
B3W M6	25.13	25.16	25.14	25.14
B5W M6	21.32	21.29	21.39	21.33
B9W M6	25.32	25.33	25.41	25.35
B11W M6	24.27	24.22	24.30	24.26

Appendix E. Critical values of the correlation coefficients for one-sided tests of the null hypothesis H0: ρ = 0. where degrees of freedom =sample size - 2 (Underhill and Bradfield, 2013).

Deg. of	Probability Level (P)										
Freedom	0.4	0.3	0.2	0.1	0.05	0.025	0.01	0.005	0.0025	0.001	0.0005
1	0.3090	0.5878	0.8090	0.9511	0.9877	0.9969	0.9995	0.9999	1.0000	1.0000	1.0000
2	0.2000	0.4000	0.6000	0.8000	0.9000	0.9500	0.9800	0.9900	0.9950	0.9980	0.9990
3	0.1577	0.3197	0.4919	0.6870	0.8054	0.8783	0.9343	0.9587	0.9740	0.9859	0.9911
4	0.1341	0.2735	0.4257	0.6084	0.7293	0.8114	0.8822	0.9172	0.9417	0.9633	0.9741
5	0.1186	0.2427	0.3803	0.5509	0.6694	0.7545	0.8329	0.8745	0.9056	0.9350	0.9509
6	0.1075	0.2204	0.3468	0.5067	0.6215	0.7067	0.7887	0.8343	0.8697	0.9049	0.9249
7	0.0990	0.2032	0.3208	0.4716	0.5822	0.6664	0.7498	0.7977	0.8359	0.8751	0.8983
8	0.0922	0.1895	0.2998	0.4428	0.5494	0.6319	0.7155	0.7646	0.8046	0.8467	0.8721
9	0.0867	0.1783	0.2825	0.4187	0.5214	0.6021	0.6851	0.7348	0.7759	0.8199	0.8470
10	0.0820	0.1688	0.2678	0.3981	0.4973	0.5760	0.6581	0.7079	0.7496	0.7950	0.8233
11	0.0780	0.1607	0.2552	0.3802	0.4762	0.5529	0.6339	0.6835	0.7255	0.7717	0.8010
12	0.0746	0.1536	0.2443	0.3646	0.4575	0.5324	0.6120	0.6614	0.7034	0.7501	0.7800
13	0.0715	0.1474	0.2346	0.3507	0.4409	0.5140	0.5923	0.6411	0.6831	0.7301	0.7604
14	0.0688	0.1419	0.2260	0.3383	0.4259	0.4973	0.5742	0.6226	0.6643	0.7114	0.7419
15	0.0664	0.1370	0.2183	0.3271	0.4124	0.4821	0.5577	0.6055	0.6470	0.6940	0.7247
16	0.0643	0.1326	0.2113	0.3170	0.4000	0.4683	0.5425	0.5897	0.6308	0.6777	0.7084
17	0.0623	0.1285	0.2049	0.3077	0.3887	0.4555	0.5285	0.5751	0.6158	0.6624	0.6932
18	0.0605	0.1248	0.1991	0.2992	0.3783	0.4438	0.5155	0.5614	0.6018	0.6481	0.6788
19	0.0588	0.1214	0.1938	0.2914	0.3687	0.4329	0.5034	0.5487	0.5886	0.6346	0.6652
20	0.0573	0.1183	0.1888	0.2841	0.3598	0.4227	0.4921	0.5368	0.5763	0.6219	0.6524
21	0.0559	0.1154	0.1843	0.2774	0.3515	0.4132	0.4815	0.5256	0.5647	0.6099	0.6402
22	0.0546	0.1127	0.1800	0.2711	0.3438	0.4044	0.4716	0.5151	0.5537	0.5986	0.6287
23	0.0534	0.1102	0.1760	0.2653	0.3365	0.3961	0.4622	0.5052	0.5434	0.5879	0.6178
24	0.0522	0.1078	0.1723	0.2598	0.3297	0.3882	0.4534	0.4958	0.5336	0.5776	0.6074
25	0.0511	0.1056	0.1688	0.2546	0.3233	0.3809	0.4451	0.4869	0.5243	0.5679	0.5974
26	0.0501	0.1036	0.1655	0.2497	0.3172	0.3739	0.4372	0.4785	0.5154	0.5587	0.5880
27	0.0492	0.1016	0.1624	0.2451	0.3115	0.3673	0.4297	0.4705	0.5070	0.5499	0.5789
28	0.0483	0.0997	0.1594	0.2407	0.3061	0.3610	0.4226	0.4629	0.4990	0.5415	0.5703
29	0.0474	0.0980	0.1567	0.2366	0.3009	0.3550	0.4158	0.4556	0.4914	0.5334	0.5621
30	0.0466	0.0963	0.1540	0.2327	0.2960	0.3494	0.4093	0.4487	0.4840	0.5257	0.5541
31	0.0458	0.0947	0.1515	0.2289	0.2913	0.3440	0.4032	0.4421	0.4770	0.5184	0.5465
32	0.0451	0.0932	0.1491	0.2254	0.2869	0.3388	0.3972	0.4357	0.4703	0.5113	0.5392
33	0.0444	0.0918	0.1468	0.2220	0.2826	0.3338	0.3916	0.4296	0.4639	0.5045	0.5322
34	0.0437	0.0904	0.1446	0.2187	0.2785	0.3291	0.3862	0.4238	0.4577	0.4979	0.5254
35	0.0431	0.0891	0.1425	0.2156	0.2746	0.3246	0.3810	0.4182	0.4518	0.4916	0.5189
36	0.0425	0.0878	0.1405	0.2126	0.2709	0.3202	0.3760	0.4128	0.4461	0.4856	0.5126
37	0.0419	0.0866	0.1386	0.2097	0.2673	0.3160	0.3712	0.4076	0.4406	0.4797	0.5066
38	0.0414	0.0855	0.1368	0.2070	0.2638	0.3120	0.3665	0.4026	0.4353	0.4741	0.5007
39	0.0408	0.0844	0.1350	0.2043	0.2605	0.3081	0.3621	0.3978	0.4301	0.4686	0.4950
40	0.0403	0.0833	0.1333	0.2018	0.2573	0.3044	0.3578	0.3932	0.4252	0.4634	0.4896
45	0.0380	0.0785	0.1257	0.1903	0.2429	0.2876	0.3384	0.3721	0.4028	0.4394	0.4647
50	0.0360	0.0744	0.1192	0.1806	0.2306	0.2732	0.3218	0.3542	0.3836	0.4188	0.4432
60	0.0328	0.0679	0.1088	0.1650	0.2108	0.2500	0.2948	0.3248	0.3522	0.3850	0.4079
70	0.0304	0.0628	0.1007	0.1528	0.1954	0.2319	0.2737	0.3017	0.3274	0.3583	0.3798
80	0.0284	0.0588	0.0942	0.1430	0.1829	0.2172	0.2565	0.2830	0.3072	0.3364	0.3568
90	0.0268	0.0554	0.0888	0.1348	0.1726	0.2050	0.2422	0.2673	0.2903	0.3181	0.3375
100	0.0254	0.0525	0.0842	0.1279	0.1638	0.1946	0.2301	0.2540	0.2759	0.3025	0.3211
110	0.0242	0.0501	0.0803	0.1220	0.1562	0.1857	0.2196	0.2425	0.2635	0.2890	0.3068
120	0.0232	0.0479	0.0769	0.1168	0.1496	0.1779	0.2104	0.2324	0.2526	0.2771	0.2943
140	0.0214	0.0444	0.0712	0.1082	0.1386	0.1648	0.1951	0.2155	0.2343	0.2572	0.2733
160	0.0201	0.0415	0.0666	0.1012	0.1297	0.1543	0.1826	0.2019	0.2195	0.2411	0.2562
180	0.0189	0.0391	0.0628	0.0954	0.1223	0.1455	0.1723	0.1905	0.2072	0.2276	0.2419
200	0.0179	0.0371	0.0595	0.0905	0.1161	0.1381	0.1636	0.1809	0.1968	0.2162	0.2298

Appendix F. Thermogravimetric analysis (TGA) for Bench 5

Bench 5 (Fresh sample)			Bench 5, two weeks (B5 W2)		
Temperature °C	**Weight %**	**Deriv. Weight %/min**	**Temperature °C**	**Weight %**	**Deriv. Weight %/min**
30.00	99.71	0.353300	30.00	99.77	0.33
40.00	99.08	0.248000	40.00	99.23	0.27
50.00	98.61	0.025970	50.00	98.78	0.09
60.00	98.54	0.093880	60.00	98.67	0.15
70.00	98.43	0.112200	70.00	98.51	0.15
80.00	98.31	0.108200	80.00	98.37	0.12
90.00	98.23	0.034450	90.00	98.26	0.12
100.00	98.15	0.060010	100.00	98.18	0.06
110.00	98.10	0.042490	110.00	98.12	0.05
120.00	98.07	0.029490	120.00	98.08	0.03
130.00	98.06	0.010250	130.00	98.06	0.02
140.00	98.06	-0.001859	140.00	98.05	0.00
150.00	98.07	-0.029000	150.00	98.05	-0.01
160.00	98.10	-0.036980	160.00	98.06	-0.02
170.00	98.14	-0.053320	170.00	98.09	-0.04
180.00	98.20	-0.070140	180.00	98.14	-0.07
190.00	98.29	-0.099850	190.00	98.22	-0.08
200.00	98.40	-0.129900	200.00	98.32	-0.11
210.00	98.53	-0.150300	210.00	98.45	-0.15
220.00	98.70	-0.184700	220.00	98.60	-0.17
230.00	98.89	-0.209200	230.00	98.79	-0.21
240.00	99.11	-0.221900	240.00	99.01	-0.23
250.00	99.33	-0.222400	250.00	99.24	-0.23
260.00	99.54	-0.196700	260.00	99.45	-0.21
270.00	99.71	-0.141900	270.00	99.63	-0.16
280.00	99.80	-0.048810	280.00	99.73	-0.06
290.00	99.80	0.069150	290.00	99.73	0.08
300.00	99.65	0.228300	300.00	99.59	0.24
310.00	99.35	0.404300	310.00	99.27	0.41
320.00	98.87	0.555500	320.00	98.77	0.60
330.00	98.22	0.720000	330.00	98.08	0.77
340.00	97.41	0.870100	340.00	97.21	0.93
350.00	96.45	1.032000	350.00	96.18	1.10
360.00	95.32	1.227000	360.00	94.97	1.30
370.00	94.00	1.437000	370.00	93.57	1.51
380.00	92.46	1.690000	380.00	91.96	1.77
390.00	90.66	2.064000	390.00	90.10	2.10
400.00	88.48	2.571000	400.00	87.90	2.57
410.00	85.76	3.461000	410.00	85.23	3.30
420.00	82.17	5.636000	420.00	81.88	4.60
430.00	77.36	31.040000	430.00	77.59	8.71

440.00	65.92	5.609000	440.00	71.13	6.77
450.00	59.30	5.361000	450.00	62.05	6.24
460.00	53.50	4.482000	460.00	55.27	5.17
470.00	48.77	3.554000	470.00	49.68	3.87
480.00	45.14	2.852000	480.00	45.67	2.97
490.00	42.29	2.275000	490.00	42.69	2.28
500.00	40.05	1.849000	500.00	40.45	1.81
510.00	38.26	1.531000	510.00	38.70	1.49
520.00	36.84	1.177000	520.00	37.31	1.15
530.00	35.81	0.807600	530.00	36.30	0.79
540.00	35.13	0.509500	540.00	35.65	0.49
550.00	34.71	0.313700	550.00	35.25	0.30
560.00	34.45	0.203800	560.00	35.00	0.20
570.00	34.28	0.142600	570.00	34.83	0.14
580.00	34.14	0.121000	580.00	34.70	0.12
590.00	34.03	0.105700	590.00	34.59	0.10
600.00	33.94	0.078110	600.00	34.50	0.08
610.00	33.87	0.065900	610.00	34.43	0.07
620.00	33.81	0.055640	620.00	34.37	0.06
630.00	33.76	0.045840	630.00	34.32	0.06
640.00	33.71	0.051440	640.00	34.26	0.06
650.00	33.66	0.046190	650.00	34.22	0.04
660.00	33.62	0.039750	660.00	34.18	0.04
670.00	33.59	0.034740	670.00	34.14	0.03
680.00	33.56	0.032140	680.00	34.12	0.03
690.00	33.52	0.053620	690.00	34.09	0.03
700.00	33.44	0.092870	700.00	34.05	0.05
710.00	33.34	0.108700	710.00	33.99	0.07
720.00	33.24	0.076280	720.00	33.90	0.10
730.00	33.18	0.042580	730.00	33.79	0.10
740.00	33.15	0.021520	740.00	33.70	0.08
750.00	33.13	0.018160	750.00	33.64	0.05
760.00	33.11	0.017910	760.00	33.59	0.04
770.00	33.10	0.014580	770.00	33.56	0.03
780.00	33.08	0.010370	780.00	33.53	0.03
790.00	33.07	0.008164	790.00	33.51	0.02
800.00	33.05	0.008288	800.00	33.50	0.02
810.00	33.04	0.012590	810.00	33.48	0.02
820.00	33.03	0.013180	820.00	33.47	0.01
830.00	33.02	0.010330	830.00	33.46	0.01
840.00	33.01	0.008296	840.00	33.45	0.00
850.00	33.00	0.010060	850.00	33.44	0.01
860.00	32.98	0.018150	860.00	33.43	0.01
870.00	32.97	0.009800	870.00	33.43	0.00
880.00	32.96	0.015250	880.00	33.42	0.00

890.00	32.95	0.012630	890.00	33.41	0.01
900.00					
890.00	99.80	31.040000			
30.00	32.95	-0.222400			
860.00	66.85	31.262400			
Bench 5, one month (B5 M1)			**Bench 5, two months (B5 M2)**		
Temperature °C	**Weight %**	**Deriv. Weight %/min**	**Temperature °C**	**Weight %**	**Deriv. Weight %/min**
20.00	99.96	0.10	30.00	99.82	0.26
30.00	99.79	0.28	40.00	98.86	-0.05
40.00	99.35	0.27	50.00	98.89	-0.03
50.00	98.83	0.06	60.00	98.86	0.07
60.00	98.75	0.11	70.00	98.77	0.09
70.00	98.62	0.14	80.00	98.66	0.13
80.00	98.47	0.16	90.00	98.55	0.07
90.00	98.29	0.14	100.00	98.45	0.09
100.00	98.18	0.10	110.00	98.39	0.04
110.00	98.08	0.08	120.00	98.36	0.02
120.00	98.02	0.05	130.00	98.34	0.01
130.00	97.98	0.03	140.00	98.33	0.00
140.00	97.96	0.02	150.00	98.34	-0.01
150.00	97.94	0.01	160.00	98.35	-0.03
160.00	97.94	0.00	170.00	98.37	-0.04
170.00	97.95	-0.01	180.00	98.41	-0.05
180.00	97.97	-0.02	190.00	98.47	-0.08
190.00	98	-0.04	200.00	98.56	-0.10
200.00	98.06	-0.07	210.00	98.67	-0.12
210.00	98.13	-0.09	220.00	98.81	-0.16
220.00	98.24	-0.12	230.00	98.97	-0.18
230.00	98.36	-0.15	240.00	99.17	-0.20
240.00	98.51	-0.16	250.00	99.37	-0.22
250.00	98.67	-0.17	260.00	99.56	-0.19
260.00	98.83	-0.15	270.00	99.72	-0.13
270.00	98.95	-0.11	280.00	99.81	-0.04
280.00	99.02	-0.03	290.00	99.79	0.09
290.00	98.99	0.09	300.00	99.64	0.24
300.00	98.83	0.23	310.00	99.31	0.42
310.00	98.53	0.40	320.00	98.8	0.61
320.00	98.06	0.56	330.00	98.12	0.77
330.00	97.43	0.71	340.00	97.26	0.93
340.00	96.64	0.86	350.00	96.24	1.10
350.00	95.7	1.01	360.00	95.04	1.29
360.00	94.59	1.20	370.00	93.64	1.53
370.00	93.3	1.42	380.00	92.01	1.79

380.00	91.79	1.66	390.00	90.12	2.13
390.00	90.03	1.98	400.00	87.87	2.62
400.00	87.95	2.44	410.00	85.12	3.37
410.00	85.4	3.14	420.00	81.72	4.68
420.00	82.16	4.35	430.00	77.21	7.24
430.00	77.95	6.50	440.00	71.18	8.67
440.00	72.35	7.92	450.00	62.85	7.43
450.00	64.82	6.98	460.00	54.81	5.84
460.00	57.36	5.67	470.00	48.54	4.54
470.00	51.32	4.55	480.00	43.79	3.49
480.00	46.55	3.58	490.00	40.28	2.56
490.00	42.91	2.65	500.00	37.79	1.92
500.00	40.33	1.97	510.00	35.96	1.51
510.00	38.45	1.52	520.00	34.56	1.15
520.00	37.04	1.13	530.00	33.54	0.80
530.00	36.05	0.76	540.00	32.88	0.51
540.00	35.41	0.49	550.00	32.47	0.31
550.00	35.02	0.30	560.00	32.22	0.20
560.00	34.77	0.20	570.00	32.05	0.15
570.00	34.6	0.15	580.00	31.92	0.12
580.00	34.47	0.12	590.00	31.82	0.09
590.00	34.37	0.11	600.00	31.73	0.07
600.00	34.28	0.08	610.00	31.66	0.06
610.00	34.21	0.06	620.00	31.6	0.05
620.00	34.15	0.05	630.00	31.55	0.04
630.00	34.09	0.05	640.00	31.51	0.08
640.00	34.04	0.06	650.00	31.46	0.04
650.00	33.99	0.05	660.00	31.42	0.03
660.00	33.95	0.03	670.00	31.39	0.03
670.00	33.92	0.04	680.00	31.37	0.02
680.00	33.89	0.03	690.00	31.35	0.03
690.00	33.86	0.02	700.00	31.31	0.06
700.00	33.83	0.00	710.00	31.24	0.07
710.00	33.79	0.06	720.00	31.15	0.10
720.00	33.73	0.07	730.00	31.05	0.10
730.00	33.66	0.07	740.00	30.95	0.07
740.00	33.59	0.06	750.00	30.89	0.05
750.00	33.54	0.05	760.00	30.86	0.02
760.00	33.5	0.03	770.00	30.83	0.02
770.00	33.48	0.03	780.00	30.81	0.02
780.00	33.46	0.02	790.00	30.79	0.01
790.00	33.44	0.02	800.00	30.78	0.01
800.00	33.43	0.02	810.00	30.77	-0.04
810.00	33.42	0.01	820.00	30.76	0.01

820.00	33.4	0.02	830.00	30.75	0.00
830.00	33.39	0.01	840.00	30.74	0.00
840.00	33.38	0.01	850.00	30.74	0.00
850.00	33.37	0.02	860.00	30.73	0.02
860.00	33.36	0.01	870.00	30.72	0.01
870.00	33.34	0.01	880.00	30.72	0.01
880.00	33.33	0.01	890.00	30.71	0.01
890.00	33.31	0.01			
Bench 5, four months (B5 M4)			**Bench 5, six months (B5 M6)**		
Temperature °C	**Weight %**	**Deriv. Weight %/min**	**Temperature °C**	**Weight %**	**Deriv. Weight %/min**
20.00	99.96	0.096	30.00	99.81	0.21
30.00	99.79	0.275	40.00	99.3	0.17
40.00	99.35	0.272	50.00	98.93	0.00
50.00	98.83	0.061	60.00	98.88	0.08
60.00	98.75	0.107	70.00	98.78	0.10
70.00	98.62	0.141	80.00	98.66	0.11
80.00	98.47	0.157	90.00	98.58	0.06
90.00	98.29	0.139	100.00	98.47	0.08
100.00	98.18	0.102	110.00	98.41	0.05
110.00	98.08	0.084	120.00	98.37	0.03
120.00	98.02	0.053	130.00	98.34	0.02
130.00	97.98	0.034	140.00	98.32	0.02
140.00	97.96	0.020	150.00	98.32	0.00
150.00	97.94	0.007	160.00	98.32	-0.01
160.00	97.94	-0.003	170.00	98.33	-0.01
170.00	97.95	-0.009	180.00	98.35	-0.02
180.00	97.97	-0.026	190.00	98.38	-0.05
190.00	98	-0.041	200.00	98.44	-0.07
200.00	98.06	-0.066	210.00	98.52	-0.09
210.00	98.13	-0.085	220.00	98.62	-0.12
220.00	98.24	-0.117	230.00	98.75	-0.14
230.00	98.36	-0.152	240.00	98.91	-0.17
240.00	98.51	-0.160	250.00	99.07	-0.17
250.00	98.67	-0.165	260.00	99.23	-0.16
260.00	98.83	-0.147	270.00	99.37	-0.12
270.00	98.95	-0.106	280.00	99.43	-0.03
280.00	99.02	-0.027	290.00	99.4	0.10
290.00	98.99	0.087	300.00	99.24	0.26
300.00	98.83	0.232	310.00	98.9	0.43
310.00	98.53	0.398	320.00	98.4	0.60
320.00	98.07	0.561	330.00	97.71	0.76
330.00	97.43	0.707	340.00	96.87	0.92
340.00	96.65	0.857	350.00	95.85	1.10

350.00	95.71	1.006	360.00	94.65	1.31
360.00	94.6	1.196	370.00	93.24	1.56
370.00	93.31	1.416	380.00	91.57	1.88
380.00	91.79	1.661	390.00	89.6	2.30
390.00	90.05	1.980	400.00	87.18	3.01
400.00	87.95	2.436	410.00	84.07	4.67
410.00	85.11	3.231	420.00	79.96	32.28
420.00	82.19	4.322	430.00	73.45	25.23
430.00	77.96	6.486	440.00	61.58	5.15
440.00	72.42	7.919	450.00	56.03	4.99
450.00	64.84	6.987	460.00	50.57	4.09
460.00	57.37	5.671	470.00	46.26	3.21
470.00	51.34	4.554	480.00	42.98	2.47
480.00	46.56	3.587	490.00	40.52	1.93
490.00	42.93	2.647	500.00	38.62	1.59
500.00	40.34	1.975	510.00	37.08	1.34
510.00	38.45	1.515	520.00	35.83	1.05
520.00	37.04	1.135	530.00	34.9	0.74
530.00	36.06	0.767	540.00	34.28	0.48
540.00	35.42	0.489	550.00	33.89	0.29
550.00	35.02	0.301	560.00	33.66	0.19
560.00	34.77	0.198	570.00	33.5	0.13
570.00	34.6	0.148	580.00	33.39	0.10
580.00	34.47	0.120	590.00	33.3	0.08
590.00	34.37	0.105	600.00	33.23	0.06
600.00	34.28	0.080	610.00	33.17	0.05
610.00	34.21	0.063	620.00	33.12	0.04
620.00	34.15	0.055	630.00	33.07	0.05
630.00	34.09	0.053	640.00	33.02	0.04
640.00	34.04	0.055	650.00	32.98	0.04
650.00	33.99	0.045	660.00	32.95	0.04
660.00	33.95	0.036	670.00	32.92	0.03
670.00	33.92	0.036	680.00	32.89	0.02
680.00	33.89	0.031	690.00	32.86	0.06
690.00	33.86	0.025	700.00	32.78	0.11
700.00	33.83	0.001	710.00	32.66	0.13
710.00	33.79	0.057	720.00	32.53	0.12
720.00	33.73	0.069	730.00	32.42	0.10
730.00	33.66	0.068	740.00	32.32	0.08
740.00	33.6	0.063	750.00	32.26	0.06
750.00	33.54	0.048	760.00	32.2	0.06
760.00	33.5	0.025	770.00	32.15	0.03
770.00	33.48	0.026	780.00	32.13	0.02
780.00	33.46	0.016	790.00	32.12	0.01

790.00	33.44	0.015	800.00	32.11	0.01
800.00	33.43	0.015	810.00	32.1	0.01
810.00	33.4	0.023	820.00	32.09	0.00
820.00	33.39	0.015	830.00	32.09	0.01
830.00	33.38	0.008	840.00	32.08	0.01
840.00	33.37	0.017	850.00	32.07	0.01
850.00	33.36	0.015	860.00	32.06	0.00
860.00	33.34	0.012	870.00	32.06	0.00
870.00	33.33	0.010	880.00	32.05	0.00
880.00	33.31	0.014	890.00	32.04	0.01
Bench 5 wet, one month (B5W M1)			**Bench 5 wet, two months (B5W M2)**		
Temperature °C	**Weight %**	**Deriv. Weight %/min**	**Temperature °C**	**Weight %**	**Deriv. Weight %/min**
30.00	99.78	0.2952	30.00	99.84	0.25
40.00	99.14	0.1645	40.00	99.23	0.12
50.00	98.77	-0.02516	50.00	98.96	-0.03
60.00	98.75	0.0507	60.00	98.95	0.05
70.00	98.67	0.09173	70.00	98.84	0.08
80.00	98.57	0.1099	80.00	98.75	0.10
90.00	98.49	0.04116	90.00	98.66	0.06
100.00	98.40	0.06548	100.00	98.58	0.12
110.00	98.35	0.03966	110.00	98.52	0.04
120.00	98.32	0.0308	120.00	98.48	0.02
130.00	98.30	0.0126	130.00	98.46	0.01
140.00	98.30	-0.003087	140.00	98.46	0.00
150.00	98.30	-0.006108	150.00	98.46	0.00
160.00	98.32	-0.02612	160.00	98.47	-0.01
170.00	98.35	-0.03644	170.00	98.5	-0.03
180.00	98.40	-0.06236	180.00	98.54	-0.05
190.00	98.46	-0.0884	190.00	98.6	-0.07
200.00	98.56	-0.08841	200.00	98.67	-0.09
210.00	98.67	-0.1265	210.00	98.78	-0.12
220.00	98.82	-0.1648	220.00	98.91	-0.15
230.00	98.99	-0.1875	230.00	99.07	-0.17
240.00	99.19	-0.2154	240.00	99.25	-0.20
250.00	99.40	-0.2084	250.00	99.44	-0.19
260.00	99.60	-0.1825	260.00	99.62	-0.17
270.00	99.75	-0.1264	270.00	99.77	-0.13
280.00	99.84	-0.0448	280.00	99.85	-0.04
290.00	99.83	0.08031	290.00	99.82	0.09
300.00	99.67	0.2411	300.00	99.67	0.24
310.00	99.35	0.4226	310.00	99.35	0.42
320.00	98.84	0.5927	320.00	98.85	0.59
330.00	98.16	0.7652	330.00	98.19	0.74

340.00	97.32	0.9088	340.00	97.36	0.90
350.00	96.32	1.075	350.00	96.37	1.06
360.00	95.15	1.251	360.00	95.22	1.25
370.00	93.79	1.496	370.00	93.87	1.48
380.00	92.20	1.743	380.00	92.3	1.75
390.00	90.33	2.085	390.00	90.45	2.09
400.00	88.14	2.567	400.00	88.24	2.63
410.00	85.45	3.316	410.00	85.46	3.57
420.00	82.07	4.578	420.00	81.79	5.59
430.00	77.63	7.192	430.00	77.06	34.24
440.00	71.80	9.542	440.00	65.05	5.72
450.00	63.11	7.09	450.00	57.1	4.97
460.00	55.22	5.584	460.00	51.67	4.03
470.00	49.23	4.418	470.00	47.47	3.09
480.00	44.60	3.383	480.00	44.37	2.43
490.00	41.20	2.508	490.00	41.98	1.96
500.00	38.76	1.907	500.00	40.07	1.63
510.00	36.93	1.512	510.00	38.5	1.36
520.00	35.54	1.14	520.00	37.24	1.05
530.00	34.53	0.7808	530.00	36.32	0.75
540.00	33.88	0.4978	540.00	35.72	0.46
550.00	33.48	0.3096	550.00	35.35	0.29
560.00	33.23	0.2031	560.00	35.12	0.18
570.00	33.05	0.1488	570.00	34.97	0.13
580.00	32.92	0.1216	580.00	34.85	0.10
590.00	32.81	0.09272	590.00	34.76	0.09
600.00	32.72	0.0811	600.00	34.69	0.07
610.00	32.65	0.06976	610.00	34.63	0.06
620.00	32.59	0.05256	620.00	34.57	0.05
630.00	32.53	0.05577	630.00	34.52	0.05
640.00	32.48	0.0572	640.00	34.48	0.04
650.00	32.43	0.04875	650.00	34.44	0.04
660.00	32.39	0.03699	660.00	34.4	0.03
670.00	32.36	0.0344	670.00	34.37	0.03
680.00	32.33	0.02015	680.00	34.34	0.03
690.00	32.31	0.02567	690.00	34.31	0.04
700.00	32.28	0.03286	700.00	34.28	0.04
710.00	32.24	0.04186	710.00	34.23	0.07
720.00	32.18	0.0699	720.00	34.17	0.07
730.00	32.11	0.07934	730.00	34.1	0.06
740.00	32.03	0.07232	740.00	34.04	0.05
750.00	31.98	0.04128	750.00	34.01	0.03
760.00	31.94	0.01866	760.00	33.98	0.02
770.00	31.92	0.01791	770.00	33.96	0.02

780.00	31.90	0.01718	780.00	33.94	0.02
790.00	31.89	0.014	790.00	33.93	0.01
800.00	31.87	0.01474	800.00	33.92	0.01
810.00	31.86	0.01082	810.00	33.91	0.01
820.00	31.85	0.01505	820.00	33.89	0.01
830.00	31.83	-0.000603	830.00	33.88	0.01
840.00	31.82	0.01543	840.00	33.87	0.01
850.00	31.81	0.01548	850.00	33.86	0.01
860.00	31.80	0.01601	860.00	33.86	0.01
870.00	31.79	0.008723	870.00	33.85	0.01
880.00	31.78	0.002262	880.00	33.84	0.01
890.00	31.77	0.01114	890.00	33.83	0.01
Bench 5 wet, four months (B5W M4)			**Bench 5 wet, six months (B5W M6)**		
Temperature °C	**Weight %**	**Deriv. Weight %/min**	**Temperature °C**	**Weight %**	**Deriv. Weight %/min**
30.00	99.77	0.33	30.00	99.72	0.31
40.00	99.17	0.20	40.00	99.08	0.23
50.00	98.95	0.20	50.00	98.61	0.09
60.00	98.77	0.21	60.00	98.5	0.14
70.00	98.56	0.19	70.00	98.34	0.15
80.00	98.38	0.16	80.00	98.2	0.13
90.00	98.22	0.14	90.00	98.08	0.10
100.00	98.11	0.12	100.00	97.96	0.13
110.00	97.97	0.08	110.00	97.84	0.09
120.00	97.91	0.05	120.00	97.78	0.05
130.00	97.88	0.03	130.00	97.74	0.03
140.00	97.86	0.01	140.00	97.71	0.02
150.00	97.85	0.01	150.00	97.69	0.02
160.00	97.85	-0.01	160.00	97.69	0.00
170.00	97.86	-0.02	170.00	97.69	-0.01
180.00	97.89	-0.03	180.00	97.71	-0.02
190.00	97.93	-0.05	190.00	97.74	-0.02
200.00	97.99	-0.07	200.00	97.8	-0.07
210.00	98.07	-0.09	210.00	97.88	-0.09
220.00	98.18	-0.12	220.00	97.98	-0.12
230.00	98.31	-0.15	230.00	98.11	-0.15
240.00	98.46	-0.17	240.00	98.26	-0.16
250.00	98.62	-0.16	250.00	98.42	-0.15
260.00	98.78	-0.15	260.00	98.57	-0.14
270.00	98.91	-0.10	270.00	98.69	-0.10
280.00	98.97	-0.03	280.00	98.75	-0.02
290.00	98.95	0.08	290.00	98.72	0.09
300.00	98.81	0.23	300.00	98.56	0.24
310.00	98.52	0.38	310.00	98.24	0.43

320.00	98.06	0.55	320.00	97.75	0.59
330.00	97.44	0.70	330.00	97.08	0.75
340.00	96.66	0.85	340.00	96.25	0.90
350.00	95.72	1.01	350.00	95.25	1.07
360.00	94.62	1.19	360.00	94.08	1.26
370.00	93.33	1.40	370.00	92.71	1.50
380.00	91.84	1.65	380.00	91.12	1.77
390.00	90.09	1.99	390.00	89.26	2.09
400.00	88.01	2.45	400.00	87.07	2.55
410.00	85.47	3.18	410.00	84.43	3.23
420.00	82.24	4.49	420.00	81.16	4.28
430.00	78.04	7.01	430.00	77.04	5.86
440.00	72.42	8.11	440.00	71.79	7.68
450.00	64.49	6.70	450.00	64.96	8.28
460.00	57.16	5.50	460.00	56.32	6.59
470.00	51.19	4.38	470.00	49.03	4.99
480.00	46.53	3.45	480.00	43.66	3.86
490.00	42.98	2.55	490.00	39.66	2.71
500.00	40.48	1.88	500.00	37.03	1.91
510.00	38.67	1.46	510.00	35.22	1.46
520.00	37.32	1.09	520.00	33.88	1.07
530.00	36.37	0.75	530.00	32.94	0.73
540.00	35.74	0.48	540.00	32.32	0.46
550.00	35.35	0.30	550.00	31.95	0.29
560.00	35.11	0.19	560.00	31.72	0.18
570.00	34.94	0.14	570.00	31.56	0.13
580.00	34.82	0.11	580.00	31.45	0.10
590.00	34.71	0.09	590.00	31.35	0.08
600.00	34.63	0.08	600.00	31.28	0.07
610.00	34.56	0.07	610.00	31.21	0.06
620.00	34.5	0.05	620.00	31.15	0.06
630.00	34.44	0.05	630.00	31.1	0.05
640.00	34.39	0.05	640.00	31.05	0.05
650.00	34.34	0.04	650.00	31.01	0.04
660.00	34.31	0.04	660.00	30.97	0.04
670.00	34.28	0.03	670.00	30.94	0.02
680.00	34.25	0.03	680.00	30.91	0.02
690.00	34.23	0.02	690.00	30.89	0.03
700.00	34.21	0.03	700.00	30.86	0.03
710.00	34.19	0.03	710.00	30.82	0.01
720.00	34.15	0.03	720.00	30.78	0.04
730.00	34.12	0.05	730.00	30.74	0.04
740.00	34.07	0.05	740.00	30.71	0.02
750.00	34.02	0.05	750.00	30.69	0.02

760.00	33.98	0.04	760.00	30.68	0.02
770.00	33.94	0.03	770.00	30.66	0.02
780.00	33.91	0.02	780.00	30.64	0.01
790.00	33.9	0.02	790.00	30.63	0.02
800.00	33.88	0.02	800.00	30.61	0.02
810.00	33.87	0.02	810.00	30.6	0.01
820.00	33.86	0.01	820.00	30.58	0.06
830.00	33.85	0.01	830.00	30.57	0.01
840.00	33.84	0.01	840.00	30.56	0.01
850.00	33.83	0.01	850.00	30.54	0.02
860.00	33.82	0.01	860.00	30.54	0.01
870.00	33.81	0.01	870.00	30.52	0.01
880.00	33.8	0.01	880.00	30.51	0.02
890.00	33.79	0.01	890.00	30.5	0.02

Appendix G. Carbonate analysis on various calcite grains (wt%) by EMPA

Bench 5 (fresh sample)										
No of grains measured	**MgO**	**CaO**	**MnO**	**FeO**	**Total**	**Mg**	**Ca**	**Mn**	**Fe**	**Total**
1 / 1	0.05	53.52	0.51	0.55	54.63	0.008	5.900	0.045	0.048	6
2 / 1	0.06	50.86	0.32	0.37	51.61	0.010	5.927	0.030	0.033	6
1 / 2	0.25	55.32	0.06	0.01	55.63	0.037	5.957	0.005	0.001	6
2 / 2	0.39	54.85	0.05	0.04	55.33	0.058	5.934	0.004	0.003	6
Bench 5, 6 months (contaminated by rainwater)										
No of grains measured	**MgO**	**CaO**	**MnO**	**FeO**	**Total**	**Mg**	**Ca**	**Mn**	**Fe**	**Total**
1 / 1	0.03	54.21	0.09	0.35	54.67	0.004	5.959	0.007	0.030	6
2 / 1	0.00	54.8	0.07	0.27	55.14	0.000	5.971	0.006	0.023	6
3 / 1	0.00	54.71	0.10	0.31	55.13	0.001	5.964	0.009	0.027	6
4 / 1	0.00	54.56	0.10	0.17	54.83	0.000	5.977	0.009	0.014	6
5 / 1	0.00	54.36	0.08	0.17	54.6	0.000	5.979	0.007	0.014	6
6 / 1	0.00	54.37	0.14	0.17	54.67	0.000	5.974	0.012	0.014	6
7 / 1	0.52	54.06	0.14	0.10	54.83	0.079	5.900	0.012	0.009	6
8 / 1	0.47	54.47	0.07	0.11	55.11	0.071	5.914	0.006	0.009	6
1 / 2	0.03	54.21	0.09	0.35	54.67	0.004	5.959	0.007	0.030	6
2 / 2	0.00	54.80	0.07	0.27	55.14	0.000	5.971	0.006	0.023	6
3 / 2	0.00	54.71	0.10	0.31	55.13	0.001	5.964	0.009	0.027	6
4 / 2	0.00	54.56	0.10	0.17	54.83	0.000	5.977	0.009	0.014	6
1 / 3	0.13	53.11	0.40	0.51	54.16	0.021	5.900	0.035	0.045	6
2 / 3	0.00	53.48	0.12	0.38	53.98	0.000	5.957	0.010	0.033	6
3 / 3	0.10	1.40	0.25	52.24	54.00	0.019	0.198	0.028	5.755	6
4 / 3	0.16	1.56	0.16	45.24	47.11	0.035	0.251	0.020	5.694	6
1 / 4	0.00	19.14	0.06	0.21	19.41	0.000	5.934	0.015	0.052	6
2 / 4	0.01	2.36	0.02	3.37	5.76	0.023	2.819	0.015	3.143	6
Bench 5 wet, 5 months										
No of grains measured	**MgO**	**CaO**	**MnO**	**FeO**	**Total**	**Mg**	**Ca**	**Mn**	**Fe**	**Total**
1 / 1	0.34	54.53	0.02	0.01	54.90	0.052	5.945	0.002	0.001	6
2 / 1	0.33	54.41	0.03	0.03	54.80	0.051	5.944	0.002	0.003	6

Appendix H. Raman spectroscopy

The Raman spectra of the weathered calcite grains in the six-month samples of Bench 5 were found to correspond to the spectra of fresh calcite as reported by Frezzotti *et al* (2012) and therefore indicate that there is no structural change in the calcite grains that appear (both optically and petrographically) to be weathered. The image below shows the Raman spectra of weathered and fresh calcite grains after six months of weathering in Bench 5. One of the measurements were taken in close proximity to vitrinite hence one of the spectra includes a graphitic band (G band) which occurred at 1605 cm^{-1} and resulted in a higher intensity

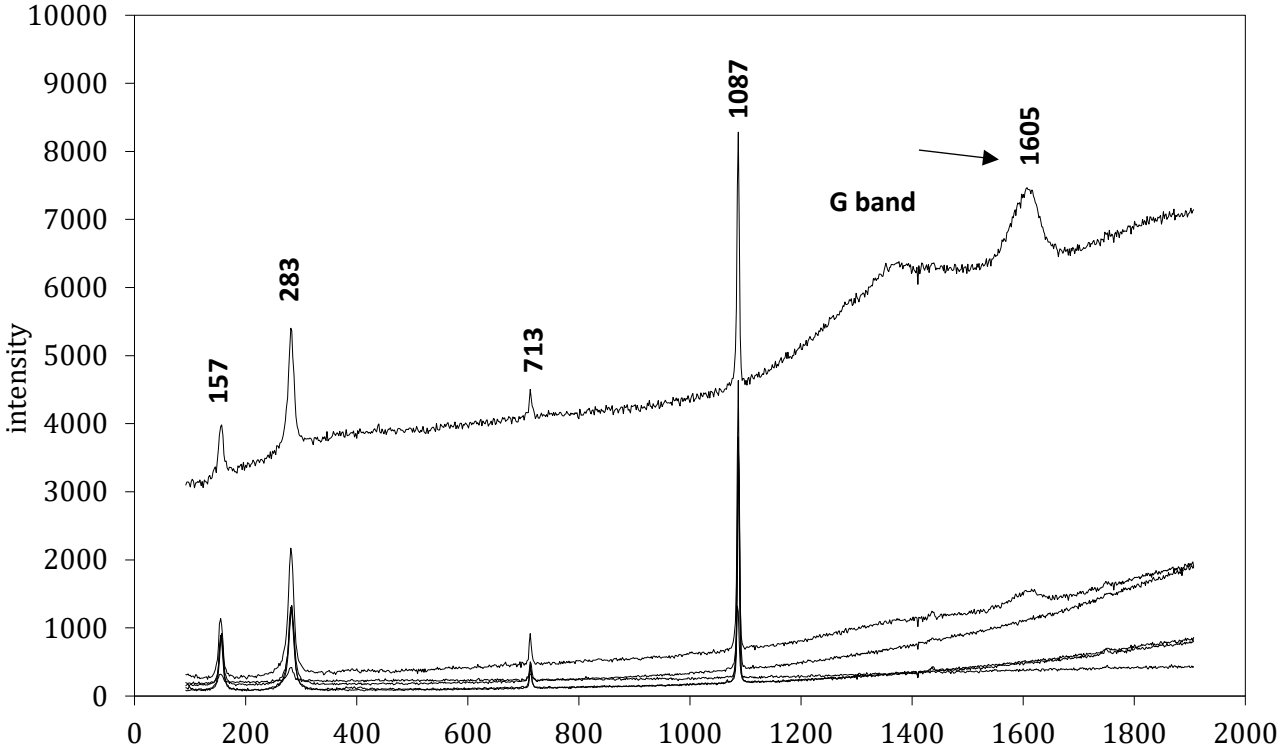


Figure 36. Raman spectra of red calcite grains

Appendix I. Major oxide composition (wt %) as determined by XRF

Middle Seam (MS)														
Days	**SiO_2**	**TiO_2**	**Al_2O_3**	**Fe_2O_3 (t)**	**MnO**	**MgO**	**CaO**	**Na_2O**	**K_2O**	**P_2O_5**	**Cr_2O_3**	**LOI**	**Total**	**H_2O^-**
0	13.01	0.17	4.23	2.33	0.014	0.23	1.70	0.04	0.45	0.08	0.02	77.53	99.80	1.59
7	12.73	0.17	4.09	2.67	0.013	0.23	1.66	0.08	0.44	0.08	0.00	78.01	100.18	1.44
14	11.65	0.16	3.82	2.05	0.013	0.21	1.72	0.04	0.40	0.07	0.01	78.22	98.37	1.53
33	11.42	0.26	5.45	2.68	0.005	0.07	1.29	0.02	0.21	0.63	0.01	77.66	99.71	1.48
73	11.78	0.16	3.77	2.96	0.014	0.22	1.85	0.05	0.41	0.07	0.02	78.64	99.95	0.61
125	12.07	0.16	3.95	3.15	0.013	0.22	1.69	0.03	0.42	0.07	0.00	77.79	99.57	0.93
188	12.72	0.17	4.23	3.72	0.014	0.23	1.74	0.03	0.44	0.08	0.01	76.59	99.97	1.87
Middle seam wet (MSW)														
Days	**SiO_2**	**TiO_2**	**Al_2O_3**	**Fe_2O_3 (t)**	**MnO**	**MgO**	**CaO**	**Na_2O**	**K_2O**	**P_2O_5**	**Cr_2O_3**	**LOI**	**Total**	**H_2O^-**
0	13.01	0.17	4.23	2.33	0.01	0.23	1.70	0.04	0.45	0.08	0.02	77.53	99.80	1.59
7	12.91	0.17	4.21	2.43	0.01	0.23	1.69	0.04	0.45	0.08	0.01	77.63	99.86	1.51
33	6.96	0.29	6.20	0.29	0.06	1.16	5.74	0.01	0.04	0.68	0.01	77.44	98.87	1.49
73	12.73	0.17	4.14	2.02	0.01	0.22	1.37	0.03	0.46	0.08	0.02	78.27	99.52	0.77
125	13.40	0.17	4.36	2.16	0.01	0.22	1.37	0.03	0.46	0.08	0.00	77.54	99.81	1.18
188	12.33	0.17	4.12	2.94	0.01	0.22	1.69	0.04	0.42	0.07	0.01	77.91	99.93	1.47
Bench 3 (B3)														
Days	**SiO_2**	**TiO_2**	**Al_2O_3**	**Fe_2O_3 (t)**	**MnO**	**MgO**	**CaO**	**Na_2O**	**K_2O**	**P_2O_5**	**Cr_2O_3**	**LOI**	**Total**	**H_2O^-**
0	17.14	0.20	5.02	1.22	0.04	0.49	0.86	0.02	0.27	0.02	0.01	74.50	99.79	2.05
7	14.82	0.19	4.40	1.71	0.04	0.53	0.95	0.04	0.25	0.02	0.00	76.21	99.17	1.74
14	15.05	0.19	4.44	1.94	0.05	0.59	1.05	0.02	0.23	0.02	0.01	76.31	99.90	1.73
33	14.64	0.19	4.30	1.51	0.04	0.52	0.92	0.02	0.22	0.02	0.01	77.25	99.64	1.88
73	15.14	0.18	4.43	1.38	0.04	0.45	0.79	0.01	0.24	0.02	0.03	77.09	99.80	0.78
125	14.24	0.18	4.18	1.30	0.04	0.50	0.88	0.01	0.22	0.02	0.01	78.13	99.71	1.02
188	15.21	0.19	4.55	1.48	0.04	0.49	0.86	0.02	0.23	0.03	0.01	76.90	100.00	1.70
Bench 3 wet (B3W)														
Days	**SiO_2**	**TiO_2**	**Al_2O_3**	**Fe_2O_3 (t)**	**MnO**	**MgO**	**CaO**	**Na_2O**	**K_2O**	**P_2O_5**	**Cr_2O_3**	**LOI**	**Total**	**H_2O^-**
0	17.14	0.20	5.02	1.22	0.04	0.49	0.86	0.02	0.27	0.02	0.01	74.50	99.79	2.05
7	16.02	0.19	4.66	1.54	0.04	0.52	0.90	0.02	0.25	0.02	0.01	75.78	99.95	1.83
33	15.13	0.18	4.42	1.80	0.04	0.52	0.92	0.02	0.23	0.02	0.01	76.08	99.37	1.90
73	17.90	0.38	8.08	3.03	0.01	0.15	1.71	0.03	0.32	0.86	0.02	67.62	100.11	0.96

125	14.27	0.18	4.18	2.08	0.04	0.53	0.93	0.02	0.22	0.02	0.00	77.27	99.74	1.30
188	14.42	0.18	4.79	2.58	0.01	0.21	1.22	0.04	0.50	0.09	0.01	75.99	100.03	1.44
Bench 5 (B5)														
Days	**SiO_2**	**TiO_2**	**Al_2O_3**	**Fe_2O_3 (t)**	**MnO**	**MgO**	**CaO**	**Na_2O**	**K_2O**	**P_2O_5**	**Cr_2O_3**	**LOI**	**Total**	**H_2O^-**
0	18.23	0.41	8.54	3.80	0.01	0.10	1.93	0.04	0.34	1.05	0.02	65.66	100.12	1.75
7	17.74	0.41	8.49	3.66	0.01	0.10	2.01	0.04	0.36	1.00	0.01	65.46	99.28	1.41
14	16.02	0.41	7.72	3.41	0.01	0.11	2.38	0.04	0.37	0.96	0.02	66.78	98.23	1.46
33	19.26	0.26	6.32	4.44	0.02	0.35	2.65	0.05	0.67	0.12	0.02	65.40	99.56	1.54
73	16.91	0.40	7.99	2.85	0.01	0.10	2.05	0.03	0.32	0.99	0.03	68.20	99.88	0.66
125	18.02	0.40	8.49	3.13	0.01	0.09	1.84	0.03	0.34	1.01	0.02	66.45	99.82	0.97
188	17.37	0.41	8.32	3.31	0.01	0.10	2.04	0.03	0.32	0.96	0.02	67.04	99.93	1.45
Bench 5 wet (B5W)														
Days	**SiO_2**	**TiO_2**	**Al_2O_3**	**Fe_2O_3 (t)**	**MnO**	**MgO**	**CaO**	**Na_2O**	**K_2O**	**P_2O_5**	**Cr_2O_3**	**LOI**	**Total**	**H_2O^-**
0	18.23	0.41	8.54	3.80	0.005	0.10	1.93	0.04	0.34	1.05	0.018	65.66	100.12	1.75
7	18.99	0.41	8.89	2.37	0.004	0.09	1.86	0.04	0.36	1.13	0.008	65.67	99.82	1.58
33	17.93	0.39	8.50	2.70	0.005	0.09	1.82	0.02	0.33	0.967	0.014	65.71	98.48	1.53
73	15.63	0.24	5.37	1.97	0.03	0.38	1.10	0.02	0.26	0.28	0.01	74.50	99.79	0.81
125	18.13	0.40	8.62	3.40	0.006	0.08	1.75	0.03	0.34	0.988	0.016	65.78	99.54	0.97
188	18.04	0.41	8.65	2.37	0.005	0.08	1.82	0.03	0.34	1.05	0.015	67.21	100.02	1.61
Bench 9B (B9)														
Days	**SiO_2**	**TiO_2**	**Al_2O_3**	**Fe_2O_3 (t)**	**MnO**	**MgO**	**CaO**	**Na_2O**	**K_2O**	**P_2O_5**	**Cr_2O_3**	**LOI**	**Total**	**H_2O^-**
0	6.22	0.25	5.52	0.18	0.055	1.03	5.22	0.01	0.04	0.617	0.007	80.11	99.25	2.44
7	5.77	0.24	5.18	0.23	0.051	0.98	4.92	0.01	0.04	0.606	0.004	80.64	98.66	1.87
14	5.77	0.24	5.12	0.25	0.052	0.99	5.03	0.01	0.04	0.579	0.007	80.79	98.87	1.75
33	10.97	0.14	3.58	2.14	0.010	0.19	1.23	0.03	0.38	0.063	0.011	80.62	99.36	2.00
73	4.84	0.22	4.40	0.27	0.05	0.93	4.81	0.01	0.04	0.49	0.02	81.45	97.52	1.19
125	5.77	0.24	5.08	0.25	0.045	0.95	4.38	0.01	0.04	0.544	0.007	81.49	98.80	1.17
188	6.15	0.25	5.54	0.26	0.052	1.03	4.89	0.01	0.04	0.581	0.009	80.47	99.27	2.21
Bench 9B wet (B9W)														
Days	**SiO_2**	**TiO_2**	**Al_2O_3**	**Fe_2O_3 (t)**	**MnO**	**MgO**	**CaO**	**Na_2O**	**K_2O**	**P_2O_5**	**Cr_2O_3**	**LOI**	**Total**	**H_2O^-**
0	6.22	0.25	5.52	0.18	0.055	1.03	5.22	0.01	0.04	0.617	0.007	80.11	99.25	2.44
7	6.09	0.24	5.4	0.23	0.047	0.9	4.53	0.01	0.04	0.64	0.004	80.92	99.04	2.07
33	12.06	0.15	3.50	1.42	0.032	0.41	0.72	0.01	0.18	0.016	0.009	80.36	98.87	2.09

73	5.41	0.22	4.84	0.20	0.05	0.88	4.60	0.01	0.04	0.59	0.01	81.50	98.34	1.51
125	6.41	0.22	4.17	1.75	0.022	0.76	1.23	0.01	0.05	0.016	0.008	84.88	99.52	1.24
188	5.98	0.24	5.46	0.22	0.048	0.92	4.64	0.01	0.04	0.642	0.006	81.11	99.31	2.09
Bench 11 (B11)														
Days	**SiO_2**	**TiO_2**	**Al_2O_3**	**Fe_2O_3 (t)**	**MnO**	**MgO**	**CaO**	**Na_2O**	**K_2O**	**P_2O_5**	**Cr_2O_3**	**LOI**	**Total**	**H_2O^-**
0	6.75	0.24	4.42	1.95	0.025	0.83	1.35	0.01	0.05	0.014	0.010	83.98	99.62	2.17
7	6.38	0.22	4.15	1.40	0.024	0.83	1.34	0.01	0.05	0.014	0.004	84.69	99.11	1.75
14	6.15	0.23	4.07	1.18	0.025	0.87	1.45	0.01	0.06	0.014	0.008	84.54	98.60	1.90
33	6.69	0.23	4.38	1.50	0.025	0.84	1.36	0.01	0.05	0.014	0.009	84.46	99.56	1.96
73	6.48	0.22	4.20	1.51	0.024	0.80	1.30	0.00	0.05	0.014	0.017	85.31	99.93	0.92
125	6.13	0.22	4.01	1.18	0.024	0.81	1.31	0.01	0.05	0.013	0.007	85.81	99.56	1.21
188	6.51	0.23	4.31	1.29	0.026	0.89	1.42	0.01	0.05	0.016	0.008	84.80	99.55	1.76
Bench 11 wet (B11W)														
Days	**SiO_2**	**TiO_2**	**Al_2O_3**	**Fe_2O_3 (t)**	**MnO**	**MgO**	**CaO**	**Na_2O**	**K_2O**	**P_2O_5**	**Cr_2O_3**	**LOI**	**Total**	**H_2O^-**
0	6.75	0.24	4.42	1.95	0.025	0.83	1.35	0.01	0.05	0.014	0.01	83.98	99.62	2.17
7	6.51	0.24	4.21	1.39	0.027	0.88	1.43	0.01	0.06	0.013	0.005	85.05	99.82	1.76
33	6.70	0.24	4.37	1.74	0.025	0.85	1.38	0.01	0.05	0.015	0.007	84.09	99.47	1.82
73	15.60	0.24	5.38	2.00	0.030	0.39	1.11	0.02	0.26	0.278	0.011	74.62	99.94	0.77
125	6.12	0.22	4.01	1.19	0.023	0.76	1.24	0.01	0.05	0.013	0.008	85.91	99.54	1.13
188	16.00	0.19	4.78	1.79	0.036	0.44	0.75	0.02	0.24	0.023	0.008	75.55	99.83	1.96

Appendix J. Presentations arising from this research project

Presentations given by the candidate during the course of the degree programme (2016-2017):

1. Fossil Fuel Foundation (FFF) conference in Sustainable Development of southern Africa's Energy Resources.
   29 – 30 November 2017. Johannesburg. South Africa.
   Oral presentation: Weathering of coals from the Waterberg and Limpopo Coalfields. South Africa
   Authors: M.T. Sebola. G.R. Drennan and N.J. Wagner

2. 35th International Geological Congress (IGC)
   27 August – 4 September 2016. Cape Town. South Africa
   Poster presentation: The effects of weathering on coal quality in the Limpopo and Soutpansberg Coalfields.
   Authors: M.T.. Sebola. G.R. Drennan. R.M.S. Falcon and N.J. Wagner
   Available from: http://www.americangeosciences.org/information